

Durham E-Theses

The Synthesis and Characterisation of Complex Branched Polymers via Living Anionic Polymerisation

OTI, MATTHEW,EBENEZER

How to cite:

OTI, MATTHEW,EBENEZER (2019) *The Synthesis and Characterisation of Complex Branched Polymers via Living Anionic Polymerisation*, Durham theses, Durham University. Available at Durham E-Theses Online: <http://etheses.dur.ac.uk/13248/>

Use policy

The full-text may be used and/or reproduced, and given to third parties in any format or medium, without prior permission or charge, for personal research or study, educational, or not-for-profit purposes provided that:

- a full bibliographic reference is made to the original source
- a [link](#) is made to the metadata record in Durham E-Theses
- the full-text is not changed in any way

The full-text must not be sold in any format or medium without the formal permission of the copyright holders.

Please consult the [full Durham E-Theses policy](#) for further details.

Academic Support Office, Durham University, University Office, Old Elvet, Durham DH1 3HP
e-mail: e-theses.admin@dur.ac.uk Tel: +44 0191 334 6107
<http://etheses.dur.ac.uk>



Durham University
Department of Chemistry



The Synthesis and Characterisation of Complex Branched Polymers via Living Anionic Polymerisation

Matthew Oti

2019

Thesis submitted in fulfilment for the degree of Doctor of Philosophy

The Synthesis and Characterisation of Complex Branched Polymers via Living Anionic Polymerisation

Matthew Oti

Abstract

This work is focused on the synthesis and characterisation of a range of branched polybutadiene materials using a combination of anionic polymerisation and post-polymerisation coupling reactions. The branched polymer architectures targeted included stars, H-shaped polymers and long-chain randomly branched polymers. Both three and four-arm star polymers were synthesised. The stars were characterised using both size exclusion chromatography (SEC) and interaction chromatography (IC) – in particular temperature gradient interaction chromatography (TGIC). TGIC was able to confirm structural dispersity within the crude and purified star polymers, which was otherwise undetectable by SEC. H-shaped polymers were synthesised using the “macromonomer” approach, which involves the use of polymers with reactive chain-end functionalities introduced via a functionalised protected initiator or a functionalised protected end capping agent. The functional macromonomers were then coupled together in a post-polymerisation Williamson coupling reaction to give the final H-shaped polymers. All macromonomers were prepared using anionic polymerisation resulting in well-defined polymers with narrow molecular weight distributions. The telechelic “crossbar” polymers were prepared in copolymerisation reactions exploiting monomer reactivity ratios, whereas the arms were prepared using an end capping agent. Normal-phase isothermal IC was employed to analyse the macromonomers by their molecular weight as well as functionality and was able to quantitatively assess the degree of functionalization for the polymers. The H-shaped polymers were synthesised using the functionalized macromonomers and TGIC analysis allowed for very detailed compositional analysis, revealing structural heterogeneity which was unclear from SEC analysis alone. Randomly branched polybutadienes were synthesised by using a crosslinking agent, a chain transfer promoter and toluene as both a chain transfer agent and solvent. This resulted in the production of soluble, highly branched, high molecular weight polymers from a one-pot facile reaction. The materials synthesised are to be used in a separate study as model polymers for structure-property correlation rheological studies.

Table of contents

List of Figures	i
List of Schemes	viii
List of Abbreviations.....	xii
Statement of Copyright	xiv
Acknowledgements	xv

Chapter 1 Introduction

1.1 Background.....	2
1.2 Classification of Polymers	4
1.2.1 Classification by Source.....	4
1.2.2 Classification by Architecture.....	5
1.2.3 Classification by Composition.....	5
1.2.4 Classification by Properties.....	6
1.3 Polymer Synthesis	8
1.3.1 Step-Growth Polymerisation	8
1.3.2 Chain-Growth Polymerisation	8
1.3.2.1 Free Radical Polymerisation	9
1.3.3 Controlled Polymerisation Methods	11
1.3.3.1 Reversible-Deactivation Radical Polymerisation	11
1.3.3.2 Atom Transfer Radical Polymerisation (ATRP)	12
1.3.3.3 Reversible Addition Fragmentation chain Transfer (RAFT).....	12
1.4 Living Polymerisation	15
1.4.1 Criteria for Living Polymerisation.....	15
1.4.2 Ionic Polymerisation	19
1.4.2.1 Cationic Polymerisation	19
1.4.2.2 Anionic Polymerisation.....	19
1.4.2.2.1 Mechanism.....	20
1.4.2.2.2 Monomers	21
1.4.2.2.3 Solvents	22
1.4.2.2.4 Initiators	23
1.4.2.2.5 Polymer Functionalisation.....	24
1.4.2.2.6 Impurities.....	25
1.5 Polymer Architectures	27
1.5.1 Linear Polymers.....	27
1.5.2 Branched Polymers	28
1.5.2.1 Star-branched Polymers	29

1.5.2.2	H-shaped Polymers.....	31
1.5.2.3	Graft/Comb polymers.....	34
1.5.3	Dendritically Branched Polymers	36
1.5.3.1	Dendrimers	37
1.5.3.2	Hyperbranched Polymers	38
1.5.3.3	Long-Chain Branched Polymers	39
1.6	The “Macromonomer” Approach.....	41
1.7	Aims and Objectives.....	45
1.8	References.....	47

Chapter 2 Synthesis and characterisation of Star-Branched Polybutadienes

2.1	Introduction.....	53
2.2	Results and Discussion	54
2.2.1	Synthesis of Three-Arm Star - Star(3)150	54
2.2.2	Synthesis of Four-Arm Star.....	58
2.2.2.1	Initial attempt - Star(4)180.....	58
2.2.2.2	Synthesis of 4-Arm Star - Star(4)130	60
2.2.3	Analysis of Stars - Interaction Chromatography	61
2.2.3.1	TGIC analysis - Crude Stars.....	67
2.2.3.2	TGIC analysis - Purified Stars	70
2.3	Experimental.....	72
2.3.1	Materials	72
2.3.2	Reaction Vessel (“Christmas Tree”).....	72
2.3.2.1	Preparation of Reaction Vessel.....	73
2.3.3	Characterisation.....	73
2.3.3.1	Nuclear Magnetic Resonance (NMR).....	73
2.3.3.2	Size Exclusion Chromatography (SEC).....	73
2.3.3.3	Temperature Gradient Interaction Chromatography (TGIC)...	74
2.3.4	Synthesis	74
2.3.4.1	Synthesis of 3-Arm Star - Star(3)150	74
2.3.4.2	Synthesis of 4-Arm Star - Star(4)180.....	75
2.3.4.3	Synthesis of 4-Arm Star - Star(4)130.....	75
2.3.5	Fractionation of Stars	75
2.4	Conclusions	77
2.5	References.....	78

Chapter 3 Synthesis and characterisation of Macromonomers

3.1 Introduction.....	80
3.2 Results and Discussion	82
3.2.1 Synthesis of Protected Functionalised Precursor (DPE-OSi)	82
3.2.2 Synthesis of Telechelic Polybutadiene “crossbars”	85
3.2.2.1 Synthesis of Telechelic Polybutadiene - “End-Capped” Approach.....	87
3.2.2.1.1 Initial attempts	87
3.2.2.1.2 Modified End-Capped Approach.....	92
3.2.2.2 Synthesis of Telechelic Polybutadiene by the “Fire and Forget” Approach.....	95
3.2.2.3 Deprotection of Crossbars.....	98
3.2.3 Synthesis of Polybutadiene “arm” Macromonomers.....	99
3.2.4 Analysis of Macromonomers by Interaction Chromatography.....	102
3.2.4.1 NP-IC Analysis of the Arms	103
3.2.4.2 NP-IC Analysis of the Crossbars.....	106
3.2.4.2.1 Impact of solvent temperature on NP-IIC analysis...	110
3.2.4.2.2 Impact of solvent composition on NP-IIC analysis ..	111
3.3 Experimental.....	117
3.3.1 Materials	117
3.3.2 Characterisation.....	117
3.3.2.1 Nuclear Magnetic Resonance (NMR).....	117
3.3.2.2 Size Exclusion Chromatography (SEC).....	117
3.3.2.3 Interaction Chromatography (IC).....	118
3.3.3 Synthesis	118
3.3.4 Synthesis of Functional Initiator/End-Capping Agent (DPE-OSi)	119
3.3.4.1 1-Bis(4- <i>tert</i> -butyldimethylsiloxyphenyl)benzophenone.....	119
3.3.4.2 1,1-Bis(4- <i>tert</i> -butyldimethylsiloxyphenyl)ethylene (DPE-OSi).....	119
3.3.5 Synthesis of Crossbar Macromonomers (telechelic polybutadiene)	119
3.3.5.1 Synthesis of Telechelic Polybutadiene - “End-capped” Approach.....	119
3.3.5.1.1 EC-XBAR62- $\alpha\omega$	119
3.3.5.1.2 EC-XBAR76- $\alpha\omega$	120
3.3.5.2 Synthesis of Telechelic Polybutadiene - Modified “End- capped” Approach.....	120
3.3.5.2.1 EC-XBAR32- $\alpha\omega$	120
3.3.5.3 Synthesis of Telechelic Polybutadiene - “Fire and Forget” Approach.....	121

3.3.5.3.1	FF-XBAR29- $\alpha\omega$	121
3.3.5.3.2	FF-XBAR52- $\alpha\omega$	122
3.3.5.3.3	FF-XBAR53- $\alpha\omega$	122
3.3.5.3.4	FF-XBAR100- $\alpha\omega$	122
3.3.5.4	Deprotection of Crossbar Macromonomers	122
3.3.6	Synthesis of Arm Macromonomers	123
3.3.6.1	Synthesis of Hydroxyl end-functionalised macromonomers .	123
3.3.6.1.1	ARM19-OH.....	123
3.3.6.1.2	ARM23-OH.....	123
3.3.6.1.3	ARM25-OH.....	123
3.3.6.1.4	ARM31-OH.....	123
3.3.6.1.5	ARM40-OH.....	123
3.3.6.2	Arm Bromination (conversion of hydroxyl groups)	124
3.4	Conclusions	125
3.5	References	126

Chapter 4 Synthesis and characterisation of H-Shaped Polybutadienes

4.1	Introduction.....	128
4.2	Results and Discussion	131
4.2.1	Synthesis of H-shaped polymers in DMF/THF.....	131
4.2.2	Synthesis of H-shaped polymers in DMAc/THF	135
4.2.2.1	RP-TGIC analysis of H-shaped polymers H-Pbd_7, H-Pbd_8 and H-Pbd_9	141
4.2.2.2	Synthesis of H-shaped polymers in DMAc/THF – Varying the Molar Ratio of Arms to Crossbar	146
4.2.2.3	Synthesis of H-shaped polymers in DMAc/THF – Varying the Molar Ratio of Cesium Carbonate	151
4.2.2.4	Synthesis of H-shaped polymers in DMAc/THF – Improved Conditions.....	156
4.2.3	Synthesis of H-shaped polymers – Large Scale Synthesis.....	159
4.2.3.1	Initial attempts.....	159
4.2.3.2	Purification of Large Scale H-shaped polymers	167
4.3	Experimental.....	173
4.3.1	Materials	173
4.3.2	Characterisation.....	173
4.3.2.1	Nuclear Magnetic Resonance (NMR).....	173
4.3.2.2	Size Exclusion Chromatography (SEC).....	173
4.3.2.3	Temperature Gradient Interaction Chromatography (TGIC).	173

4.3.3	Synthesis	174
4.3.3.1	Synthesis of H-Pbd_1.....	174
4.3.3.2	Synthesis of H-Pbd_2.....	174
4.3.3.3	Synthesis of H-Pbd_3.....	174
4.3.3.4	Synthesis of H-Pbd_4.....	175
4.3.3.5	Synthesis of H-Pbd_5.....	175
4.3.3.6	Synthesis of H-Pbd_6.....	175
4.3.3.7	Synthesis of H-Pbd_7.....	175
4.3.3.8	Synthesis of H-Pbd_8.....	175
4.3.3.9	Synthesis of H-Pbd_9.....	176
4.3.3.10	Synthesis of H-Pbd_10.....	176
4.3.3.11	Synthesis of H-Pbd_11.....	176
4.3.3.12	Synthesis of H-Pbd_12.....	176
4.3.3.13	Synthesis of H-Pbd_13.....	177
4.3.3.14	Synthesis of H-Pbd_14.....	177
4.3.3.15	Synthesis of H-Pbd_15.....	177
4.3.3.16	Synthesis of H-Pbd_16.....	177
4.3.3.17	Synthesis of H-Pbd_17.....	178
4.3.3.18	Synthesis of H-Pbd_18.....	178
4.3.3.19	Synthesis of H-Pbd_19.....	178
4.3.4	Fractionation of H-shaped polymers.....	178
4.4	Conclusions	179
4.5	References.....	181
 Chapter 5 Synthesis and characterisation of Randomly Branched Polybutadienes		
5.1	Introduction.....	183
5.1.1	The Strathclyde Route.....	183
5.1.2	Adapting the Strathclyde Route for Anionic Polymerisation.....	184
5.2	Results and Discussion	189
5.2.1	Synthesis of Randomly Branched Polybutadiene with Divinylbenzene	189
5.2.1.1	Synthesis of Randomly Branched Polybutadiene with Divinylbenzene using Potassium <i>tert</i> -butoxide.....	189
5.2.1.2	Synthesis of Randomly Branched Polybutadiene with Divinylbenzene using TMEDA	199
5.3	Experimental.....	206
5.3.1	Materials	206
5.3.2	Characterisation.....	206

5.3.2.1	Nuclear Magnetic Resonance (NMR).....	206
5.3.2.2	Size Exclusion Chromatography (SEC).....	206
5.3.3	Synthesis.....	206
5.3.3.1	Synthesis of Randomly Branched Polybutadiene with Potassium <i>tert</i> -Butoxide	207
5.3.3.1.1	R-Pbd_1	207
5.3.3.1.2	R-Pbd_2	208
5.3.3.1.3	R-Pbd_3	208
5.3.3.1.4	R-Pbd_4	208
5.3.3.1.5	R-Pbd_5	208
5.3.3.1.6	R-Pbd_6	209
5.3.3.2	Synthesis of Randomly Branched Polybutadiene with Potassium <i>tert</i> -Butoxide solution (1.0 M in THF)	209
5.3.3.2.1	R-Pbd_7	209
5.3.3.2.2	R-Pbd_8	209
5.3.3.2.3	R-Pbd_9	210
5.3.3.3	Synthesis of Randomly Branched Polybutadiene with TMEDA.....	210
5.3.3.3.1	R-Pbd_10	210
5.3.3.3.2	R-Pbd_11	210
5.3.3.3.3	R-Pbd_12	211
5.3.3.3.4	R-Pbd_13	211
5.3.3.3.5	R-Pbd_14	211
5.3.3.3.6	R-Pbd_15	211
5.4	Conclusions	212
5.5	References.....	215

Chapter 6 Concluding Remarks

6.1	Conclusions	217
6.2	Future Work.....	223
6.3	References.....	226

List of Figures

Figure 1.1 - An example of the tyre label required for all tyres sold in the EU ³	2
Figure 1.2 - Macromolecule architectures.....	5
Figure 1.3 - Polymer types by composition.....	6
Figure 1.4 - AIBN radical formation.....	9
Figure 1.5 - Free radical termination reaction mechanisms	10
Figure 1.6 - Common strategy for Reversible-Deactivation Radical Polymerisation techniques.....	11
Figure 1.7 - Types of RAFT agent	13
Figure 1.8 - Monomers capable of anionic polymerisation.....	21
Figure 1.9 - Resonance stabilisation of the negative charge in vinyl monomers	22
Figure 1.10 - Various end-group functionalisation paths for polydienes.....	24
Figure 1.11 - Branched polymers of different structures: (a) star, (b) H-shaped, (c) comb, (d) dendritically branched and (e) hyperbranched polymers.....	28
Figure 1.12 - Star polymer synthetic methodologies: “arm-first” and “core-first”	29
Figure 1.13 - Synthesis of a star polymer via the use of a multifunctional initiator	30
Figure 1.14 - Schematic description of dendritically branched polymers ¹⁰⁰ Reprinted with permission from [Gao, C.; Yan, D., <i>Prog. Polym. Sci.</i> 2004, 29 (3), 183-275]. Copyright [2004] Elsevier.....	37
Figure 1.15 - The divergent and convergent approaches to dendrimer synthesis.....	38
Figure 1.16 - Synthesis of an AB ₂ hyperbranched polymer by the single monomer method	38
Figure 2.1 - ¹ H-NMR spectrum of precursor arm polybutadiene Star(3)150_Arm	55
Figure 2.2 - Polydiene microstructures	55
Figure 2.3 - SEC chromatograms (RI detector) of polybutadiene Star(3)150. Comparison of the linear arm precursor (blue) and the final crude star mixture (red).	56
Figure 2.4 - SEC chromatograms (RI detector) of three-arm polybutadiene Star(3)150 from the initial crude material through four cycles of fractionation.....	57
Figure 2.5 - SEC chromatogram (RI detector) of crude polybutadiene Star(4)180	59
Figure 2.6 - SEC chromatograms (RI detector) of crude four arm polybutadiene Star(4)130. Comparison of the linear arm precursor (blue) and the final crude star mixture (red).	60
Figure 2.7 - SEC chromatograms (RI detector) of four-arm polybutadiene Star(4)130 before and after four cycles of fractionation.....	61

Figure 2.8 - Polymer molecular weight vs. retention volume in three different chromatographic separation regimes: Size Exclusion Chromatography (SEC), Liquid Chromatography at the Critical Condition (LCCC) and Interaction Chromatography (IC)	62
Figure 2.9 - SEC (A) and TGIC (B) chromatograms (UV detector) of branched PS prepared by linking polystyryl anion with CDMSS. Reprinted with permission from Chang, T., J. Polym. Sci., Part B: Polym. Phys. 2005, 43 (13), 1591-1607. Copyright 2005 Wiley.	64
Figure 2.10 - TGIC separation of PS samples with different end groups (hydrogen terminated vs. hydroxyl terminated) by (a) NP-TGIC and (b) RP-TGIC. Temperature programs are also drawn in each figure. Reprinted (adapted) with permission from Lee, W.; Cho, D.; Chun, B. O.; Chang, T.; Ree, M., J. Chromatogr. A 2001, 910 (1), 51-60. Copyright 2001 Elsevier.	65
Figure 2.11 - Schematic diagram of an IC apparatus	66
Figure 2.12 - SEC and RP-TGIC chromatograms of the crude polybutadiene three arm and four arm stars recorded with an RI detector (Δn) and RALS detector (R_{90}). SEC samples were analysed in THF at 40 °C at a flow rate of 1 ml/min. TGIC samples were analysed in 1,4-dioxane at a flow rate of 0.4 ml/min. Temperature profiles are shown on the plot.	68
Figure 2.13 - SEC and RP-TGIC chromatograms of the polybutadiene three arm and four arm stars (post fractionation) recorded with an RI detector (Δn) and RALS detector (R_{90}). SEC samples were analysed in THF at 40 °C at a flow rate of 1 ml/min. TGIC samples were analysed in 1,4-dioxane at a flow rate of 0.4 ml/min. Temperature profiles are shown on the plot.	70
Figure 2.14 - RP-TGIC chromatograms of the precursor arm, crude and pure polybutadiene three arm and four arm stars recorded with an RI detector (Δn). TGIC samples were analysed in 1,4-dioxane at a flow rate of 0.4 ml/min. Temperature profiles are shown on the plot.	71
Figure 2.15 - "Christmas tree" reactor used for living anionic polymerisation, (i) Flask A containing living polystyryllithium, (ii) Flask B, (iii) Sidearm Flask, (iv) Reaction Flask, (v) Septum.	72
Figure 3.1 - General schematic for the synthesis of H-Shaped polymers via the macromonomer approach	80
Figure 3.2 - ^1H -NMR spectrum of 1-bis(4- <i>tert</i> -butyldimethylsiloxyphenyl)benzophenone	83

Figure 3.3 - ^1H -NMR spectra comparison between 4,4'-dihydroxybenzophenone (top) and 1-bis(4- <i>tert</i> -butyldimethylsiloxyphenyl)benzophenone (bottom)	84
Figure 3.4 - ^1H -NMR spectrum of 1,1-Bis(4- <i>tert</i> -butyldimethylsiloxyphenyl)ethylene (DPE-OSi)	84
Figure 3.5 - Introduction of functionality to polymer chain ends	85
Figure 3.6 - General schematic for the synthesis of telechelic “crossbar” polymers via the use of the (a) “End-capped” approach and (b) “Fire and Forget” approach.....	87
Figure 3.7 - Structures of protected functionalised polymers at each stage of reaction.....	89
Figure 3.8 - ^1H -NMR spectra of “crossbar” telechelic polybutadiene EC-XBAR62- $\alpha\omega$ synthesised by the “end-capped” approach with TMEDA present from initiation. Expansion between 0.1 ppm and 1.10 ppm focusing on the protection groups introduced to the polymer chain ends.....	90
Figure 3.9 - Illustration depicting the effect of TMEDA on DPE-OSi incorporation.....	91
Figure 3.10 - ^1H -NMR spectra of “crossbar” telechelic polybutadiene EC-XBAR32 synthesised by the “end-capped” approach.....	94
Figure 3.11 - ^1H -NMR spectra of telechelic polybutadiene crossbar FF-XBAR52. Comparison of the polymer spectra before and after deprotection is reported.....	98
Figure 3.12 - ^1H -NMR spectra (700 MHz) of polybutadienes ARM31-H, ARM31-OH and ARM31-Br. Expansion between 3.0 ppm and 4.2 ppm focusing on the functional groups introduced to the polymer chain ends.	101
Figure 3.13 - Isothermal (50 °C) NP-IIC chromatograms (RALS detector) of ARM40-H, ARM40-OH and ARM40-Br at a solvent composition of 96/4 isooctane/THF.	103
Figure 3.14 - Isothermal ((a) 50 °C, (b) 60 °C (c) 50 °C, (d) 60 °C) NP-IIC chromatograms (RALS detector) of linear polybutadiene arm macromonomers at a solvent composition of 96/4 isooctane/THF.	105
Figure 3.15 - SEC chromatogram (RI detector) of crude polybutadiene FF-XBAR29 samples	107
Figure 3.16 - Isothermal (22 °C) NP-IIC chromatograms (UV detector) of samples FF-XBAR29-(OX) ₂ , FF-XBAR29-(OX) ₄ , FF-XBAR29-(OH) ₂ and FF-XBAR29-(OH) ₄ at a solvent composition of 88-12 isooctane-THF.	107
Figure 3.17 - Isothermal 50 °C (Red Line) and 60 °C (Blue line) NP-IIC chromatogram (UV detector) of FF-XBAR29-(OX) ₄ at a solvent composition of 88/12 isooctane/THF	110
Figure 3.18 - Isothermal (22 °C) NP-IIC chromatogram (UV detector) of FF-XBAR29-(OX) ₄ and FF-XBAR52-(OX) ₄ at a solvent composition of 87/13 isooctane/THF.....	112

Figure 3.19 - Isothermal (22 °C) NP-IIC chromatograms (UV detector) of samples FF-XBAR52-(OX) ₄ , FF-XBAR52-(OH) ₂ and FF-XBAR52-(OH) ₄ at a solvent composition of 84/16 isooctane/THF.	114
Figure 3.20 - “Christmas tree” reactor used for living anionic polymerisation, (i) Flask A containing living polystyryllithium, (ii) Flask B, (iii) Sidearm Flask, (iv) Reaction Flask, (v) Septum.	118
Figure 4.1 - General schematic for the synthesis of H-shaped polymers via the macromonomer approach.....	131
Figure 4.2 - SEC chromatograms ((a) RI and (b) RALS detector) of polymer H-Pbd_2. Comparison of the samples between the start (0 hr) and end of reaction.....	133
Figure 4.3 - Potential incomplete by-products of H-shaped polymer synthesis by the Williamson coupling reaction.....	134
Figure 4.4 - SEC chromatograms (RI detector) of polymers: (a) H-Pbd_4, (FF-XBAR29, ARM31-Br) (b) H-Pbd_5 (FF-XBAR52, ARM31-Br) and (c) H-Pbd_6 (FF-XBAR100, ARM31-Br). Comparison of the samples between the start (0 hr) and end of reaction. ...	136
Figure 4.5 - SEC chromatograms (RI detector) of polymers H-Pbd_2 (FF-XBAR52, ARM31-Br; solvent: DMF/THF) (blue line) and H-Pbd_5 (FF-XBAR52, ARM31-Br; solvent: DMAc/THF) (red line)	137
Figure 4.6 - SEC chromatograms (RI detector) of polymers H-Pbd_3 (FF-XBAR100, ARM31-Br; solvent: DMF/THF) (blue line) and H-Pbd_6 (FF-XBAR100, ARM31-Br; solvent: DMAc/THF) (red line)	138
Figure 4.7 - SEC chromatograms (RI detector) of polymers: (a) H-Pbd_7 (FF-XBAR29, ARM31-Br), (b) H-Pbd_8 (FF-XBAR52, ARM31-Br) and (c) H-Pbd_9 (FF-XBAR52, ARM31-Br), from the reactions using a new bottle of cesium carbonate. Comparison of the samples between the start (0 hr) and end of reaction.	139
Figure 4.8 - SEC chromatograms (RI detector) of polymers H-Pbd_2 (FF-XBAR52, ARM31-Br; solvent: DMF/THF) (blue line), H-Pbd_5 (FF-XBAR52, ARM31-Br; solvent: DMF/THF) (red line) and H-Pbd_8 (FF-XBAR52, ARM31-Br; solvent: DMF/THF; new bottle cesium carbonate) (green line).....	140
Figure 4.9 - SEC chromatograms (RI detector) of polymers H-Pbd_6 (FF-XBAR100, ARM31-Br; solvent: DMF/THF) (blue line) and H-Pbd_9 (FF-XBAR100, ARM31-Br; solvent: DMF/THF; new bottle cesium carbonate) (red line).....	140

Figure 4.10 - SEC (a) and RP-TGIC (b) chromatograms of polymer H-Pbd_7. TGIC samples were analysed in 1,4-dioxane at a flow rate of 0.4 ml/min. Temperature profiles are shown on the plot.	142
Figure 4.11 - SEC (a) and RP-TGIC (b) chromatograms of polymer H-Pbd_8. TGIC samples were analysed in 1,4-dioxane at a flow rate of 0.4 ml/min. Temperature profiles are shown on the plot.	143
Figure 4.12 - TGIC chromatograms (RALS detector) of polymers H-PBD_8 and linear polybutadiene standard PB170K. TGIC samples were analysed in 1,4-dioxane at a flow rate of 0.4 ml/min. Temperature profile is shown on the plot.	144
Figure 4.13 - SEC (a) and RP-TGIC (b) chromatograms of polymer H-Pbd_9. TGIC samples were analysed in 1,4-dioxane at a flow rate of 0.4 ml/min. Temperature profiles are shown on the plot.	144
Figure 4.14 - SEC chromatograms (RI and RALS detectors) of polymers: (a) H-Pbd_10 (FF-XBAR52, ARM23-Br (7 equivalents arm : crossbar)), and (b) H-Pbd_11 (FF-XBAR52, ARM31-Br (10 equivalents arm : crossbar)). Comparison of the samples between the start (0 hr) and end of reaction.	147
Figure 4.15 - SEC chromatograms (RI detector) of polymers H-Pbd_8 (5 equivalents arm : crossbar), H-Pbd_10 (7 equivalents arm : crossbar) and H-Pbd_11 (10 equivalents arm : crossbar).	147
Figure 4.16 - SEC (a) and RP-TGIC (b) chromatograms of polymer H-Pbd_10 (FF-XBAR52, ARM23-Br (7 equivalents arm : crossbar)). TGIC samples were analysed in 1,4-dioxane at a flow rate of 0.4 ml/min. Temperature profiles are shown on the plot.	148
Figure 4.17 - SEC (a) and RP-TGIC (b) chromatograms of polymer H-Pbd_11 (FF-XBAR52, ARM31-Br (10 equivalents)). TGIC samples were analysed in 1,4-dioxane at a flow rate of 0.4 ml/min. Temperature profiles are shown on the plot.	150
Figure 4.18 - SEC chromatograms (RI detector) of polymers: (a) H-Pbd_12 (FF-XBAR29, ARM23-Br), and (b) H-Pbd_13 (FF-XBAR52, ARM23-Br). Comparison of the samples between the start (0 hr) and end of reaction. Reaction conditions: 10 equivalents arm : crossbar; 50 equivalents cesium carbonate : crossbar.	152
Figure 4.19 - SEC chromatograms (RI detector) of polymers: (a) H-Pbd_7 and H-Pbd_12, and (b) H-Pbd_11 and H-Pbd_13.	152
Figure 4.20 - SEC (a) and RP-TGIC (b) chromatograms of polymer H-Pbd_12 (FF-XBAR29, ARM23-Br). TGIC samples were analysed in 1,4-dioxane at a flow rate of 0.4 ml/min. Temperature profiles are shown on the plot.	153

Figure 4.21 - SEC (a) and RP-TGIC (b) chromatograms of polymer H-Pbd_13. TGIC samples were analysed in 1,4-dioxane at a flow rate of 0.4 ml/min. Temperature profiles are shown on the plot.	155
Figure 4.22 - SEC chromatograms (RI and RALS detectors) of polymer H-Pbd_14 (FF-XBAR52 and ARM25-Br). Reaction conditions: 7 equivalents arm : crossbar; 50 equivalents cesium carbonate : crossbar. Comparison of the samples between the start (0 hr) and end of reaction.	157
Figure 4.23 - TGIC chromatograms of polymer H-Pbd_14 recorded with RI and RALS detectors. TGIC samples were analysed in 1,4-dioxane at a flow rate of 0.4 ml/min. Temperature profile is shown on the plot.	158
Figure 4.24 - SEC (a) and RP-TGIC (b) chromatograms of H-Pbd_15 (FF-XBAR52, ARM25-Br) recorded with RI and RALS detectors. Reaction conditions: 7 equivalents arm : crossbar; 50 equivalents cesium carbonate : crossbar. TGIC analysis was carried out in 1,4-dioxane at a flow rate of 0.4 ml/min. Temperature profile is shown on the plot.....	160
Figure 4.25 - SEC chromatograms (RI and RALS detectors) of polymers: (a) H-Pbd_16, (b) H-Pbd_17, (c) H-Pbd_18 and (d) H-Pbd_19 via a Williamson coupling reaction. Reaction conditions: 7 equivalents arm : crossbar; 50 equivalents cesium carbonate : crossbar.	162
Figure 4.26 - TGIC chromatograms of polymers: (a,b) H-Pbd_16, (c,d) H-Pbd_17, (e,f) H-Pbd_18 and (g,h) H-Pbd_19 recorded with RI and RALS detectors. Expansions of the chromatograms on the left are presented on the right, to better observe the presence of the peaks due to coupled products. TGIC samples were analysed in 1,4-dioxane at a flow rate of 0.4 ml/min. Temperature profiles are shown on the plot.	164
Figure 4.27 - SEC chromatograms (RI and RALS detectors) of H-Pbd_15 through three cycles of fractionation	168
Figure 4.28 - SEC chromatograms (RI and RALS detectors) of H-Pbd_16 through two cycles of fractionation	169
Figure 4.29 - SEC chromatograms (RI and RALS detectors) of H-Pbd_18 through two cycles of fractionation	170
Figure 4.30 - SEC chromatograms (RI and RALS detectors) of H-Pbd_19 through two cycles of fractionation	171
Figure 5.1 - Synthesis of branched vinyl polymer using a balance of divinyl monomer and radical transfer agent ³ Reprinted with permission from [O'Brien, N.; McKee, A.; Sherrington, D. C.; Slark, A. T.; Titterton, A., Polymer 2000, 41 (15), 6027-6031]. Copyright [2000] Elsevier	184

Figure 5.2 - Mechanism of chain transfer to solvent in the presence of potassium <i>tert</i> -butoxide in the anionic polymerisation of butadiene.	185
Figure 5.3 - Reaction of butadiene and divinylbenzene in the absence of chain transfer.	186
Figure 5.4 - SEC chromatograms (RI Detector) of random polybutadienes. Group (a) represents high vinyl content (HVC) polymers R-Pbd_1, R-Pbd_3 and R-Pbd_5. Group (b) represents low vinyl content (LVC) polymers R-Pbd_2, R-Pbd_4 and R-Pbd_6.	192
Figure 5.5 - Mark-Houwink plots for LVC polymers: R-Pbd_1, R-Pbd_3 and R-Pbd_5; and HVC polymers: R-Pbd_2, R-Pbd_4 and R-Pbd_6	196
Figure 5.6 - SEC chromatograms (RI Detector) of random polybutadienes using potassium <i>tert</i> -butoxide in THF (1.0 M)	198
Figure 5.7 - SEC chromatograms (RI detector) of randomly branched polybutadienes prepared using TMEDA as chain transfer agent	202
Figure 5.8 - Proposed route of branching of randomly branched polybutadienes prepared using TMEDA as chain transfer agent	202
Figure 5.9 - SEC chromatogram (RI detector) of randomly branched polybutadiene R-Pbd_15 using TMEDA as chain transfer agent.	204
Figure 5.10 - “Christmas tree” reactor used for living anionic polymerisation, (i) Flask A containing living polystyryllithium, (ii) Flask B, (iii) Sidearm Flask, (iv) Reaction Flask, (v) Septum.	207

List of Schemes

Scheme 1.1 - Mechanism of ATRP	12
Scheme 1.2 - Mechanism of RAFT polymerisation	14
Scheme 1.3 - Anionic polymerisation of styrene by sodium naphthalide	20
Scheme 1.4 - Termination reaction of polymeric alkyllithium with a) oxygen and b) carbon dioxide	25
Scheme 1.5 - Synthesis of linear polybutadiene by anionic polymerisation	27
Scheme 1.6 - Original synthetic strategy for H-shaped polystyrene	32
Scheme 1.7 - Synthesis of H-shaped polyisoprene	32
Scheme 1.8 - Synthetic route to H-shaped polybutadiene using DCMSDPE	33
Scheme 1.9 - Schematic diagram of a comb polymer synthesis by the “grafting from” method	34
Scheme 1.10 - Schematic diagram of a comb polymer synthesis by the “grafting onto” method	35
Scheme 1.11 - Schematic diagram of a comb polymer synthesis by the “grafting through” method	35
Scheme 1.12 - Synthesis of an exact comb poly(isoprene)-g-polystyrene	36
Scheme 1.13 - Synthesis of polystyrene AB ₂ macromonomer	41
Scheme 1.14 - Synthesis of G2 polystyrene DendriMac. Reproduced from Ref 125 with permission of The Royal Society of Chemistry)	42
Scheme 1.15 - Synthesis of polystyrene HyperMacs. Reproduced from Ref 125 with permission of The Royal Society of Chemistry)	42
Scheme 1.16 - General schematic for the synthesis of asymmetric three-arm stars via macromonomer approach. ¹³⁷ Reprinted with permission from [Agostini, S.; Hutchings, L. R., Eur. Polym. J. 2013, 49 (9), 2769-2784]. Copyright [2013] Elsevier	43
Scheme 2.1 - Synthesis of three-arm star polybutadiene	54
Scheme 2.2 - Synthesis of four-arm polybutadiene Star(4)180	58
Scheme 3.1 - Synthesis of 1,1-bis(4- <i>tert</i> -butyldimethylsiloxyphenyl)ethylene (DPE-OSi)	82
Scheme 3.2 - Initial synthetic route of “crossbar” telechelic polybutadiene by the “end- capped” approach.	88
Scheme 3.3 - Modified synthesis of “crossbar” telechelic polybutadiene by the modified “end-capped” approach	93
Scheme 3.4 - Synthesis of bromine end functionalised linear polybutadiene arms	100

Scheme 4.1 - Williamson coupling reaction for the synthesis of H-shaped polybutadiene	132
Scheme 5.1 - Synthesis of randomly branched polybutadiene in toluene.....	190

List of Tables

Table 2.1 - Molecular weight, dispersity and microstructure values for three-arm star polybutadiene Star(3)150 obtained by SEC	58
Table 2.2 - Molecular weight and dispersity values for incomplete four-arm star polybutadiene Star(4)180 obtained by SEC	59
Table 2.3 - Molecular weight, dispersity and microstructure values for four-arm star polybutadiene Star(4)130 obtained by SEC	60
Table 2.4 - Molecular weight (M_n) values for crude star polybutadienes obtained by TGIC analysis	69
Table 3.1 - Molecular weight data, dispersity and end-capping amount for “crossbar” telechelic polybutadiene synthesised by the “end-capped” path	90
Table 3.2 - Molecular weight data, dispersity and end-capping for “crossbar” telechelic polybutadiene synthesised by the modified “end-capped” approach.....	94
Table 3.3 - Molecular weight data, dispersity and extent of end-capping for “crossbar” telechelic polybutadiene synthesised by the “fire and forget” approach	96
Table 3.4 - Molar mass data of arm polymers (solvent THF; $dn/dc = 0.124 \text{ ml g}^{-1}$)	100
Table 4.1 - Molar mass data of macromonomer polymers (solvent THF; $dn/dc = 0.124 \text{ ml g}^{-1}$)	131
Table 4.2 - Molar mass data for H-Pbd_2 (solvent THF; $dn/dc = 0.124 \text{ ml g}^{-1}$).....	133
Table 4.3 - Molar mass data for H-Pbd_2 and H-Pbd_5 (solvent THF; $dn/dc = 0.124 \text{ ml g}^{-1}$)	137
Table 4.4 - Molar mass data for H-Pbd_6 and H-Pbd_9 (solvent THF; $dn/dc = 0.124 \text{ ml g}^{-1}$)	141
Table 4.5 - Molar mass data for H-Pbd_10 and H-Pbd_11 (solvent THF; $dn/dc = 0.124 \text{ ml g}^{-1}$)	147
Table 4.6 - Theoretical molar masses for the expected polymeric species in H-Pbd_10 (7 equivalents arm : crossbar)) and H-Pbd_11 (10 equivalents arm : crossbar)).....	149
Table 4.7 - Molar mass data for H-Pbd_10 obtained by triple detection RP-TGIC analysis (solvent 1,4-dioxane; $dn/dc = 0.095 \text{ ml g}^{-1}$)	149
Table 4.8 - Theoretical molar masses for the expected polymeric species in H-Pbd_12. Reaction conditions: 10 equivalents arm : crossbar; 50 equivalents cesium carbonate : crossbar.....	154

Table 4.9 - Molar mass data for H-Pbd_12 obtained by triple detection RP-TGIC analysis (solvent 1,4-dioxane; $dn/dc = 0.095 \text{ ml g}^{-1}$)	154
Table 4.10 - Theoretical molar masses for the expected polymeric species in H-Pbd_13. Reaction conditions: 10 equivalents arm : crossbar; 50 equivalents cesium carbonate : crossbar.	155
Table 4.11 - Molar mass data for H-Pbd_13 obtained by triple detection RP-TGIC analysis (solvent 1,4-dioxane; $dn/dc = 0.095 \text{ ml g}^{-1}$)	155
Table 4.12 - Molar mass data for H-Pbd_14 obtained by triple detection RP-TGIC analysis (solvent 1,4-dioxane; $dn/dc = 0.095 \text{ ml g}^{-1}$)	158
Table 4.13 - Molar mass data for H-Pbd_15 obtained by triple detection RP-TGIC analysis (solvent 1,4-dioxane; $dn/dc = 0.095 \text{ ml g}^{-1}$)	160
Table 4.14 - Molar mass data for the large scale synthesis of polymers H-Pbd_16, H-Pbd_17, H-Pbd_18 and H-Pbd_19 via a Williamson coupling reaction.....	162
Table 4.15 - Molar mass data for H-Pbd_16 (EC-XBAR32, ARM19-Br) obtained by triple detection RP-TGIC analysis (solvent 1,4-dioxane; $dn/dc = 0.095 \text{ ml g}^{-1}$).....	166
Table 4.16 - Molar mass data for H-Pbd_17 (EC-XBAR32, ARM40-Br) obtained by triple detection RP-TGIC analysis (solvent 1,4-dioxane; $dn/dc = 0.095 \text{ ml g}^{-1}$).....	166
Table 4.17 - Molar mass data for H-Pbd_18 (EC-XBAR53, ARM19-Br) obtained by triple detection RP-TGIC analysis (solvent 1,4-dioxane; $dn/dc = 0.095 \text{ ml g}^{-1}$).....	166
Table 4.18 - Molar mass data for H-Pbd_19 (EC-XBAR53, ARM40-Br) obtained by triple detection RP-TGIC analysis (solvent 1,4-dioxane; $dn/dc = 0.095 \text{ ml g}^{-1}$).....	167
Table 4.19 - Molar mass data for the initial crude polymer and the final series of fractionations for large scale polymers H-Pbd_15, H-Pbd_16 H-Pbd_18 and H-Pbd_19 (solvent THF; $dn/dc = 0.124 \text{ ml g}^{-1}$).....	172
Table 5.1 - Reaction conditions, molar mass data and microstructure values for randomly branched polybutadienes using solid potassium <i>tert</i> -butoxide	190
Table 5.2 - Reaction conditions, molar mass data and microstructure values for randomly branched polybutadienes using potassium <i>tert</i> -butoxide in THF (1.0 M)	197
Table 5.3 - Reaction conditions, molar mass data and microstructure values for randomly branched polybutadienes prepared using TMEDA as chain transfer agent	200
Table 5.4 - Reaction conditions, molar mass data and microstructure values for randomly branched polybutadienes R_PBd_14 and R_PBd_15 prepared using TMEDA as chain transfer agent	204

List of Abbreviations

ATRP	Atom Transfer Radical Polymerisation
BHT	3,5-di- <i>tert</i> -butyl-4-hydroxytoluene
CT	Chain Transfer
CDMSS	4-(chlorodimethylsilyl)styrene
D	Dispersity
DB	Degree of Branching
DCC	<i>N,N'</i> -Dicyclohexylcarbodiimide
DCM	Dichloromethane
DCMSDPE	4-(dichloromethylsilyl)diphenylethylene
DFI	1,2-bis-(4-(1-phenylethenyl)phenyl)ethane
DMAc	Dimethylacetamide
DMAP	4-Dimethylaminopyridine
DMF	Dimethylformamide
DMM	Double Monomer Method
DMSO	Dimethylsulfoxide
dn/dc	Refractive index increment
DNA	Deoxyribonucleic Acid
DPE	1,1-Diphenylethylene
DPE-OSi	1,1-Bis(4- <i>tert</i> -butyldimethylsiloxyphenyl)ethylene
DP _n	Number Average Degree of Polymerisation
DP _w	Weight Average Degree of Polymerisation
DTHFP	2,2'-Ditetrahydrofurylpropane
DVB	Divinylbenzene
HCT	High Chain Transfer
HPLC	High Performance Liquid Chromatography
IC	Interaction Chromatography
IUPAC	International Union of Pure and Applied Chemistry
KO ^t Bu	Potassium <i>tert</i> -butoxide
LC	Liquid Chromatography
LCCC	Liquid Chromatography at Critical Condition
LCT	Low Chain Transfer
MH	Mark-Houwink Plot
M _n	Number Average Molecular Weight
M _w	Weight Average Molecular Weight

MW	Molecular Weight
NMR	Nuclear Magnetic Resonance
NP	Normal-Phase
PB	Polybutadiene
PCL	poly(ϵ -caprolactone)
PE	Polyethylene
PEEK	Poly(ether ether ketone)
PMMA	Poly(methyl methacrylate)
PP	Polypropylene
PVC	Poly(vinyl chloride)
PI	Polyisoprene
PS	Polystyrene
PTFE	Polytetrafluoroethylene
RAFT	Reversible Addition-Fragmentation Transfer
RALS	Right Angle Light Scattering
RDRP	Reversible-Deactivation Radical Polymerisation
RI	Refractive Index
ROMBP	Ring-Opening Multibranching Polymerisation
RP	Reversed-Phase
SBR	Styrene/Butadiene Rubber
sSBR	Solution Styrene/Butadiene Rubber
SCT	Semi-Crystalline Thermoplastics
SCROP	Self-Condensing Ring-Opening Polymerisation
SCVP	Self-Condensing Vinyl Polymerisation
SEC	Size Exclusion Chromatography
<i>sec</i> -BuLi	<i>sec</i> -Buthyllithium
SGIC	Solvent Gradient Interaction Chromatography
SMM	Single Monomer Methodology
T_g	Glass Transition Temperature
TGIC	Temperature Gradient Interaction Chromatography
THF	Tetrahydrofuran
T_m	Melting Temperature
TMEDA	<i>N,N,N',N'</i> -tetramethylethylenediamine
TPE	Thermoplastic Elastomer

Statement of Copyright

The copyright of this thesis rests with the author. No quotation from it should be published without the author's prior written consent and information derived from it should be acknowledged.

Acknowledgements

I would like to express my deepest gratitude to my academic supervisor Professor Lian Hutchings for his continued support, guidance, and encouragement shown to me throughout these years. The opportunities granted as well as the mentorship provided by him throughout the project have been invaluable. The project has been wonderful to work on, and much of that was due to having such a great supervisor.

I would especially like to thank Dr Serena Agostini for all of her incredible help and friendship during my first years at Durham. Her knowledge, positivity and patience both in and out the lab was infinitely treasured and a vital part of the shaping of this work.

I would like to thank Michelin for providing the funding of this research and making all of this possible. I would also like to thank Florent Vaultier, Michel Valtier, and Magali Heurtefeu, as well as all of the people that contributed during our meetings between here and France for their scientific input.

I would very much like to thank all the members of our research group past and present, in particular Roberto, Brunella, Tatiana, Gabriele, Paul, Anne-Charlotte, Jenny, Jon, Natasha, Antonella, Utku, Mareike, and Dan that made the years in Durham so enjoyable.

I would like to extend a thanks to Professor Harald Pasch and his research group for making my time in Stellenbosch University very welcoming, and to Douglas Murima for always being available to help.

I would like to acknowledge to Dr Richard Thompson and Carl Reynolds and am glad that the materials synthesised in the project were of such use to them. I would also like to thank the Durham University Analytical Services and glassblowers Mr Malcolm Richardson and Mr Aaron Brown who were always willing to mend all those Christmas trees.

Finally, a special thanks goes my family, both immediate and extended; to my parents that supported and encouraged me endlessly during this period and to my brothers for the fun, stress relief, and joy. Without the faith we share, none of this would have been possible.

Chapter 1

Introduction

1.1 Background

The tyre industry is one of the most economically important industries on the planet. In 2014 in Europe alone it was responsible for the generation of €46 billion in turnover, and the production of 4.67 million tonnes of tyres, compromising roughly 21% of world tyre production.¹ The global demand for mobility has increased over the past few decades, especially in the emerging economies of China and India, as the number of vehicles in these countries has increased substantially.² Concurrently, the general requirements of tyres have been getting more sophisticated and complex each year. Tyres have to be able to bear heavier loads, be more fuel efficient, have longer lifetimes, as well as meet more stringent safety requirements. In 2012 the European Parliament introduced regulations that specified that all tyres to be sold in the European Union will be graded on specific guidelines, ranking a tyre's rolling resistance, rolling noise, wet grip and fuel efficiency, and labelled according to their performance (Figure 1.1).³

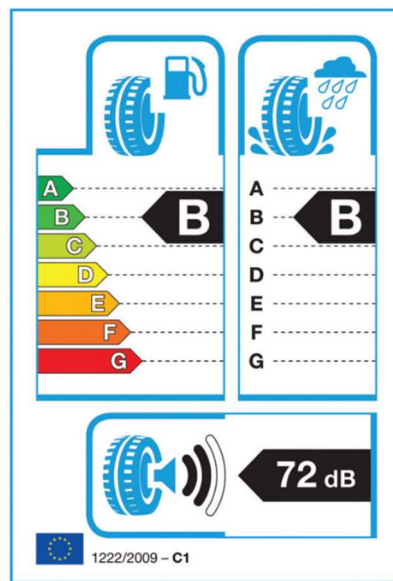


Figure 1.1 - An example of the tyre label required for all tyres sold in the EU³

A tyre is a complex assembly of many elements, but a key ingredient of tyres is polymers, more specifically rubber(s), both natural and synthetic. The tyre industry is one of the major consumers of rubber on the planet, with the production of automobile tyres being roughly 1.4 billion units per annum.⁴ Historically, the rubber that went into the makeup of a typical tyre was natural rubber, although today in general most tyres are made from synthetic rubbers such as polybutadiene (PB) or styrene/butadiene rubber (SBR) copolymers. Rheology is used to determine and tune the properties of the industrial rubbers. Several polymer properties such as molecular weight, microstructure, and

polymer architecture can have significant impacts on the rheology and the processability of industrial polymers, which in turn affect the overall properties of the resultant tyre. For instance, tyre rubber needs to produce high friction when brakes are applied, in order to have short braking distances and better wet grip, requiring softer, more viscous polymers; conversely, tyre rubber also needs to produce minimal friction during normal driving conditions to lower rolling resistance requiring harder, more elastic polymers.⁵ Melt viscosity and cold flow in particular are very important properties as they can determine a polymer's processability – a material that may behave as a liquid when poured could act as a solid when pushed through pipes.⁶ As such, branched polymers are of significant industrial importance due to their advantageous rheological properties in comparison to their linear analogues, including low solution and melt viscosities, improved cold flow, and solubility, all of which improve the processability of a polymer.⁷⁻⁸ Industrially, branched polymers have also been shown to demonstrate desired characteristics such as high wet grip and excellent processabilities such as milling processability and extrusion processability required for tyre manufacture.⁹

The tyre industry is currently facing numerous challenges to meet the future demands of consumers and regulators with regards to both the volume of tyres to be manufactured, as well as the higher performance criteria that new tyres must attain. A key factor in being able to meet these future targets is being able to develop polymers that are capable of achieving the standards set. One of the major ways in assisting in how to develop future generations of polymers is to have a fundamental understanding of the synthetic and rheological properties of well-defined, complex model branched polymers with fully characterised architectures. In this way, a better understanding of the rheology and characteristics of branched and crosslinked polymers obtained from industrial processing can be formulated, aiding in the development of tyre rubbers capable of enhanced performance and hence tyres capable of meeting more demanding properties.

What follows in the remainder of this chapter is an introduction to the various synthetic methods, techniques and procedures used in the synthesis of polymer architectures. Emphasis is given to the practice and principles of anionic polymerisation, as this is the dominant synthetic method used in this thesis and widely used in the production of synthetic rubber for the tyre industry. There is also comprehensive discussion on the types of polymer architectures of relevance to this thesis, with the specific aims of the project detailed at the end of the chapter.

1.2 Classification of Polymers

The word polymer refers to a large and diverse group of both natural and synthetic materials. A polymer is any macromolecule built up by the covalent linking of smaller unit molecules, referred to as monomers. The chemical reactions of these monomer units to create polymers are known as polymerisations. Polymers may be formed with many different combinations of monomer units, affording materials with a wide range of architectures and desirable properties. Polymers are used in daily life in numerous applications including but not limited to clothing, food packaging, in paint, as additives and of course in tyres. There is no single method for the classification of all polymer types. Polymers can be simple or complex materials; occur in nature or be produced synthetically; possess a wide variety of architectures and display a wide array of properties. Due to the myriad polymers that have been identified and the guaranteed development of new polymers, a number of methods have been developed for their classification, usually depending on a set aspect of a particular polymer. These classifications have become necessary for the efficient description of polymers.

1.2.1 Classification by Source

Polymers are obtained from a wide variety of sources and can be classified accordingly. Polymers produced by nature such as cellulose, lignin or natural rubber can be grouped together along with polymers from biological sources including proteins, lipids, starches and DNA.¹⁰⁻¹¹ Synthetic polymers, that is, polymers created from man-made chemical processes, can then be used to classify the spectrum of other polymeric materials including those derived from inorganic sources such as silicones to polymers derived from organic sources such as synthetic rubber analogues, polyisoprene and polybutadiene, or aromatic polymers such as polystyrene. The work in this thesis is concerned with polymers that fall into the synthetic organic class of polymers.

1.2.2 Classification by Architecture

Polymers can exist in a range of architectural configurations, which strongly affect a polymer's properties including rheology, crystallinity and mechanical properties. In general, these can be grouped into three main classes: linear, branched and crosslinked (network) structures, schematically represented in Figure 1.2.

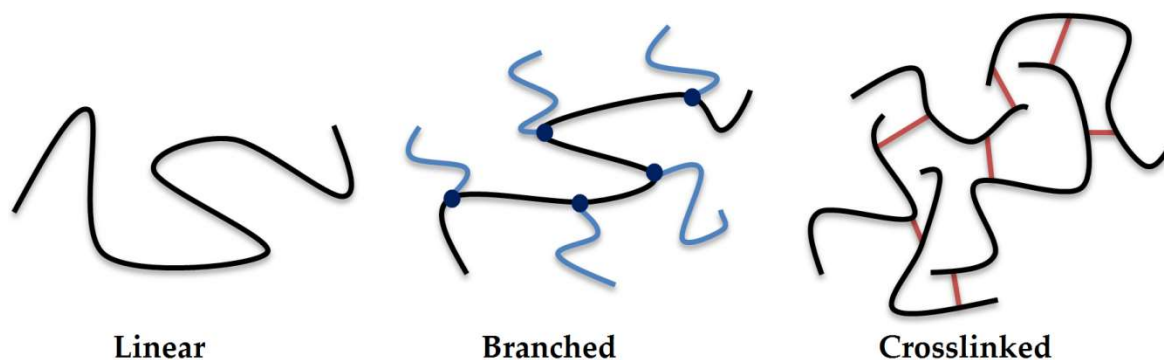


Figure 1.2 - Macromolecule architectures

These classifications, particularly the branched class, are of importance in the current work and many of the different types of these polymers will be discussed further.

1.2.3 Classification by Composition

Polymers can also be classified according to the number, type and distribution of monomer units present in the polymer. A homopolymer consists of one type of monomer, whereas a copolymer consists of two or more monomer types. Copolymers can be further classified depending on the exact sequential arrangement of the monomer units in the copolymer. For example, a copolymer may have a strictly alternating sequence; a random or statistical sequence arrangement; a block copolymer containing long sequences of one monomer, followed by a block of a different monomer or gradient copolymers in which the comonomer sequence undergoes a gradual transition along the chain from one monomer to another. These particular copolymer compositions are illustrated in Figure 1.3, although due to the almost infinite combinations of different monomers in an untold number of sequences, there are still many other possible structures, for example terpolymers which contain three different monomer types and discussion continues today on what to name a new class of sequence-defined polymers, currently known as “aperiodic copolymers”.¹²

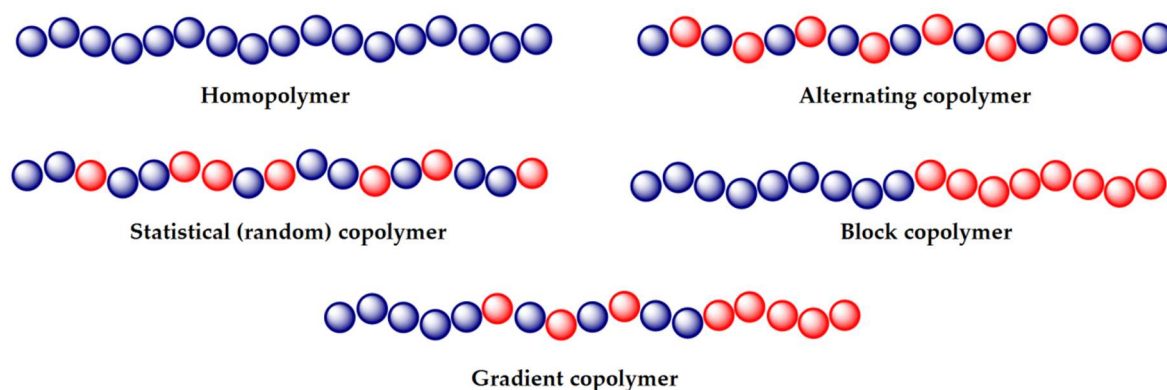


Figure 1.3 - Polymer types by composition

1.2.4 Classification by Properties

A very common method for classifying industrial polymers is according to their properties. In this way polymers can be sorted into three main classes - thermosets, thermoplastics and elastomers.

Thermoset polymers are produced by the direct formation of polymer networks from either monomers or the crosslinking of linear prepolymers. Once formed, these polymers cannot be manipulated any further, and are hence set due to the high degree of crosslinking present. One of the first examples of a commercially successful thermosetting polymer was Bakelite, developed in 1909 by Dr Leo Baekeland, which marked the beginning of the commercial plastics industry.¹³

Thermoplastics consist of linear or branched polymers that can be processed as viscous liquids, when temperatures above their glass transition temperature (T_g) or melting point (T_m) are applied, and re-solidify when cooled. This allows them to be processed into different shapes, sizes and to be recycled. Thermoplastics can be sub-divided further into two sub-classes; namely amorphous thermoplastics, in which all the polymer chains are disordered and entangled, resulting in materials which only have a T_g , and semi-crystalline thermoplastics (SCT) which have both disordered domains and highly ordered crystalline domains, giving SCT polymers both a T_g and T_m . When heated above their T_g , amorphous polymers can be processed as liquids, SCT polymers require heating above both their T_g and T_m to be processed, as they remain solid at their glass transition temperatures due to their crystalline domains. Thermoplastics are the most abundant materials in the commercial plastics market, mainly due to their adaptability and reprocessability. Thermoplastics, unlike thermosets do not crosslink during manufacture.

Examples of amorphous thermoplastics include polystyrene (PS), poly(methyl methacrylate) (PMMA), and poly(vinyl chloride) (PVC) whereas semi-crystalline thermoplastics include polyethylene (PE), polypropylene (PP) and poly(ether ether ketone) (PEEK).

The third class, elastomers, are polymers that most resemble vulcanised natural rubber but are produced from synthetic methods. Their main property is their ability to be stretched to high extension and revert back to their initial form once said stress is removed. These rubbery polymers are comprised of lightly crosslinked polymer networks. Unlike thermosets, the degree of crosslinking is not as high, allowing for their elasticity. These are the polymers that comprise the bulk of importance to the tyre industry, and many are produced from elastomeric pre-cursors including styrene-butadiene rubber (SBR) copolymers, polybutadiene (PB), and polyisoprene (PI). However, once rubbery polymers are crosslinked to give elastomers by curing or vulcanization, they lose their processability. In some cases, polymers can be formed from the mixing of two different classes; these hybrid materials contain properties from both their constituent classes, such as in the case of thermoplastic elastomers.

1.3 Polymer Synthesis

Polymers are synthesised by a wealth of polymerisation reactions.¹¹ These reactions can be classified into two broad types: step-growth polymerisation and chain-growth polymerisation.

1.3.1 Step-Growth Polymerisation

Step-growth polymerisation involves the step-wise reaction between mutually reactive functional groups on two or more monomers. Initially, two monomers react to form a dimer, a monomer may add to dimer forming a trimer, two dimers reacting to give a tetramer and so forth, until the formation of long polymer chains. In general, this addition can be summarised as follows:



As all monomers present contain reactive functionalities, there is no need for an initiator to begin the polymerisation, although these reactions are often catalysed as they can be slow. In the simplest case, where each monomer is a bifunctional unit, reaction affords linear polymers, whereas if the monomers contain multiple functionalities this can lead to the formation of branched and hyperbranched polymers. It was commonly assumed that all step-growth polymerisations occur by polycondensation where a small molecule such as water would be lost during reaction, as is the case for polyesters obtained from diols.¹⁴⁻¹⁵ This resulted in the term “condensation polymerisation” becoming a generic reference for all step-growth polymerisation. However, step-growth can also occur by polyaddition reactions in which no elimination takes place, for example, the reaction of diols and diisocyanates to form polyurethanes.¹⁶⁻¹⁸ A wide range of polymers are commercially synthesised using step-growth polymerisation reactions including polyesters, polycarbonates, polyurethanes, polysiloxanes, and polyamides such as nylons.

1.3.2 Chain-Growth Polymerisation

Chain-growth polymerisations are mechanisms in which the monomer is only consumed one unit at a time, by an active centre located on the chain-end of the reactive species, rapidly decreasing the time taken for the formation of polymer in comparison to step-growth polymerisation. These reactions can continue and involve tens of thousands of

monomer units until the reaction eventually ceases by either the complete consumption of monomer or by the deactivation of the active centre via a number of possible termination reactions. Chain-growth polymerisation has been the subject of much academic and commercial interest due to its desirable reaction times and defined products; leading to the development of many different polymerisation routes including Ziegler-Natta polymerisation, metallocene catalysed polymerisation, free radical polymerisation, ring-opening metathesis polymerisation, and ionic polymerisation.

1.3.2.1 Free Radical Polymerisation

Free radical polymerisation,¹⁹ first reported by Flory in 1937 involves the initiation and propagation of polymer chains by the use of radical species.²⁰ It is accessible to a very diverse range of vinyl monomers and tolerant of many functional groups and solvents, including water, as long as oxygen is not present. As a result, conventional free radical polymerisation accounts for the synthesis of around 50% of all commercial polymer.²¹ While it is possible to control (reproducibly) the molar mass and distribution of a polymer sample using free radical polymerisation, the resultant polymer is always heterogeneous in terms of molar mass, and composition in the case of copolymers. This makes it unsuitable for the creation of well-defined polymers of any sort. Free radical polymerisation comprises of three key stages; initiation, propagation and termination. The initiation step begins the reaction and involves (i) the formation of the radical initiator which will ultimately (ii) react with the monomer in question.



Radicals can be formed by several processes, but most are generated in decomposition reactions such as thermolysis, where heat is used to form the radical, for example in peroxides where the (-O-O-) bond is split forming two (-O•) radical species, or by photolysis where radiation is used to form the radical; a very common radical initiator which undergoes photolysis and thermolysis is azobisisobutyronitrile (AIBN) (Figure 1.4).

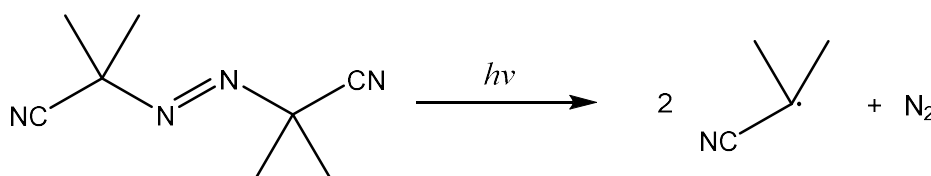


Figure 1.4 - AIBN radical formation

Radicals are very reactive and (usually) unstable species, so once formed will undergo reaction with any monomer present in the system forming a new, propagating radical species which leads onto the next stage of polymerisation, propagation.



Propagation between this radical species and monomer continues until either all monomer is consumed or as is often the case in free radical polymerisation, the active centre on the propagating chain end is terminated.



Termination involves the deactivation of the active radical chains, ending chain growth. It occurs mainly via two mechanisms: disproportionation, where a proton is abstracted from another chain, resulting in two deactivated chains (Figure 1.5a) or recombination where two radical chains couple together resulting in one deactivated chain (Figure 1.5b).

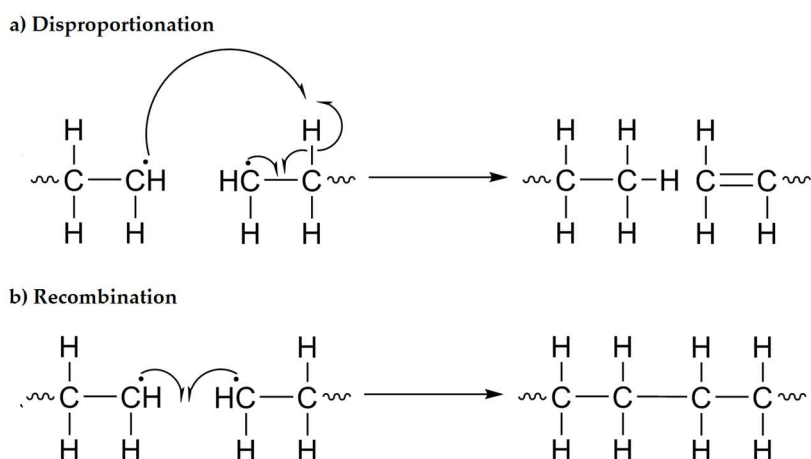


Figure 1.5 - Free radical termination reaction mechanisms

Other factors may inhibit chain growth such as reactions with impurities or the transfer of an active centre to another molecule, be it solvent, initiator or monomer in a process known as chain transfer. The lack of control over potential termination reactions, as well as the undisciplined nature of free radical polymerisation in general, makes it very unsuitable for the creation of well-defined polymers. This has led to the development of many controlled radical polymerisation techniques which aim to have better control over the polymers while still accessing a diverse range of monomers.

1.3.3 Controlled Polymerisation Methods

In both academia and industry, polymerisation mechanisms in which it is possible to control a polymer's size, shape, molecular weight and molecular weight distribution (MWD) are of significant interest. As a result, in the late 1980s this led to a search for radical-based routes affording much greater control over these parameters such as seen in living polymerisation, combined with the versatility of free radical polymerisation, which resulted in the family of controlled radical polymerisation mechanisms.

1.3.3.1 Reversible-Deactivation Radical Polymerisation

Reversible-Deactivation Radical Polymerisation (RDRP) techniques are some of the most academically popular routes for the creation of well-defined polymers. Most RDRP methods operate under the same principle – by dramatically lowering the concentration of a growing radical species by establishing a fast equilibrium between the growth-active radical species and a dormant species, where the equilibrium very strongly favours the dormant species (Figure 1.6).²² This in turn minimises (but does not eliminate) termination, as well as allowing frequent interconversion between the active and dormant species.

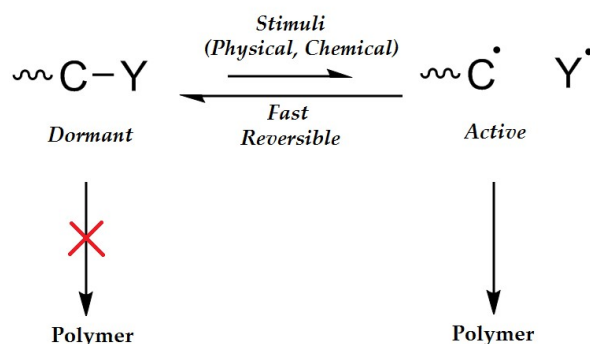
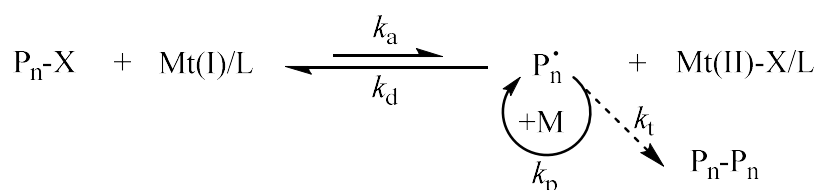


Figure 1.6 - Common strategy for Reversible-Deactivation Radical Polymerisation techniques

Many controlled radical techniques utilise these (IUPAC termed) “reversible-deactivation radical polymerisation” (RDRP)²³ mechanisms and two RDRP techniques in particular have had much success in the last quarter century with regards to their development for the synthesis of well-defined polymers, these being: Atom Transfer Radical Polymerisation (ATRP) and Reversible Addition Fragmentation chain Transfer (RAFT).

1.3.3.2 Atom Transfer Radical Polymerisation (ATRP)

Atom Transfer Radical Polymerisation (ATRP) is a popular RDRP technique that was first reported independently by both Sawamoto²⁴ and Matyjaszewski²⁵ in 1995. ATRP, in essence, is a reversible-deactivation process based on transferring an atom to generate a new C-C bond. In a typical ATRP reaction, a halogen atom (X) is transferred from an alkyl halide to a metal centre (Mt), both oxidising the metal catalyst and producing the active organic radical species. This radical species can then be deactivated by the reverse transfer of the halogen atom and the reduction of the metal (Scheme 1.1). The metal is often coordinated to multidentate ligands (L). This deactivation reaction is kinetically favourable ensuring the low concentration of radical species present in the system, allowing for controlled reaction with monomer (M), producing polymers with low dispersity values. Termination although minimised, will still occur in an ATRP system, thus limiting its ability to have absolute control over molecular weight as well as produce very high molecular weight polymers.



Scheme 1.1 - Mechanism of ATRP

ATRP is accessible to a wide variety of monomers including styrenes, acrylates, methacrylates, acrylonitriles and acrylamides, however, all potential monomers must be able to tolerate its reaction conditions. The use of transition metal catalysts, in particular copper (the most popular metal used for ATRP), and their removal after polymerisation may also cause problems with industrial applications.

1.3.3.3 Reversible Addition Fragmentation chain Transfer (RAFT)

Another popular RDRP technique is Reversible Addition Fragmentation chain Transfer (RAFT) polymerisation. This technique, developed by Moad, Rizzardo, Thang and co-workers in 1998 was very quickly adopted due its applicability to a very wide range of monomers and relatively facile reaction conditions.²⁶ The key for every RAFT polymerisation is the use of a suitable chain transfer agent, known as a RAFT agent. RAFT agents are used to trap the propagating chains into a dormant state. The choice of

RAFT agent (Figure 1.7) is an important factor, with the type of substituent group at Z and R affecting polymerisation efficiency. Many RAFT agents use Z groups that also increase the radical stability; some examples of this are given below.

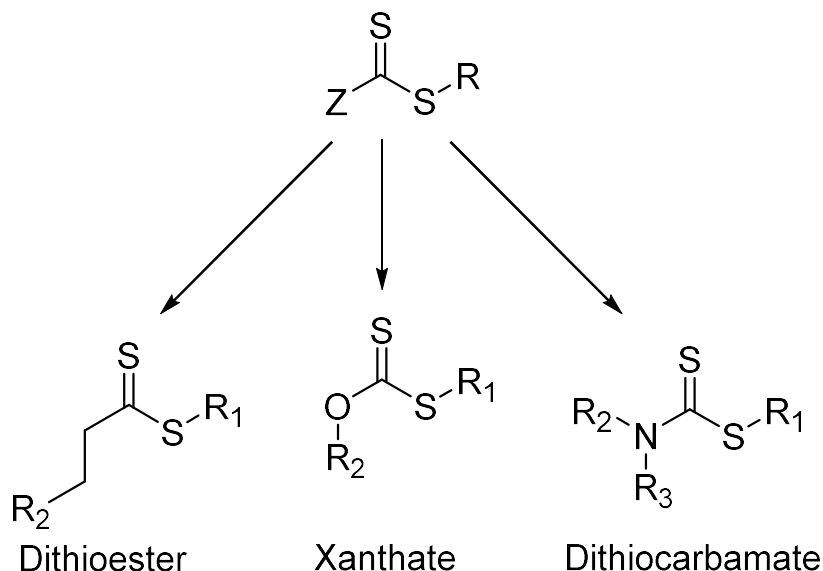
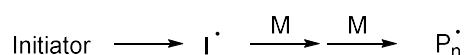
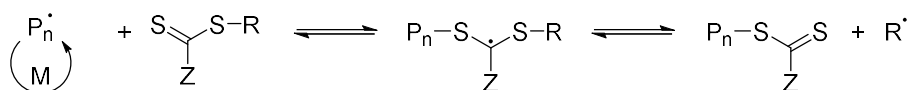
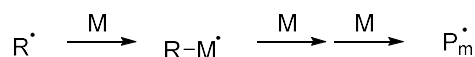
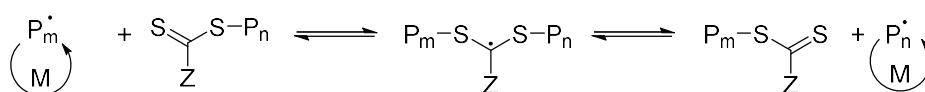
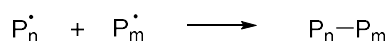


Figure 1.7 - Types of RAFT agent

A generic RAFT polymerisation mechanism is presented overleaf in Scheme 1.2. The first stage (a) is the initiation of the monomer with a typical radical initiator, for example AIBN. The propagating radical (P_n^\bullet) then reacts with the reactive thioketene bond in the RAFT agent producing an intermediate radical. This intermediate radical can then fragment either backwards to release the propagating chains or forwards to release a new radical (b) which can further initiate monomer (c) forming a new active polymer chain (P_m^\bullet). The newly active chain then reacts with the RAFT agent (d) and a rapid equilibrium/propagation occurs between both of the active polymer chains (P_n^\bullet and P_m^\bullet). As further reaction of monomer with either chain occurs at the same rate and leads to the same intermediate step, polymers with low dispersities can be achieved. After termination (e), chains with a RAFT agent attached at one end are obtained.²⁷

(a) *Initiation*(b) *Reversible chain transfer*(c) *Reinitiation*(d) *Chain equilibrium/propagation*(e) *Termination***Scheme 1.2 - Mechanism of RAFT polymerisation**

Although RAFT polymerisation offers many advantages, it also suffers from the fact that there is at present, no generic RAFT agent which is suitable for all monomer types, thus a RAFT agent needs to be synthesised for a particular monomer and the synthesis of copolymers of monomers with differing reactivity can be a problem. Moreover, as the RAFT agents themselves are often brightly coloured, the final polymers may also retain their colour, which might require an additional step post-polymerisation to cleave the RAFT agent residue from the chain end. Due to these limitations and associated expenses, industrial uptake of RAFT is still limited.²⁸

The main advantage offered by many controlled radical polymerisation techniques is their access to a wide variety of vinyl monomers, using fairly facile reaction conditions to achieve polymers with control over molecular weight and relative control over molecular weight distribution. Termination, while limited, will still occur in most CRP systems meaning absolute control over any given polymerisation cannot be obtained, as there will always be the possibility of prematurely deactivated polymer chains. It would be best for well-defined polymers to be synthesised with a technique that does not contain any termination or chain transfer reactions, such as in a living system.

1.4 Living Polymerisation

Living polymerisation is a versatile concept for the creation of narrow dispersity homopolymers and copolymers and well-defined, complex polymers. Synthetically speaking it is the approach offering the most control over molecular weight, molecular weight distribution, copolymer composition, and microstructure whilst also retaining the option for the chain-end functionalisation of polymers. The desirable characteristics possessed by a living system have led to a number of techniques claiming to be such in the literature, many of which are based on the “degree of livingness” that may be present. Terms such as quasi-living, pseudo-living, controlled living, truly living and immortal have all been used to describe polymerisations. For simplicity’s sake, living polymerisation is defined as a chain reaction polymerisation where chain transfer and termination are absent; any other qualification needed to justify the livingness of a system, principally excludes it from being considered living, including systems with reversible deactivation reactions. Furthermore, as the rate of chain initiation is comparable or faster than the rate of propagation, polymer chain growth is essentially constant during polymerisation, leading to polymers with very narrow dispersities. The absence of termination or chain transfer reactions allows the reactive species generated to remain active even after the complete consumption of monomers. Living polymerisation can be carried out with a number of monomers, solvents and initiators, as well as with Lewis acids and end capping agents, all of which may have a direct effect on the exact type of polymer synthesised with regards to molecular weight, dispersity (\bar{M}_w/\bar{M}_n) and microstructure.

1.4.1 Criteria for Living Polymerisation

For any polymerisation mechanism to be regarded as living, there is a number of criteria that the system must adhere to, both experimentally and physically.^{6, 29} The following is a list of these criteria:

1. *Polymerisation proceeds until all monomer is consumed and addition of further monomer results in further polymerisation.*

This criterion is perhaps the most important regarding whether a system is living. The key facet of this criterion is that all polymer chain ends retain their active centres during the time scale of the experiment and beyond, meaning that upon addition of further

quantities of monomer there is continued polymerisation. In free radical polymerisation, while all monomer may be consumed, all chain ends do not retain their active centres and therefore these may not be described as “living”. Fulfilment of this criterion can be confirmed by size exclusion chromatography (SEC), by determining the molecular weight before and after the second monomer addition, with the molecular weight increasing if a living polymerisation has occurred. However, alone this criterion cannot define a living polymerisation.

2. *The number average molecular weight (M_n) is a linear function of conversion.*

This criterion exploits the fact that the degree of polymerisation is related to the stoichiometry of the reactants and the degree of monomer conversion. The number average molecular weight (M_n) of the polymer is related to the mass (in grams) of monomer by the following equation:

$$M_n = \frac{\text{mass of monomer (g)}}{\text{moles of initiator (mol)}} \quad [1.5]$$

It therefore follows that at an intermediate degree of conversion the equation becomes:

$$M_n = \frac{\text{mass of monomer consumed (g)}}{\text{moles of initiator (mol)}} \quad [1.6]$$

This relationship, however, does not account for termination reactions, which although limiting the number of active chains, does not alter the total number of chains in the reaction. This means the linear relationship defining this criterion is not robust enough (in isolation) to determine whether or not a system is living.

3. *The number of polymer molecules (and active centres) is constant, which is sensibly independent of conversion.*

This is one of the more robust criteria, as it is sensitive to different aspects of a living polymerisation. Firstly, it establishes that termination does not occur so long as the number of active centres is constant. This criterion is also sensitive to the possibility of chain transfer reactions, which would increase the number of polymer molecules. For both criteria 2 and 3, termination and chain transfer reactions would result in peak broadening detected in the SEC chromatograms of the resulting polymer.

4. *The molecular weight can be controlled by the stoichiometry of the reaction.*

It has been previously shown in criterion 2 that the theoretical molecular weight can be determined by the ratio of the grams of monomer to moles of initiator. As such, deviations between this calculated value and experimentally obtained molecular weights can indicate whether the system is stoichiometrically controlled. Active chains are deactivated by chain transfer reactions leading to an increase in the concentration of lower molecular weight chains. Again, this criterion alone is not sufficient to establish livingness in a polymerisation.

5. *Narrow molecular weight distribution polymers are produced.*

A narrow Poisson molecular weight distribution is generally an indication of several factors associated with a polymerisation reaction. In particular, it indicates that all active centres are introduced at the onset of polymerisation; the rate of initiation and propagation are competitive; there are no chain transfer or termination reactions occurring; all active centres are readily available to react with monomer and that propagation must be irreversible. Conversely, broad molecular weight distributions can also be found in living polymerisation systems depending on what type of initiator has been used, or even what type of monomer is being polymerised. Narrow molecular weight distribution polymers have also been shown to be attainable even in non-living systems. Due to these limitations, a narrow molecular weight distribution cannot alone be used as a criterion for living polymerisation.

6. *Block copolymers can be prepared by sequential monomer addition.*

This criterion, much like criterion 1, states that upon further addition of monomer polymerisation continues. This allows for the creation of block copolymers of different monomers such as poly(styrene-*b*-butadiene). This criterion is also sensitive to competing chain transfer or terminating reactions, which can be detected by SEC. This is a very important criterion in defining a living polymerisation.

7. *Chain-end functionalities can be introduced in quantitative yield.*

Theoretically, each of the active centres in a living polymerisation should be available for end-capping reactions with various terminating or functionalising agents. There may be problems, however, with the analysis of end-capped polymers since end-groups become increasingly difficult to detect by NMR (and other techniques) with increasing molecular weight.

8. *Linearity of a kinetic plot of rate of propagation as a function of time given by the equation:*

$$\ln \frac{[M]_0}{[M]} = k_{obs} t \quad [1.7]$$

This determines that the kinetics of propagation should be pseudo first order, resulting in a linear plot, which should arise when there is no chain termination. This is useful in supplementing criterion 2 which is sensitive to chain transfer but not termination, whereas criterion 8 is sensitive to chain termination, but not chain transfer.

9. *A plot of the left side of Equation [1.8] vs. time will be linear.*

$$\ln \left(1 - \frac{[I]_0}{[M]_0} \overline{DP}_n \right) = -k_p [I]_0 t \quad [1.8]$$

The number average degree of polymerisation (\overline{DP}_n) can be calculated using an equation similar to that of equation [1.6] giving:

$$\overline{DP}_n = \frac{[M]_0 - [M]_t}{[P^*]_0} = \frac{[M]_0 - [M]_t}{[I]_0} \quad [1.9]$$

Thus:

$$[M]_t = [M]_0 - \overline{DP}_n \cdot [I]_0 \quad [1.10]$$

The rate of polymerisation is expressed as:

$$\frac{d[M]}{dt} = -k_p [P^*] [M]_t = -k_p [I]_0 [M]_t \quad [1.11]$$

Thus:

$$\ln \frac{[M]_t}{[M]_0} = k_{obs} t \quad [1.12]$$

Substituting $[M]_0$ from Equation [1.10] and rearranging gives Equation [1.8]. A plot of these data is a simple way of determining whether chain transfer or termination is present in the system, with a linear plot being obtained if both are absent.³⁰

It can clearly be seen that no single criterion can be used to determine whether or not a system is a living polymerisation. Each criterion is sensitive to different aspects of polymerisation, but in utilising all criteria we can define a living polymerisation as one in which: there are no chain transfer or termination reactions present; all polymer chains are initiated at the onset of polymerisation and polymerisation occurs until all monomer is consumed; additional batches of monomer will result in continued polymerisation resulting in increasing molecular weight polymers or block copolymers. The increase of

molecular weight is directly proportional to the amount of monomer and initiator in the system and narrow dispersity polymers can be achieved. As there are no termination reactions, end capping and functionalisation reactions are possible to obtain functionalised polymers. There are few polymerisation techniques that fulfil each criterion, but those that do include cationic polymerisation, anionic polymerisation and ring opening metathesis polymerisation.

1.4.2 Ionic Polymerisation

Ionic polymerisation occurs when the reactive propagating species carries an ionic charge. The monomers used in these reactions must also be stable enough to carry the charge for polymerisation to occur.

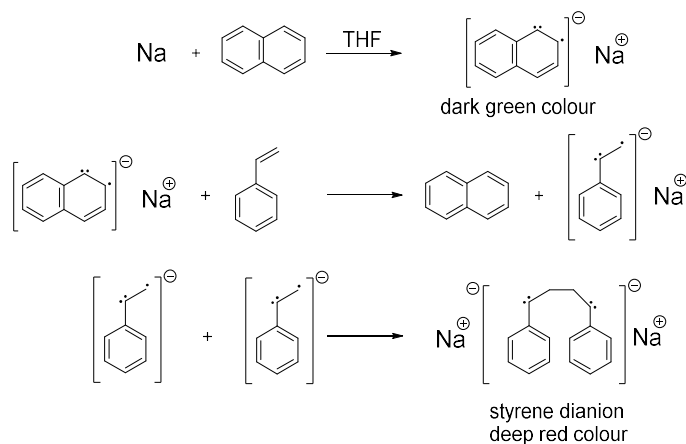
1.4.2.1 Cationic Polymerisation

Cationic polymerisation is a type of chain growth polymerisation which occurs when the active chain end is a positively charged species. Cationic polymerisations consist of initiation, propagation and termination reactions, although when the latter is excluded they can be classed as living polymerisation. Initiators in these reactions are typically Lewis acids such as boron trifluoride or tin tetrachloride. These reactions are usually carried out at low temperatures in order to inhibit side reactions such as chain transfer, due to the very high reactivity of the propagating species, even when compared to anionic polymerisation. There must also be great care taken to eliminate impurities that may terminate the reactions.³¹

1.4.2.2 Anionic Polymerisation

Anionic polymerisation meets each of the living polymerisation criteria listed above and can therefore be considered living. As living anionic polymerisation provides more control over both molecular weight and dispersity than that of other chain growth methods, it is the optimal candidate for the synthesis of well-defined model polymers of different architectures. Much like cationic polymerisation, anionic polymerisation occurs when the active chain end centre is a charged species, for example an anion or a radical anion. In 1956 Szwarc and co-workers first discovered “living” anionic polymerisation and published their seminal papers describing the living nature of these polymerisations

based on the polymerisation of styrene monomers, the mechanism of which is given in Scheme 1.3.³²⁻³³



Scheme 1.3 - Anionic polymerisation of styrene by sodium naphthalide

The initial step is the formation of the dark green sodium naphthalene radical anion, which subsequently reacts with a unit of styrene, forming styrene radical anions. These styrene radical anions then rapidly couple, forming the deep red styrene dianion, which acts as the true initiator of this living polymerisation, which then goes on to propagate polystyrene chains from both ends. Szwarc and co-workers noted that the polymer solution remained red even after complete monomer consumption and upon further addition of monomer, polymerisation continued. Based on these observations, they concluded that termination had not occurred. Anionic polymerisation, along with free radical polymerisation, has become one of the most commercially utilised techniques for polymer synthesis. It remains the dominant synthetic technique favoured by the tyre and rubber industry and is one of the most important commercial polymerisation procedures for the synthesis of elastomers, thermoplastic elastomers, thermoplastic resins, and other specialty polymers.⁶

1.4.2.2.1 Mechanism

A general mechanism for living anionic polymerisation is given below, for a monomer M , where I is an initiator. Initiation occurs when a monomer unit is activated by an initiator molecule, forming an active centre. Propagation occurs when this unimer reacts with further monomer units until all monomer is completely consumed.

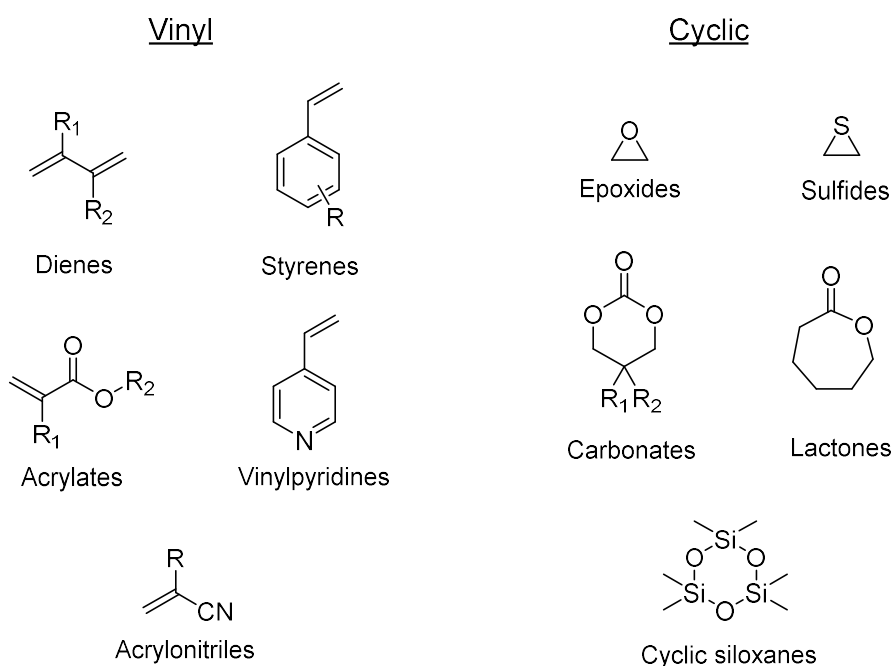




Under normal circumstances there is no chain transfer or inherent termination. In order to deactivate the propagating species, the reaction is usually quenched with an alcohol, for example methanol. When carried out precisely, this will result in predictable, reproducible, very well-defined polymers.

1.4.2.2.2 Monomers

Monomer choice is not as broad as the choice of monomers available to radical based polymerisation. For anionic polymerisation, monomers are generally classified into two groups. The first being vinyl monomers including styrene, diene and carbonyl-type monomers, with difunctionality provided by one or more double bonds, and the second being cyclic monomers of various ring sizes with difunctionality provided by a ring that can open by reaction with nucleophiles. Some of the monomers capable of anionic polymerisation are shown below in Figure 1.8.



R = H, alkyl, aryl or electron withdrawing aprotic functional group

Figure 1.8 - Monomers capable of anionic polymerisation

Any monomer that is used in an anionic polymerisation must stabilise the negative charge of the generated propagating carbanionic species (Figure 1.9). If a monomer contains a substituent group that is not able to stabilise the anionic charges, it is not

suitable for anionic polymerisation; this excludes most acidic, proton donating groups (e.g. amino, hydroxyl, carboxyl, acetylene functional groups) as well as strongly electrophilic functional groups or bases that react with nucleophiles.

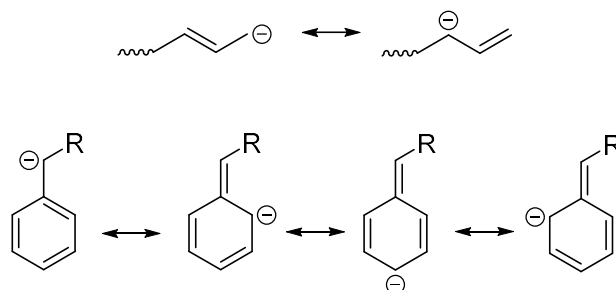


Figure 1.9 - Resonance stabilisation of the negative charge in vinyl monomers

In order to use monomers with functional groups which are not stable to the anionic charges, such groups need to be protected first, ideally with a protection group which remains stable during polymerisation and is easily removed afterwards. For example, with hydroxyl based functionalities, this can usually be achieved by protection to their corresponding silyl ether derivatives, which can then be removed via mild acid deprotection. The work in this project is mainly focused on the vinyl class of monomers, with butadiene being of particular importance. Butadiene is one of the most commercially used monomers and is used extensively in the tyre industry.⁶

1.4.2.2.3 Solvents

Solvent choice is limited due to the high reactivity of the initiators and propagating anionic species present. Halogenated and protic solvents are unsuitable for use in anionic polymerisation because of their reaction with active centres. For styrene and diene monomers, solvent choice is limited to alkanes, cycloalkanes, aromatic hydrocarbons and ethers.³⁴⁻³⁵ Benzene provides enhanced rates of initiation; and toluene can undergo chain transfer reactions in styrene and diene polymerisations under some circumstances, the degree of which increases with increasing temperature or in the presence of polar additives such as ethers, amines or group I metal alkoxides.³⁶⁻³⁷ Chain transfer can also occur when using alkenes as the solvent.³⁸

1.4.2.2.4 Initiators

Anionic polymerisation can be initiated with radical anions and alkali metals but most commonly is achieved with group I organometallic compounds based on lithium, sodium and potassium. Alkylolithium compounds have seen the most usage because of their fast initiation rates, hydrocarbon solubility, commercial availability and for diene polymerisation in particular, their ability to form diene polymers with predominantly 1,4-microstructures. The rate of initiation by alkylolithiums in hydrocarbon solvents is dependent on monomer and solvent choice, as well as the temperature and the structure of the initiator itself. The relative reactivity of these initiators in hydrocarbon solvents is related to their degree of aggregation which in turn is mainly dependent on steric factors. For example *n*-butyllithium aggregates into hexamers whereas *sec*-butyllithium associates into tetramers.³⁹ The relative rates of reaction for styrenes and dienes with commonly used alkylolithium initiators can be summarised as follows (known degree of association in parenthesis):

Diene polymerisation: Menthylolithium (2) > *sec*-butyllithium (4) > *iso*-propyllithium (4-6) > *tert*-butyllithium (4) > *iso*-butyllithium > *n*-butyllithium (6)

Styrene polymerisation: Menthylolithium (2) > *sec*-butyllithium (4) > *iso*-propyllithium (4-6) > *iso*-butyllithium > *n*-butyllithium (6) > *tert*-butyllithium (4).

It can be seen that the less associated an alkylolithium complex, the faster is the rate of initiation. All previously mentioned alkylolithium initiators are monofunctional, as in they are only able to generate one living chain end of a propagating species. It is also possible to have initiators that are difunctional, trifunctional or multifunctional, which may be of use when synthesising polymers that require specific branching, such as in the synthesis of H-shaped polymers. Functionalised initiators have also seen use in the synthesis of protected end-functionalised polymers.

The fastest initiation possible is preferable in most cases; as such *sec*-butyllithium is the initiator preferred over *n*-butyllithium for both styrene and diene polymerisations. This initiator's solubility in a wide range of both non-polar organic solvents such as benzene is also favourable for its use.

1.4.2.2.5 Polymer Functionalisation

Living anionic polymerisation is particularly suited to the synthesis of end-group functionalised polymers, especially in the cases of the alkyllithium-initiated polymerisations of styrene or dienes.⁶ The propagating anionic chain ends remain active and are very reactive, enabling many post-polymerisation reactions to be carried out, with a range of electrophilic agents, as illustrated in Figure 1.10.

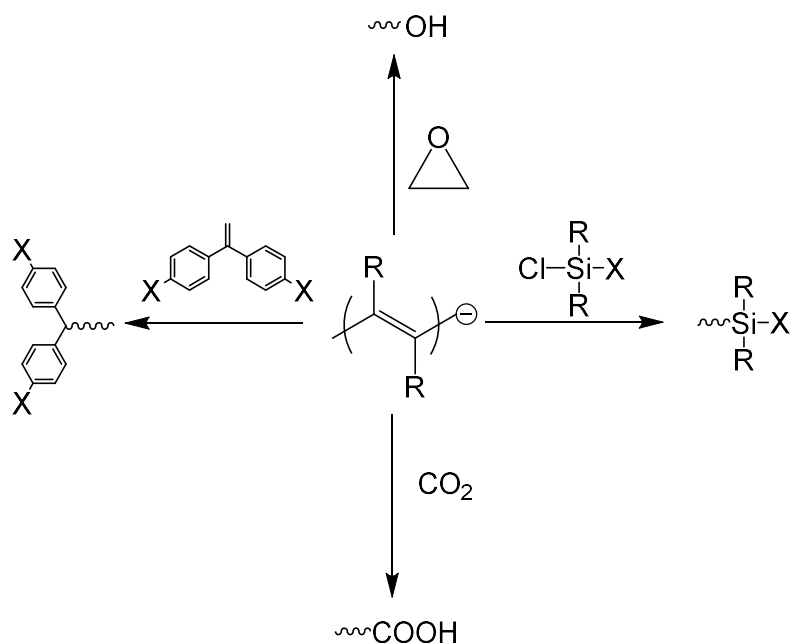


Figure 1.10 – Various end-group functionalisation paths for polydienes

Carbocation reactions can be carried out using polystyrene or polydienes and carbon dioxide to introduce a terminal carboxyl group, although this reaction suffers from the production of a mixture of products (see 1.4.2.2.6).⁴⁰ It has been reported that addition of THF in large quantities (25 vol%) is sufficient to eliminate side product formation if added prior to the addition of carbon dioxide.⁴¹ Hydroxylation reactions are also possible for generating functionalised polymers with a single hydroxyl group at the end of each chain; this is achieved by the addition of excess ethylene oxide as an end-capping agent of organolithium-initiated polystyrenes and polydienes (in benzene). Following reaction with ethylene oxide the end-groups become lithium alkoxides, which strongly associate to each other, making the polymer chains less reactive and unable to propagate resulting in quantitative (>90%) chain end-capping, and no ethylene oxide polymerisation.⁴² Other general functionalities can be introduced to polymer chains, through the use of suitable, protected end-capping agents, with silyl halides and (substituted) 1,1-diphenylethylene

(DPE) derivatives being of particular importance to living anionic polymerisation.⁴³ Silyl halides containing functional or protected functional groups provide a facile route to a number of end-group functionalised polymers, for example chlorosilane derivatives being used to introduce chain-end fluoroalkyl groups has been previously reported.⁴⁴⁻⁴⁵ DPE-based methods have also proven to be very useful for introducing a range of end-group functionalities to polymers. The addition reactions involving this monomer are simple, quantitative and, can result in several functionalities being incorporated along a polymer chain depending on the monomers used. Copolymerization of styrene with substituted DPE, can result in several functional groups being placed along a polymer chain,⁴⁶ and introducing several perfluorooctyl (C_8F_{17}) chain end-groups by exploiting DPE-substituted monomers and chlorosilane chemistry has been demonstrated.⁴⁷⁻⁴⁸

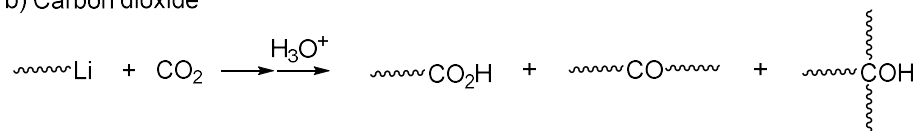
1.4.2.2.6 Impurities

Living anionic polymerisation is not immortal! The most important feature of any living anionic polymerisation reaction is the elimination of all potential impurities which may cause unwanted termination reactions. The species in use during living anionic polymerisations, namely the alkyllithium initiators and the carbanionic propagating species, are highly susceptible to reactions with environmental impurities such as carbon dioxide, oxygen, water and other protic impurities which can prematurely terminate the active centres. These side reactions can also lead to unwanted chain coupling reactions (see Scheme 1.4).⁴⁹⁻⁵⁰

a) Oxygen



b) Carbon dioxide



Scheme 1.4 - Termination reaction of polymeric alkyllithium with a) oxygen and b) carbon dioxide

As such, strict care is taken to eliminate all possible impurities before the commencement of any polymerisation. In most laboratory-scale reactions, this is achieved via the purification and degassing of all reagents and monomers used, in conjunction with the use of high vacuum techniques with specialised glass reaction apparatus, which have

proven to be quite effective in the elimination of impurities.⁵¹⁻⁵² If necessary, reactions can also be undertaken under an atmosphere of an inert gas such as nitrogen or argon. These specialised reaction vessels can also be washed with a living polymer solution before polymerisation in order to completely purify the vessel of any residual impurities.

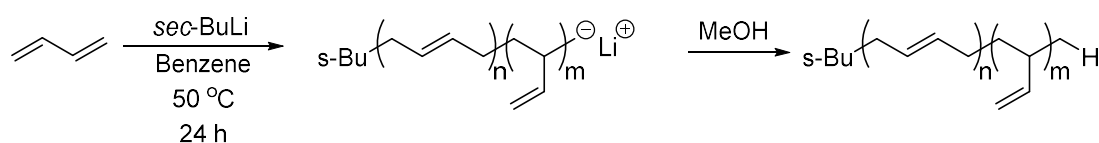
In summary, living anionic polymerisation is a powerful, versatile method for the creation of polymers. It is possible to control the molecular weight, molecular weight distribution, chain end functionalities and microstructure of these materials to a fine degree, despite being somewhat limited in monomer choice. Despite the challenges associated with potential side reactions due to impurities, it is still the most useful polymerisation technique for the synthesis of well-defined polydiene materials.

1.5 Polymer Architectures

Since the initial definition of macromolecules by Staudinger in 1922,⁵³ polymer architecture has played a tremendous role in polymer development. Seminal scientists including Staudinger, Flory, Ziegler, Natta, Shirakawa, Sharpless and of course Szwarc have made many important discoveries related to polymer architecture. Architecture itself can greatly affect a material's properties. Branched polymers in particular are of significant interest, in terms of their synthesis, structural characterisation and rheological properties. It still remains a challenge to both synthesise and characterise complex polymer architectures, and as such, they are regarded (along with complete sequence controlled polymerisation) as one of the most valuable targets for polymer science.

1.5.1 Linear Polymers

Linear polymers are the simplest polymer structures to synthesise and can be created using all previously mentioned polymerisation techniques. When using anionic polymerisation, polymers with predictable molecular weights and very narrow dispersities ($\mathcal{D} \leq 1.05$) can be obtained with relative ease.⁵⁴ They consist of straight chain polymers that can be prepared in one pot polymerisations. Molecular weights of linear polymers are controlled by the monomer : initiator ratio. The synthesis of linear polybutadiene is achieved by the reaction of butadiene in a hydrocarbon solvent such as benzene and a butyllithium initiator such as *sec*-butyllithium; a general route for this reaction is given in Scheme 1.5.



Scheme 1.5 - Synthesis of linear polybutadiene by anionic polymerisation

Propagation occurs via a Michael addition to the chain ends of the active species, leading to a polymer that can contain both 1,2- and 1,4-microstructures, with vinyl units incorporated randomly into the chain. Solvent choice plays a key role in determining the microstructure in alkylolithium-initiated diene polymerisations. If polymerisation is carried out in a polar solvent, the 1,2-content of the resultant polymer increases; for example, when THF is the solvent, the vinyl content of polybutadiene is above 80%, whereas in an exclusively non-polar hydrocarbon solvent such as benzene the vinyl

content is generally less than 10%.⁵⁵⁻⁵⁶ The drastic differences in microstructure are namely a result of the interaction between the propagating chain ends and the lithium counter ion. In polar solvents, the solvent molecules occupy the coordination sites around the lithium counter ion, increasing the ionic character of the propagating chain/lithium ion pair. As such, steric effects around the chains are alleviated, both the rate of initiation and propagation increase, and polydienes more readily undergo 1,2- addition.⁵⁵ In a non-polar hydrocarbon solvent, the bonding between the propagating chain end and the lithium atom is much more covalent in nature and aggregates are formed, increasing steric effects on the polymer as well as concentrating the negative charge at the chain ends, thus increasing the 1,4-content.^{6, 57}

1.5.2 Branched Polymers

A branched polymer is one composed of two or more linked chains and is essentially non-linear. Branch points indicate the point at which two or more chains are connected. Numerous types of branched polymers exist, some of which are depicted in Figure 1.11.

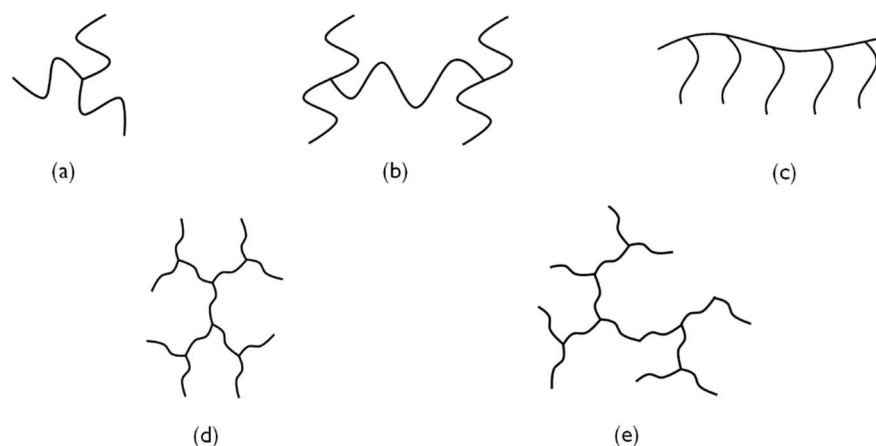


Figure 1.11 - Branched polymers of different structures: (a) star, (b) H-shaped, (c) comb, (d) dendritically branched and (e) hyperbranched polymers

Industrially produced polymers often have randomly branched architectures and high dispersities, making them difficult to study from both synthetic and rheological perspectives. Typically, chemists, physicists and engineers have instead employed well-defined materials, which are structurally homogeneous, for structure-property correlation studies. The study of these model polymers enables a clear correlation between structure and properties to be understood, which in time, can be extrapolated to better understand these inherently disperse industrial materials.

1.5.2.1 Star-branched Polymers

A star-branched polymer is one comprised of several chains attached to a single branch point. They can be synthesised using ionic⁵⁸ and controlled radical polymerisation methods.⁵⁹⁻⁶² The synthesis of star-branched polymers via living anionic polymerisation is well-documented and there has been a number of reviews that cover a range of synthetic methods including a comprehensive review on complex polymer architectures by Hadjichristidis *et al.* in 2017.⁶³⁻⁶⁴ Stars are the simplest type of branched polymer with only one branch point and numerous examples have been synthesised via living anionic polymerisation including stars based on polybutadiene,⁶⁵⁻⁶⁷ polyisoprene,⁶⁸⁻⁷⁰ and polystyrene.⁷¹⁻⁷³ There are two main strategies for the synthesis of star polymers: the “core first” approach and the “arm first” approach (Figure 1.12).



Figure 1.12 - Star polymer synthetic methodologies: “arm-first” and “core-first”

The “core-first” approach involves the use of a multifunctional initiator which will grow all arms simultaneously around the “core” molecule. The number of arms per star is determined by the number of initiation sites present on the initiator, but this approach experiences a number of issues. Firstly, the initiator needs to have initiation sites that are all equally reactive and possess the same rate of initiation, otherwise the arms will be initiated at different times, thus producing stars with significant dispersity in arm length – this in itself is a challenge. Many multifunctional alkyllithium initiators are both difficult to make and often insoluble, even in polar solvents. To overcome these issues, Burchard demonstrated a method in which a multifunctional initiator was generated from reaction of divinylbenzene (DVB) with *sec*-butyllithium in dilute benzene solution, creating a microgel suspension, illustrated in Figure 1.13. Each gel particle contains numerous active sites, thus allowing the growth of polymer chains when reacted with styrene, giving high molecular weight star polymers.⁷⁴ This method was developed further by Rempp, Gnanou and Lutz to be used with other monomers.⁷⁵

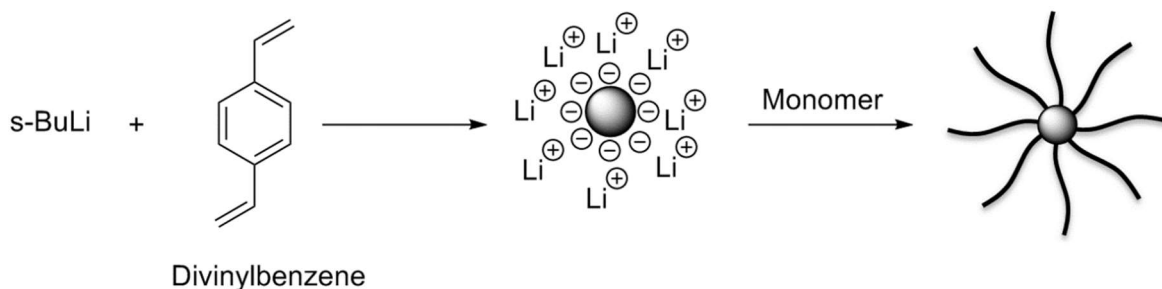


Figure 1.13 - Synthesis of a star polymer via the use of a multifunctional initiator

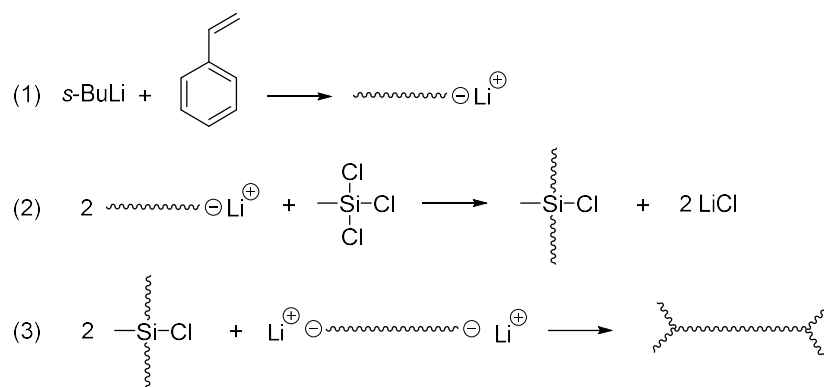
A further significant issue with the core-first method is that it does not allow for the characterisation of the molecular weights of the polymer arms independently. There are also steric hindrance issues when using multifunctional initiators, especially when using particularly bulky monomers. There are very few initiators that fulfil these requirements and as such this method is not commonly used. The “arm-first” approach involves the synthesis of living polymer chains first which are then coupled around a multifunctional electrophilic “core” coupling agent to give the star. This approach provides control over every step of the reaction, as well as allowing molecular weight characterisation of both the arms and the star polymer independently. The use of silyl halides, particularly chlorosilane compounds has been most widely employed for the synthesis of star polymers by this approach.⁷⁶⁻⁷⁸ The number of reactive functionalities on the silane determines the number of arms on the resultant polymer. Highly functional chlorosilanes have been used for the synthesis of polybutadiene stars with 32, 64 and 128 arms, as reported by Hadjichristidis and co-workers.⁷⁹⁻⁸¹ The disadvantage of this technique is mainly related to the time taken for the final linking reactions to occur, with chains of higher molecular weight or the synthesis of stars with many arms, potentially taking weeks to result in complete coupling. In general, for a given multifunctional chlorosilane compound the reactivity decreases in the order polybutadienyllithium > polyisoprenyllithium > polystyryllithium due to the steric influences of the polymer species in question. However, steric crowding around the core can be alleviated by the use of more sterically spaced chlorosilane linking agents. Another method for decreasing steric hindrance is to end cap the living polymer chains with a few units of butadiene before coupling. The arm-first technique usually requires a molar excess of polymer chains with respect to silane functionality, to ensure maximum coupling efficiency, which in turn requires the use of fractionation to remove any unreacted linear arm remaining in the polymer product. Another moiety that has been used to make stars is 1,1-diphenylethylene (DPE) based derivatives. This differs from the chlorosilane based

couplings because when the linking agent is added to a living polymer chain, rather than resulting in termination, as is the case with chlorosilanes, the chain retains the active centre allowing for further reaction. These “living linking agents” have found much use in the preparation of heteroarm or miktoarm star polymers, where each arm in the star comprises a different monomer. Such a strategy was used for the creation of miktoarm polystyrene and polybutadiene stars by Quirk⁸²⁻⁸³ and Fujimoto.⁸⁴ Recently, another method for star polymer synthesis has expanded on this concept and been developed by Hirao and co-workers - the iterative methodology.⁸⁵ This approach exploits use of anionic polymerisation and multiple functionalised DPE derivatives to generate stars with a large number of arms, through their repeated coupling reactions, i.e. “iterations”. Hirao *et al.* have had success in the synthesis of polystyrene stars with multiple arms including 4, 8 and 16 arm stars.⁸⁶ The advantages of this approach include the ability to produce multiple generations of homogenous stars as well as the precise control anionic polymerisation grants. The disadvantage, however, is the time consuming synthesis and reaction, as well as the need for stoichiometric reaction conditions.

Star polymers are of some industrial interest and have often been the bases of model branched polymers for studies of their mechanical, physical and rheological properties. The synthesis of star polymers of various arm numbers and molecular weights by anionic polymerisation and chlorosilane linking agents is often used to synthesise well-defined branched polymers, owing to their facile synthesis.

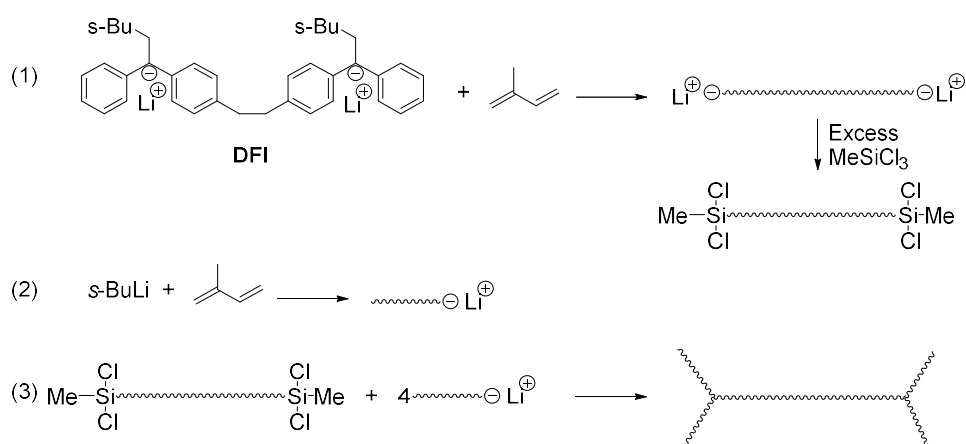
1.5.2.2 H-shaped Polymers

H-shaped polymers constitute the next level of complexity in branched polymers, differing from stars in that there are two branch points i.e. linking agents located at each end of the main chain backbone. Most syntheses used for H-shaped polymers exploit anionic polymerisation with difunctional initiators and chlorosilane coupling reactions. The first H-shaped polymer was prepared from styrene by Roovers and Toporowski using living anionic polymerisation in a three step process (Scheme 1.6).⁸⁷ Step (1) involves the synthesis of the polystyrene arms, with *sec*-BuLi as the initiator, in step (2), these chains are reacted with excess methyltrichlorosilane – the stoichiometry of this step being controlled to avoid production of a three arm star. The crossbar backbone polymer was synthesised in a separate reaction with the difunctional initiator sodium naphthalide, and then coupled with the arms in step (3), giving the final H-polymer.



Scheme 1.6 - Original synthetic strategy for H-shaped polystyrene

This route was not without issues and required the use of a polar solvent, such as THF, in order to generate the crossbar, while the use of sodium naphthalide further limited its use to styrene based materials, as the solvent would greatly increase the percentage of 1,2-microstructure in diene based materials. This route was modified by McLeish and Young for the production of high 1,4-cis H-shaped polyisoprene in benzene, using 1,2-bis-(4-(1-phenylethenyl)phenyl)ethane (**DFI**, Scheme 1.7) as a difunctional initiator; its sterically bulky structure aids its solubility in hydrocarbon solvents.⁸⁸ In step (1) DFI is used to create the “crossbar” polymer backbone with two living chain ends which are subsequently coupled in a large excess methyltrichlorosilane (50:1). The arms of the polymer, formed as independent living chains in step (2) are then coupled with the crossbar to form the final H-polymer in step (3).



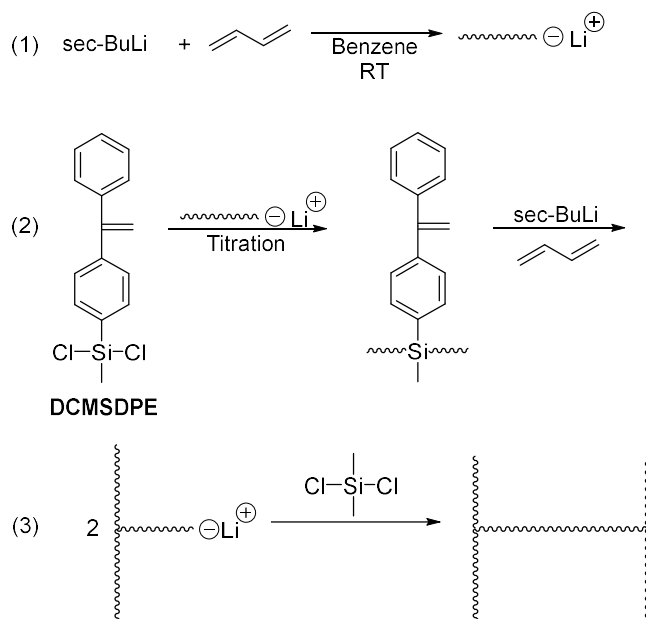
Scheme 1.7 - Synthesis of H-shaped polyisoprene

These previously described strategies, whilst successful, are still accompanied by the production of both high and low molecular weight by-products, formed due to backbone coupling or incomplete coupling of the arms to the backbone. Both approaches are also time consuming processes, requiring fractionation to purify the final product. The use of

difunctional initiators in itself is also problematic, as there is always a possibility of incomplete activation.

Despite these caveats, the synthesis of various H-shaped polymers has been reported using chlorosilane coupling agents including H-shaped (4-arms), super-H (6 arms)⁸⁹⁻⁹⁰ and pom-pom polymers (8-arms or more),⁹¹ these being produced by using linking agents with corresponding number of functionalities.

In 2008, Mays *et al.* described a novel approach for the synthesis of H-shaped polymers, with the intention of avoiding unwanted high molecular weight side products, using 4-(dichloromethylsilyl)diphenylethylene (DCMSDPE, Scheme 1.8) as a living linking agent.⁹² This strategy involves the generation of living three-arm star polymers, which were then linked together around dimethyldichlorosilane to form H-shaped polybutadiene. This route exploits the fact that carbanion species react with chlorosilane groups preferentially in the presence of vinyl groups, as well as the steric nature of the DCMSDPE molecule hindering reaction with the double bond even further.



Scheme 1.8 - Synthetic route to H-shaped polybutadiene using DCMSDPE

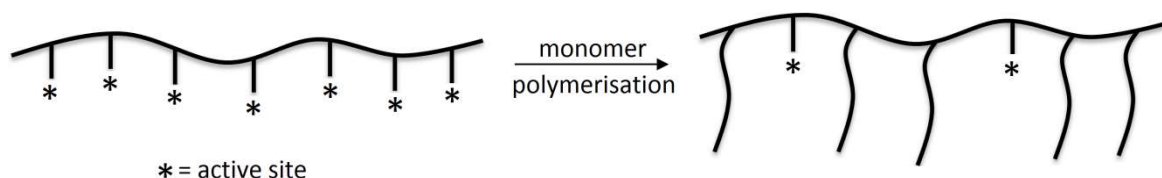
This living star coupling method, although complex, has proven effective for the creation of polymers of this architecture, although complications may arise when using this approach. The use of living macromolecules may also potentially generate unwanted side reactions due to their high reactivity. H-shaped polymers make for interesting materials themselves, the presence of two branch points allows for the study of effects such as long

chain branching on rheological properties, however, when compared with stars and other branched architectures, there are relatively few studies focused on these materials in particular, despite interest in them from both industrial and rheological standpoints. Synthetic challenges may be the contributing factor in limiting the number of previous studies on H-polymers.⁹³

1.5.2.3 Graft/Comb polymers

Graft polymers, also referred to as comb polymers, are polymers with multiple chains attached to a main linear backbone through multiple branching points, in contrast to H-shaped polymers which only have branch points at each end of the backbone. Comb polymers are usually prepared by one of three methods: “grafting from”, “grafting to”, and “grafting through”, the latter also called the “macromonomer” approach.

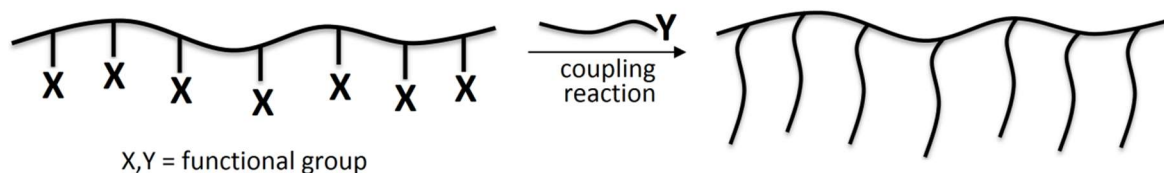
The “grafting from” method involves the synthesis of a backbone which has active centres generated on it, used to initiate polymerisation with another monomer forming the graft branches; an overview of this is illustrated in Scheme 1.9. This method is often used with radical polymerisation⁹⁴ and has been used to synthesise poly(isoprene-g-styrene)⁹⁵ and PMMA-g-poly(β -butyrolactone) by anionic polymerisation.⁹⁶ However, it remains an unpopular method due to the uncontrolled nature of the grafting reactions, resulting in polymers where the level of grating cannot be quantitatively known.



Scheme 1.9 - Schematic diagram of a comb polymer synthesis by the “grafting from” method

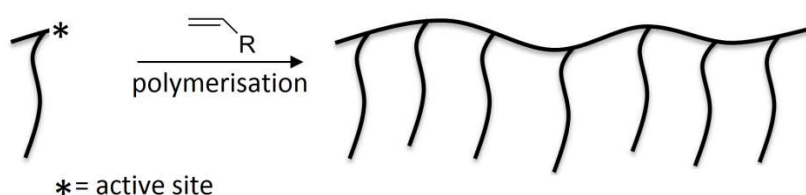
The “grafting to” method employs the synthesis of a backbone polymer chain containing randomly-distributed reactive functional groups, which undergo reaction with functional groups on the chain-end of a second polymer, forming the graft branches – i.e. preformed branches are coupled to the backbone; this is illustrated in Scheme 1.10. This method allows for the separate characterisation of both backbone and polymer branches. As both polymers are premade, it is possible to quantify the average degree of branching by a simple comparison of the molecular weight of starting materials and product. Although, since the distribution of reactive functional groups on the polymer backbone is usually

uncontrolled, the resulting combs will contain a random distribution of branches. Deffieux and Schappacher used the method to synthesise poly(2-chloroethylvinylether)-g-polystyrene.⁹⁷



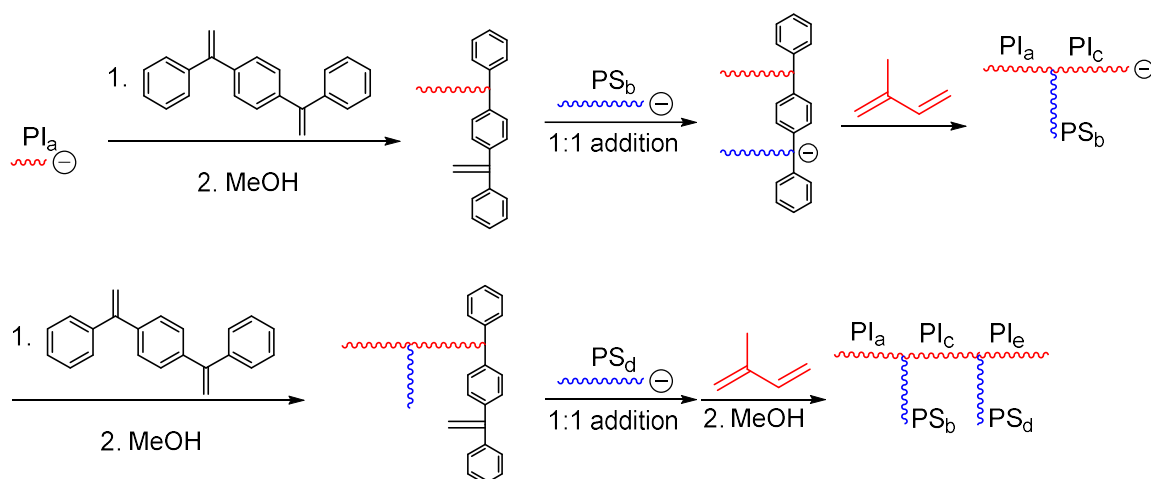
Scheme 1.10 - Schematic diagram of a comb polymer synthesis by the "grafting onto" method

The third method, "grafting through", is one in which preformed macromonomers are copolymerised with another monomer in order to produce the graft copolymer - illustrated in Scheme 1.11. Matyjaszewski *et al.* were able to synthesise poly(*n*-butyl acrylate)-g-polyethylene using the "grafting through" method.⁹⁸ A branched polyethylene macromonomer was first synthesised by palladium-mediated olefin polymerisation, which was then copolymerised with *n*-butyl acrylate via ATRP.



Scheme 1.11 - Schematic diagram of a comb polymer synthesis by the "grafting through" method

The ability to control the molecular weight of the arms and the backbone independently by controlled or living polymerisation is facile. However, to create exact graft polymers where one can control: (a) the molecular weight between each branch point on the main chain; (b) the total number of branch chains and (c) the position of each side chain on the main chain still remains a challenge. Paraskeva and Hadjichristidis were the first to report on the synthesis of exact comb polybutadienes with two and three branches as well as the synthesis of exact comb poly(isoprene)-g-polystyrene with the use of living anionic polymerisation and DPE derivatives (Scheme 1.12).⁹⁹



Scheme 1.12 - Synthesis of an exact comb poly(isoprene)-g-polystyrene

Polyisoprene (PI_a) was first reacted with 1,4-bis(phenylethenyl)-benzene, giving functionalised chain end PI. This chain then undergoes reaction with a stoichiometric amount of living PS (PS_b), followed by reaction with isoprene, forming a 3-arm living star polymer anion. The star polymer anion was then reacted again with 1,4-bis(phenylethenyl)-benzene, and the process repeated, giving a final polymer of poly(isoprene)-g-polystyrene. This stepwise strategy, although allowing for complete control over branch points, molecular weight and dispersity of the backbone and side chains, relies heavily on exact 1:1 stoichiometric control and due to the nature of anionic polymerisation is still very sensitive to impurities leading to the formation of unwanted by-products.

1.5.3 Dendritically Branched Polymers

Dendritically branched polymers are highly branched polymers with complex, dendritic architectures. In some respects, they can be regarded as a “fourth” class of polymers alongside the traditional linear, branched and crosslinked classes. The class itself is comprised of six subclasses, these being: (a) dendrons and dendrimers; (b) linear-dendritic hybrids; (c) dendrigrafts or dendronised polymers; (d) hyperbranched polymers; (e) multi-arm star polymers and (f) hypergrafts or hypergrafted polymers as shown in (Figure 1.14).¹⁰⁰

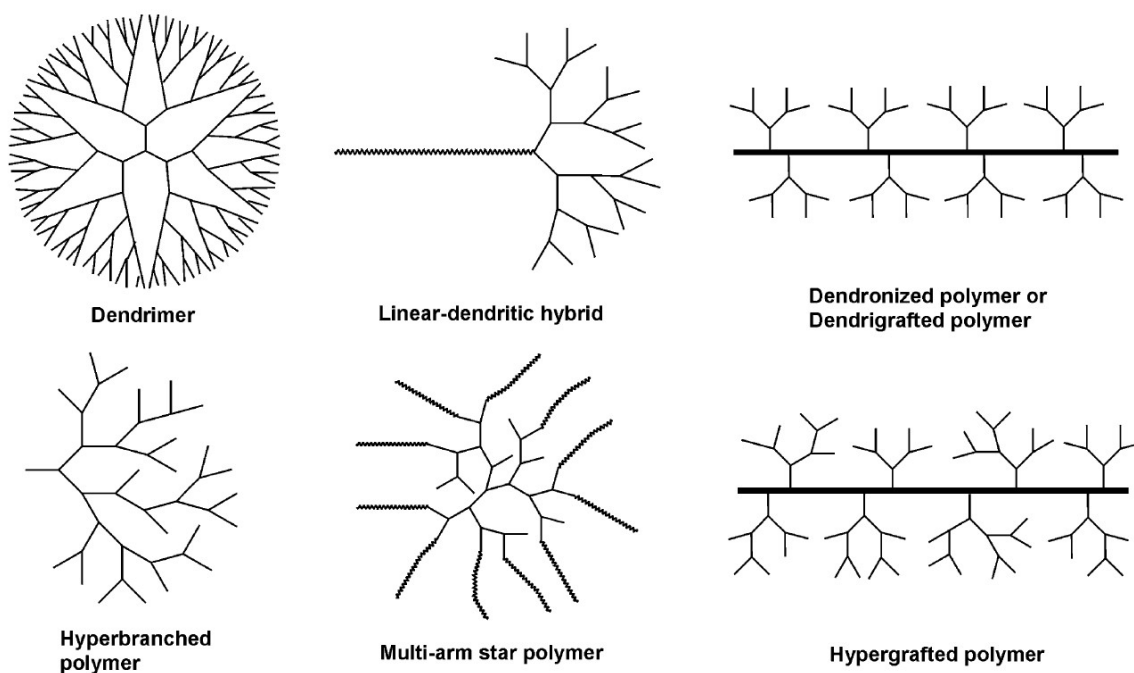


Figure 1.14 - Schematic description of dendritically branched polymers¹⁰⁰ Reprinted with permission from [Gao, C.; Yan, D., *Prog. Polym. Sci.* 2004, 29 (3), 183-275]. Copyright [2004] Elsevier

The unique architectures of this class have led to their development in a range of applications from potential as drug delivery systems¹⁰¹⁻¹⁰² to uses in nanoscience and nanotechnology.¹⁰³ Due to the high number of branch points, as well as the complexities of these structures, dendrimers and hyperbranched polymers in particular, have been the focus of a number of synthetic reviews¹⁰⁴⁻¹⁰⁵ and rheological studies.¹⁰⁶⁻¹⁰⁷

1.5.3.1 Dendrimers

Dendrimers are very well-defined, perfectly branched polymers. They were first theorised of by Flory¹⁰⁸ in the 1940s, but it was not until the mid-1980s that their synthesis was reported, first by Tomalia¹⁰⁹ *et al.* in 1984 and then, independently, by Newkome¹¹⁰ *et al.* in 1985. There are two general methods for the synthesis of dendrimers: the divergent approach and the convergent approach, a visual representation of each is given in Figure 1.15.¹¹¹ Both methods, unfortunately, remain extremely time consuming techniques for the creation of dendrimers.

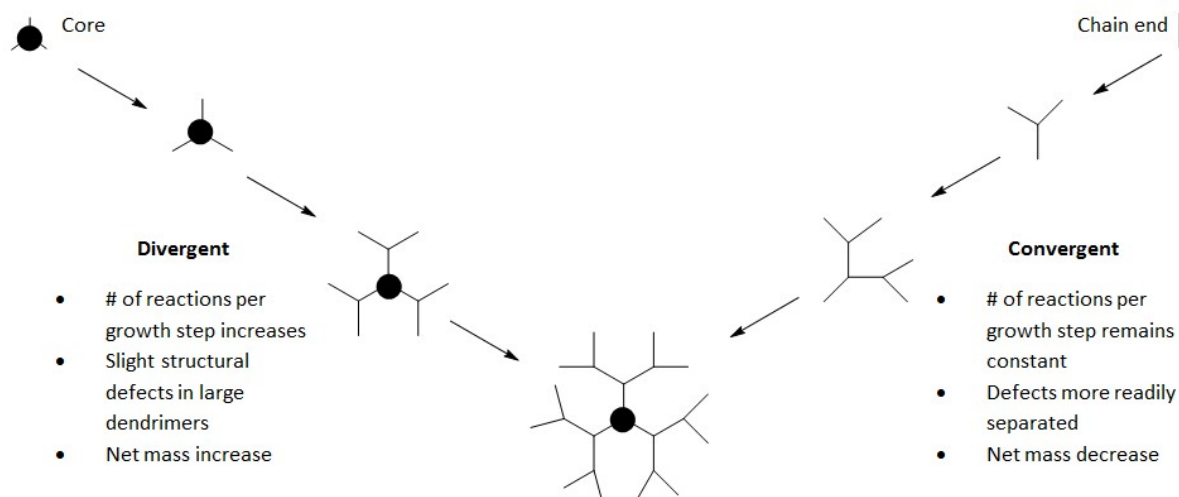


Figure 1.15 - The divergent and convergent approaches to dendrimer synthesis

1.5.3.2 Hyperbranched Polymers

Hyperbranched polymers are multiply branched polymers, but possess features that distinguish them from regular dendrimers. Hyperbranched polymers are not as structurally homogeneous as dendrimers, with functional groups not located at an ordered position; this is due to the statistical coupling steps involved in their syntheses as well as other factors including steric hindrance and the reactivity of the functional groups used.¹¹² There are several synthetic strategies for the preparation of hyperbranched polymers, with the most common method being the single monomer method (SMM), in which an AB_n ($n \geq 2$) monomer will react with itself – i.e. functional group A reacts with functional group B, eventually forming a hyperbranched polymer, with an initial focal point A and terminal B groups, an example of this is given in Figure 1.16 for a typical AB_2 monomer.¹¹³

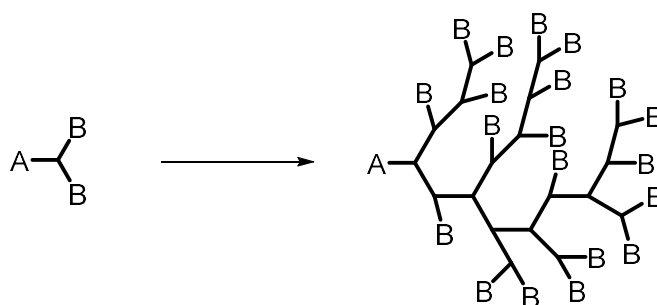


Figure 1.16 - Synthesis of an AB_2 hyperbranched polymer by the single monomer method

Hyperbranched polymers synthesised by polycondensation reactions,¹¹⁴ self-condensing vinyl polymerisation (SCVP),¹¹⁵ ring opening multibranching polymerisation (ROMBP),¹¹⁶ as well as polymerisations using a double monomer method (DMM)¹¹⁷ have all been reported. The synthetic routes to hyperbranched polymers are more facile, 'one-pot' reactions when compared to multistep dendrimer syntheses. These economical reaction conditions have generated large commercial interest for their applicability to large scale production of random, highly branched materials.

1.5.3.3 Long-Chain Branched Polymers

The previously discussed synthetic methods for dendritically branched polymers were concerned with synthetic routes that often start from monomers or small molecules, resulting in the final polymers having high degrees of branching and branching density. However, if those materials are modified to increase the distance between branch points with, long chain linear segments, this would decrease the polymer's degree of branching and branching density. These new types of polymers are collectively known as long-chain branched polymers, although they have been given a multitude of other names to describe them such as Cayley Trees,¹¹⁸ dendrimer-like,¹¹⁹ DendriMacs¹²⁰ and dendritically star branched polymers¹²¹ to describe the more well-defined analogues, and comb-burst,¹²² dendrigraft,¹²³ arborescent¹²⁴ and HyperMacs¹²⁵ to describe the less well-defined analogues. They are essentially the long-chain analogues of conventional dendrimers and hyperbranched polymers. The unique architectures these systems possess have garnered much academic and industrial interest, with recent reviews on these polymers by both Gauthier¹²⁶ and Perrier.¹²⁷

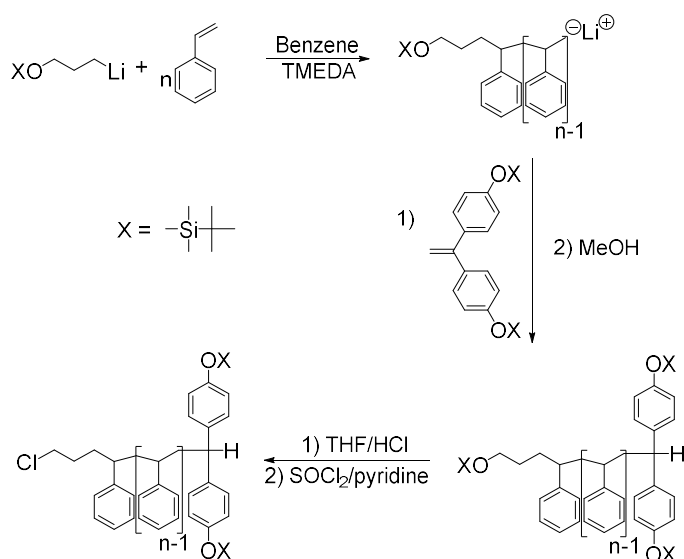
The linear segments in long-chain branched polymers can be linear homopolymers or block copolymer chains. Various methodologies have been reported for synthesis of these polymers, frequently involving the combination of living or controlled polymerisation techniques to generate the linear segments, with the branched segments formed using coupling/branching reactions. Tomalia *et al.* were among the first to report on the synthesis of comb-burst dendrimer-like polymers.¹²² Hadjichristidis *et al.* have reported the use of a stepwise convergent anionic polymerisation methodology combined with DPE/chlorosilane based coupling reactions to synthesise well-defined first and second generation dendrimer-like polybutadienes, after fractionation.¹²⁸ Long-chain hyperbranched polybutadiene and polyisoprenes were prepared by Frey *et al.* also using

an AB_n macromonomer based strategy.¹²⁹⁻¹³⁰ Anionic polymerisation was used to synthesise linear polydiene chains with a high number of side vinyl groups, subsequently end-capped with chlorodimethylsilane, giving an AB_n polydiene. The macromonomer was then bulk polymerised in a polycondensation reaction with Karstedt's catalyst producing branched polybutadiene or polyisoprene. Although effective, this reaction also may generate other problems related to side reactions with the high concentration of vinyl groups.

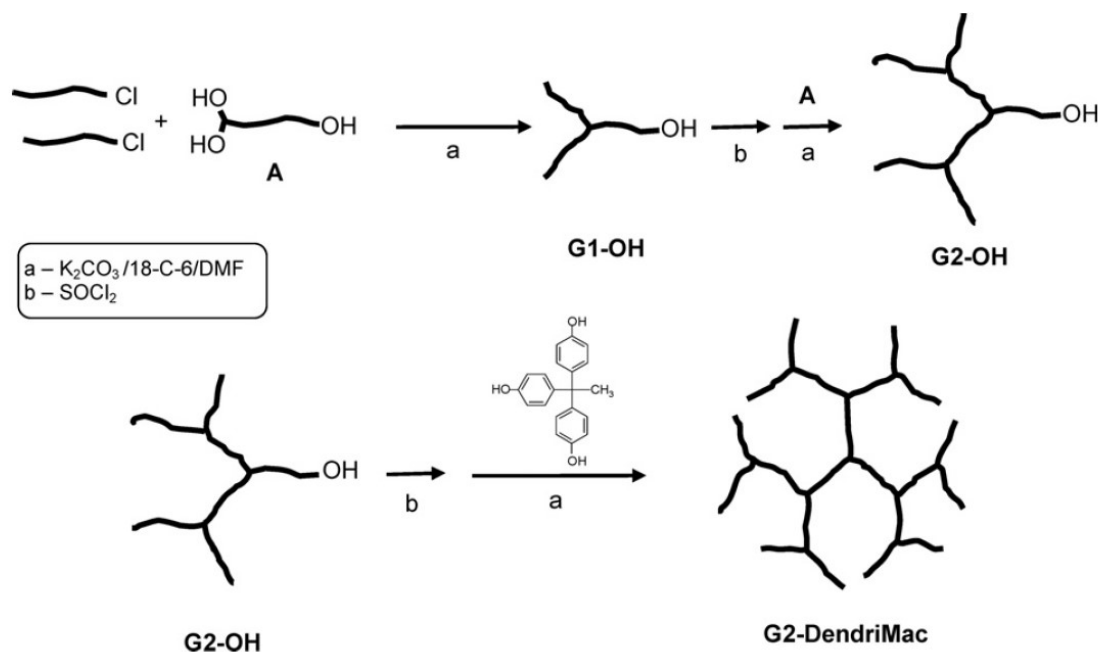
1.6 The “Macromonomer” Approach

For the creation of long-chain branched polymers another strategy, the “Macromonomer” approach, has been developed. The previous techniques for long chain branched synthesis, although effective, do not allow for the tailoring of specific polymers or control over the molecular weight of linear segments between branching points. In the macromonomer approach, end group functionalised linear polymers i.e. macromonomers are used as well-defined building blocks to form long-chain branched polymers, in this way the molecular weight between the branched points can be controlled. This approach was first reported by Hedrick *et al.* to synthesise long-chain hyperbranched poly(ϵ -caprolactone) (PCL) from an AB₂ poly(ϵ -caprolactone) macromonomer.¹³¹

Hutchings *et al.* have developed this method extensively, widely expanding its versatility and first reported its use with vinyl monomers with the synthesis of long-chain branched polystyrene “DendriMacs” using an iterative convergent AB₂ macromonomer approach.¹³² For the preparation of polystyrene DendriMacs, polystyrene chains were synthesised by living anionic polymerisation initiated with a protected functionalised initiator, 3-*tert*-butyldimethylsiloxy-1-propyllithium and end-capped with a difunctional (protected) derivative of DPE. The primary alcohol group was converted to a chloride functionality, producing the AB₂ macromonomer (Scheme 1.13). This macromonomer, after undergoing a series end-group modification and Williamson coupling reactions was then used to produce long-chain branched segments which were then coupled around a core trifunctional molecule giving a G2-DendriMac, (Scheme 1.14).

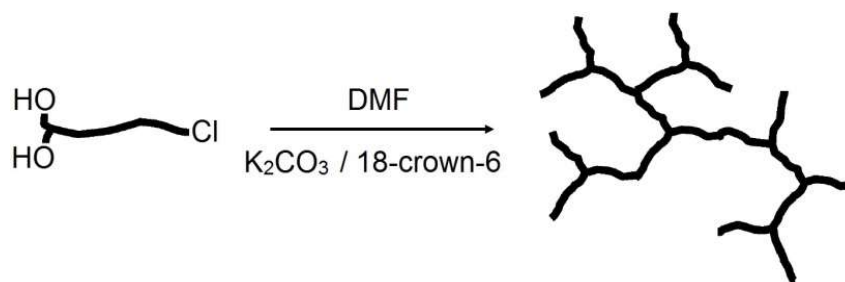


Scheme 1.13 - Synthesis of polystyrene AB₂ macromonomer



Scheme 1.14 - Synthesis of G2 polystyrene DendriMac. Reproduced from Ref 125 with permission of The Royal Society of Chemistry).

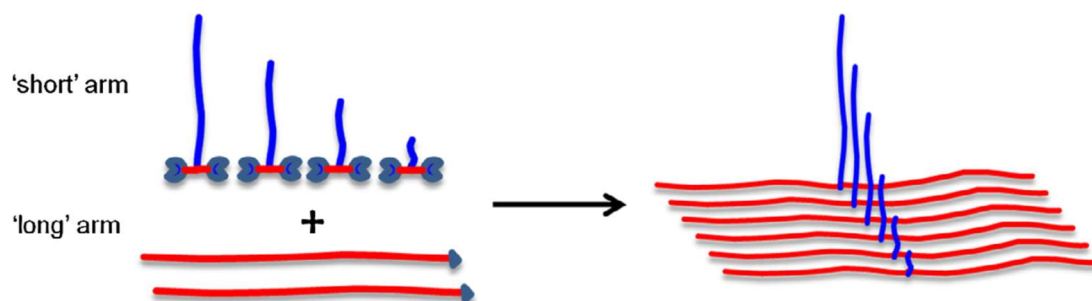
This “macromonomer” approach is extremely versatile for long-chain branched polymer synthesis. It allows for the full characterisation of each polymer segment between each branch point. Hutchings *et al.* have also extended the use of AB_2 macromonomers to synthesise long chain hyperbranched polymers, coined “HyperMacs” using a polycondensation methodology (Scheme 1.15). Polystyrene,¹³³⁻¹³⁴ polybutadiene and poly(methyl methacrylate) HyperMacs have all been reported.¹³⁵



Scheme 1.15 - Synthesis of polystyrene HyperMacs. Reproduced from Ref 125 with permission of The Royal Society of Chemistry).

The strategy has also been extended for the synthesis of “Hyperblocks” – long chain hyperbranched block copolymers.¹³⁵⁻¹³⁶ Anionic polymerisation was used to synthesise an ABA poly(styrene-*b*-isoprene-*b*-styrene) block AB_2 macromonomer, which was subsequently used to synthesise Hyperblocks using a similar synthetic strategy as seen for HyperMacs. This approach has also been adapted for well-defined branched polymer

synthesis. In 2013, Agostini and Hutchings created a series of asymmetric polystyrene three arm stars in which the molecular weight of two “long” arms were kept fixed and the remaining “short” arm’s molecular weight was varied, a schematic of this is given in Scheme 1.16.¹³⁷



Scheme 1.16 - General schematic for the synthesis of asymmetric three-arm stars via macromonomer approach.¹³⁷ Reprinted with permission from [Agostini, S.; Hutchings, L. R., *Eur. Polym. J.* 2013, 49 (9), 2769-2784]. Copyright [2013] Elsevier

The long arm of the asymmetric stars was produced on a large scale, allowing for the same macromonomer to be used in all experiments, permitting for the generation of complete series of homologous star-branched polymers which differ only in the length of the “short” arm; some of these materials were then used as model polymers in a separate rheological study.¹³⁸ The modular approach allows the creation of a range of branched polymers, as macromonomers of any molecular weight can be produced and reacted with any other macromonomer, so long as the end-group functionalities are compatible. However, the macromonomer approach is not without its disadvantages when it comes to creating well-defined model polymers. The ether linkage reactions used to form the final polymers, most often via a Williamson coupling reaction between a primary alcohol functional group and a halide functional group, can often result in incomplete coupling reactions. The use of excess starting materials can minimise this issue but this in turn leads to the need for time-consuming fractionation and purification of products. Even following careful purification, the resultant branched materials themselves may contain small quantities of branched by-products, arising from incomplete coupling. Such a mixture will contain polymers with similar hydrodynamic volumes, making their quantification via size exclusion chromatography (SEC) difficult. In this case, the use of more stringent polymer characterisation methods becomes paramount for quantitative analysis. Nonetheless if such methods are available precise synthesis and characterisation of well-defined model polymers has been demonstrated.

The macromonomer approach remains a versatile, relatively facile and currently the only possible method for the creation of a series of well-defined branched polymers wherein all the components of a final branched material can be fully and independently synthesised, characterised and used in repeated experiments which would be of great use in rheological studies. It also remains the only possible method for the synthesis of long chain branched polymers in which the linear segments of the final polymer can be completely well-defined, characterised and controlled. As such the use of this methodology for the creation of complex well-defined materials is more than viable.

1.7 Aims and Objectives

As mentioned previously, the tyre industry is facing ongoing challenges related to the complex nature of their industrially manufactured polymers. Industrial polymers are often complex, heterogeneous mixtures which are complicated even further by standard industrial processes such as vulcanisation. More specifically, these challenges relate to the processing of raw materials before curing processes such as vulcanisation that these polymers are put through. These materials are often highly heterogeneous polymers with varying degrees of branching and crosslinking. This in turn impacts upon the processability and properties of these polymers when they are eventually vulcanised.

The principal aim of this project is to synthesise and characterise branched polymeric materials of increasingly complex architectures i.e. from linear materials to star-branched, H-shaped and long-chain, randomly-branched polymers, based on monomers used in the tyre industry, principally polybutadiene. This will be achieved using both traditional and novel synthetic methods exploiting anionic polymerisation. These model polymers of complex architectures and mixtures of architectures will then be used as an excellent stepping stone towards understanding the inherently disperse branched polymers encountered in industry.

A key aim of this project will also be the analysis of the materials using a variety of analytical techniques, including size exclusion chromatography and interaction chromatography. Total and accurate characterisation of materials will help build a better understanding of polymer structure, for future rheological studies.

This thesis aims:

- 1) To synthesise and characterise star-branched polymers using temperature gradient interaction chromatography for total structural analysis
- 2) To synthesise, for the first time, a series of H-shaped polymers using the macromonomer approach. This will be achieved by:
 - a. Synthesis of a series of “crossbar” AB₄ macromonomers of increasing molecular weights (30 kg mol⁻¹ to 100 kg mol⁻¹) with chain-end functionality at both ends of the polymer
 - b. Synthesis of a series of complementary “arm” macromonomers (20 kg mol⁻¹ to 50 kg mol⁻¹) for reaction with the crossbars

- c. Creating a homologous series of H-shaped polymers from reaction of a chosen crossbar with each arm.
- 3) To synthesise soluble long-chain, randomly-branched polybutadiene by anionic polymerisation using various chain transfer agents to inhibit gelation.

The chapters in this thesis, although interconnected, are written as stand-alone projects. Thus the following chapters each report on distinct themes. Chapter 2 discusses the synthesis and characterisation of a number of star-branched polymers in relation to the first aim. Chapter 3 details the synthesis and characterisation of polybutadiene macromonomers which are to be used as the “building blocks” for the range of H-shaped polymers, which are then discussed in Chapter 4 in relation to the second aim. Chapter 5 is focused on the synthesis of long-chain, randomly branched polybutadienes by the adaptation of a free-radical based synthetic method to anionic polymerisation in relation to the third aim. Due to the structure of the thesis, there may be some repetition regarding the materials used, the synthetic and characterisation methods, and other details reported in the experimental sections of Chapters 2 – 5. Although the focus of this PhD project was on the synthesis of such polymers, this project was carried out in collaboration with a second PhD project strictly focussing on the rheological properties of the described materials.

1.8 References

1. *ETRMA Annual Report 2013/2014*; European Tyre & Rubber Manufacturers' Association: Brussels, 2014.
2. *Statistics Edition 2015*; European Tyre & Rubber Manufacturers' Association: 2015.
3. European Parliament, On the Labelling of Tyres with respect to Fuel Efficiency and other Essential Parameters. In *No 1222/2009*, EU, Ed. 2009; pp 46-58.
4. Sienkiewicz, M.; Kucinska-Lipka, J.; Janik, H.; Balas, A., *Waste Manag.* **2012**, *32* (10), 1742-51.
5. Wang, M.-J., *Rubber Chem. Technol.* **1998**, *71* (3), 520-589.
6. Hsieh, H. L.; Quirk, R. P., *Anionic Polymerization: Principles and Practical Applications*. Marcel Dekker: New York, 1996.
7. England, R. M.; Rimmer, S., *Polym. Chem.* **2010**, *1* (10), 1533-1544.
8. Hutchings, L. R.; Kimani, S. M.; Hoyle, D. M.; Read, D. J.; Das, C.; McLeish, T. C. B.; Chang, T.; Lee, H.; Auhl, D., *ACS Macro Letters* **2012**, *1* (3), 404-408.
9. Yamamoto K; Nobuyuki Y; Yasushi O; Akio I; Tomoaki S; Furukawa, A; Yuichi S. US Patent 4523618; 1985.
10. Braun, D.; Cherdrón, H.; Rehahn, M.; Ritter, H.; Voit, B., *Polymer Synthesis: Theory and Practice : Fundamentals, Methods, Experiments* 5th ed.; Springer: Germany, 2013; p 432.
11. Young, R. J.; P.A, L., *Introduction to Polymers*. 2nd ed.; Chapman & Hall: United Kingdom, 1991.
12. Rowan, S. J.; Barner-Kowollik, C.; Klumperman, B.; Gaspard, P.; Grubbs, R. B.; Hillmyer, M. A.; Hutchings, L. R.; Mahanthappa, M. K.; Moatsou, D.; O'Reilly, R. K.; Ouchi, M.; Sawamoto, M.; Lodge, T. P., *ACS Macro Letters* **2016**, *5* (1), 1-3.
13. Baekeland LH. US Patent 0942699; 1907.
14. Carothers, W. H., *Trans. Faraday Soc.* **1936**, *32* (0), 39-49.
15. Signer, R.; Houwink, R.; Weiser, H. B.; Meyer, K. H.; Mark, H.; Staudinger, H.; Carothers, W. H., *Trans. Faraday Soc.* **1936**, *32* (0), 49-53.
16. Billiet, L.; Fournier, D.; Du Prez, F., *Polymer* **2009**, *50* (16), 3877-3886.
17. Radhakrishnan, B.; Cloutet, E.; Cramail, H., *Colloid. Polym. Sci.* **2002**, *280* (12), 1122-1130.
18. Zhang, M.; June, S. M.; Long, T. E.; Kong, J., Principles of Step-Growth Polymerization (Polycondensation and Polyaddition). In *Reference Module in Materials Science and Materials Engineering*, Elsevier: 2016.
19. Braun, D., *Int. J. Polym. Sci.* **2009**, 2009.
20. Flory, P. J., *J. Am. Chem. Soc.* **1937**, *59* (2), 241-253.
21. Braunecker, W. A.; Matyjaszewski, K., *Prog. Polym. Sci.* **2007**, *32* (1), 93-146.
22. Kamigaito, M.; Ando, T.; Sawamoto, M., *Chem. Rev.* **2001**, *101* (12), 3689-3746.
23. Jenkins Aubrey, D.; Jones Richard, G.; Moad, G., Terminology for reversible-deactivation radical polymerization previously called "controlled" radical or "living" radical polymerization (IUPAC Recommendations 2010). In *Pure Appl. Chem.*, 2009; Vol. 82, p 483.
24. Kato, M.; Kamigaito, M.; Sawamoto, M.; Higashimura, T., *Macromolecules* **1995**, *28* (5), 1721-1723.
25. Wang, J.-S.; Matyjaszewski, K., *J. Am. Chem. Soc.* **1995**, *117* (20), 5614-5615.

26. Chiefari, J.; Chong, Y. K.; Ercole, F.; Krstina, J.; Jeffery, J.; Le, T. P. T.; Mayadunne, R. T. A.; Meijs, G. F.; Moad, C. L.; Moad, G.; Rizzardo, E.; Thang, S. H., *Macromolecules* **1998**, *31* (16), 5559-5562.
27. Moad, G.; Rizzardo, E.; Thang, S. H., *Aust. J. Chem.* **2012**, *65* (8), 985-1076.
28. Nesvadba, P., **2012**.
29. Quirk, R. P.; Lee, B., *Polym. Int.* **1992**, *27* (4), 359-367.
30. Penczek, S.; Kubisa, P.; Szymanski, R., *Macromol Rapid Commun.* **1991**, *12* (2), 77-80.
31. Aoshima, S.; Kanaoka, S., *Chem. Rev.* **2009**, *109* (11), 5245-5287.
32. Szwarc, M.; Levy, M.; Milkovich, R., *J. Am. Chem. Soc.* **1956**, *78* (11), 2656-2657.
33. Szwarc, M., *Nature* **1956**, *178* (4543), 1168-1169.
34. Morton, M.; Fetters, L. J., *Rubber Chem. Technol.* **1975**, *48* (3), 359-409.
35. Young, R. N.; Quirk, R. P.; Fetters, L. J., Anionic polymerizations of non-polar monomers involving lithium. In *Anionic Polymerization*, Springer Berlin Heidelberg: Berlin, Heidelberg, 1984; pp 1-90.
36. Luxton, A. R., *Rubber Chem. Technol.* **1981**, *54* (3), 596-626.
37. Gatzke, A. L., *J. Polym. Sci., Part A-1: Polym. Chem.* **1969**, *7* (8), 2281-2292.
38. Beikhol'd, G. A.; Matkovskii, P. Y.; Kissin, Y. V.; Brikshtein, K. M. A.; D'Yachkovskii, F. S., *Polymer Science U.S.S.R.* **1971**, *13* (1), 149-158.
39. Reich, H. J., *Chem. Rev.* **2013**, *113* (9), 7130-7178.
40. Quirk, R. P.; Yin, J.; Fetters, L. J., *Macromolecules* **1989**, *22* (1), 85-90.
41. Quirk, R. P.; Chen, W.-C., *Die Makromolekulare Chemie* **1982**, *183* (9), 2071-2076.
42. Quirk, R. P.; Ma, J.-J., *J. Polym. Sci., Part A: Polym. Chem.* **1988**, *26* (8), 2031-2037.
43. Hirao, A.; Goseki, R.; Ishizone, T., *Macromolecules* **2014**, *47* (6), 1883-1905.
44. Jackson, A. T.; Bunn, A.; Hutchings, L. R.; Kiff, F. T.; Richards, R. W.; Williams, J.; Green, M. R.; Bateman, R. H., *Polymer* **2000**, *41* (20), 7437-7450.
45. Hunt, M. O.; Belu, A. M.; Linton, R. W.; DeSimone, J. M., *Macromolecules* **1993**, *26* (18), 4854-4859.
46. Natalello, A.; Hall, J. N.; Eccles, E. A.; Kimani, S. M.; Hutchings, L. R., *Macromol. Rapid Commun.* **2011**, *32* (2), 233-7.
47. Sugiyama, K.; Nemoto, T.; Koide, G.; Hirao, A., *Macromol. Symp.* **2002**, *181* (1), 135-154.
48. El-Shehawy, A. A.; Yokoyama, H.; Sugiyama, K.; Hirao, A., *Macromolecules* **2005**, *38* (20), 8285-8299.
49. Fetters, L. J.; Firer, E. M., *Polymer* **1977**, *18* (3), 306-307.
50. Wyman, D. P.; Allen, V. R.; Altares, T., *J. Polym. Sci., Part A: Gen. Pap.* **1964**, *2* (10), 4545-4550.
51. Uhrig, D.; Mays, J. W., *J. Polym. Sci., Part A: Polym. Chem.* **2005**, *43* (24), 6179-6222.
52. Hadjichristidis, N.; Iatrou, H.; Pispas, S.; Pitsikalis, M., *J. Polym. Sci., Part A: Polym. Chem.* **2000**, *38* (18), 3211-3234.
53. Staudinger, H.; Fritsch, J., *Helv. Chim. Acta* **1922**, *5* (5), 785-806.
54. Mykhaylyk, O. O.; Fernyhough, C. M.; Okura, M.; Fairclough, J. P. A.; Ryan, A. J.; Graham, R., *Eur. Polym. J.* **2011**, *47* (4), 447-464.
55. Bywater, S.; Firat, Y.; Black, P. E., *J. Polym. Sci., Part A: Polym. Chem.* **1984**, *22* (3), 669-672.

56. Morton, M.; Rupert, J. R., Factors Affecting the Isomeric Chain Unit Structure in Organolithium Polymerization of Butadiene and Isoprene. In *Initiation of Polymerization*, American Chemical Society: 1983; Vol. 212, pp 283-289.
57. Bywater, S.; Worsfold, D. J.; Hollingsworth, G., *Macromolecules* **1972**, 5 (4), 389-393.
58. Kanaoka, S.; Sawamoto, M.; Higashimura, T., *Macromolecules* **1991**, 24 (9), 2309-2313.
59. Baek, K.-Y.; Kamigaito, M.; Sawamoto, M., *Macromolecules* **2001**, 34 (2), 215-221.
60. Baek, K.-Y.; Kamigaito, M.; Sawamoto, M., *Macromolecules* **2001**, 34 (22), 7629-7635.
61. Gao, H.; Matyjaszewski, K., *Macromolecules* **2006**, 39 (15), 4960-4965.
62. Gao, H.; Matyjaszewski, K., *Macromolecules* **2008**, 41 (4), 1118-1125.
63. Hadjichristidis, N.; Pitsikalis, M.; Pispas, S.; Iatrou, H., *Chem. Rev.* **2001**, 101 (12), 3747-3792.
64. Polymeropoulos, G.; Zapsas, G.; Ntetsikas, K.; Bilalis, P.; Gnanou, Y.; Hadjichristidis, N., *Macromolecules* **2017**, 50 (4), 1253-1290.
65. Adams, C. H.; Hutchings, L. R.; Klein, P. G.; McLeish, T. C. B.; Richards, R. W., *Macromolecules* **1996**, 29 (17), 5717-5722.
66. Richards, R. W., *Macromolecules* **1999**, 32 (3), 880-891.
67. Hwang, J.; Foster, M. D.; Quirk, R. P., *Polymer* **2004**, 45 (3), 873-880.
68. Lee, J. H.; Fetters, L. J.; Archer, L. A.; Halasa, A. F., *Macromolecules* **2005**, 38 (9), 3917-3932.
69. Lee, J. H.; Goldberg, J. M.; Fetters, L. J.; Archer, L. A., *Macromolecules* **2006**, 39 (19), 6677-6685.
70. Ratkanthwar, K. R.; Hadjichristidis, N.; Pudukulathan, Z., *Chemistry Journal* **2013**, 1 (3), 90-96.
71. Gervasi, J. A.; Gosnell, A. B., *J. Polym. Sci., Part A-1: Polym. Chem.* **1966**, 4 (6), 1391-1399.
72. Lebreton, A.; Kallitsis, J. K.; Héroguez, V.; Gnanou, Y., *Macromol. Symp.* **2004**, 215 (1), 41-50.
73. Morton, M.; Helminiak, T. E.; Gadkary, S. D.; Bueche, F., *J. Polym. Sci.* **1962**, 57 (165), 471-482.
74. Eschwey, H.; Burchard, W., *Polymer* **1975**, 16 (3), 180-184.
75. Gnanou, Y.; Lutz, P.; Rempp, P., *Die Makromolekulare Chemie* **1988**, 189 (12), 2885-2892.
76. Hadjichristidis, N.; Guyot, A.; Fetters, L. J., *Macromolecules* **1978**, 11 (4), 668-672.
77. Hadjichristidis, N.; Fetters, L. J., *Macromolecules* **1980**, 13 (1), 191-193.
78. Hutchings, L. R.; Richards, R. W., *Polym. Bull.* **1998**, 41 (3), 283-289.
79. Zhou, L. L.; Roovers, J., *Macromolecules* **1993**, 26 (5), 963-968.
80. Zhou, L. L.; Hadjichristidis, N.; Toporowski, P. M.; Roovers, J., *Rubber Chem. Technol.* **1992**, 65 (2), 303-314.
81. Roovers, J.; Zhou, L. L.; Toporowski, P. M.; van der Zwan, M.; Iatrou, H.; Hadjichristidis, N., *Macromolecules* **1993**, 26 (16), 4324-4331.
82. Quirk, R. P.; Lee, B., *Makromol. Chem., Macromol. Symp.* **1992**, 53 (1), 201-210.
83. Quirk, R. P.; Yoo, T., *Polym. Bull.* **1993**, 31 (1), 29-36.
84. Fujimoto, T.; Zhang, H.; Kazama, T.; Isono, Y.; Hasegawa, H.; Hashimoto, T., *Polymer* **1992**, 33 (10), 2208-2213.

85. Hirao, A.; Hayashi, M.; Loykulnant, S.; Sugiyama, K.; Ryu, S. W.; Haraguchi, N.; Matsuo, A.; Higashihara, T., *Prog. Polym. Sci.* **2005**, *30* (2), 111-182.
86. Hirao, A.; Inoue, K.; Higashihara, T., *Macromol. Symp.* **2006**, *240* (1), 31-40.
87. Roovers, J.; Toporowski, P. M., *Macromolecules* **1981**, *14* (5), 1174-1178.
88. Hakiki, A.; Young, R. N.; McLeish, T. C. B., *Macromolecules* **1996**, *29* (10), 3639-3641.
89. Iatrou, H.; Avgeropoulos, A.; Hadjichristidis, N., *Macromolecules* **1994**, *27* (21), 6232-6233.
90. Iatrou, H.; Willner, L.; Hadjichristidis, N.; Halperin, A.; Richter, D., *Macromolecules* **1996**, *29* (2), 581-591.
91. Hadjichristidis, N.; Xenidou, M.; Iatrou, H.; Pitsikalis, M.; Poulos, Y.; Avgeropoulos, A.; Sioula, S.; Paraskeva, S.; Velis, G.; Lohse, D. J.; Schulz, D. N.; Fetters, L. J.; Wright, P. J.; Mendelson, R. A.; García-Franco, C. A.; Sun, T.; Ruff, C. J., *Macromolecules* **2000**, *33* (7), 2424-2436.
92. Rahman, M. S.; Aggarwal, R.; Larson, R. G.; Dealy, J. M.; Mays, J., *Macromolecules* **2008**, *41* (21), 8225-8230.
93. Li, S. W.; Park, H. E.; Dealy, J. M., *J. Rheol.* **2011**, *55* (6), 1341.
94. Ito, S.; Goseki, R.; Ishizone, T.; Hirao, A., *Polym. Chem.* **2014**, *5* (19), 5523-5534.
95. Hadjichristidis, N.; Roovers, J., *J. Polym. Sci. B* **1978**, *16* (5), 851-858.
96. Kowalczyk, M.; Adamus, G.; Jedlinski, Z., *Macromolecules* **1994**, *27* (2), 572-575.
97. Deffieux, A.; Schappacher, M., *Macromolecules* **1999**, *32* (6), 1797-1802.
98. Hong, S. C.; Jia, S.; Teodorescu, M.; Kowalewski, T.; Matyjaszewski, K.; Gottfried, A. C.; Brookhart, M., *J. Polym. Sci., Part A: Polym. Chem.* **2002**, *40* (16), 2736-2749.
99. Nikopoulou, A.; Iatrou, H.; Lohse, D. J.; Hadjichristidis, N., *J. Polym. Sci., Part A: Polym. Chem.* **2009**, *47* (10), 2597-2607.
100. Gao, C.; Yan, D., *Prog. Polym. Sci.* **2004**, *29* (3), 183-275.
101. Twyman, L. J.; Beezer, A. E.; Esfand, R.; Hardy, M. J.; Mitchell, J. C., *Tetrahedron Lett.* **1999**, *40* (9), 1743-1746.
102. Liu, M.; Kono, K.; Fréchet, J. M. J., *J. Control. Release* **2000**, *65* (1-2), 121-131.
103. Fréchet, J. M. J., *J. Polym. Sci., Part A: Polym. Chem.* **2003**, *41* (23), 3713-3725.
104. Voit, B. I.; Lederer, A., *Chem. Rev.* **2009**, *109* (11), 5924-5973.
105. Zheng, Y.; Li, S.; Weng, Z.; Gao, C., *Chem. Soc. Rev.* **2015**, *44* (12), 4091-4130.
106. Uppuluri, S.; Keinath, S. E.; Tomalia, D. A.; Dvornic, P. R., *Macromolecules* **1998**, *31* (14), 4498-4510.
107. Dodds, J. M.; De Luca, E.; Hutchings, L. R.; Clarke, N., *J. Polym. Sci., Part B: Polym. Phys.* **2007**, *45* (19), 2762-2769.
108. Flory, P. J., *J. Am. Chem. Soc.* **1941**, *63* (11), 3083-3090.
109. Tomalia, D. A.; Baker, H.; Dewald, J.; Hall, M.; Kallos, G.; Martin, S.; Roeck, J.; Ryder, J.; Smith, P., *Polym. J.* **1985**, *17* (1), 117-132.
110. Newkome, G. R.; Yao, Z.; Baker, G. R.; Gupta, V. K., *J. Org. Chem.* **1985**, *50* (11), 2003-2004.
111. Tomalia, D. A.; Fréchet, J. M. J., *J. Polym. Sci., Part A: Polym. Chem.* **2002**, *40* (16), 2719-2728.
112. Inoue, K., *Prog. Polym. Sci.* **2000**, *25* (4), 453-571.
113. Kim, Y. H.; Webster, O. W., *Macromolecules* **1992**, *25* (21), 5561-5572.
114. Shu, C.-F.; Leu, C.-M., *Macromolecules* **1999**, *32* (1), 100-105.

115. Fréchet, J. M. J.; Henmi, M.; Gitsov, I.; Aoshima, S.; Leduc, M. R.; Grubbs, R. B., *Science* **1995**, 269 (5227), 1080.
116. Sunder, A.; Hanselmann, R.; Frey, H.; Mülhaupt, R., *Macromolecules* **1999**, 32 (13), 4240-4246.
117. Emrick, T.; Chang, H.-T.; Fréchet, J. M. J., *Macromolecules* **1999**, 32 (19), 6380-6382.
118. van Ruymbeke, E.; Orfanou, K.; Kapnistos, M.; Iatrou, H.; Pitsikalis, M.; Hadjichristidis, N.; Lohse, D. J.; Vlassopoulos, D., *Macromolecules* **2007**, 40 (16), 5941-5952.
119. Taton, D.; Feng, X.; Gnanou, Y., *New J. Chem.* **2007**, 31 (7), 1097.
120. Kimani, S. M.; Hutchings, L. R., *Macromol. Rapid Commun.* **2008**, 29 (8), 633-637.
121. Hirao, A.; Yoo, H.-S., *Polym. J.* **2011**, 43 (1), 2-17.
122. Tomalia, D. A.; Hedstrand, D. M.; Ferritto, M. S., *Macromolecules* **1991**, 24 (6), 1435-1438.
123. Grubbs, R. B.; Hawker, C. J.; Dao, J.; Fréchet, J. M. J., *Angew. Chem. Int. Ed.* **1997**, 36 (3), 270-272.
124. Gauthier, M., *J. Polym. Sci., Part A: Polym. Chem.* **2007**, 45 (17), 3803-3810.
125. Hutchings, L. R., *Soft Matter* **2008**, 4 (11), 2150-2159.
126. Teertstra, S. J.; Gauthier, M., *Prog. Polym. Sci.* **2004**, 29 (4), 277-327.
127. Konkolewicz, D.; Monteiro, M. J.; Perrier, S., *Macromolecules* **2011**, 44 (18), 7067-7087.
128. Orfanou, K.; Iatrou, H.; Lohse, D. J.; Hadjichristidis, N., *Macromolecules* **2006**, 39 (13), 4361-4365.
129. López-Villanueva, F.-J.; Wurm, F.; Kilbinger, A. F. M.; Frey, H., *Macromol. Rapid Commun.* **2007**, 28 (6), 704-709.
130. Wurm, F.; López-Villanueva, F.-J.; Frey, H., *Macromol. Chem. Phys.* **2008**, 209 (7), 675-684.
131. Trollsås, M.; Atthoff, B.; Claesson, H.; Hedrick, J. L., *Macromolecules* **1998**, 31 (11), 3439-3445.
132. Hutchings, L. R.; Roberts-Bleming, S. J., *Macromolecules* **2006**, 39 (6), 2144-2152.
133. Hutchings, L. R.; Dodds, J. M.; Roberts-Bleming, S. J., *Macromol. Symp.* **2006**, 240 (1), 56-67.
134. Hutchings, L. R.; Dodds, J. M.; Roberts-Bleming, S. J., *Macromolecules* **2005**, 38 (14), 5970-5980.
135. Hutchings, L. R.; Dodds, J. M.; Rees, D.; Kimani, S. M.; Wu, J. J.; Smith, E., *Macromolecules* **2009**, 42 (22), 8675-8687.
136. Hutchings, L. R.; Agostini, S.; Hamley, I. W.; Hermida-Merino, D., *Macromolecules* **2015**, 48 (24), 8806-8822.
137. Agostini, S.; Hutchings, L. R., *Eur. Polym. J.* **2013**, 49 (9), 2769-2784.
138. Huang, Q.; Agostini, S.; Hengeller, L.; Shivokhin, M.; Alvarez, N. J.; Hutchings, L. R.; Hassager, O., *Macromolecules* **2016**, 49 (17), 6694-6699.

Chapter 2

**Synthesis and characterisation of Star-Branched
Polybutadienes**

2.1 Introduction

The study of well-defined model branched polymers has, for synthetic chemists and rheologists alike, been of critical importance in understanding the relationships between polymer architecture and physical/mechanical properties. Since its discovery in 1956 by Szwarc,¹ living anionic polymerisation has been a vital tool in the creation of well-defined polymers with narrow dispersities (below $\bar{D} = 1.05$), with fine control over both molecular weight and architecture.

Presently, most synthetic polymers are characterised (in terms of molecular weight and composition) using size exclusion chromatography (SEC). Moreover, SEC is often incapable of separating polymers with different molecular weights but similar hydrodynamic volumes, which may be the case in mixtures of branched polymers. However, in recent years, interaction chromatography (IC) and in particular, temperature gradient interaction chromatography (TGIC) has developed as a technique for the analysis of complex polymers and is capable of significantly enhanced resolution compared to SEC. Due to the substantial importance of IC to the work described in this thesis, it will be discussed in full later in the chapter.

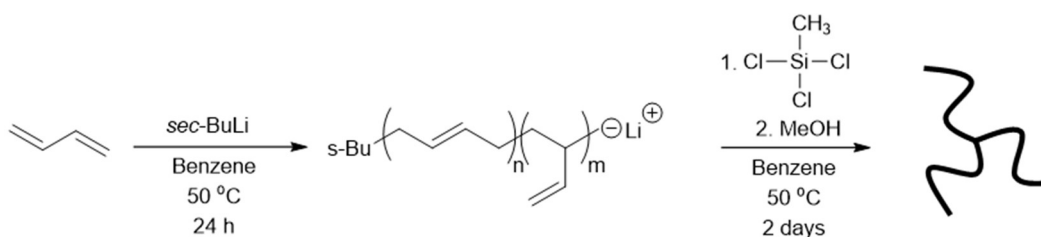
We describe here the use of the living anionic polymerisation for the synthesis of both three-arm and four-arm star-branched polybutadiene polymers, to be used as model polymers for structure-property correlation rheological studies. The polymers produced have been characterised using both size exclusion chromatography and interaction chromatography for total structural characterisation.

2.2 Results and Discussion

Three- and four-arm star-branched polybutadienes were prepared using an arm-first approach via living anionic polymerisation and chlorosilane chemistry, as outlined in Chapter 1 (section 1.5.2.1). The code to refer to the star polymers is “Star(X)Y” – with X referring to the number of arms present for the respective star and Y referring to the molecular weight (M_n) in kg mol^{-1} .

2.2.1 Synthesis of Three-Arm Star - Star(3)150

The first polymer to be prepared was a three-arm star-branched polybutadiene (Star(3)150); the synthetic route is given below in Scheme 2.1.



Scheme 2.1 - Synthesis of three-arm star polybutadiene

The initiator chosen was *sec*-butyllithium (*sec*-BuLi) due to its speed of initiation in hydrocarbon solvents with regards to diene polymerisations.² Benzene was chosen as the solvent owing to its advantageous properties for the anionic polymerisation of dienes at low to moderate temperatures while avoiding the onset of chain transfer or termination reactions, as well as producing polydienes with high 1,4-content.³

The target molecular weight for the three-arm star was $150,000 \text{ g mol}^{-1}$, with each branch having a molecular weight of $50,000 \text{ g mol}^{-1}$. In the first step, 1,3-butadiene was polymerised with *sec*-BuLi for 24 hours at 50°C to generate the linear precursor polybutadiene “arms”. Before addition of the linking agent, a small sample of the precursor arms was collected into a side flask and terminated, with methanol, for molecular weight analysis. To maximize the extent of the coupling reaction, methyltrichlorosilane was then added to the remaining living polymer solution in sufficient quantity that there was a 25% molar excess of living polymer (chain ends) to the chlorosilane groups, which was then left to react with the arms for two days to form the three-arm star polymer.

^1H -NMR characterisation was carried out on the precursor arm polymer (Star(3)150_Arm) in order to determine its microstructure and is given in Figure 2.1.

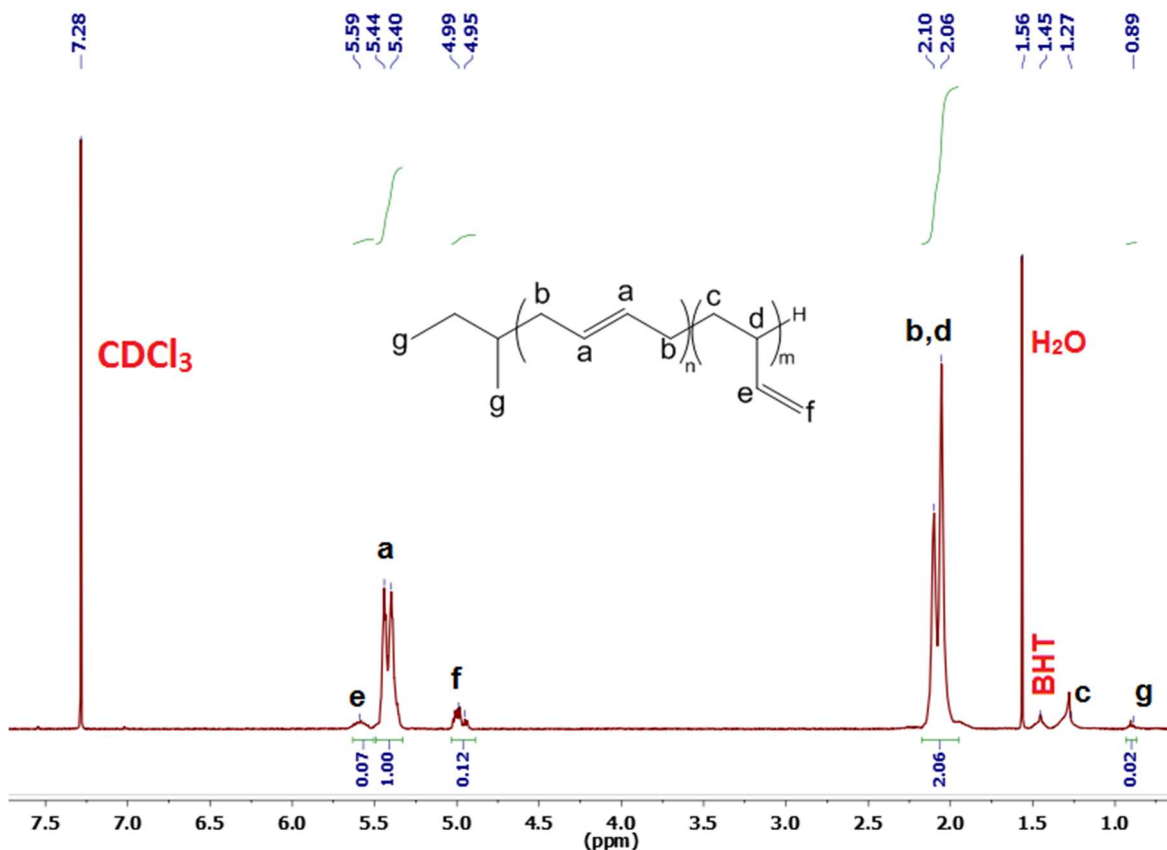


Figure 2.1 - ^1H -NMR spectrum of precursor arm polybutadiene Star(3)150_Arm

Microstructure is a very important attribute for polydiene materials. The microstructure can determine certain mechanical and thermal properties of a polydiene polymer. Conjugated 1,3-polydienes can polymerise to form four isomeric microstructures, illustrated in Figure 2.2. When $\text{R} = \text{H}$, 1,2- microstructure is equivalent to 3,4-, which is the case for polybutadiene.

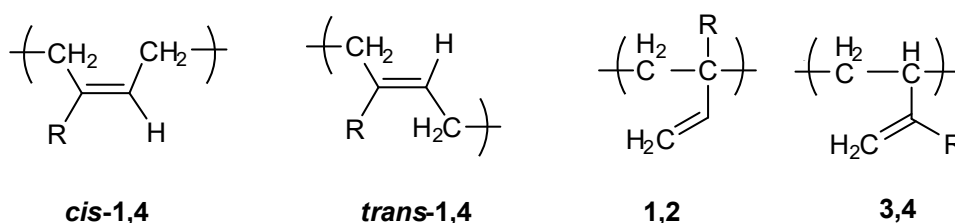


Figure 2.2 - Polydiene microstructures

Polydiene microstructure is determined by the reaction conditions in which polymerisation is carried out and is affected by a number of factors including the metal counterion of the initiator, solvent and the presence of a Lewis base such as Group I metal

alkoxides.² High *cis*-1,4-polybutadiene has good heat stability, low glass transition temperatures (T_g), and desirable elastomeric properties above room temperature, making its processing and blending with other materials advantageous for industrial purposes; as such in this work it was important that the 1,2- or pendant vinyl content of polymers synthesised was kept to a minimum, which again justified the use of alkyllithium initiators and non-polar hydrocarbon solvents. ^1H -NMR spectroscopy is a valuable way of characterising the microstructure of polydienes. In polybutadiene, the peak at 5.4 ppm is representative of the two “a” protons present on the main linear chain backbone i.e. the 1,4-content present in the polymer and the peak at 5.0 ppm is representative of the two “f” protons present on the pendant groups attached to the main chain i.e. the amount of 1,2- or vinyl content present in the polymer. Integration of these peaks to determine their areas is then used to determine the exact percentage of 1,4-content present in the polymer in question, which was determined to be 94% for the precursor arm polymer (Star(3)150_Arm).

Triple detection size exclusion chromatography (SEC) was used for molecular weight measurements for both the precursor arm and the crude star and their chromatograms are presented in Figure 2.3.

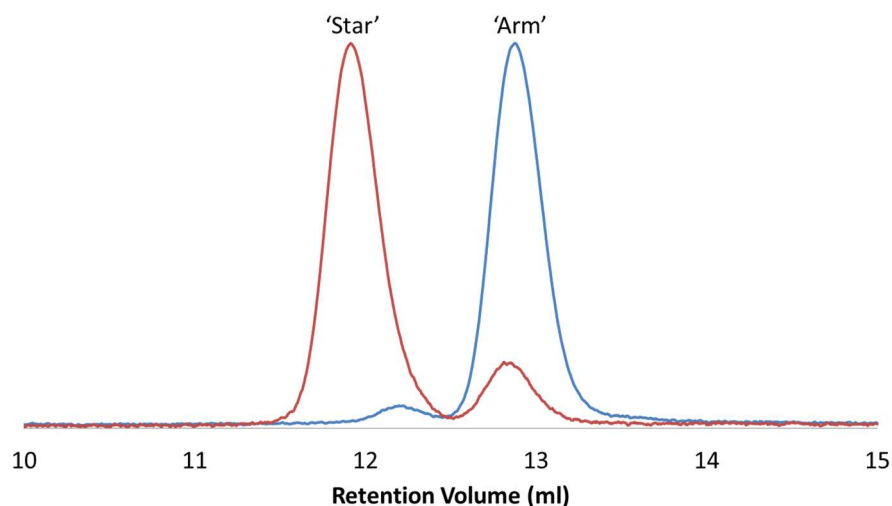


Figure 2.3 - SEC chromatograms (RI detector) of polybutadiene Star(3)150. Comparison of the linear arm precursor (blue) and the final crude star mixture (red).

It can be seen from the chromatograms above that a high level of arm coupling has been achieved in the star synthesis, with the peak eluting at 11.9 ml representing the branched product. There is also a decrease in size of the peak representing the precursor arm at 12.8 ml, which can still be detected in the chromatogram of the crude star, due to the arm

being used in excess with respect to the methyltrichlorosilane. The three-arm star was then purified by fractionation, to remove the excess unreacted arm (a complete description of the fractionation process is given in the experimental section of this chapter). It can be seen in Figure 2.4, that with each fractionation cycle, low molecular weight impurity is removed from the crude mixture until no more can be detected by SEC. Four cycles of fractionation were completed in total and SEC analysis of the fractions in the final cycle indicated the detection of excess arm polymer was no longer possible and the purification of the crude star polymer was completed.

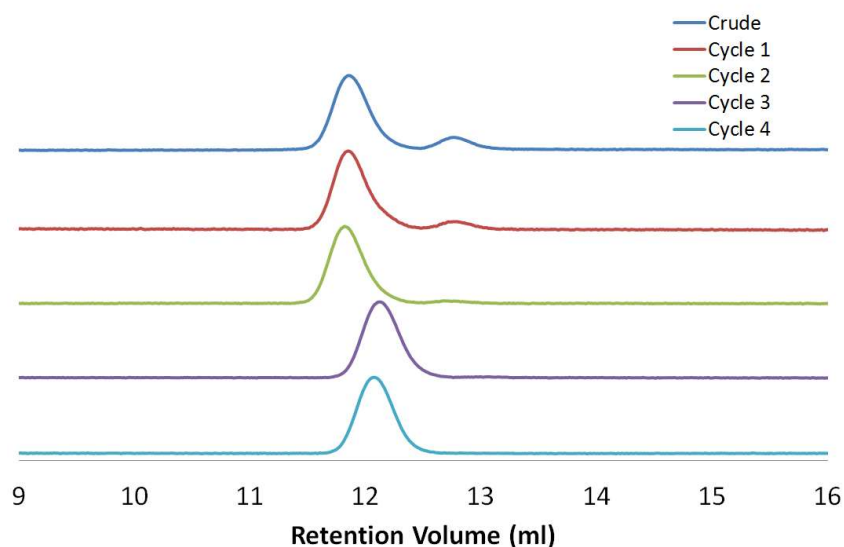


Figure 2.4 - SEC chromatograms (RI detector) of three-arm polybutadiene Star(3)150 from the initial crude material through four cycles of fractionation

Molecular weight analysis (SEC) was carried out on the linear precursor arm, the crude star and the purified star and these are presented overleaf in Table 2.1. A dn/dc value of 0.124 ml/g was used for polybutadiene in THF.⁴ It can be seen that the linear precursor arms had an M_n of 53,000 g mol⁻¹, an M_w of 56,000 g mol⁻¹, and a low dispersity value (\mathcal{D}) of 1.05, closely matching that of the target M_n of 50,000 g mol⁻¹. The crude star polymer possessed an M_n of 123,000 g mol⁻¹, an M_w of 142,000 g mol⁻¹, and a \mathcal{D} of 1.16. The functionality of the star gives an indication of the efficiency of the linking reaction, i.e. the number of arms per star. This is calculated simply by the ratio of the M_n (star)/ M_n (arm), which in the case of Star(3)150 gave a value of 2.32 for the unfractionated crude star. While this figure may seem low, it is important to note that the crude polymer still contains a significant amount of low molecular weight unreacted arm material, lowering its M_n , as well as increasing its dispersity. The purified star polymer produced an M_n of 148,000 g mol⁻¹, an M_w of 151,000 g mol⁻¹, and a \mathcal{D} of 1.02. The functionality of the purified

star was 2.79, with this number being more representative of the final star due to the removal of the lower molecular weight excess arm and again indicating that the linking reaction had gone to a high level of completion.

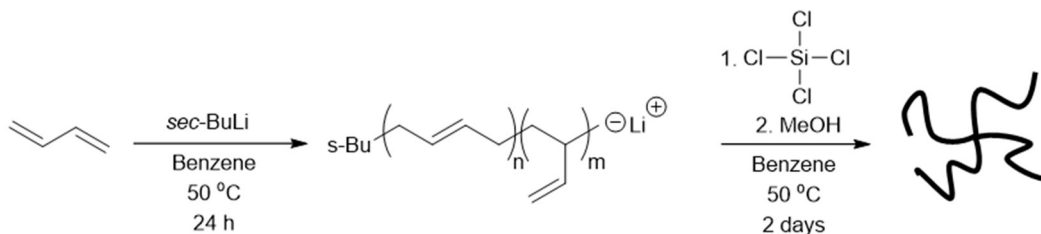
Table 2.1 - Molecular weight, dispersity and microstructure values for three-arm star polybutadiene Star(3)150 obtained by SEC

Polymer	Target M_n (g mol ⁻¹)	M_n (g mol ⁻¹)	M_w (g mol ⁻¹)	\bar{D}	Functionality of star	% 1,4- microstructure
Star(3)150						
Arm	50,000	53,000	56,000	1.05	-	94
Crude Star	150,000	123,000	142,000	1.16	2.32	94
Pure Star	150,000	148,000	151,000	1.02	2.79	94

Having successfully prepared and purified a 3-arm star-branched polybutadiene the synthesis of a 4-arm star was attempted.

2.2.2 Synthesis of Four-Arm Star

2.2.2.1 Initial attempt - Star(4)180



Scheme 2.2 - Synthesis of four-arm polybutadiene Star(4)180

A four-arm polybutadiene star polymer was prepared under the same reaction conditions used for Star(3)150, except that silicon tetrachloride was used as the coupling agent (Scheme 2.2). A molar ratio of 5 : 4 - precursor arm chains : chlorosilane groups - was used to maximise the extent of coupling. The precursor arm target molecular weight was 50,000 g mol⁻¹. Although the coupling reaction initially appeared successful (Figure 2.5), SEC analysis of the resultant crude polymer indicated that arm coupling was incomplete (Table 2.2).

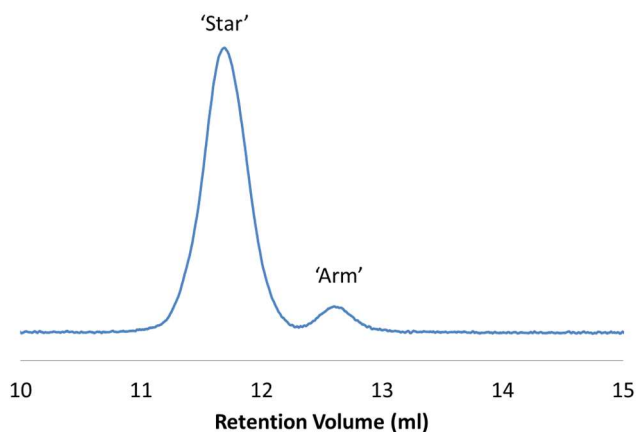


Figure 2.5 - SEC chromatogram (RI detector) of crude polybutadiene Star(4)180

Table 2.2 - Molecular weight and dispersity values for incomplete four-arm star polybutadiene Star(4)180 obtained by SEC

Polymer	Target M_n (g mol ⁻¹)	M_n (g mol ⁻¹)	M_w (g mol ⁻¹)	\bar{D}	Functionality of star	% 1,4- microstructure
Star(4)180						
Arm	50,000	67,500	71,300	1.06	-	94
Crude Star	270,000	183,100	198,200	1.08	2.71	94

SEC analysis of the precursor arm peak at 12.6 ml gave molecular weight values of M_n 67,500 g mol⁻¹, M_w 71,300 g mol⁻¹ and \bar{D} 1.06 – significantly above the target M_n of 50,000 g mol⁻¹. Bearing the higher than expected M_n of the precursor arms in mind, the target molecular weight of the final four arm star should theoretically be around 270,000 g mol⁻¹. However, analysis of the crude product indicated molecular weight values of M_n 183,100 g mol⁻¹, M_w 198,200 g mol⁻¹ and \bar{D} 1.08, with the functionality of this polymer calculated to be 2.71, suggesting that at most, only a three-arm star has formed. A number of reasons could be the cause of these results and the incomplete coupling. The time allowed for the linking reaction (2 days) could have been insufficient for the complete coupling to take place, and extra time may have been needed to couple the remaining arm onto the core linking agent. Another possibility is that the molecular weight of the linear arm chains themselves was too large for the precursor to link effectively around the multifunctional coupling agent; linking linear polymers with high molecular weights has been reported to be more challenging.⁵ Silicon tetrachloride in itself is a relatively small linking agent, which again may lead to steric problems when trying to link together high molecular weight polymer chains.

2.2.2.2 Synthesis of 4-Arm Star – Star(4)130

A second attempt was undertaken using the reaction conditions detailed in Scheme 2.2. However, to maximize the extent of coupling the precursor arm target molecular weight was lowered from 50,000 g mol⁻¹ to 30,000 g mol⁻¹ and the linking reaction time was increased from two days to four. The 5 : 4 molar ratio of arms to chlorosilane groups was unchanged. These conditions proved successful, and SEC analysis of the crude polymer obtained (Star(4)130) produced results supporting the production of the desired four-arm star.

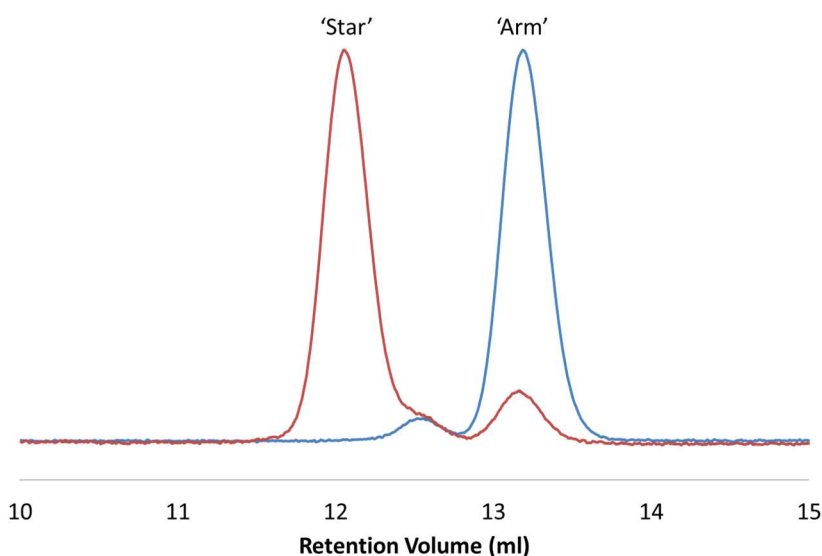


Figure 2.6 - SEC chromatograms (RI detector) of crude four arm polybutadiene Star(4)130. Comparison of the linear arm precursor (blue) and the final crude star mixture (red).

The peak at 12.0 ml in the crude star polymer chromatogram represents the formation of a branched polymer with a high degree of coupling and with a large decrease in the peak at 13.2 ml which represents the excess unreacted arm. Molecular weight data for Star(4)130 is given in Table 2.3.

Table 2.3 - Molecular weight, dispersity and microstructure values for four-arm star polybutadiene Star(4)130 obtained by SEC

Polymer	Target M _n	M _n	M _w	Đ	Functionality	% 1,4-
Star(4)130	(g mol ⁻¹)	(g mol ⁻¹)	(g mol ⁻¹)		of Star	microstructure
Arm	30,000	33,600	34,600	1.03	-	94
Crude Star	136,000	109,200	123,400	1.16	3.25	94
Pure Star	136,000	134,200	138,400	1.03	3.99	94

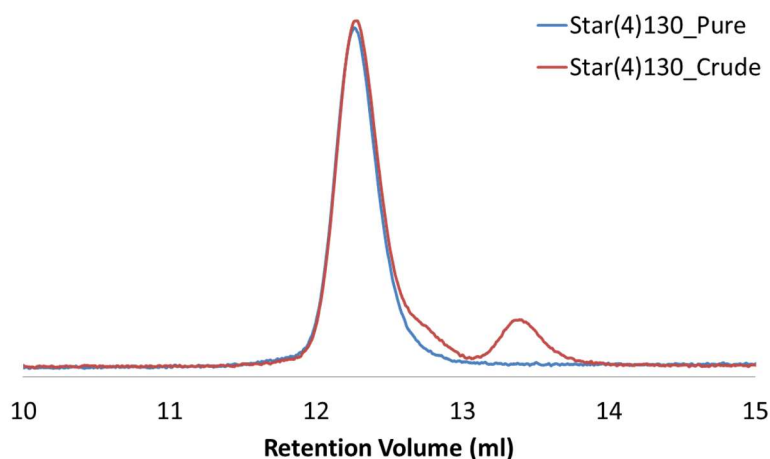


Figure 2.7 - SEC chromatograms (RI detector) of four-arm polybutadiene Star(4)130 before and after four cycles of fractionation

The linear precursor arms had molar mass values of M_n 33,600 g mol⁻¹, M_w 34,600 g mol⁻¹, and a dispersity value (\bar{D}) of 1.03, in excellent agreement with the target M_n of 30,000 g mol⁻¹. The higher molecular weight shoulder peak of the precursor arm visible at 12.6 ml (Figure 2.6) is the result of chain coupling competing with termination - the arm is sampled into a side vessel and nitrogen-sparged methanol injected to terminate the living chains. This can result in the coupling of a small quantity of chains via reaction with any traces of impurities such as oxygen or carbon dioxide. As the precursor arm sample is terminated in a separate side vessel to the main reaction these “dead” double molecular weight chains are not expected to be present in the crude branched polymer. The crude star polymer produced values of M_n of 109,200 g mol⁻¹, an M_w of 123,400 g mol⁻¹, and a dispersity value (\bar{D}) of 1.16, giving a crude functionality value of 3.25. Purification by fractionation was carried out to remove the excess linear arm and SEC analysis indicated this was complete after four cycles (Figure 2.7). The purified star produced values of M_n 134,200 g mol⁻¹, M_w 138,400 g mol⁻¹ and \bar{D} 1.03, giving a pure functionality value of 3.99, indicating that the desired four-arm star polymer was formed and isolated successfully.

In summary, both a three arm and four arm star-branched polybutadiene sample were synthesised, purified and characterised both ¹H-NMR spectroscopy and SEC.

2.2.3 Analysis of Stars - Interaction Chromatography

Interaction Chromatography (IC) is an analytical technique in which polymers are separated by molecular weight; it can be carried out isothermally or with a temperature

gradient. IC can be seen as a variation of the HPLC method, which is a technique that is mostly used in the separation of small molecules.⁶ Presently, most synthetic polymer molecular weight and molecular weight distributions are characterised using size exclusion chromatography (SEC). However, SEC is incapable of separating polymer chains of similar molecular sizes or hydrodynamic volumes, which may be the case in complex mixtures of linear polymers and/or branched polymers.⁷ In recent years IC and in particular temperature gradient interaction chromatography (TGIC) has developed as a technique for the analysis of complex polymers and is capable of significantly enhanced resolution compared to SEC. SEC and IC are similar in many respects and both techniques require the use of porous packing materials as the stationary phase in their columns. SEC columns are often packed with styrene-divinylbenzene resins whereas HPLC/IC columns are packed with silica based materials bonded with a specific end group dependent on the interaction mode of the column.⁷ However, in IC, the specific analytical conditions used, determines which mode of separation is dominant. Polymers can be separated chromatographically in three different regimes - size exclusion chromatography (SEC), liquid chromatography at the critical condition (LCCC) and interaction chromatography (IC), these are graphically represented in Figure 2.8.

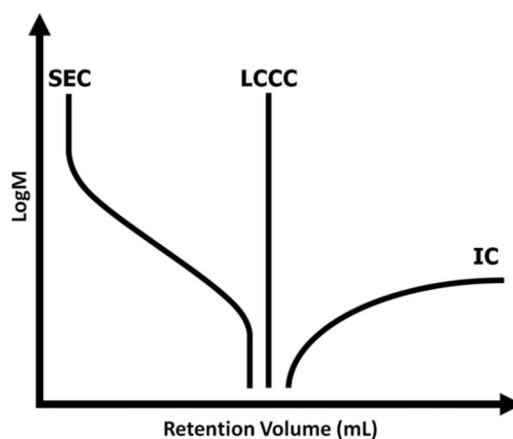


Figure 2.8 - Polymer molecular weight vs. retention volume in three different chromatographic separation regimes: Size Exclusion Chromatography (SEC), Liquid Chromatography at the Critical Condition (LCCC) and Interaction Chromatography (IC)

In SEC mode, polymer chains are eluted from high molecular weight chains to low molecular weight chains and all chains are eluted before the solvent peak, whereas in IC mode the order of elution is reversed, with low molecular weight polymer chains eluted first and all chains are eluted after the solvent peak. This is due to mode of interaction of the polymer chains in solution. In SEC mode, separation is predominantly driven by entropic factors between the polymer chains and the size of the pores of the stationary

phase, with no enthalpic interactions between the polymer analyte and the column packing. In IC mode, separation/retention is predominantly driven by enthalpic interactions, i.e. adsorption/desorption between the solute molecules with the surface of the stationary phase, including the inside of the pore surface. In the event where the entropic and enthalpic contributions exactly compensate each other, all non-functionalised polymer chains elute at the same point regardless of molecular weight, this mode is defined as liquid chromatography at the critical condition (LCCC).⁸⁻⁹

SEC principally separates polymer chains by their hydrodynamic size in solution, not by their molecular weight. For linear polymers, the correlation between retention volume (hydrodynamic volume) and molecular weight is excellent. However, if a polymer consists of a mixture of chains with similar hydrodynamic volumes, such as is often the case for non-homogenous or branched polymers, it becomes extremely difficult for SEC to separate, or even detect any potential imperfections or different species present.¹⁰ IC has a much higher sensitivity to a polymer's molecular weight, architecture, chemical composition and chain functionality than SEC, making identification and separation of polymer molecules by all these parameters possible. The strength of enthalpic adsorption interactions of polymers in IC are mainly controlled by either altering the solvent (polarity) composition during elution, in a process known as solvent gradient interaction chromatography (SGIC) or altering the temperature during elution i.e. temperature gradient interaction chromatography (TGIC).¹¹

In SGIC, a solute is injected into a column which is filled with a mobile phase that is initially a poor solvent for the polymer in question, promoting retention of the polymer on the stationary phase. The mobile phase composition is then gradually altered by the addition of a good solvent, increasing the solvent strength of the mobile phase. SGIC can also be performed on the basis of the polarity of the solvent in question i.e. going from a solvent with poor polarity for the analyte in question to a good polarity. The lowest molecular weight polymer chains will be released by the column before the higher molecular weight polymer chains, which are more strongly retained by the stationary phase, until such point where the mobile phase solvent strength is sufficient for release of the remaining polymer. This method is often used for the separation of small molecules; however, for polymers it has many disadvantages. The nature of the technique involves the modification of the mobile phase, and this often limits which detectors can be used. Refractive index, light scattering and viscometry detectors are all extremely sensitive to

mobile phase changes and differences in solvent composition often lead to signal drift, which in turn makes obtaining information about molecular weight or molecular weight distribution impossible and any information gained is often qualitative.⁷

TGIC was first reported by Chang in 1996.¹² In TGIC, the strength of interactions between polymer chains and stationary phase is controlled by a temperature gradient. Elution is started at a (low) temperature at which all polymer chains are retained by the stationary phase, and the temperature is increased during elution with separation largely based on molecular weight, not molecular size. Lower molecular weight polymer chains are eluted first at lower temperatures and higher molecular weight polymer chains are eluted at higher temperatures. In contrast to SEC, the resolution in TGIC is much higher, especially with regards to branched polymers, making the technique very useful for the analysis of complex mixtures. This is observable below in Figure 2.9, in which a highly branched sample of polystyrene, prepared by linking living polystyrene chains using chlorodimethylsilyl styrene (CDMSS) is analysed.¹¹ Tetrahydrofuran (THF) was used as the eluent in the SEC analysis and the temperature was held at a constant 40 °C, whereas a 55/45 mixture of dichloromethane/acetonitrile was used as the eluent in the TGIC analysis and the temperature was varied from 5 °C to 40 °C. For the SEC analysis, two columns were used (Polymer Labs, mixed C). For the TGIC analysis, the column used was a C18 bonded silica column (Zorbax, 250×9.3 mm, 100 Å) and the flow rate was 0.7 ml/min.

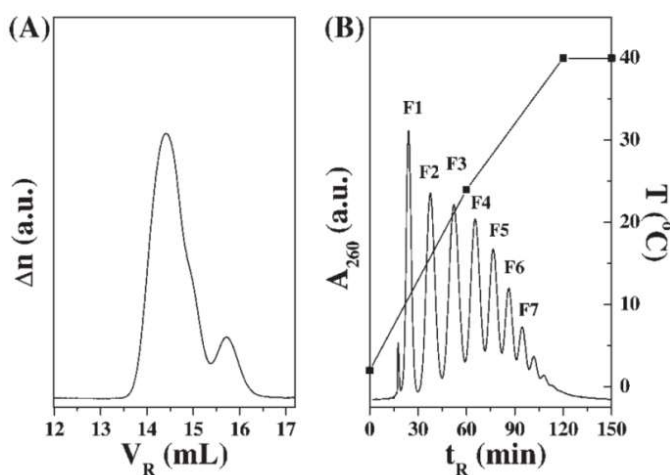


Figure 2.9 - SEC (A) and TGIC (B) chromatograms (UV detector) of branched PS prepared by linking polystyryl anion with CDMSS. Reprinted with permission from Chang, T., J. Polym. Sci., Part B: Polym. Phys. 2005, 43 (13), 1591-1607. Copyright 2005 Wiley.

It can be seen in Figure 2.9, that whereas the SEC chromatograms can only distinguish two relatively broad peaks in this highly branched sample, the TGIC chromatogram is able to resolve the existence of a number of different branched species of various molecular weights. This high level of resolution in IC compared to SEC makes the technique very valuable for branched polymer analysis.

Akin to other LC techniques, IC can be carried out as either reversed-phase (RP) or normal-phase (NP) chromatography. RP-IC uses a non-polar, hydrophobic stationary phase such as C18 bonded silica and a mobile phase that is more polar than the stationary phase. RP-TGIC has been used to study a range of branched polymers and the technique was reviewed in detail in 2012.¹³

NP-IC exploits a polar stationary phase such as bare silica or diol bonded silica and a mobile phase with a polarity that is dependent on the polymer under investigation but is normally less polar than the stationary phase. Normal-phase IC, although much less widely exploited, is capable of similar molecular weight-based separation as RP-IC, but has also demonstrated its potential as a tool for the characterisation of chain end-functionalised polymers. This was initially demonstrated by Chang *et al.* in the separation of hydroxyl chain end-functionalised polystyrene (Figure 2.10).¹⁴

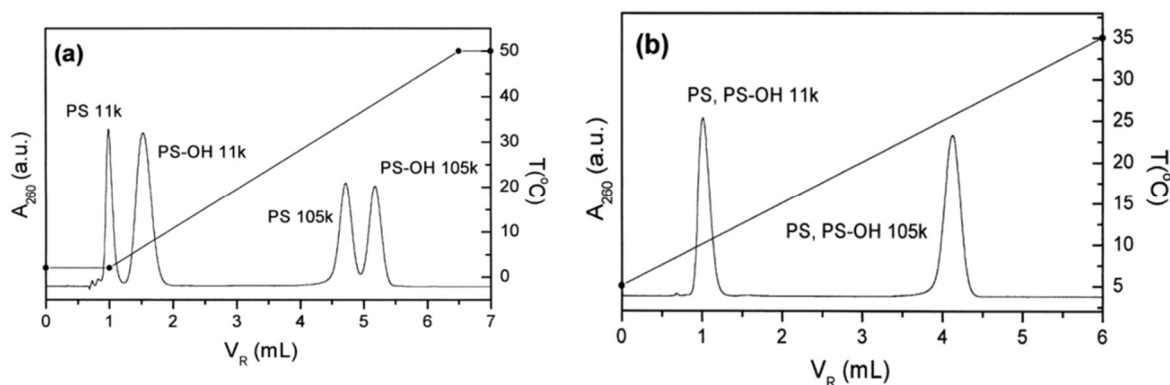


Figure 2.10 - TGIC separation of PS samples with different end groups (hydrogen terminated vs. hydroxyl terminated) by (a) NP-TGIC and (b) RP-TGIC. Temperature programs are also drawn in each figure.

Reprinted (adapted) with permission from Lee, W.; Cho, D.; Chun, B. O.; Chang, T.; Ree, M., J. Chromatogr. A 2001, 910 (1), 51-60. Copyright 2001 Elsevier.

Polystyrene (PS) samples of molar masses 11,000 g mol⁻¹ and 105,000 g mol⁻¹ were prepared by living anionic polymerisation. Each polymer sample was split into two batches, one of which was terminated with methanol producing non-functionalised linear polystyrene while the other was end-capped with ethylene oxide before termination, producing hydroxyl end-functionalised PS (PS-OH). A mixture of the two pairs of

samples (PS 11K, PS-OH 11K, PS-105K and PS105K-OH) were subjected to RP-TGIC and NP-TGIC analysis. RP-TGIC analysis showed no distinction between the non-functionalised and end-capped polymers, with separation only occurring based on molecular weight (Figure 2.10b), whereas the NP-TGIC analysis was able to resolve all four samples separating by both molecular weight and functionality (Figure 2.10a), demonstrating the utility of this mode of separation.

A schematic diagram of the apparatus setup for IC is given below in Figure 2.11. It very much resembles a HPLC or SEC instrument with various modifications.

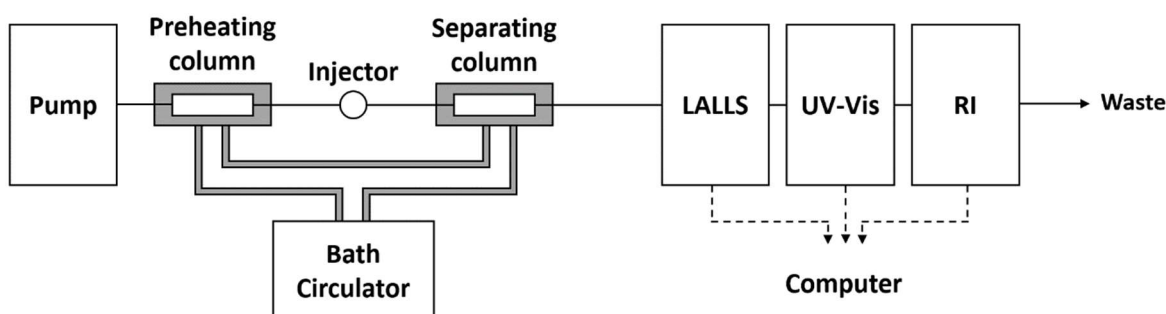


Figure 2.11 - Schematic diagram of an IC apparatus

The columns of the IC apparatus are placed inside jacketed columns which allows for the control of the column temperature through the use of a bath circulator to circulate the fluid. A preheating column is placed before the separating column to pre-equilibrate the eluent to the separation column temperature. Eluents used in IC analysis are often theta solvents, to minimise potential polymer-solvent interactions which may further complicate polymer-stationary phase interactions. If a mixed eluent is used, it is often premixed to the desired composition before usage, to improve reproducibility, rather than using a gradient pump. It is important to note that while IC is capable of much higher resolution than SEC, the technique itself is much less universal. SEC can be carried out using a wide variety of good solvents for a large range of polymers, with no enthalpic interactions between solute and column. IC methods need to be developed for every different polymer type analysed to ensure optimal separation and characterisation. This often means finding a suitable flow rate, stationary phase, pore size, mobile phase, mobile phase composition, polarity, temperature range and temperature gradient, if a gradient is employed. It has been demonstrated that small changes in temperature and mobile phase composition can have a large effect on the separation mechanism.⁷ IC method development can be a very time-consuming process, which may have hindered its wider

adoption. Nevertheless, IC (in particular TGIC) has been used to characterise and analyse a range of model polymers including star-shaped polymers,^{10, 15-16} H-shaped polymers,¹⁷⁻¹⁸ comb polymers,¹⁹⁻²⁰ dendritically branched polymers²¹ and a series of asymmetric stars.²²

In order to quantify the success of the prepared star polymers it was decided to use RP-TGIC analysis for further characterisation. While the SEC analysis indicated high levels of coupling in the crude samples, there remains the possibility that there could be undetected impurities as a result of incomplete coupling – e.g. the presence of a “two-arm star” that may not be detected and may still be present even after purification. For structure-property correlation studies, even small amounts of impurities can drastically affect the subsequent rheological data if not taken into account beforehand. Therefore, when synthesising samples created for these studies, it is best to have samples that have been fully characterised, including the detection of any imperfections present in “perfect” model polymers.

2.2.3.1 TGIC analysis - Crude Stars

RP-TGIC was carried out on Star(3)150 (three-arm PB), Star(4)180 (incomplete four-arm PB) and Star(4)130 (four-arm PB) before their purification by fractionation. A Nucleosil C18 column was used with 1,4-dioxane (a theta solvent for PB)²³ as the eluent. The temperature was varied during the elution run and the flow rate kept constant at 0.4 ml/min. The SEC and RP-TGIC chromatograms for the crude polymers are presented overleaf in Figure 2.12 and the differences between the SEC and TGIC chromatograms for each polymer are stark. In each SEC chromatogram two peaks can clearly be resolved, as explained earlier the largest peak, at lower retention times, in all cases represents the branched products and the smaller peak at longer retention time corresponds to the excess precursor arm. For Star(3)150, four major peaks can be detected in the TGIC chromatogram (Figure 2.12b), the first large peak at 3.2 ml is the solvent peak, confirming that elution is in IC mode. The next peak at 5.0 ml corresponds to the excess unreacted arm still present in the sample. There is then a peak at 9.3 ml which corresponds to the “two-arm” incomplete star which was undetected in the SEC elution. The major peak 13.2 ml is then representative of the three-arm star product.

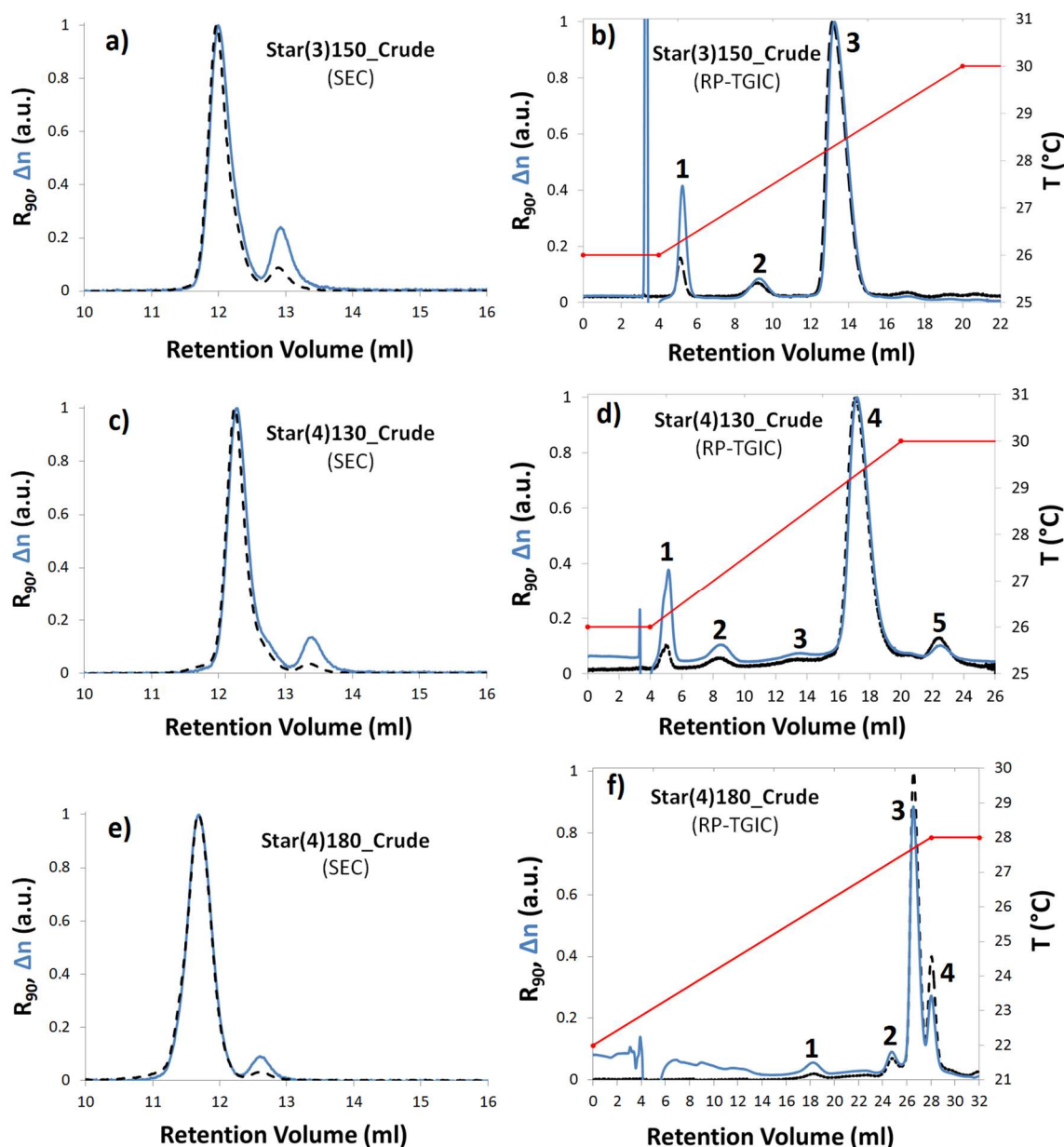


Figure 2.12 - SEC and RP-TGIC chromatograms of the crude polybutadiene three arm and four arm stars recorded with an RI detector (Δn) and RALS detector (R_{90}). SEC samples were analysed in THF at 40 °C at a flow rate of 1 ml/min. TGIC samples were analysed in 1,4-dioxane at a flow rate of 0.4 ml/min. Temperature profiles are shown on the plot.

A similar result can be seen in Star(4)130 (Figure 2.12d) with the peaks at 5.0 ml, 8.3 ml, 13.3 ml, and 17.3 ml, corresponding to the unreacted arm, the “two-arm” incomplete star, the incomplete “three-arm” star and the major four-arm star product. There is also a peak at 22.6 ml which may be the result of a high molecular weight by-product from the result of a side/unintended coupling reaction. Star(4)180 was also analysed in order to detect if there had been the formation of any four-arm star or if there was only three-arm present as the SEC indicated. There are four polymer peaks (peaks 1-4) which correspond to the unreacted arm, the “two-arm” incomplete star, the “three-arm” incomplete star - which

represents the majority of the sample, and a peak at 28.1 ml believed to represent the four-arm star product. The analysis once again showcases that even in a complex mixture such as Star(4)180, TGIC is able to detect all polymer chains present at a much higher resolution than SEC, as SEC is unable to distinguish between the polymer chains of similar hydrodynamic volumes.

Table 2.4 - Molecular weight (M_n) values for crude star polybutadienes obtained by TGIC analysis

Sample Code	Peak Molar Mass (M_n) (g mol ⁻¹)				
	Peak 1	Peak 2	Peak 3	Peak 4	Peak 5
Star(3)150_crude	42,000	85,000	133,000	No Peak	No Peak
Star(4)130_crude	26,800	-	-	110,900	-
Star(4)180_crude	76,100	128,400	176,900	250,700	No Peak

Molecular weight analysis was also carried out for all samples analysed by TGIC and these are presented in Table 2.4. It should be noted that in comparison to SEC, TGIC molecular weight data may be of slightly lower accuracy. The refractive index detector is very sensitive to changes in temperature and this can result in unstable baselines, which in turn effect the accuracy of any molecular weight calculations.²⁴ However, results obtained by TGIC are often indicative and accurate enough to separate and assign the distinctive polymer peaks. The peaks listed in Table 2.4 correspond to the peaks listed for each respective polymer in Figure 2.12. For Star(3)150_crude molecular weight (M_n) values were calculated for every peak present in its TGIC chromatogram. Peak 1 has an M_n of 42,000 g mol⁻¹, which is in reasonable agreement with the value calculated by SEC (53,000 g mol⁻¹). Peak 2 has an M_n of 85,000 g mol⁻¹, in good agreement with the theoretical value that would be expected for an incomplete “two-arm” star (84,000 g mol⁻¹), and peak 3 has a value of 133,000 g mol⁻¹, again in agreement with the number expected for a three-arm star. In the case of Star(4)130_crude, analysis was only possible for peaks 1 and 4, with peak 1 having an M_n of 26,800 g mol⁻¹, with peak 4 having an M_n of 110,900 g mol⁻¹ close to four times of that of peak 1. For Star(4)180_crude it can be seen that there is roughly a 50-70,000 g mol⁻¹ increase from peak 1, which has an M_n of 76,100 g mol⁻¹ as an additional arm is added, through to peak 4 which has an M_n of 250,700 g mol⁻¹. Although there are some discrepancies between the molecular weight measurements from TGIC and the SEC calculations, nonetheless, the data help to confirm the identity of each component of the crude materials.

2.2.3.2 TGIC analysis - Purified Stars

The purified three-arm and four-arm star polymers, Star(3)150 and Star(4)130 respectively were also subjected to RP-TGIC analysis in order to more accurately determine how successful their purification by fractionation had been. The success of the fractionation process was initially evaluated using SEC, which indicated the polymers had indeed had any excess unreacted arm or partially coupled polymers successfully removed, evidenced by a single peak in their chromatograms as can be seen for Star(3)150 (a), and Star(4)130 (c) in Figure 2.13. The TGIC analysis once again gives more information than the SEC, revealing that although the products are more or less as expected following fractionation, total purification was incomplete and there still remain traces of impurities in both “purified” samples.

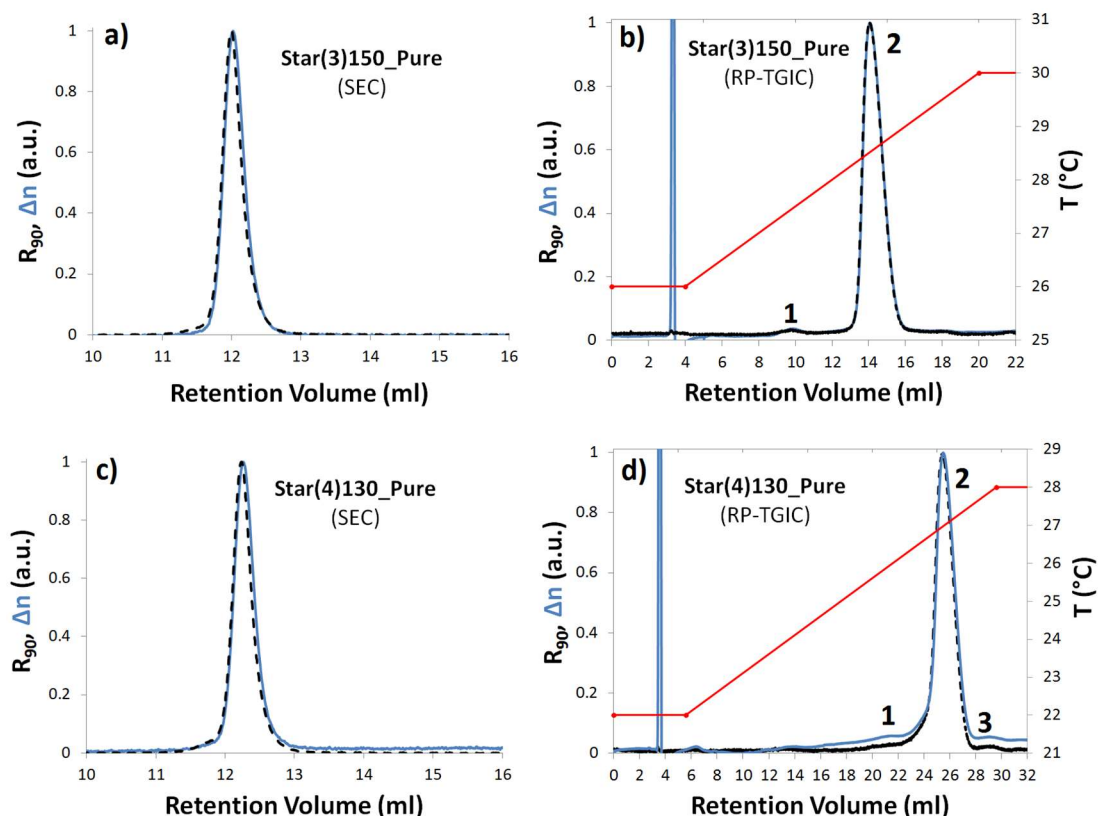


Figure 2.13 - SEC and RP-TGIC chromatograms of the polybutadiene three arm and four arm stars (post fractionation) recorded with an RI detector (Δn) and RALS detector (R_{90}). SEC samples were analysed in THF at 40 °C at a flow rate of 1 ml/min. TGIC samples were analysed in 1,4-dioxane at a flow rate of 0.4 ml/min. Temperature profiles are shown on the plot.

For Star(3)150, the TGIC chromatogram (Figure 2.13b) indicates there has been a complete removal of the excess precursor arm and no peak can be detected for it. However, there remains a residual small peak at 9.9 ml, which corresponds to a trace of the “2-arm” partially coupled product, even after four cycles of fractionation. The large peak at 15.0 ml

retention volume corresponds to the 3-arm star. It was possible to quantify the amount of this residual impurity using the RI detector, which measures concentration. Peak 1 (Figure 2.13b) was calculated and represents 1.1 weight percent of the sample with the remaining 98.9% being the desired 3-arm star. That TGIC was able to detect a relatively low amount of impurity again showcases the sensitivity of this method. The purified four-arm polymer Star(4)130 was also analysed and produced similar results. In its TGIC chromatogram (Figure 2.13d) there is no peak for the excess arm, or for the “2-arm” partially coupled product that were spotted previously. There remains however, a small peak at 21.3 ml representative of the “3-arm” partially coupled product, and the major peak at 25.4 ml corresponding to the desired 4-arm product and a small peak at 29.3 ml which may correspond to traces of a high molecular weight by-product. The quantities of impurities were calculated (RI detector): peak 1 (Figure 2.13d) was measured to be 1.2% and peak 3 was measured to be 1.1%, giving peak 2, the desired 4-arm star, a total weight percent of 97.7%.

TGIC analysis was also carried out independently for the precursor arms of each star, and the results were superimposed with the crude and purified samples for their respective star. The temperature program was the same for each respective sample and the chromatograms are shown below in Figure 2.14.

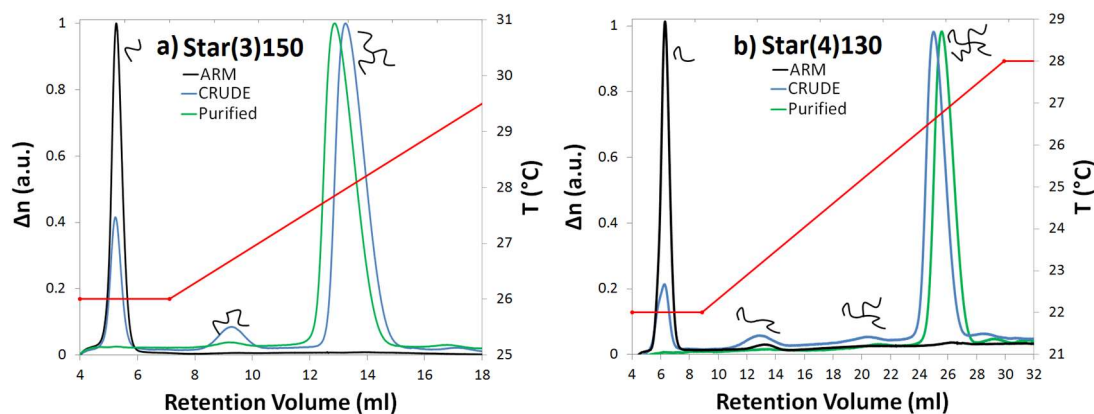


Figure 2.14 – RP-TGIC chromatograms of the precursor arm, crude and pure polybutadiene three arm and four arm stars recorded with an RI detector (Δn). TGIC samples were analysed in 1,4-dioxane at a flow rate of 0.4 ml/min. Temperature profiles are shown on the plot.

It can be seen that the first peak eluted for each sample (5 ml for Star(3)150; 6 ml for Star(4)130) belongs to the precursor arm. There is also no residual arm peak detected in the final purified sample for each star, again confirming its successful removal. It can be seen again that TGIC has provided far more detail into the nature of the star-branched polymers than traditional SEC has been able to.

2.3 Experimental

2.3.1 Materials

Benzene (Aldrich, HPLC grade, $\geq 99.9\%$), was dried and degassed over calcium hydride (CaH_2) (Acros Organics, 93%) and stored under high vacuum. 1,3-Butadiene (Aldrich, +99%) was passed through columns of Carbosorb (Aldrich) and molecular sieves (Aldrich) to remove any inhibitor and moisture respectively. Methyltrichlorosilane (Aldrich, 99%), and silicon tetrachloride (Aldrich, 99%) were used as received. The solvents were degassed by a number of freeze-pump-thaw cycles and freshly distilled prior to use. *sec*-Butyllithium (Aldrich, 1.4 M solution in cyclohexane) and *n*-butyllithium (Sigma-Aldrich, 2.5 M in hexanes) were used as received. 1,4-dioxane (HPLC grade, Fischer Scientific) was used as received.

2.3.2 Reaction Vessel (“Christmas Tree”)

The reaction vessel pictured below, (Figure 2.15), colloquially referred to as a “Christmas Tree” is an example of the type of reactor used in all polymerisation experiments. It has been designed to ensure that both a high vacuum is sustainable for prolonged periods of time for reaction, as well being fully sealable for the elimination of environmental impurities. The vessel is configured with numerous J Young’s taps for both the setting of the vacuum and the transfer of solvents or monomers into or out of the system. Precision rubber septa are also used to seal the vessel in order to allow the injection of initiating, coupling or terminating species into the system. All solvents and monomers are transferred into the reactor by distillation. Most initiating and terminating agents were introduced to the system by injection with gas tight syringes through a septum.

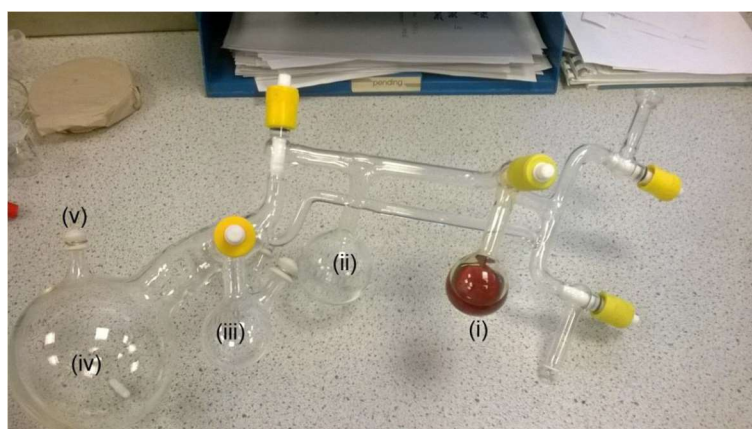


Figure 2.15 - “Christmas tree” reactor used for living anionic polymerisation, (i) Flask A containing living polystyryllithium, (ii) Flask B, (iii) Sidearm Flask, (iv) Reaction Flask, (v) Septum.

2.3.2.1 Preparation of Reaction Vessel

Before all polymerizations were carried out, necessary procedures are undertaken with the specialised “Christmas Tree” vessel (Figure 2.15) to ensure that both premature termination and unwanted side reactions are avoided. Firstly, the reactor is connected to a high vacuum line and left to dry under high vacuum for one hour. The reactor is then fully sealed by closing all of its Young’s taps and removed from the line maintaining its vacuum. The entire reactor is then washed completely on the inside with the orange-red living polystyryllithium (PSLi) in benzene solution contained in Flask A once; this is done to react any leftover impurities contained within the reactor. The living PSLi/benzene solution is then collected back into Flask A. Flask B is then cooled with liquid nitrogen and benzene distilled directly from the living PS mixture into Flask B and this benzene used to clean the remainder of the reactor before being returned to Flask A and distilled again. This is repeated until all remaining living PSLi is returned into Flask A and the benzene used to clean the reactor remains colourless (often around 4 or 5 times). The benzene is then finally collected into Flask A and said flask is frozen completely with liquid nitrogen, with a heat gun used to collect any residual benzene in the reactor into Flask A. The flask is then closed and the reactor returned to the vacuum line and evacuated overnight, finally preparing the Christmas tree for polymerization.

2.3.3 Characterisation

2.3.3.1 Nuclear Magnetic Resonance (NMR)

^1H -NMR spectra were measured on a Varian VNMRs 700 MHz or a Bruker DRX-400 MHz spectrometer using either CDCl_3 or DMSO-d_6 as solvents.

2.3.3.2 Size Exclusion Chromatography (SEC)

Triple detection size exclusion chromatography (SEC) was carried out for the analysis of molecular weight, molecular weight distribution and dispersity of the synthesised polymers, using a Viscotek TDA 302 with refractive index, right angle light scattering (RALS – 690 nm) and viscosity detectors and two PLgel 5 μm mixed C columns (300 \times 75 mm). Tetrahydrofuran was used as the eluent at a flow rate of 1.0 ml/min and at a temperature of 35 $^\circ\text{C}$. The calibration was carried out with a single narrow distribution polystyrene standard purchased from Polymer Laboratories. A value of 0.124 mL/g (measured in house) was used as the dn/dc of polybutadiene for the analysis of prepared polymers.

2.3.3.3 Temperature Gradient Interaction Chromatography (TGIC)

Temperature gradient interaction chromatography analysis was carried out in reversed-phase conditions. Polymer solution concentrations of approximately 4 mg/ml dissolved in the eluent mixture were used and the injection volume was 100 μ l. Reversed-phase temperature gradient interaction chromatography (RP-TGIC) analysis was carried out using a single C18 bonded silica column (Nucleosil C18, 100 Å pore 250×4.6 mm I.D., 5 μ m). 1,4-dioxane was used as the eluent at a flow rate of 0.40 ml/min. The RP-TGIC system used a modified Viscotek TDA 302 with refractive index, viscosity, RALS detectors (Viscotek) and an external UV detector (Knauer). The temperature of the column in both systems was controlled by a Thermo Scientific thermostatically controlled circulating bath. A value of 0.095 mL/g was used as the dn/dc of polybutadiene which was obtained from a previous report.¹⁷

2.3.4 Synthesis

All polymerisations carried out during this work utilise the same general procedure but with varying amounts of monomer, solvents and reagents being used. The main solvent used in all the following polymerisations was benzene. Any extra steps taken are detailed in that polymer's synthetic description.

2.3.4.1 Synthesis of 3-Arm Star - Star(3)150

Benzene (200 ml) and butadiene (22.66 g, 419 mmol) were added via distillation under vacuum into the reaction flask of the Christmas tree. In order to obtain the target arm M_n of 50 Kg mol⁻¹, 0.32 ml of *sec*-BuLi in cyclohexane (0.45 mmol) was injected directly into the reaction flask via the septum and reacted under vacuum at 50 °C for 24 hours for complete conversion, after which a sample of the precursor arm was collected for molar mass characterisation. Methyltrichlorosilane (0.013 mL, 0.11 mmol) was then added to the solution via injection and the reaction continued under vacuum at 50 °C for 2 days, after which it was terminated via injection of nitrogen-sparged methanol. The polymer was precipitated in methanol in the presence of anti-oxidant butylated hydroxytoluene (BHT). The excess solution was then removed, the polymer fully dissolved in THF and the polymer then precipitated again by adding to BHT/methanol and dried to constant mass under vacuum for several days. Yield 91%.

Star(3)150_Arm: M_n 53,000 g mol⁻¹, M_w 56,000 g mol⁻¹, Đ 1.05.

Star(3)150_Crude: M_n 123,000 g mol⁻¹, M_w 142,000 g mol⁻¹, Đ 1.16.

2.3.4.2 Synthesis of 4-Arm Star - Star(4)180

Star(4)180 was prepared according to the procedure described above in 2.3.4.1. To a solution of butadiene (20.90 g, 364 mmol) in benzene (200 ml), *sec*-BuLi (0.30 ml, 0.42 mmol) was injected and reacted under vacuum at 50 °C for 24 hours. A sample of the precursor arm was collected for molar mass characterisation. Silicon tetrachloride (0.010 mL, 0.13 mmol) was then added via injection and the reaction was continued under vacuum at 50 °C for 2 days, after which the reaction was terminated via injection of nitrogen-sparged methanol. The polymer was precipitated into methanol, redissolved in THF, precipitated again into methanol and dried under vacuum. Yield 97%.

Star(4)180_Arm: M_n 67,500 g mol⁻¹, M_w 71,300 g mol⁻¹, Đ 1.06.

Star(4)180_Crude: M_n 183,100 g mol⁻¹, M_w 198,200 g mol⁻¹, Đ 1.08.

2.3.4.3 Synthesis of 4-Arm Star - Star(4)130

Star(4)130 was prepared according to the procedure described above in 2.3.4.1. To a solution of butadiene (19.74 g, 364 mmol) in benzene (200 ml), *sec*-BuLi (0.47 ml, 0.66 mmol) was injected and reacted under vacuum at 50 °C for 24 hours. A sample of the precursor arm was collected for molar mass characterisation. Silicon tetrachloride (0.015 mL, 0.13 mmol) was then added via injection and the reaction was continued under vacuum at 50 °C for 4 days, after which it was terminated via injection of nitrogen-sparged methanol. The polymer was precipitated into methanol, redissolved in THF, precipitated again into methanol and dried under vacuum. Yield 83%.

Star(4)130_Arm: M_n 33,600 g mol⁻¹, M_w 34,600 g mol⁻¹, Đ 1.03.

Star(4)130_Crude: M_n 109,200 g mol⁻¹, M_w 123,400 g mol⁻¹, Đ 1.16.

2.3.5 Fractionation of Stars

In a three-necked, 3 litre separating funnel, the recovered polymer (ca. 20 g) was dissolved in 2 litres of toluene. The separating funnel was then transferred to a temperature controlled water bath and equipped with an overhead stirrer. The temperature of the water bath was set 25 °C). While stirring, methanol (a non-solvent) was added slowly to the funnel until the polymer solution became cloudy, after which point the temperature was raised slowly until the polymer solution became clear again. Methanol was added again until the solution turned cloudy again, and this process was repeated until a suitable temperature (5-10 °C above original temperature) was reached.

Stirring was then stopped, the overhead stirrer was removed from the separating funnel, and the funnel fully stoppered. The clear solution was then allowed to cool overnight to the original starting temperature, resulting in a phase-separation which produced a lower fraction that was rich in high molecular weight material and a higher fraction which was rich in lower molecular weight polymer. The lower (high molar mass) fraction was collected and the polymer recovered by precipitation into methanol. The remaining upper phase of the polymer solution in the separating funnel was subjected to the fractionation process again. This resulted in multiple fractions being generated for a given fractionation cycle (e.g. Series A, fraction A1, A2, A3, etc.). After a cycle was completed, all of the collected fractions were analysed by SEC, with the most suitable fractions combined, unwanted fractions discarded and a new fractionation cycle started. The fractionation cycle was repeated until a fraction of pure star-branched polymer was recovered. The SEC analysis of a pure fraction should be mono-modal with a narrow dispersity.

Star(3)150_Pure: M_n 148,000 g mol⁻¹, M_w 151,000 g mol⁻¹, \bar{D} 1.02.

Star(4)130_Pure: M_n 134,200 g mol⁻¹, M_w 138,400 g mol⁻¹, \bar{D} 1.03.

2.4 Conclusions

A number of star polymers have been synthesised using a combination of living anionic polymerisation and coupling reactions via the use of chlorosilane coupling agents. Three-arm polybutadiene (Star(3)150) and four-arm polybutadiene (Star(4)130) were synthesised and purified to be used as model branched polymers for rheological studies. The polymers were analysed extensively using both size exclusion chromatography (SEC) and temperature gradient interaction chromatography (TGIC) both before and after purification by fractionation. In all cases TGIC proved itself to be capable of superior separation and able to provide a level of characterisation far beyond what is capable when using SEC alone. For the analysis of polymers before fractionation, TGIC was able to show the presence of incomplete, partially coupled products, in contrast to SEC which was only able to show the fully coupled product as well as any excess precursor still present. For the purified samples TGIC was also able to detect and quantify the amount of traces of impurities still present after fractionation, where SEC analysis had indicated complete purity. It was demonstrated that TGIC in combination with SEC allows for much more detailed structural analysis of branched polymer mixtures improving the case for IC to be used alongside SEC as a fundamental technique for branched polymer analysis.

2.5 References

1. Szwarc, M., *Nature* **1956**, *178* (4543), 1168-1169.
2. Hsieh, H. L.; Quirk, R. P., *Anionic Polymerization: Principles and Practical Applications*. Marcel Dekker: New York, 1996.
3. Halasa, A. F.; Schulz, D. N.; Tate, D. P.; Mochel, V. D., Organolithium Catalysis of Olefin and Diene Polymerization. In *Adv. Organomet. Chem.*, Stone, F. G. A.; West, R., Eds. Academic Press: 1980; Vol. 18, pp 55-97.
4. Kimani, S. M.; Hardman, S. J.; Hutchings, L. R.; Clarke, N.; Thompson, R. L., *Soft Matter* **2012**, *8* (12), 3487.
5. Bauer, B. J.; Fetters, L. J., *Rubber Chem. Technol.* **1978**, *51* (3), 406-436.
6. Park, S.; Cho, D.; Ryu, J.; Kwon, K.; Lee, W.; Chang, T., *Macromolecules* **2002**, *35* (15), 5974-5979.
7. Chang, T.; Lee, H. C.; Lee, W.; Park, S.; Ko, C., *Macromol. Chem. Phys.* **1999**, *200* (10), 2188-2204.
8. Ziebarth, J. D.; Wang, Y., *Soft Matter* **2016**, *12* (24), 5245-5256.
9. Pasch, H., *Polymer* **1993**, *34* (19), 4095-4099.
10. Lee, H. C.; Lee, W.; Chang, T.; Yoon, J. S.; Frater, D. J.; Mays, J. W., *Macromolecules* **1998**, *31* (13), 4114-4119.
11. Chang, T., *J. Polym. Sci., Part B: Polym. Phys.* **2005**, *43* (13), 1591-1607.
12. Lee, H. C.; Chang, T., *Polymer* **1996**, *37* (25), 5747-5749.
13. Hutchings, L. R., *Macromolecules* **2012**, *45* (14), 5621-5639.
14. Lee, W.; Cho, D.; Chun, B. O.; Chang, T.; Ree, M., *J. Chromatogr. A* **2001**, *910* (1), 51-60.
15. Lee, H. C.; Chang, T.; Harville, S.; Mays, J. W., *Macromolecules* **1998**, *31* (3), 690-694.
16. Lee, H.; Yang, J.; Chang, T., *Polymer* **2017**, *112*, 71-75.
17. Li, S. W.; Park, H. E.; Dealy, J. M.; Maric, M.; Lee, H.; Im, K.; Choi, H.; Chang, T.; Rahman, M. S.; Mays, J., *Macromolecules* **2011**, *44* (2), 208-214.
18. Perny, S.; Allgaier, J.; Cho, D.; Lee, W.; Chang, T., *Macromolecules* **2001**, *34* (16), 5408-5415.
19. Chambon, P.; Fernyhough, C. M.; Im, K.; Chang, T.; Das, C.; Embery, J.; McLeish, T. C. B.; Read, D. J., *Macromolecules* **2008**, *41* (15), 5869-5875.
20. Lee, S.; Lee, H.; Chang, T.; Hirao, A., *Macromolecules* **2017**, *50* (7), 2768-2776.
21. Hutchings, L. R.; Kimani, S. M.; Hoyle, D. M.; Read, D. J.; Das, C.; McLeish, T. C. B.; Chang, T.; Lee, H.; Auhl, D., *ACS Macro Letters* **2012**, *1* (3), 404-408.
22. Agostini, S.; Hutchings, L. R., *Eur. Polym. J.* **2013**, *49* (9), 2769-2784.
23. Roovers, J.; Toporowski, P.; Martin, J., *Macromolecules* **1989**, *22* (4), 1897-1903.
24. Snijkers, F.; van Ruymbeke, E.; Kim, P.; Lee, H.; Nikopoulou, A.; Chang, T.; Hadjichristidis, N.; Pathak, J.; Vlassopoulos, D., *Macromolecules* **2011**, *44* (21), 8631-8643.

Chapter 3

Synthesis and characterisation of Macromonomers

3.1 Introduction

This chapter concerns the synthesis and characterisation of a range of polybutadiene “Macromonomers” for the eventual synthesis of H-shaped polymers. Although the “macromonomer” approach in which polymers are coupled together post-polymerisation, has been used previously for the synthesis of a variety of branched polymers,¹⁻⁵ this thesis describes the first attempts to use this strategy for the synthesis of H-shaped polymers. As previously discussed in the Introduction (Chapter 1, Section 1.5.2.2), the traditional methods of H-shaped polymer synthesis often lead to problems with incomplete coupling and poor initiator solubility. The “macromonomer” approach allows for the creation of a homologous series of branched polymers where macromonomers of differing molecular weights can be coupled together, and crucially, full characterisation data for each component of the final H-shaped polymer is known. The macromonomers themselves are of great importance to the success of this approach as they must contain the necessary functionalities in order for the coupling reactions to be successful.

The approach chosen in this instance involves the design and synthesis of a range of telechelic polybutadiene macromonomers, which have been end-functionalised at both chain ends to generate a “crossbar” polymer for an H-shaped polymer. These “crossbars” will then be coupled with complementary linear “arm” polymers to give the final H-shaped polymer (Figure 3.1).

Crossbar:

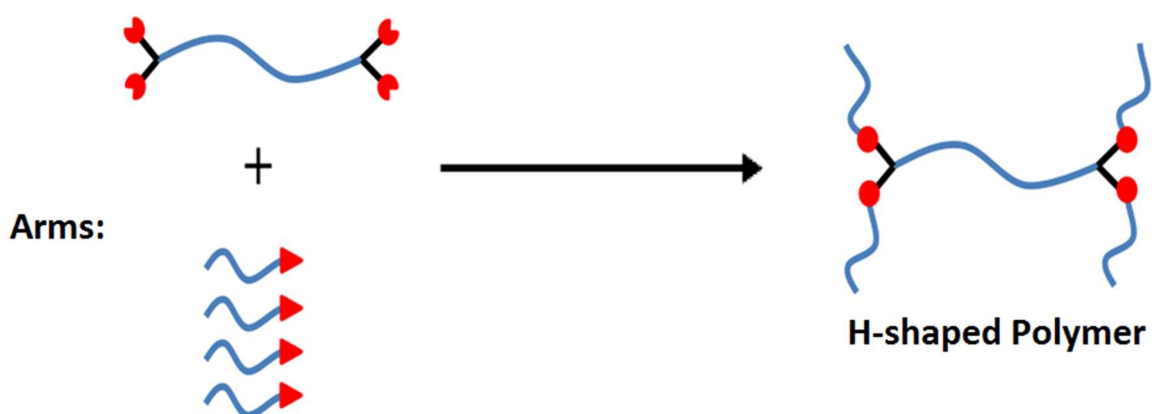


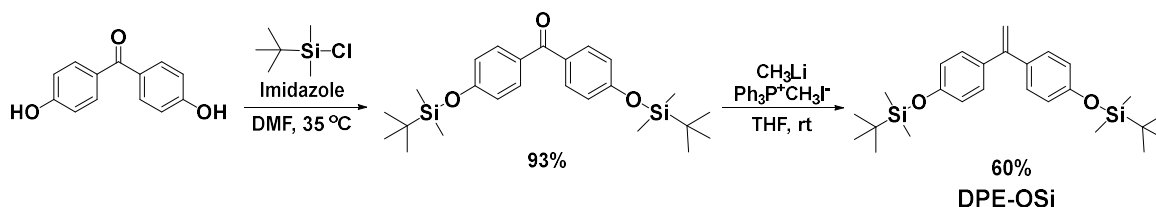
Figure 3.1 - General schematic for the synthesis of H-Shaped polymers via the macromonomer approach
A series of crossbar polymers was synthesised, with two methods for their synthesis being tested – an “end-capped” approach in which chain end-functionality is introduced to the

crossbar in two stages; and a “fire and forget” approach in which the end-capping agent is introduced at the beginning of the reaction, exploiting reactivity ratios and additives to ensure complete end-capping is achieved - both of these approaches are discussed in detail later in the chapter (Section 3.2.2). The linear “arm” macromonomers were synthesised using traditional living anionic polymerisation in conjunction with end-capping post-polymerisation methods. The telechelic crossbars and arms were characterised by size exclusion chromatography (SEC), ^1H -NMR spectroscopy and normal-phase isothermal interaction chromatography (NP-IIC). The two methods of synthesis for the telechelic crossbars were evaluated, as well as the efficacy of using NP-IIC for the characterisation of high molecular weight end-functionalised polymers.

3.2 Results and Discussion

A series of telechelic “crossbar” polybutadienes of varying molecular weights has been prepared by living anionic polymerisation via the use of a protected monomer that serves as both functionalised initiator and end-capping agent. Linear bromine-end-capped polybutadienes have also been synthesised for their eventual use as “arms” for the final H-shaped polymer synthesis. High molecular weights ($20,000 \text{ g mol}^{-1}$ to $100,000 \text{ g mol}^{-1}$) were targeted for the macromonomers to create samples of rheological interest. Polymers were characterised using ^1H -NMR spectroscopy, triple detection size exclusion chromatography (SEC) as well as interaction chromatography (IC).

3.2.1 Synthesis of Protected Functionalised Precursor (DPE-OSi)



Scheme 3.1 - Synthesis of 1,1-bis(4-*tert*-butyldimethylsiloxyphenyl)ethylene (DPE-OSi)

The protected monomer used for the synthesis of the telechelic “crossbar” polymers was 1,1-bis(4-*tert*-butyldimethylsiloxyphenyl)ethylene (DPE-OSi). This silyl ether-protected derivative of 1,1-diphenylethylene (DPE) was chosen as it has the ability to act as both a functionalised initiator and end-capping agent in anionic polymerisation, allowing for a facile, one-pot synthesis. The DPE-OSi itself can also be deprotected by a simple acid hydrolysis, restoring the original hydroxyl (-OH) functionalities. These properties have led to DPE-OSi and other DPE derivatives being used quite extensively in the synthesis of functionalised polymers via anionic polymerisation, by both the Hutchings’ group and others.⁶⁻⁷ DPE-OSi was synthesised in a two-step reaction from 4,4’-dihydroxybenzophenone according to the procedure of Quirk and Wang as shown above in Scheme 3.1.⁸ The first step of this reaction involves the protection of the phenol groups of 4,4’-dihydroxybenzophenone into their silyl ether derivatives. This protection step is required in order to eliminate unwanted side reactions, since the functionalised precursor is to be used as an initiator/end-capping agent in anionic polymerisation. The product was prepared in a high yield (93%), purified by column chromatography (toluene eluent) and the protection confirmed by ^1H -NMR spectroscopy (Figure 3.2).

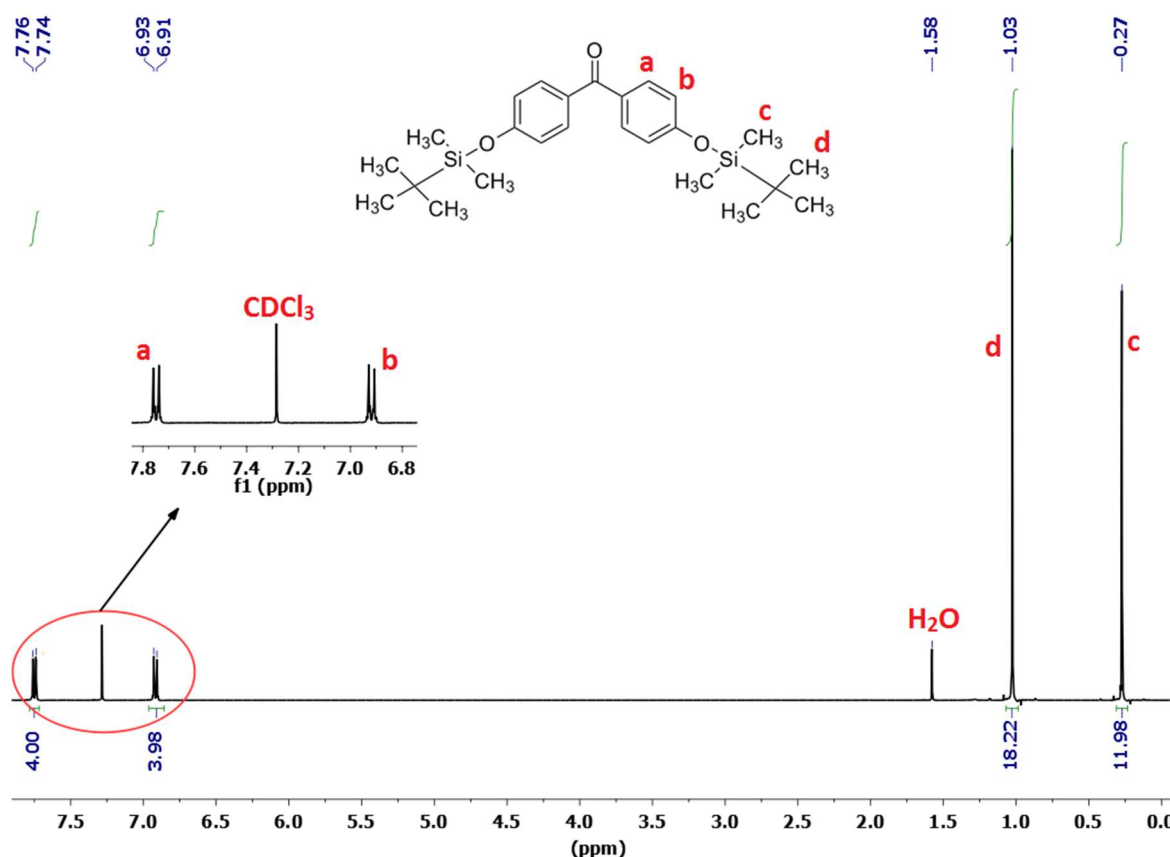


Figure 3.2 - ^1H -NMR spectrum of 1-bis(4-*tert*-butyldimethylsiloxyphenyl)benzophenone

The doublet signal at δ 7.76 ppm represents the four aromatic 'a' protons closest to the ketone group in the structure, with the doublet signal at δ 6.93 ppm corresponding to the four aromatic 'b' protons closest to the silyl ether linkage. The singlet signal at δ 1.03 ppm belongs to the eighteen 'd' methyl protons of the *tert*-butyl group with the singlet signal at δ 0.27 ppm corresponding to the twelve 'c' methyl protons attached to the silicon atom. The signal at δ 7.28 ppm is that of the chloroform solvent and the peak at δ 1.58 ppm is the result of water. This spectrum was also compared to the starting material to confirm the singlet peaks at δ 1.03 ppm and δ 0.27 ppm were due to the silyl ether groups and that protection had occurred (Figure 3.3). A slight shift in between the aromatic doublets can be seen in Figure 3.2; this is due to the different NMR solvents the materials were carried out in – 4,4'-dihydroxybenzophenone in dimethyl sulfoxide (DMSO) and DPE-OSi in chloroform (CDCl_3).

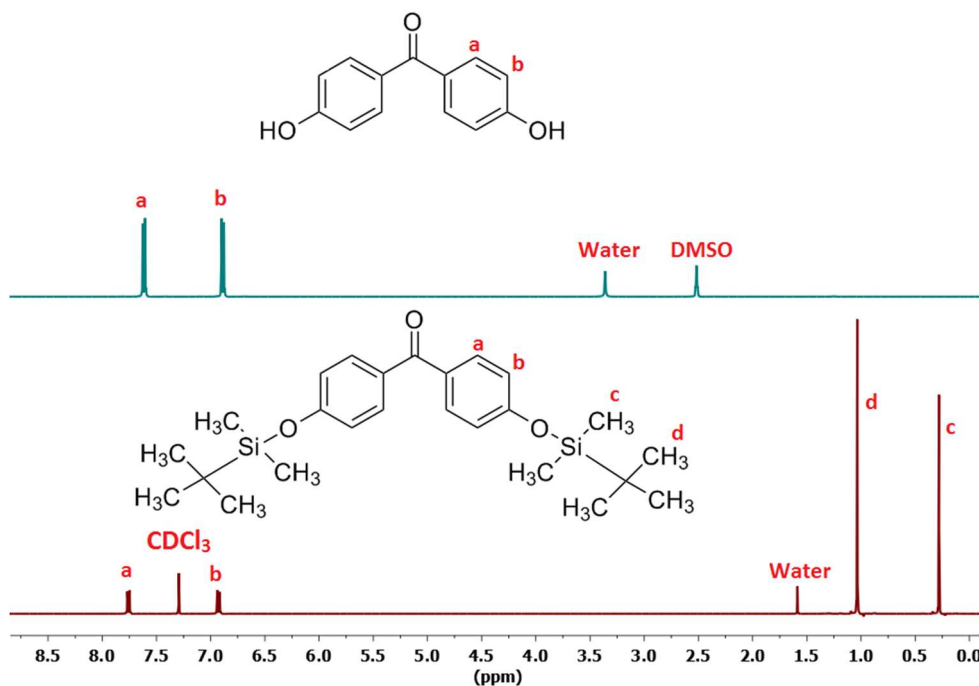


Figure 3.3 - ¹H-NMR spectra comparison between 4,4'-dihydroxybenzophenone (top) and 1-bis(4-*tert*-butyldimethylsiloxyphenyl)benzophenone (bottom)

Step two of the synthesis involved the conversion of the ketone group to an alkene using a Wittig reaction. The product was obtained in a moderate yield (60%), and purified by recrystallisation from ethanol. DPE-OSi was characterised with ¹H-NMR spectroscopy and its spectrum is given below (Figure 3.4).

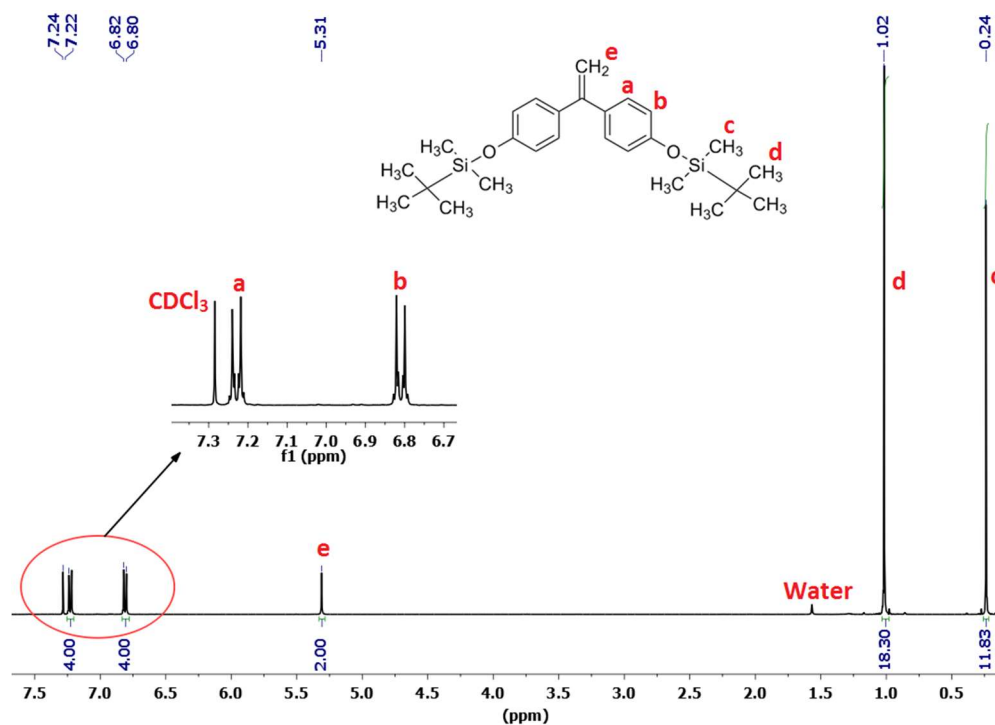


Figure 3.4 - ¹H-NMR spectrum of 1,1-Bis(4-*tert*-butyldimethylsiloxyphenyl)ethylene (DPE-OSi)

The doublet signal at δ 7.24 ppm represents the four aromatic 'a' protons ortho to the alkene substituent in the structure, with the doublet signal at δ 6.82 ppm corresponding to the four aromatic 'b' protons ortho to the silyl ether linkage. The singlet signals at δ 1.02 ppm and δ 0.24 ppm correspond to the eighteen 'd' methyl protons of the *tert*-butyl group and the twelve 'c' methyl protons adjacent to the silyl ether linkage respectively. The signal at δ 7.28 ppm is that of the chloroform solvent; the peak at δ 1.58 ppm is from water. The signal at δ 5.31 ppm is due to the two protons present on the alkene group, confirming the conversion of the ketone to the alkene. The upfield shift of the 'a' protons doublet signal from δ 7.76 ppm seen previously (Figure 3.3) to δ 7.24 ppm is also another indication that that alkene conversion has been achieved. With DPE-OSi produced, the crossbar synthesis could proceed.

3.2.2 Synthesis of Telechelic Polybutadiene "crossbars"

Telechelic polymers are generally defined as homopolymers which are functionalised at each terminal chain end. These reactive functional groups can be introduced to the polymer chain either via chain initiation or end-capping (Figure 3.5). Hutchings' *et al.* have previously reported the use of DPE-OSi as a functional initiator to introduce two phenol functionalities at the initiating end of a polymer chain, this being used to synthesise functionalised PMMA macromonomers for use in the synthesis of HyperMacs.⁹ Conversely, DPE-OSi has also been used as an end-capping agent to introduce the phenol functionalities at the terminating end of a polymer chain.

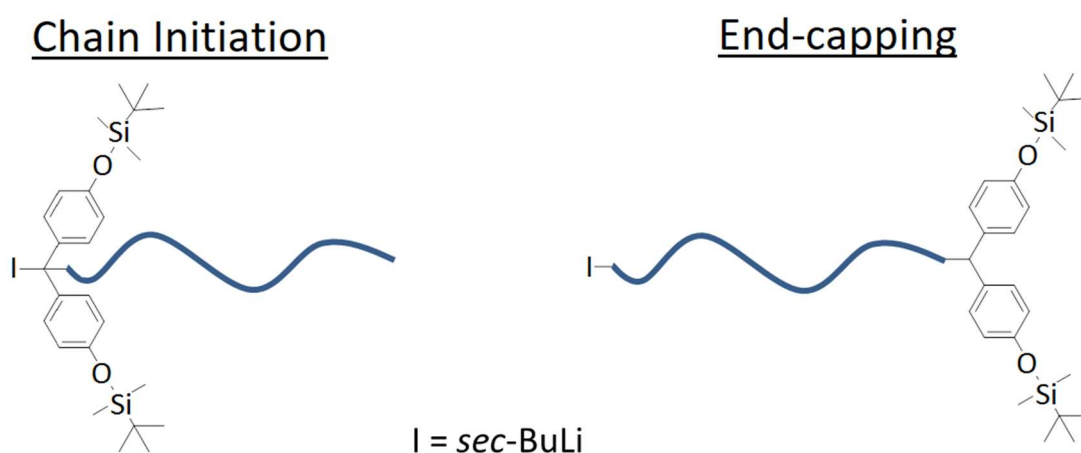


Figure 3.5 - Introduction of functionality to polymer chain ends

For the synthesis of telechelic polymers it can be seen that a combination of methods can be used to introduce the desired functionalities at both chain ends. Moreover, the

introduction of DPE-OSi at the terminal end of each chain can itself be carried out in two ways. For the preparation of telechelic polybutadiene using DPE derivatives, two approaches can be undertaken; for simplicity's sake these will be referred to as the "end-capped" approach and the "fire and forget" approach. Both approaches begin with the same step – namely, the purification and activation of DPE-OSi with *sec*-butyllithium (*sec*-BuLi) to generate the functionalised initiator, which then goes on to polymerise butadiene, introducing functionality at the beginning of each polymer chain.

In the "end-capped" approach, a stoichiometric (or small molar excess) amount of DPE-OSi, with respect to *sec*-BuLi, is introduced at the beginning of the reaction. Butadiene monomer is then added to the reaction vessel and polymerisation initiated by the activated DPE-OSi, generating a polymer with a single unit of DPE-OSi at the initiating end of each polymer chain. Following complete consumption of butadiene, end-capping is achieved by the injection of further DPE-OSi (titrated with *sec*-BuLi prior to addition, to remove impurities) prepared in a separate vessel, producing the final telechelic polymer; as illustrated in Figure 3.6a.

In the "fire and forget" approach, DPE-OSi is introduced at the beginning of the reaction in molar excess with respect to *sec*-BuLi (at least 2.5 : 1 DPE-OSi : Li). DPE-OSi is incapable of homopolymerisation or oligomerisation when reacted with alkyllithium initiators, resulting in the activation of a single equivalent of DPE-OSi with respect to the amount of *sec*-BuLi, with the excess DPE-OSi remaining unreacted. Butadiene monomer is then added to the reaction vessel and is initiated by the activated DPE-OSi. In a non-polar hydrocarbon solvent such as benzene, rather than copolymerise with DPE-OSi, butadiene has a very strong preference to self-propagate. There is no reactivity ratio data for the copolymerisation of butadiene and DPE-OSi, however, the reported reactivity ratio for butadiene and unfunctionalised DPE in non-polar hydrocarbon solvents, is $r_1 = 54$, $r_2 = 0$, and where m_1 is butadiene.¹⁰ The presence of the electron-donating substituents in the para-position of DPE-OSi increases the electron density of the alkene double bond of the molecule, reducing the likelihood of nucleophilic attack from the propagating carbanion, which in turn enhances the preference for butadiene to self-propagate. DPE-OSi is thus excluded from propagation until the all of the butadiene has been consumed. The addition of an end-capping promoter such as TMEDA is then required to accelerate the end-capping of the living chain ends with DPE-OSi, generating the final telechelic polymer; this is illustrated in Figure 3.6b.

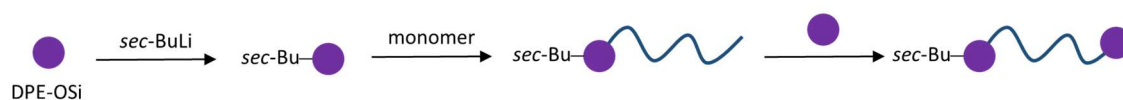
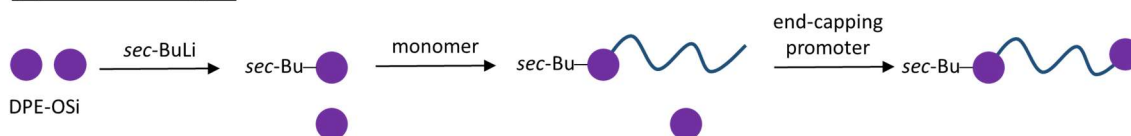
(a) End-capped**(b) Fire and Forget**

Figure 3.6 - General schematic for the synthesis of telechelic “crossbar” polymers via the use of the (a) “End-capped” approach and (b) “Fire and Forget” approach

Both approaches have advantages and disadvantages. In the “fire and forget” approach the main disadvantage arises from the possibility of more than one DPE-OSi unit becoming incorporated into the chains, despite the unfavourable copolymerisation kinetics, due to the DPE-OSi being present in excess. This approach, however, has the advantage that, theoretically, all chains should be end-capped with DPE-OSi. The main disadvantage of the “end-capped” path is the greater potential to introduce environmental impurities at the end-capping step associated with the injection of the DPE-OSi. This in turn will likely lead to a larger percentage of chains not being end-capped. In exploiting the “end-capped” approach, however, there should be no risk of inserting more than the desired number of DPE-OSi units into the polymer chains if a stoichiometric (or excess) amount of DPE-OSi are used. As each approach has its merits, both were carried out in the synthesis of telechelic polymers, discussion of which follows.

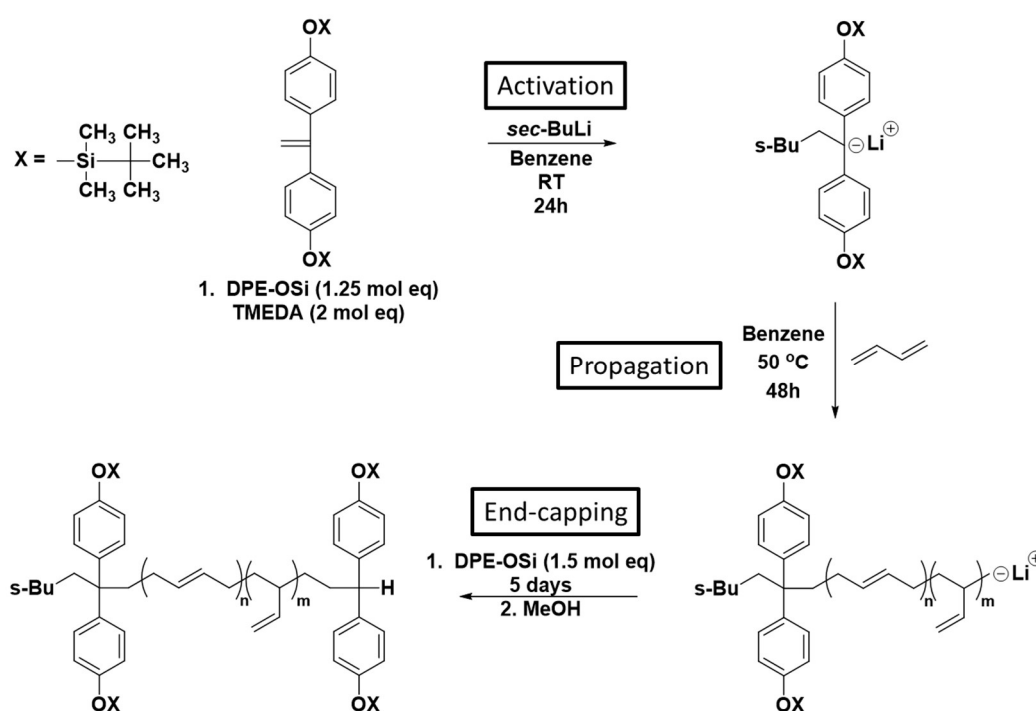
3.2.2.1 Synthesis of Telechelic Polybutadiene - “End-Capped” Approach

3.2.2.1.1 Initial attempts

Two attempts at the synthesis of telechelic polybutadiene were initially carried out via an end-capped approach as shown in Scheme 3.2. In this reaction a small stoichiometric excess of DPE-OSi (with respect to *sec*-BuLi) was azeotropically dried with benzene (three times) to remove any traces of impurities and any water before being dissolved in the required amount of benzene for the reaction. In order to enhance the rate of reaction between *sec*-BuLi and DPE-OSi during activation and subsequent propagation, *N,N,N',N'*-tetramethylethylenediamine (TMEDA) was added, in a 2 : 1 ratio with respect to the

initiating amount of *sec*-BuLi. The DPE-OSi/TMEDA mixture was then titrated with *sec*-BuLi until the appearance of a persistent pale red colour, indicating the formation of the activated DPE-OSi species and the elimination of all impurities. The required amount of *sec*-BuLi for the polymerisation was then added and the reaction between DPE-OSi and *sec*-BuLi allowed to proceed at room temperature for one hour to activate the DPE-OSi. DPE and its derivatives such as DPE-OSi are unable to undergo homopolymerisation, resulting in the formation of a single 1:1 adduct of *sec*-BuLi and DPE-OSi (Scheme 3.2 – Activation).

Butadiene was then added and polymerisation was allowed to proceed for 24 hours at 50 °C, to consume the butadiene fully (Scheme 3.2 – Propagation). At this point a sample of the polymer was collected for analysis and terminated with nitrogen-sparged methanol. It was expected that this sample should consist of polybutadiene with a single DPE-OSi attached only at the initiating α -end of the polymer chains. In a separate vessel, DPE-OSi (1.5 mol equivalent with respect to *sec*-BuLi) was titrated/purified with *sec*-BuLi until the appearance of a persistent red colour. The red-coloured solution was injected into the polymerisation vessel and the reaction was allowed to continue for five days to end-cap the living polybutadiene chains; this length of time was necessary due to the slow reaction of DPE-OSi with the propagating polymer chain ends, even in the presence of TMEDA (Scheme 3.2 – End-capping). The polymer was then terminated with nitrogen-sparged methanol and collected.



Scheme 3.2 - Initial synthetic route of "crossbar" telechelic polybutadiene by the "end-capped" approach.

Two protected telechelic “crossbar” polybutadienes (Scheme 3.2 – End-capping) of differing molecular weights were produced, analysed with both triple detection SEC and ^1H -NMR spectroscopy and the results are given in Table 3.1. The samples collected before the second addition of DPE-OSi in each reaction (Scheme 3.2 – Propagation) were also analysed by SEC and ^1H -NMR. The code to refer to these polymers is “EC-XBAR##- α ” or “EC-XBAR##- $\alpha\omega$ ” – with “##” referring to the molecular weight (M_n) in kg mol^{-1} , “- α ” referring to polymer samples where only the α -end of the polymer chains have been capped with DPE-OSi, “- $\alpha\omega$ ” referring to polymer samples where both the α -end and ω -end of the polymer chains have been capped with DPE-OSi (Figure 3.7). The prefix “EC” denotes that these polymers were synthesised by the end-capped approach.

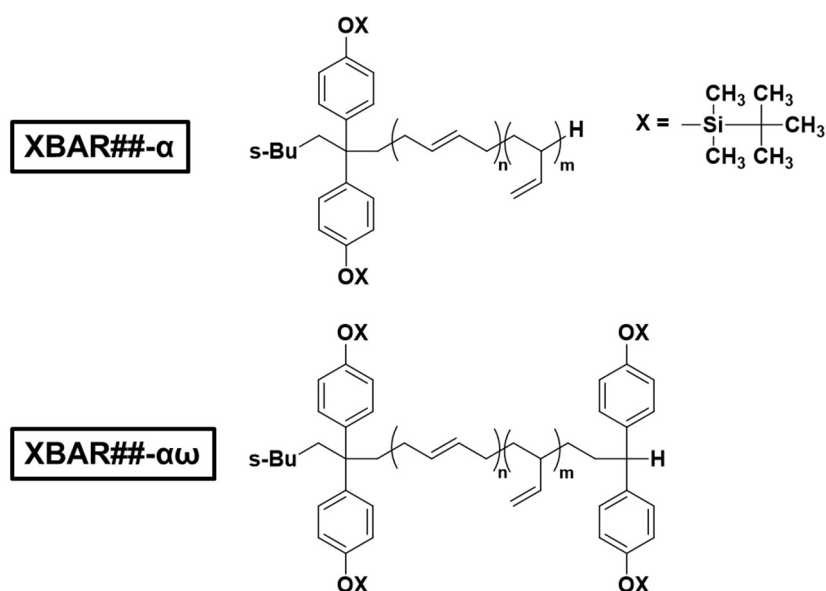


Figure 3.7 - Structures of protected functionalised polymers at each stage of reaction

Although the resulting polymers had low dispersity values, the M_n values obtained for EC-XBAR62 and EC-XBAR76 were in poor agreement with the target M_n values of $10,000 \text{ g mol}^{-1}$ and $20,000 \text{ g mol}^{-1}$ respectively. This may be a consequence of impurities in the reaction vessel lowering the concentration of initiator available for polymerisation, which would increase the molecular weight of the obtained polymers. The impact of TMEDA being present from the start in each reaction also had an adverse effect on the microstructure of the polymers, increasing the vinyl content such that the chains were only 60% 1,4-content. In order to determine the extent of functionalisation of the polymers, ^1H -NMR spectroscopy was used to calculate the average number of DPE-OSi units per chain. A high degree of end-capping (*ca.* 2 DPE-OSi units per chain) of the crossbars is essential for the successful synthesis of H-shaped polymers.

Table 3.1 - Molecular weight data, dispersity and end-capping amount for “crossbar” telechelic polybutadiene synthesised by the “end-capped” path

Crossbar	Target M_n (g mol ⁻¹)	M_n (g mol ⁻¹)	\bar{D}	Average number of DPE-OSi units per chain	1,4-content (%)
EC-XBAR62- α	10,000	62,100	1.02	2.00	60
EC-XBAR62- $\alpha\omega$	10,000	62,300	1.02	2.50	60
EC-XBAR76- α	20,000	78,400	1.03	2.00	60
EC-XBAR76- $\alpha\omega$	20,000	76,300	1.03	2.30	60

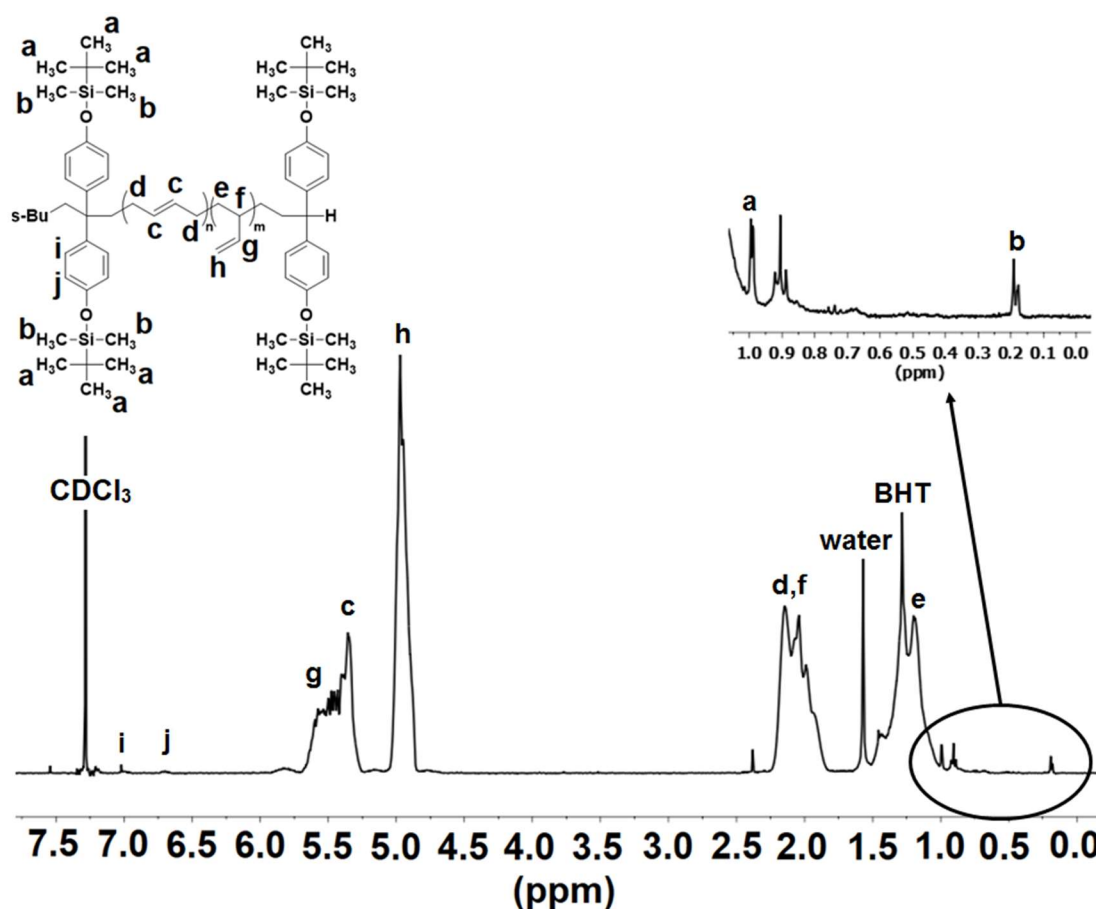
Figure 3.8 - ¹H-NMR spectra of “crossbar” telechelic polybutadiene EC-XBAR62- $\alpha\omega$ synthesised by the “end-capped” approach with TMEDA present from initiation. Expansion between 0.1 ppm and 1.10 ppm focusing on the protection groups introduced to the polymer chain ends.

Figure 3.8 shows the ¹H-NMR spectrum for EC-XBAR62- $\alpha\omega$, which is typical of the spectra obtained for both of these polymers, with expansion between δ 0.10 ppm and δ 1.10 ppm to focus on the region where the signals of the end groups are expected. The singlet at δ 0.99 ppm corresponds to the [(CH₃)₃C-Si] protons and the singlet at δ 0.19 ppm corresponds to the [(CH₃)₂Si] protons of the DPE-OSi protecting groups, indicating successful end-capping. The slight upshift of these signals when compared to the free DPE-OSi (δ 1.02 ppm

to δ 0.99 ppm and δ 0.24 ppm to δ 0.19 ppm respectively) in addition to signal broadening, is further evidence that these signals are due to the protected DPE-OSi units being attached directly to polymer chains.

With the molecular weight data obtained from SEC, and analysis of the ^1H -NMR integrals for the end group signals at δ 0.99 ppm and δ 0.19 ppm, the average number of DPE-OSi units per chain can be calculated for both the “ α ” (mono-DPE-OSi capped) and “ $\alpha\omega$ ” (telechelic) polymers, the results of which are also shown in Table 3.1. It is clear that for polymers EC-XBAR62 and EC-XBAR78 the degree of “end-capping” is higher than expected; in the samples taken before the second addition of DPE-OSi, for which an average of one unit of DPE-OSi was expected, two DPE-OSi units are present per chain. The α,ω -end-capped samples (EC-XBAR62 and EC-XBAR78) have 2.5 and 2.3 DPE-OSi units per chain indicating that more than the expected number of two DPE-OSi units are present per chain. DPE (and its derivatives) are incapable of homopolymerisation; they can however undergo copolymerisation with styrenes and dienes.¹¹ In the two described polymerisation reactions, the presence of TMEDA from the start has had a marked effect on the copolymerisation kinetics. Although previous work suggested that the copolymerisation kinetics of DPE-OSi with butadiene are extremely unfavourable for the incorporation of DPE-OSi into the chains, the presence of TMEDA would appear to have changed the kinetics such that DPE-OSi is not excluded from copolymerising with butadiene. In this case it would appear that any excess DPE-OSi remaining after the activation step, is able to copolymerise with butadiene resulting in DPE-OSi units in-chain, as well as at the chain ends; this is illustrated in Figure 3.9. The high molecular weight of the polymers arising as a result of *sec*-BuLi deactivation by impurities, would also increase the stoichiometric excess of DPE-OSi per chain and allow copolymerisation with butadiene.

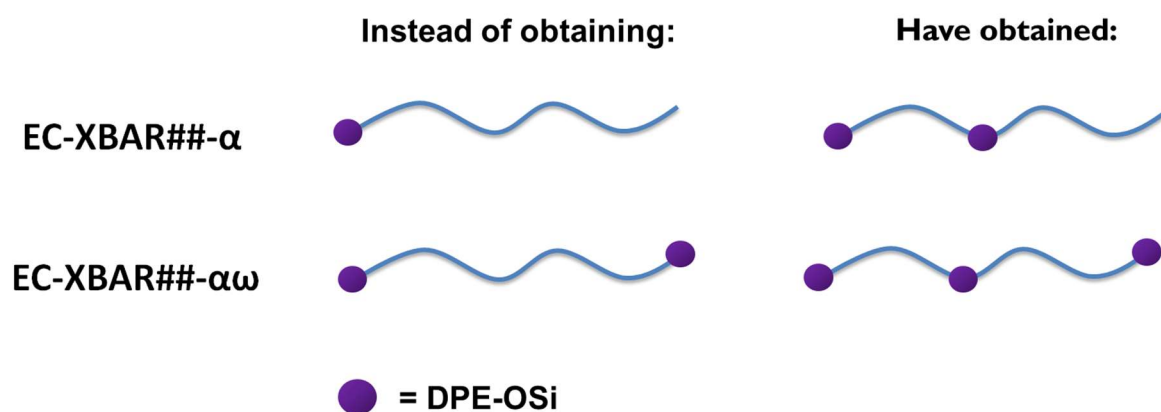
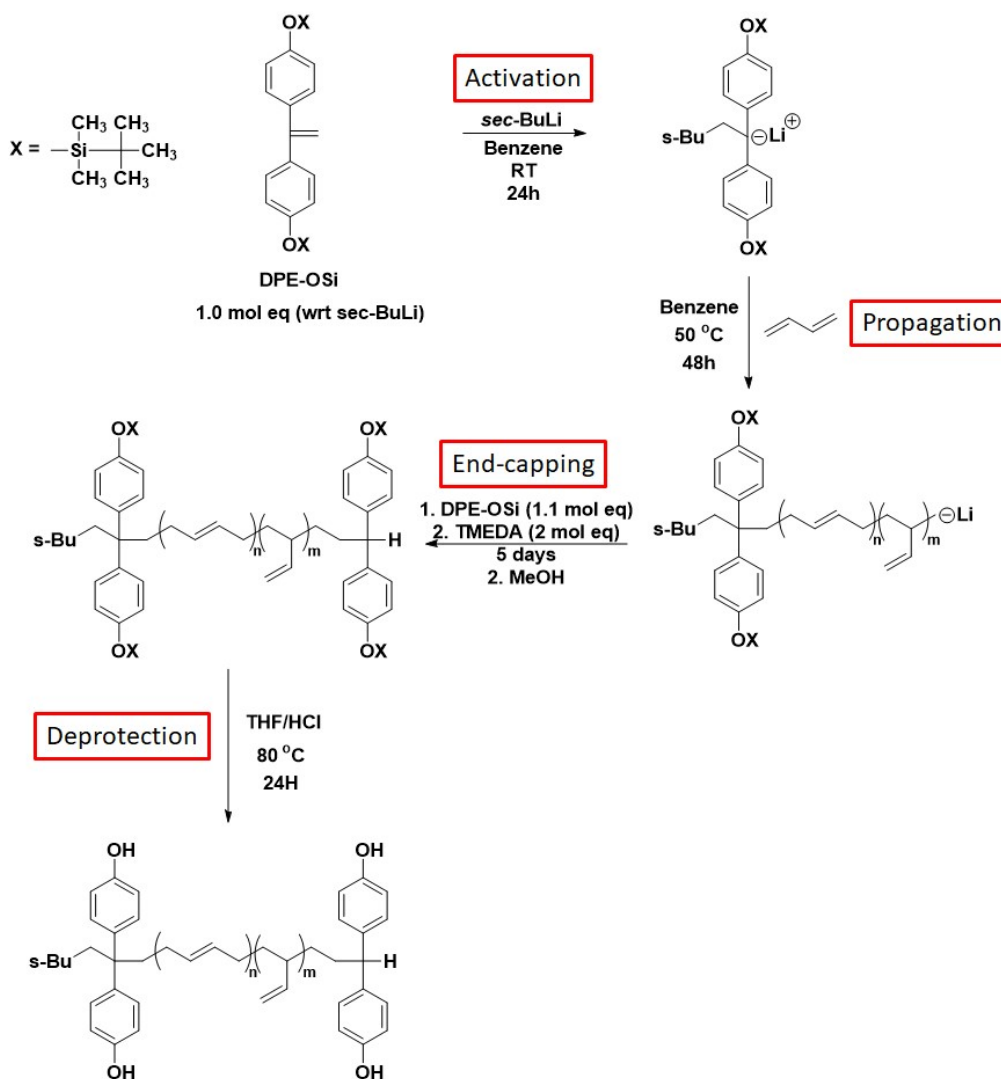


Figure 3.9 - Illustration depicting the effect of TMEDA on DPE-OSi incorporation

The polymers obtained are far from ideal as crossbars for H-polymer synthesis. While the synthesis has been successful from the perspective of generating protected functionalised polymers, it has also introduced a degree of randomness into the polymer chains, with extra DPE-OSi units being incorporated mid-chain. In a subsequent coupling reaction, this would lead to higher degrees of branching and structural heterogeneity. The lower 1,4-microstructure also may present challenges if these are to be used as macromonomers for the eventual synthesis of H-shaped polymers. As such it was necessary to modify the end-capping route in order to overcome these problems.

3.2.2.1.2 Modified End-Capped Approach

In 2015, it was reported that in non-polar, hydrocarbon solvents such as benzene, DPE-OSi is unable to copolymerise with butadiene due to the very low reactivity ratio between butadiene and DPE-OSi in such solvents. It was shown that under these conditions, end-capping only proceeds in the presence of polar promoters such as TMEDA.¹² Exploiting this attribute allowed for the successful synthesis of telechelic polybutadienes with a high 1,4-content, as TMEDA was only added after complete consumption of butadiene, to promote the end-capping reaction. Thus in the current study, the synthesis of telechelic polybutadiene as described above, was modified to delay the addition of TMEDA until post-propagation; this is shown in Scheme 3.3.



Scheme 3.3 - Modified synthesis of “crossbar” telechelic polybutadiene by the modified “end-capped” approach

The (modified) reaction shown in Scheme 3.3 is similar to the one seen in Scheme 3.2 with a few key differences. Thus i) the reaction between DPE-OSi and *sec*-BuLi (Scheme 3.3 – Activation) was allowed to proceed at room temperature overnight rather than for one hour, to ensure complete DPE-OSi activation; ii) TMEDA (2 mol eq with respect to *sec*-BuLi), instead of being present pre-propagation, was added alongside the second batch of DPE-OSi (1.1 mol equivalent with respect to *sec*-BuLi) in benzene (5 ml) post-propagation. The TMEDA/DPE-OSi mix was titrated with *sec*-BuLi and purified overnight. The resulting red solution of TMEDA/DPE-OSi was then injected directly into the polymerisation mixture to end-cap the living polybutadiene chains (Scheme 3.3 – End-capping). One example of a protected telechelic “crossbar” polybutadiene (EC-XBAR32- $\alpha\omega$) was prepared by this (modified) procedure, analysed using triple detection SEC and

^1H -NMR spectroscopy and the data for this sample, along with the data for the intermediate α -end-capped polymer are presented Table 3.2.

Table 3.2 - Molecular weight data, dispersity and end-capping for “crossbar” telechelic polybutadiene synthesised by the modified “end-capped” approach

Crossbar	Target M_n (g mol^{-1})	M_n (g mol^{-1})	\bar{D}	Average number of DPE-OSi units per chain	1,4-content (%)
EC-XBAR32- α	25,000	32,700	1.06	0.93	94
EC-XBAR32- $\alpha\omega$	25,000	32,900	1.06	1.92	94

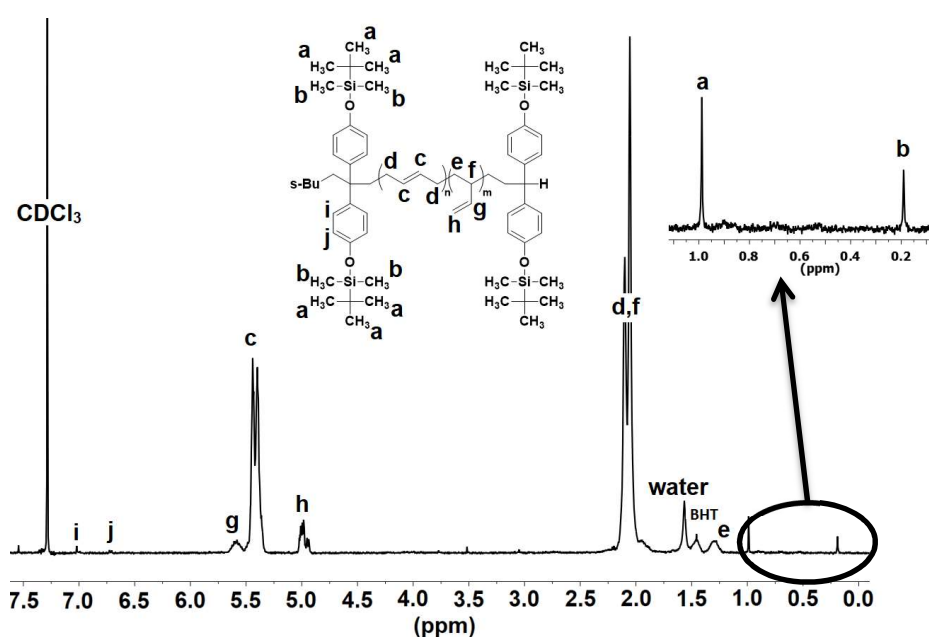


Figure 3.10 - ^1H -NMR spectra of “crossbar” telechelic polybutadiene EC-XBAR32 synthesised by the “end-capped” approach.

Figure 3.10 shows the ^1H -NMR spectrum for EC-XBAR32 and when compared to the ^1H -NMR spectrum for XBAR62- $\alpha\omega$ (Figure 3.8) the difference in the polybutadiene microstructure is clear. The vinyl proton peak at 5.0 ppm is much less intense for EC-XBAR32, as expected. The high (94%) level of 1,4-microstructure obtained arises due to the absence of TMEDA during propagation, as well as the use of a non-polar hydrocarbon reaction solvent. The silyl ether peaks again appear in the expected region between δ 1.00 ppm and δ 0.10 ppm as seen for the previous polymers. Using molecular weight data obtained from SEC combined with analysis of the ^1H -NMR integrals of end group signals at δ 0.99 ppm and δ 0.19 ppm, it was possible to calculate the average number of DPE-OSi units per chain. A value of 0.93 DPE-OSi units per chain was obtained for EC-XBAR32- α (one end-capped) and a value of 1.92 DPE-OSi units per chain was obtained for EC-

XBAR32- $\alpha\omega$ (both ends-capped). These numbers suggest that the majority of the chains of EC-XBAR32- α have a single unit of DPE-OSi, and the majority of the chains of EC-XBAR32- $\alpha\omega$ have two units of DPE-OSi.

The “end-capped” approach (both initial and modified approaches) has been used to synthesise three telechelic polybutadiene polymers, however, initial attempts met with limited success. A modified approach in which TMEDA was added to promote the end-capping reaction, only after propagation, yielded a polymer with good control over molecular weight, microstructure and the degree of end-capping. As EC-XBAR32- $\alpha\omega$ was the only polymer generated with the required characteristics a very high degree of the desired level of end-capping, it was retained for subsequent deprotection by mild acid hydrolysis to obtain the fully functionalised telechelic macromonomer.

3.2.2.2 Synthesis of Telechelic Polybutadiene by the “Fire and Forget” Approach

The synthesis of telechelic polybutadiene by the “fire and forget” approach is more facile with significant advantages, yet in many respects is similar to the “end-capping” approach. The key difference is that a 2.5 molar excess (with respect to *sec*-BuLi) of DPE-OSi is present from the start of the reaction. The “end-capped” approach, described above, experienced problems caused by the deactivation/termination of propagating chains by impurities introduced with the DPE-OSi at the end-capping stage. It was therefore reasoned that the addition of all the required DPE-OSi before initiation would eliminate said issue. So with the “fire and forget” approach, DPE-OSi was purified by titration with *sec*-BuLi until the appearance of a persistent pale red colour, indicating the formation of a small portion of the activated DPE-OSi species. The required amount of *sec*-BuLi to initiate polymerisation was then added and the reaction between DPE-OSi and *sec*-BuLi allowed to proceed at room temperature for 24 hours (Scheme 3.3 – Activation). Butadiene was then added to the reaction vessel and propagation was allowed to continue for another 24 hours at 50 °C to ensure complete consumption of the butadiene (Scheme 3.3 – Propagation). A sample was collected for analysis and terminated with nitrogen-sparged methanol. TMEDA (2 mol equivalents with respect to *sec*-BuLi) was then injected directly into the polymerisation flask and the reaction was allowed to proceed for a further five days at 50 °C to end-cap the living polybutadiene chains with the excess DPE-OSi, which is effectively unreactive until the addition of TMEDA (Scheme 3.3 – End-capping). TMEDA is a Lewis base, and its

addition results in the dissociation of Pbd-Li aggregates, resulting in Pbd-Li chains which are more reactive to DPE-OSi end-capping.⁹ The end-capped polymer was then terminated with nitrogen-sparged methanol and recovered. A range of protected telechelic “crossbar” polybutadienes of differing molecular weights were produced by the “fire and forget” approach and analysed by triple detection SEC and ¹H-NMR spectroscopy - the SEC results are reported in Table 3.3. The code to refer to these polymers is “FF-XBAR##-α”, with “##” referring to the molecular weight (M_n) in kg mol⁻¹, “-α” referring to polymer samples where only the α-end of the polymer chains have been DPE-OSi capped, “-αω” referring to polymer samples where both the α-end and ω-end of the polymer chains have been DPE-OSi capped and “FF” denoting that these polymers were synthesised by the “fire and forget” approach.

Table 3.3 - Molecular weight data, dispersity and extent of end-capping for “crossbar” telechelic polybutadiene synthesised by the “fire and forget” approach

Crossbar	Target M_n (g mol ⁻¹)	M_n (g mol ⁻¹)	Đ	Average number of DPE-OSi units per chain	1,4-content (%)
FF-XBAR29-α	20,000	28,700	1.08	0.95	94
FF-XBAR29-αω	20,000	29,000	1.07	1.90	94
FF-XBAR52-α	25,000	52,300	1.04	0.90	94
FF-XBAR52-αω	25,000	52,400	1.04	1.80	94
FF-XBAR53-α	50,000	51,100	1.03	0.95	94
FF-XBAR53-αω	50,000	53,000	1.03	1.90	94
FF-XBAR100-α	50,000	101,200	1.09	0.90	94
FF-XBAR100-αω	50,000	101,600	1.13	1.80	94

Crossbar polymers FF-XBAR29 and FF-XBAR53 with M_n values of 29,000 g mol⁻¹ and 51,100 g mol⁻¹ were obtained, in good agreement with their target M_n values of 20,000 g mol⁻¹ and 50,000 g mol⁻¹ respectively. However, for polymers FF-XBAR52 and FF-XBAR100, M_n values of 52,400 g mol⁻¹ and 101,600 g mol⁻¹ were roughly double the target M_n values of 25,000 g mol⁻¹ and 50,000 g mol⁻¹ respectively. This is most likely due to the presence of impurities which deactivated a portion of the initiator prior to or during initiation. The extent of end-capping by ¹H-NMR was calculated using the same procedure as described above for the polymers produced by the “end-capping” route.

^1H -NMR analysis indicated that the polymers synthesised by the “fire and forget” approach have high degrees of end-capping in every case. The average number of DPE-OSi units at the α -end -was greater than 0.9 in each case, and 0.95 for samples FF-XBAR29- α and FF-XBAR52- α , indicating that the majority of chains had 1 DPE-OSi unit present. After TMEDA was introduced to promote end-capping, the average number of DPE-OSi units per chain was between 1.80 and 1.90, indicating that the majority of chains have 2 units of DPE-OSi. The value for polymers FF-XBAR52- $\alpha\omega$ and FF-XBAR100- $\alpha\omega$, is slightly lower than for FF-XBAR29- $\alpha\omega$ and FF-XBAR52- $\alpha\omega$, which is probably due to the introduction of traces of impurities with the TMEDA, leading to termination of some chains.

The synthesis of telechelic polybutadiene by the fire and forget approach was performed with DPE-OSi present in a 2.5 molar ratio with respect to *sec*-BuLi. This ratio should ensure that the reaction between *sec*-BuLi and DPE-OSi is highly efficient, leading to a majority of chains having DPE-OSi present at the initiating chain-end. Additionally, in a non-polar solvent the excess DPE-OSi should play no further part in the polymerisation of butadiene due to the extremely low reactivity between polybutadienyllithium and DPE-OSi. Thus DPE-OSi is expected to be totally excluded from the polymerisation of butadiene and it can be assumed that polymerization of butadiene in the presence of a small fraction of DPE-OSi should result in a homopolymer of polybutadiene with the overwhelming majority of chains having only a single DPE-OSi unit, present at the initiating chain end.¹²

The “fire and forget” approach has been used to synthesise four telechelic polybutadienes. ^1H -NMR analysis indicates that a high degree of end-capping was achieved in all cases. When comparing the results obtained by the “end-capping” and “fire and forget” approaches, it can be concluded that the “fire and forget” approach is more facile and results in better outcomes. The addition of 2 equivalents of TMEDA after the propagation step would appear to result in the introduction of much lower levels of impurities when compared to the addition of DPE-OSi post propagation with the “end-capped” approach. The post-polymerisation addition of TMEDA also means that a high 1,4-microstructure is retained. All four “fire and forget” crossbar polybutadienes, FF-XBAR29, FF-XBAR52, FF-XBAR53 and FF-XBAR100 were retained for subsequent deprotection.

3.2.2.3 Deprotection of Crossbars

In order to generate the final crossbar macromonomers, it was necessary to remove the silyl protection groups and restore the hydroxyl functionalities. This was achieved with mild acid hydrolysis, as detailed in Scheme 3.3. The selected crossbar was dissolved (10 wt.% w/v) in THF. Concentrated aqueous hydrochloric acid (HCl, 37.0 wt%) was then added in 10 molar excess (with respect to protected phenol groups) and the solution was stirred at reflux overnight to ensure complete deprotection.⁸ The reaction was followed by ¹H-NMR spectroscopy and stopped when the peaks for the methyl groups present on the silyl ether were no longer detected. A typical ¹H-NMR spectrum (Figure 3.11) is shown demonstrating FF-XBAR52 before and after deprotection. The methyl group signals at 0.19 ppm [(CH₃)₂Si] and at δ 0.99 ppm [(CH₃)₃C-Si] disappear completely indicating that deprotection was successful.

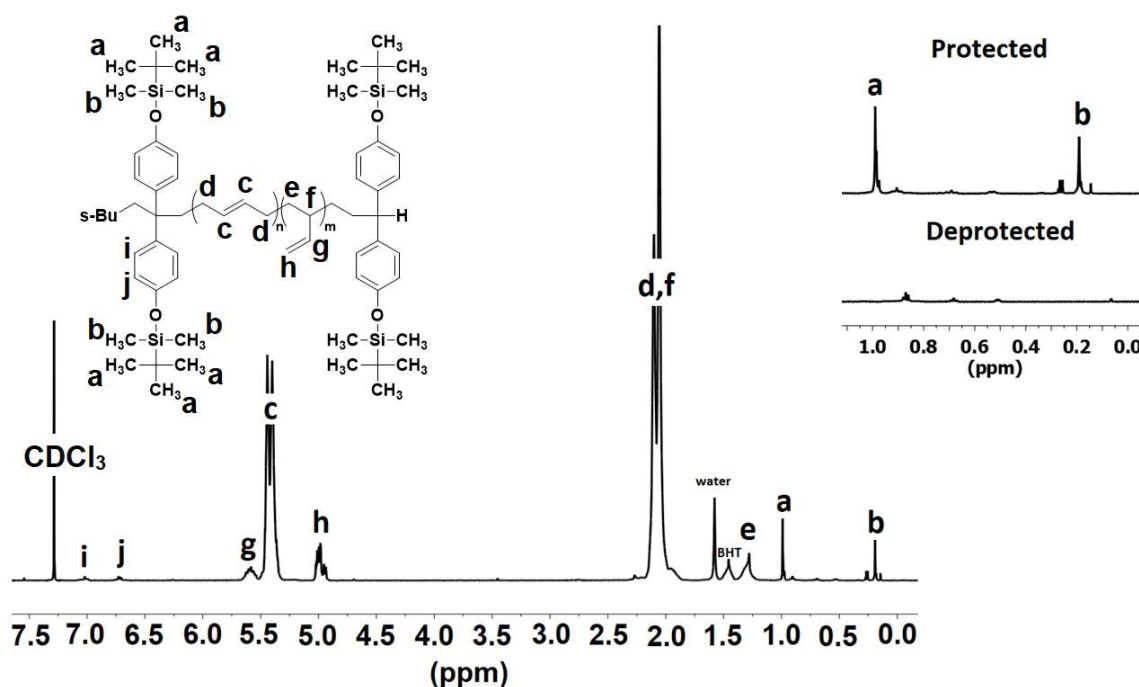
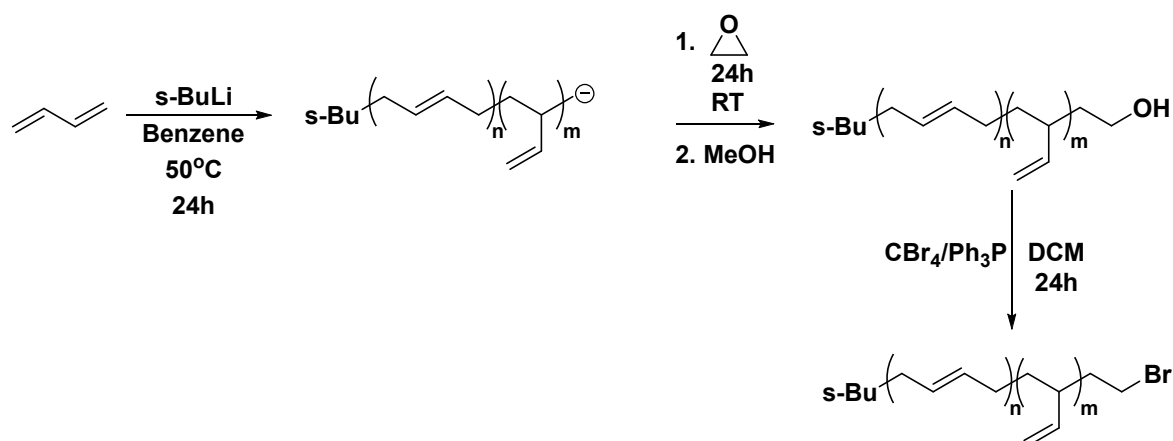


Figure 3.11 - ¹H-NMR spectra of telechelic polybutadiene crossbar FF-XBAR52. Comparison of the polymer spectra before and after deprotection is reported.

All four “Fire and Forget” telechelic polybutadienes, FF-XBAR29, FF-XBAR52, FF-XBAR53 and FF-XBAR100 as well as “end-capped” polymer EC-XBAR32 were all fully deprotected using the described methodology.

3.2.3 Synthesis of Polybutadiene “arm” Macromonomers

Complementary macromonomers that would constitute the linear “arm” segments of the H-shaped polymers were also synthesised using the macromonomer approach. As shown previously (Figure 3.5), the introduction of functionality to a polymer chain-end can either be carried out pre-polymerisation, using a functionalised initiator or post-polymerisation using end-capping agents. In a previous project in Durham focussed on the synthesis of a range of asymmetric polystyrene stars, living anionic polymerisation was exploited by Agostini and Hutchings, using a protected initiator, 3-*tert*-butyldimethylsiloxy-1-propyllithium, to generate linear polystyrene macromonomers with a single silyl protected hydroxyl functionality at the initiating chain end.¹³ The advantage of using a protected initiator in this way, ensures that 100% of the chains will contain the desired functionality. However, the lack of availability of this initiator led to the use of more traditional post-polymerisation end-capping methods. For a subsequent Williamson coupling reaction, an alkyl halide is required for reaction with the phenolic hydroxyl groups present on the crossbars. It has been shown previously that bromine-terminated polymers couple very effectively with -OH (phenol) functionalised polymers,¹⁴ hence it was decided that the polybutadiene arm macromonomers for the H-shaped polymers would be prepared with bromide functionalised chain ends and a series of such polymers was synthesised by the method shown overleaf in Scheme 3.4. Linear polybutadiene was first synthesised via living anionic polymerisation and a single -OH functionality was introduced to the polymer chain ends via end-capping with an excess of ethylene oxide with respect to *sec*-BuLi. Samples (terminated with nitrogen-sparged methanol) were taken before the addition of ethylene oxide, to obtain non-functionalised polymers for comparative analysis. The hydroxyl functionalised polymers then underwent conversion to give bromine-terminated polymers via an Appel reaction, using CBr₄/PPh₃ in dichloromethane (DCM). Triple detection SEC characterisation was carried out on all intermediate samples and final (end-capped) polymers and the results are reported in Table 3.4. The code used in these samples is “ARMX-H/OH/Br” with X corresponding to the molecular weight (M_n) in kg mol⁻¹ and H/OH/Br denoting the end group present on the polymer in question.



Scheme 3.4 - Synthesis of bromine end functionalised linear polybutadiene arms

Table 3.4 - Molar mass data of arm polymers (solvent THF; $dn/dc = 0.124 \text{ ml g}^{-1}$)

Arm	Target M_n	M_n (g mol^{-1})	M_w (g mol^{-1})	\bar{D}	% Functionalisation*
ARM19-H	20,000	18,800	19,100	1.02	-
ARM19-OH	20,000	19,700	20,200	1.03	91
ARM19-Br	20,000	19,200	19,900	1.04	91
ARM23-H	20,000	23,300	25,200	1.08	-
ARM23-OH	20,000	23,200	24,700	1.06	86
ARM23-Br	20,000	24,900	26,800	1.08	86
ARM25-H	25,000	24,900	26,400	1.06	-
ARM25-OH	25,000	24,600	25,600	1.04	92
ARM25-Br	25,000	24,300	25,100	1.03	92
ARM31-H	30,000	28,400	29,400	1.04	-
ARM31-OH	30,000	28,400	29,700	1.05	96
ARM31-Br	30,000	31,400	33,800	1.08	96
ARM40-H	40,000	40,800	42,600	1.04	-
ARM40-OH	40,000	40,800	42,600	1.04	95
ARM40-Br	40,000	40,300	41,600	1.03	95

*Percentage of functionalised arm formed during the end-capping reaction with ethylene oxide calculated by deconvolution of the IC chromatograms (RI and/or UV detectors) using a Gaussian distribution.

^1H -NMR analysis was carried out on all polymers and samples in an attempt to determine the extent of end-capping, with the resonance of the $\text{CH}_2\text{-X}$ protons being expected between δ 3.00 – 4.00 ppm. An example of this is shown in Figure 3.12 for ARM31. It can be seen in the ^1H -NMR spectrum of ARM31-OH that a signal is visible at δ 3.66 ppm (Figure 3.12 - 2)). This signal is visible only after the addition of ethylene oxide which is evident when

compared with the unfunctionalised ARM31-H (Figure 3.12 - 1)) suggesting it belongs to the $\text{CH}_2\text{-OH}$ protons. ^1H -NMR analysis also revealed the extent of the bromination, with an upfield shift of the signal at δ 3.66 ppm ($-\text{CH}_2\text{-OH}$) expected as the protons will be attached to a (less electronegative) $-\text{Br}$ group rather than an $-\text{OH}$ group. This shift was detected (Figure 3.12 - 3)) with the signal between δ 3.30 – δ 3.40 ppm arising due to the $\text{CH}_2\text{-Br}$ protons, in line with previous reports.¹³

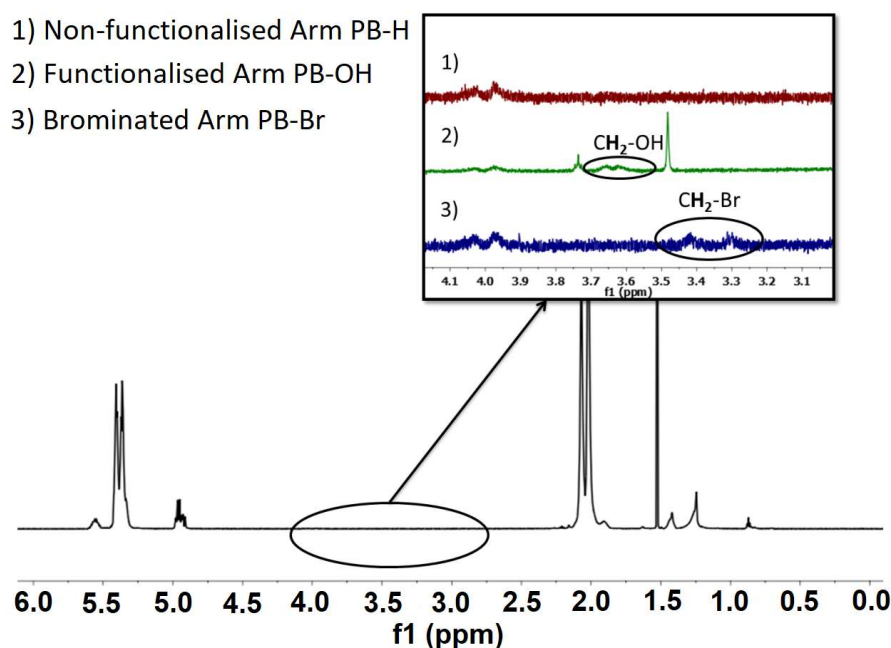


Figure 3.12 - ^1H -NMR spectra (700 MHz) of polybutadienes ARM31-H, ARM31-OH and ARM31-Br. Expansion between 3.0 ppm and 4.2 ppm focusing on the functional groups introduced to the polymer chain ends.

The use of ethylene oxide as a terminating agent in living anionic polymerisation has traditionally proven efficient with (nearly) quantitative ($> 99\%$) end-capping being reported.¹⁵ However, due to the relatively high molecular weight of the polymers synthesised in the current work, the NMR peaks associated with expected chain-end functionalities are, whilst visible, not very clear and accurate analysis of the degree of end-capping is significantly hampered by a very poor signal to noise ratio, even with the use of a 700 MHz ^1H -NMR instrument and expansion of the spectra obtained. As a result, the calculated integrals from these signals will be inaccurate. In order to try and gain a more consistent, quantitative determination of the extent of chain end functionalisation of the arm polymers, interaction chromatography (IC) – specifically normal-phase interaction chromatography (NP-IC) analysis was employed.

3.2.4 Analysis of Macromonomers by Interaction Chromatography

Interaction Chromatography (IC) is an analytical technique in which polymers are separated by molecular weight; it can be carried out isothermally, with a solvent gradient or with a temperature gradient, however, solvent gradient IC has not been used in the current work. Reversed-phase interaction chromatography (RP-IC) as well as Normal-phase interaction chromatography (NP-IC) have been shown to be powerful chromatographic techniques in which polymers can be separated by their molecular weight, rather than molecular size as is the case with SEC. This can lead to superior separation and resolution when compared to SEC. A more detailed description of interaction chromatography is included in Chapter 2 (section 2.2.3). NP-IC analysis can, in addition to separation based on molecular weight, also enable the separation of polymers via their chain-end functionality, thus providing an alternative method for the quantification of the extent of end-capping.

In 2015, Hutchings, Oti *et al.* for the first time used both normal-phase isothermal interaction chromatography (NP-IIC) and normal-phase temperature-gradient interaction chromatography (NP-TGIC) for the quantitative characterization of high molecular weight, chain end-functionalised polymers.¹⁶ A series of end-functionalised polystyrene (PS) samples with an identical molecular mass ($M_n = 89,000 \text{ g mol}^{-1}$) but varying chain-end functionality (PS-H, PS-OH and PS-Br), as well as a series of high molecular weight chain end-functionalised polybutadiene samples (PB-H and PB-OH) were analysed. The hydroxyl functionalized linear polybutadiene samples were prepared using identical synthetic techniques to those reported in this work (Scheme 3.4 - Synthesis of bromine end functionalised linear polybutadiene arms) and ranged in molar mass from $28,000 \text{ g mol}^{-1}$ to $200,000 \text{ g mol}^{-1}$. For both the polystyrene and polybutadiene samples it was possible to obtain complete (baseline) separation, only as a function of chain-end functionality, for all polymers investigated. The capacity of NP-IC for the quantitative analysis of high molecular weight, end-functionalised polymers makes the technique extremely valuable for the analysis/quantification of end-group functionalisation and modification, especially considering that other analytical techniques such as MALDI-ToF mass spectrometry and NMR spectroscopy are often incapable of allowing quantitative end-group analysis at high molar masses ($>20,000 \text{ g mol}^{-1}$).

3.2.4.1 NP-IC Analysis of the Arms

Normal-phase isothermal interaction chromatography (NP-IIC) was used to analyse the linear polybutadiene arms synthesised in this work, enabling quantitative analysis of the extent of end-capping. Examples of typical chromatograms obtained from the NP-IIC analysis of the linear arms are given in Figure 3.13 for the highest molecular weight linear polybutadiene, ARM40. Samples of the i) non-functionalised, ii) hydroxyl terminated and iii) brominated polymers (ARM40-H, ARM40-OH and ARM40-Br respectively) were subjected to analysis using a mobile phase of isooctane/THF in a 96/4 (v/v) ratio under isothermal conditions (50 °C) at a flow rate of 1.0 ml/min and the three chromatograms compared.

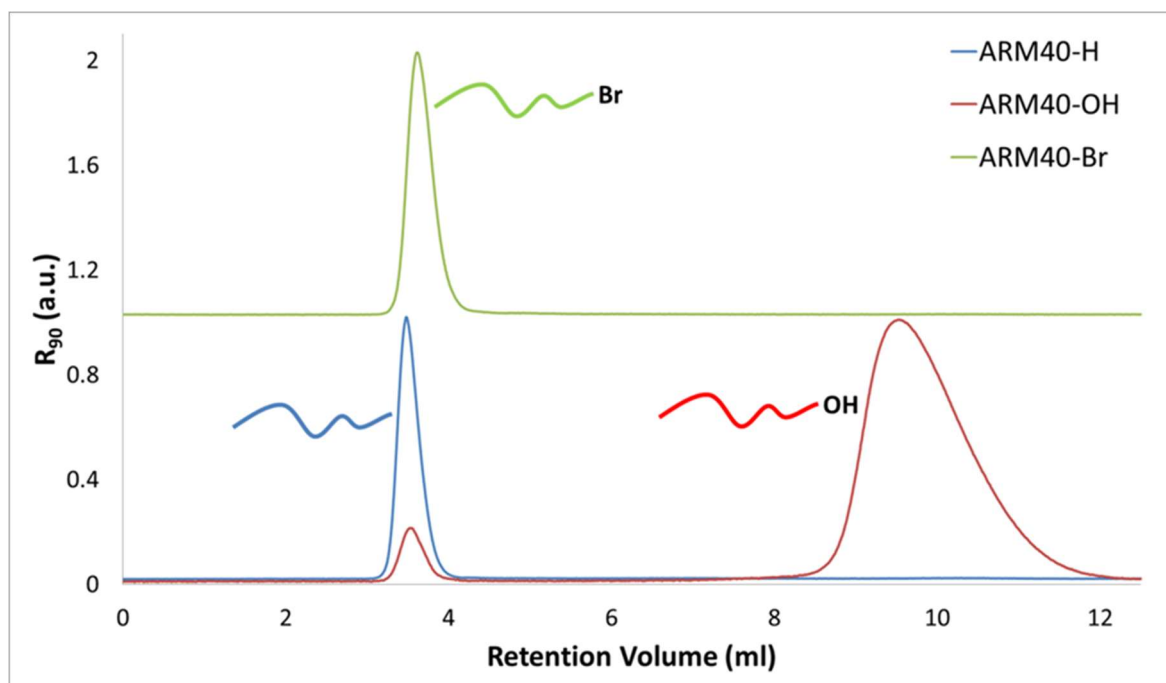


Figure 3.13 - Isothermal (50 °C) NP-IIC chromatograms (RALS detector) of ARM40-H, ARM40-OH and ARM40-Br at a solvent composition of 96/4 isooctane/THF.

The non-functionalised polymer ARM40-H, shows a single peak (in blue) at a retention volume of 3.3 ml, whereas the -OH functionalised polymer ARM40-OH (in red) shows two peaks, one small peak at 3.3 ml and another much larger, broader peak at 9.5 ml - these represent the unfunctionalised chains and the -OH end-functionalised chains respectively. Normal-phase IC utilises a polar stationary phase, in this case a single diol modified silica HPLC column, therefore the non-polar sample - the non-functionalised ARM40-H and the weakly polar brominated sample ARM40-Br (in green) interact less strongly with the stationary phase and are eluted much earlier. However, the hydroxyl group present on

ARM40-OH interacts more strongly with the polar stationary phase and these chains are retained for longer by the column, which also leads to the broader nature of the peak. Analysis of the areas under each peak for sample ARM40-OH indicated that 95% of chains (peak at 9.5 ml) have been -OH end-capped with 5% of chains (peak at 3.3 ml) remaining unfunctionalised. The success of end-capping reaction depends on the purity of the ethylene oxide added to the reaction vessel. Unfortunately, it is usually impossible to avoid unwanted termination due to environmental impurities which results in less than 100% functionalisation. Nevertheless, NP-IIC allows quantitative and accurate analysis of the degree of functionalisation and confirms a very high degree of functionalisation.

Finally, the ARM40-Br chromatogram shows one peak at 3.5 ml, representing the -Br functionalised polymer chains. Since the -Br peak at 3.5 ml overlaps with the peak recorded for the unfunctionalised -H peak at 3.3 ml it is not possible to obtain baseline separation of the residual unfunctionalised polymer and bromine functionalised samples. However, the absence of any trace of a peak at 9.5 ml does suggest that the complete conversion of all -OH end-functionalised chains into -Br chains has taken place, indicating that ARM40-Br is the desired -Br terminated product, with some remaining unfunctionalised chains.

The non-functionalised, -OH functionalised and -Br functionalised samples of the other arm polymers (ARM19, ARM21, ARM25, and ARM31) were also subjected to analysis under similar conditions and provided comparable results to that of ARM40 which are reported in Figure 3.14. The chromatograms shown in Figure 3.14 clearly illustrate that each of the -OH functionalised polymers have achieved a high degree of end-capping, as evidenced by a broad -OH peak in the chromatograms of the ARMX-OH samples analysed. However, in each case there also remains a smaller peak at a lower retention volume, corresponding to a small fraction of unfunctionalised polymer, indicating that 100% end-capping has not been achieved. The exact extent of end-capping was calculated simply using the area of the sample's constituent peaks, in this case either the RI or UV (concentration) detectors, the results of which were presented in Table 3.4 (page 97). In all cases, at least 90% of the chains have been -OH functionalised with the exception of ARM23 in which only 86% were functionalised. NP-IIC chromatograms also confirm that the -OH groups were fully converted into the desired -Br group. A small fraction of non-functionalised (ARMX-H) polymer will probably also be present in the brominated samples of the ARM19-Br and ARM25-Br (Figure 3.14a and Figure 3.14c respectively); however, it seems that this (unfunctionalised) sample co-elutes with the brominated sample peak,

owing to their identical molecular weights and similar polarities. Separation of these two species was not possible under these conditions, but the fraction of unfunctionalised chains in the final samples should have a limited impact on the use of the macromonomer. It is interesting to note, however, for samples ARM23-Br and ARM31-Br (Figure 3.14b and Figure 3.14d respectively) that the peaks for the brominated samples do not appear at quite the same elution volume as the -H or -OH. This may be due to the higher temperature (60 °C) these samples were run at compared to ARM19 and ARM23, which were carried out at 50 °C. The use of higher temperature appears to have resulted in shorter elution of the ARM-H sample allowing for slightly better separation between the non-polar ARM-H and slightly polar ARM-Br samples respectively.

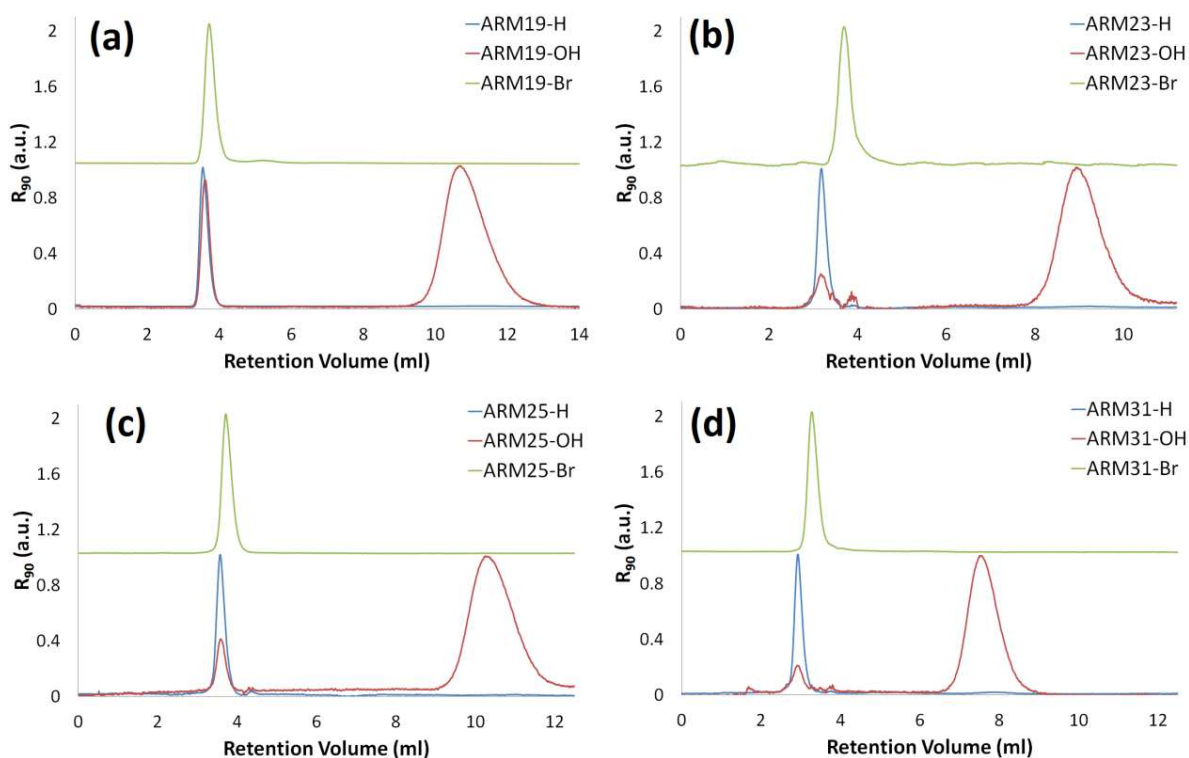


Figure 3.14 - Isothermal ((a) 50 °C, (b) 60 °C (c) 50 °C, (d) 60 °C) NP-IIC chromatograms (RALs detector) of linear polybutadiene arm macromonomers at a solvent composition of 96/4 isooctane/THF.

Five bromine end-functionalised polybutadiene samples have been synthesised by living anionic polymerisation and characterised by ^1H -NMR, SEC and IC, with molecular weights ranging from 18,000 g mol⁻¹ to 40,000 g mol⁻¹. Normal-phase IC analysis in particular, has enabled the quantitative analysis of the extent of the end-capping of the polymer chain-ends with ethylene oxide, where ^1H -NMR failed to do so, showcasing the usefulness of this technique for the analysis of chain end-functionalised polymers.

3.2.4.2 NP-IC Analysis of the Crossbars

Normal-phase isothermal interaction chromatography (NP-IIC) analysis was also carried out on the crossbar polymers in an attempt to quantify the proportion of chains that had been fully end-capped. However, since a fully coupled and deprotected crossbar would have two or hopefully four hydroxyl groups per chain, their separation would not be as straightforward compared to the singly-functionalized arm polymers.

Normal-phase IC utilises a polar stationary phase, in this case a single diol, modified silica HPLC column, and is very sensitive to the polarity of the analysed sample. If the sample that has to be analysed itself contains multiple polar end-groups, it is quite possible for the sample to be retained by the column and not eluted at all! In order to establish some base analytical conditions for the crossbars, analysis was carried out initially with polymer FF-XBAR29 which was the lowest molecular weight polymer and the easiest to dissolve in the mobile phase. Four variants of FF-XBAR29 with different end-groups were analysed under SEC and NP-IIC conditions. For clarity these are referred to as: FF-XBAR29-(OX)₂ (α -end-capped and protected), FF-XBAR29-(OX)₄ ($\alpha\omega$ -end-capped and protected) and the deprotected analogues, FF-XBAR29-(OH)₂ and FF-XBAR29-(OH)₄. SEC chromatograms are presented overleaf for all FF-XBAR29 samples in Figure 3.15. SEC is incapable of distinguishing polymers based on functionality, and as expected a single narrow major peak can be observed for all samples at 13.5 ml, which can be ascribed to the required polymer backbone. There is, however, also a second small peak at a lower retention volume (12.9 ml) present in each sample; this peak is due to chain-coupling from termination reactions with oxygen or CO₂ (see Chapter 1, section 1.4.2.2.5) which result in a double molecular weight polymer.

For the NP-IIC analysis, a series of initial elution optimisation runs were carried out and a solvent mixture of isooctane/THF at a ratio of 88-12 (v/v) and a temperature of 22 °C was chosen for elution of all samples. The chromatograms of each sample are given in Figure 3.16.

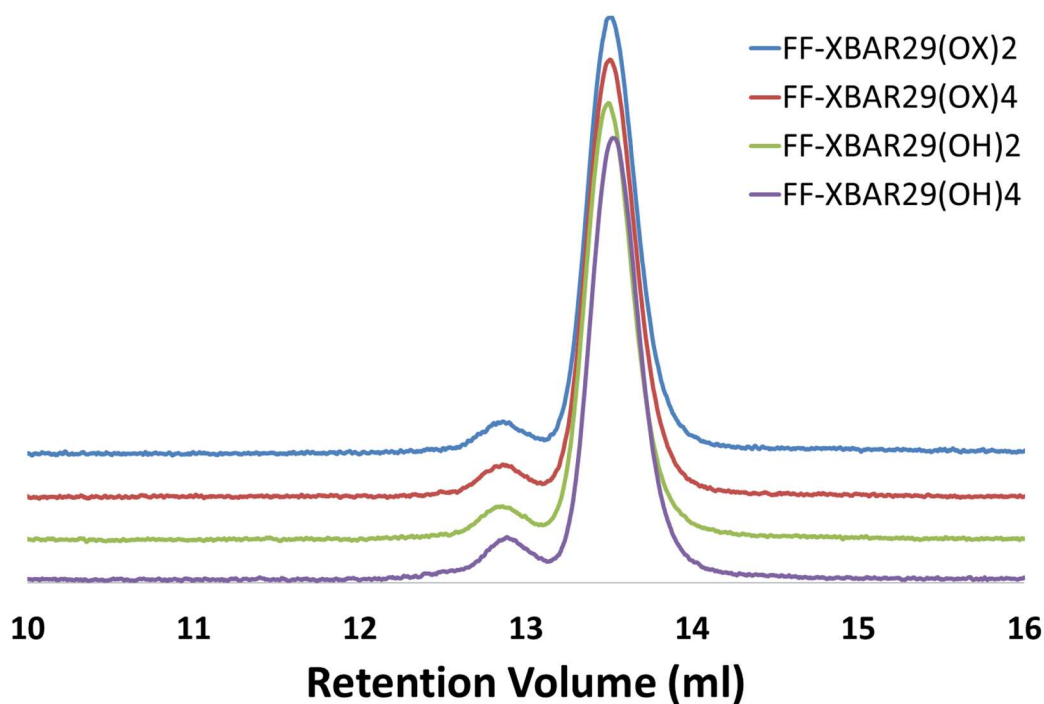


Figure 3.15 - SEC chromatogram (RI detector) of crude polybutadiene FF-XBAR29 samples

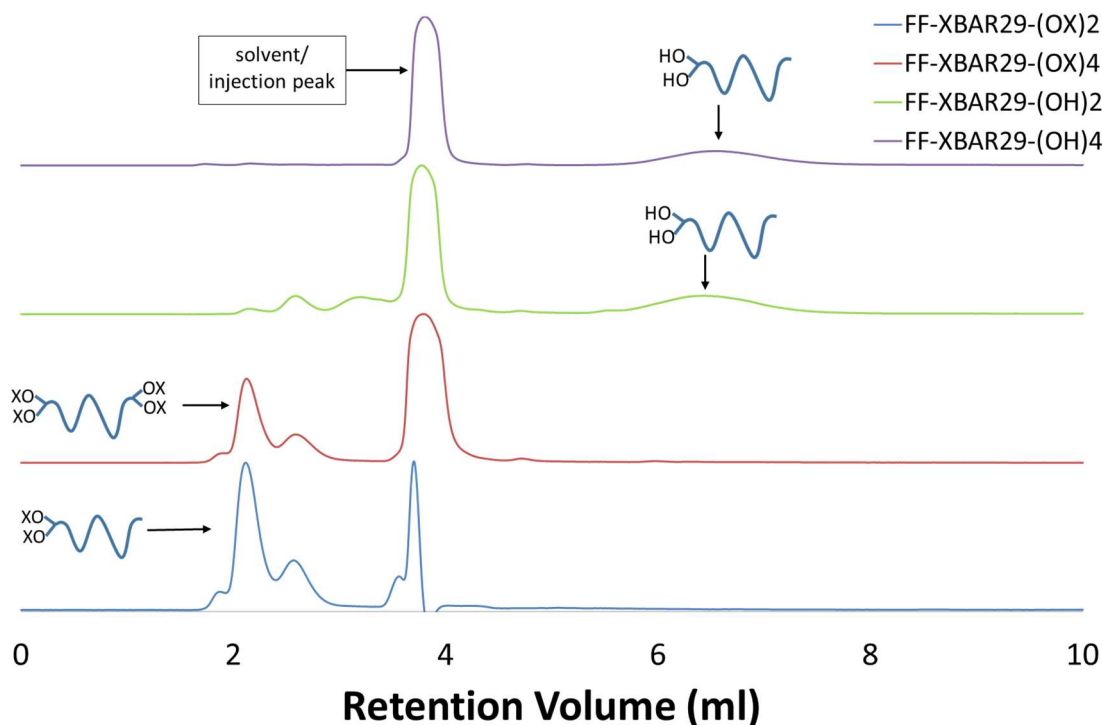


Figure 3.16 - Isothermal (22 °C) NP-IIC chromatograms (UV detector) of samples FF-XBAR29-(OX)₂, FF-XBAR29-(OX)₄, FF-XBAR29-(OH)₂ and FF-XBAR29-(OH)₄ at a solvent composition of 88-12 isooctane-THF.

In SEC mode, polymer chains are eluted in the order of high molecular weight chains to low molecular weight chains and all chains are eluted before the solvent peak, whereas in IC mode, the order of elution is reversed, with low molecular weight polymer chains eluted

first and all chains eluted after the solvent peak. The NP-IIC chromatograms of protected samples FF-XBAR29-(OX)₂ and FF-XBAR29-(OX)₄ resemble what was seen previously in their SEC chromatograms. Both show a major peak at 2.3 ml which can be attributed to the α -end-capped protected chains and the fully α,ω -end-capped protected crossbar chains respectively; molecular weight analysis of this peak produced an M_n of 28,600 g mol⁻¹, in line with the molar mass by SEC analysis. Both these chains elute at the same volume, as both are the same molecular weight. Both eluted before the solvent/injection peak at 3.8 ml (in SEC mode) as the protected, non-polar end groups do not interact strongly with the polar column. There is also a smaller peak/shoulder present at lower retention volume (1.9 ml) which can be ascribed to the chain-coupled polymers with double the molar mass – this confirms that these two polymers are in SEC mode where higher molar mass chains elute first. The peak at 2.7 ml in the samples of the protected polymers was unexpected. Molecular weight analysis of this peak reveals it is the same molecular weight as the peak at 2.3 ml (M_n ca. 29,000 g mol⁻¹). The peak may be a result of a polymer chain that has been partially deprotected, resulting in a polymer chain that has one silyl group and one -OH group i.e. FF-XBAR29(OX)(OH). Another possible reason is that this unexpected peak may be due the result of chains terminated by impurities. When an anionic chain is terminated by oxygen, an -OH or -O-OH end-group can be introduced to a polymer chain. Termination by carbon dioxide may also result in an -OH or carboxylic acid end group (see Chapter 1, section 1.4.2.2.5), resulting in a fraction of the protected polymer chains with an additional unprotected polar functionality. Finally, in all chromatograms there is a solvent/injection peak at 3.8 ml which appears broad in three of the four samples. The broadness is currently thought to be a result of the presence of BHT (antioxidant) in the samples which is co-eluting with the solvent peak.

In the chromatograms for the deprotected samples, some significant changes are observed. After deprotection, the non-polar -(OX) protected phenol groups are converted to polar phenol groups. The result is a deprotected polymer, which now comprises of chains with multiple polar end groups, capable of strong interactions with the column. In NP-IC, this should result in the deprotected chains being eluted much later than previously seen for the protected chains, even though both protected and deprotected chains are the same molecular weight. This is evident in the chromatogram for FF-XBAR29-(OH)₂. There is a significant decrease in the intensity of the peak at 2.3 ml, indicating a much reduced concentration of protected polymer chains and a new broad peak can be seen at 6.6 ml -

this peak can be ascribed to the α -end-capped deprotected $-(OH)_2$ polymer chains. Molecular weight analysis of the peak at 6.6 ml gave an M_n of 29,100 g mol⁻¹, confirming (as expected) it is the same molecular weight as the peaks at 2.3 ml and 2.7 ml. The broad nature of the peak is a result of there being two $-OH$ groups present, leading to even stronger retention and peak broadening than was seen previously in the single $-OH$ arm macromonomers. The NP-IIC chromatogram of FF-XBAR29- $(OH)_4$ resembles the FF-XBAR29- $(OH)_2$ chromatogram, with the peaks before the solvent injection peak disappearing or at least, significantly reduced, due to the deprotection reaction. There is again a broad peak at 6.6 ml which can be assumed to represent the α -end-capped deprotected chains. It is possible that the FF-XBAR29- $(OH)_4$ sample may be rather heterogeneous and contain chains which are functionalised (and deprotected) at just one end and at both ends. NP-IC should have an advantage over ¹H-NMR, SEC and RP-IC in this instance, and be able to separate these two types of polymer chains if present in the same sample. However, no peak was detected for the deprotected $\alpha\omega$ -end-capped chains at 22 °C. The deprotected $\alpha\omega$ -end-capped crossbar will have four $-OH$ groups attached, making it more polar and more likely to be retained via interaction with the polar stationary phase, leading to much higher retention volumes.

It has been shown above that (at 22 °C) the peaks representing the deprotected α -end-capped chains also had significant peak broadening, an effect that was previously seen in the NP-IIC analysis of the arm macromonomers (Figure 3.14). A possible reason for the peak broadening seen for the functional chains is mass transfer resistance due to the interaction between the polar end groups and the stationary phase of the column. The $-OH$ groups on the polymer can interact by hydrogen bonding with the diol groups present on the surface of the stationary phase.¹⁷⁻¹⁸ The main chain backbone of the polymer continues to flow down the column in the mobile phase whereas the end groups are still attached to the stationary phase, increasing the overall analyte elution zone and hence increasing peak broadening.¹⁹ This effect is exacerbated as the number of $-OH$ groups is increased as more hydrogen bonding can occur, further increasing interaction strength between the end groups and the stationary phase, in turn increasing mass transfer resistance and broadening the peak areas. A consequence of peak broadening is the peak height decreases whereas the peak width increases, impacting the ease of detection. If this trend continues it can be surmised that a polymer with four ($-OH$) end groups could produce a peak so broad that its detection would be extremely difficult under the current conditions.

3.2.4.2.1 Impact of solvent temperature on NP-IIC analysis

Chang *et al.* has previously shown that for a series of polystyrene standards, performing IC at elevated temperatures in both reversed-phase and normal-phase results in faster elution of all samples.²⁰ The NP-IIC analysis of FF-XBAR29-(OH)₄ was repeated at 50 °C and at 60 °C, in order to determine whether the use of the higher temperatures would also result in shorter retention times for the sample and ensure the elution of all species, including the $\alpha\omega$ -end-capped chains that were not evident at 22 °C, possibly due to retention in the column. The resulting chromatograms, obtained at elevated temperatures, are shown below in Figure 3.17.

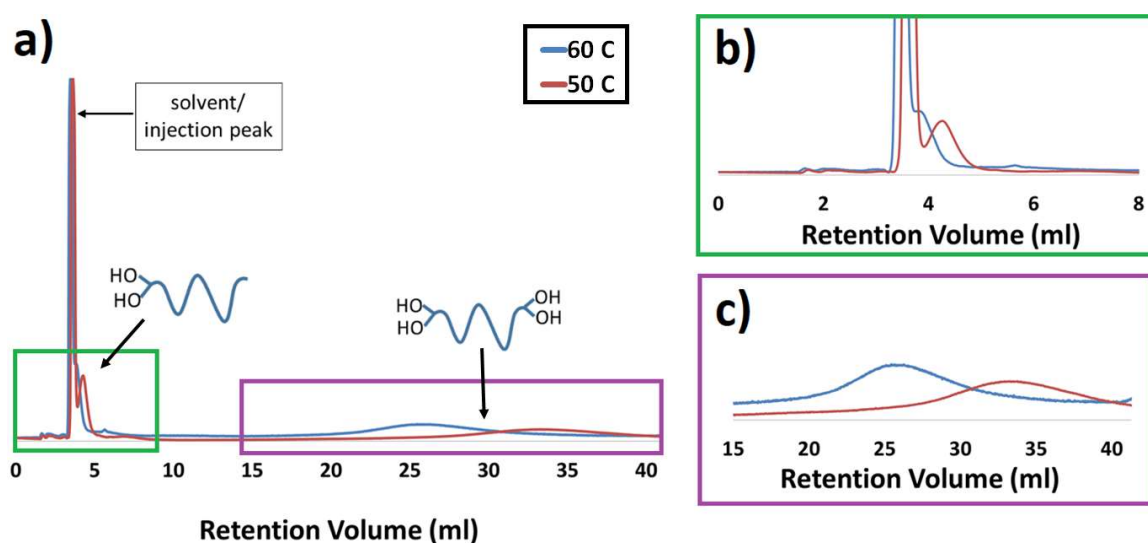


Figure 3.17 - Isothermal 50 °C (Red Line) and 60 °C (Blue line) NP-IIC chromatogram (UV detector) of FF-XBAR29-(OX)₄ at a solvent composition of 88/12 isooctane/THF

When the sample was analysed at 50 °C, two peaks were detected after the solvent injection peak at 3.4 ml; the first (reasonably sharp) peak eluted at 4.3 ml and a second (very broad) peak eluted at 32.5 ml. It was posited that the higher temperature has resulted in the elution of the entire sample from the column. We believe that the peak at 4.3 ml can be ascribed to the α -end-capped deprotected chains (with 2 phenol groups), whereas the peak at 32.5 ml corresponds to the $\alpha\omega$ -end-capped deprotected chains with 4 phenol groups, which was undetectable at 22 °C. The very broad nature of the peak at 32.5 ml indicates that very strong interaction between the four -OH groups present on the polymer chains and the column, even at this higher temperature. Analysis of the sample at 60 °C provides further evidence of the correlation between solvent temperature and elution behaviour. Thus in Figure 3.17b the peak which eluted at 4.3 ml at 50 °C, is shifted to a lower retention volume (3.9 ml) at 60 °C. Moreover, in Figure 3.17c, the peak which eluted at 32.5 ml at 50 °C, can

now be seen to elute at 25.2 ml. The faster elution and the less broad nature of the peaks at 60 °C compared to 50 °C is further evidence that the strength of interaction between the polymer chains and the column is moderated by the higher temperatures. This in turn is consistent with the conclusion that the later eluting peaks can be ascribed to chains with a higher degree of (polar) functionality. Further analysis of the peak areas at 50 °C (using the UV detector) was carried out for sample FF-XBAR29(OH)₄ in order to calculate how much (the percentage) of each polymer structure was present in the sample. It was determined that the peak at 4.3 ml constitutes 27% of the sample whereas the peak at 32.5 ml constitutes 73% of the sample. There may be some potential error in calculation due to peak overlap with the solvent peak at 4.3 ml and the very broad peak at 32.5 ml – where the baseline ends and the peak starts is fairly subjective. The NP-IIC analysis for this polymer has shown that the FF-XBAR29 is a more complex material than initially assumed, suggesting that the synthesis is not as clean as hoped, and that the sample contains a significant (ca. 25%) portion of chains which are only capped with DPE-OSi at one end. This is in contrast with the ¹H-NMR analysis which suggested that the “fire and forget” crossbars mostly consisted of chains containing at least two DPE-OSi units and a more successful end-capping average. It should be stated that the ¹H-NMR analysis could only at the maximum provide an average number for the protected polymers, whereas the NP-IIC analysis is conducted on the deprotected polymers, inhibiting the possibilities for direct comparison.

3.2.4.2.2 Impact of solvent composition on NP-IIC analysis

The composition of the elution solvent can also have an effect on the sample elution and IC is very sensitive to solvent composition, with even a 0.5% change in composition having a marked effect on elution behaviour.²⁰ As the polarity of the eluent is increased - in this case by increasing the amount of THF - the interaction between (the polar end groups of) polymer chains and the stationary phase (column) weakens as the polar end-groups interact more with the elution solvent, lowering retention volume. Thus, crossbars FF-XBAR29 and FF-XBAR52 were analysed using a solvent composition of 87/13 isooctane/THF in order to demonstrate this behaviour, with the results presented below in Figure 3.18.

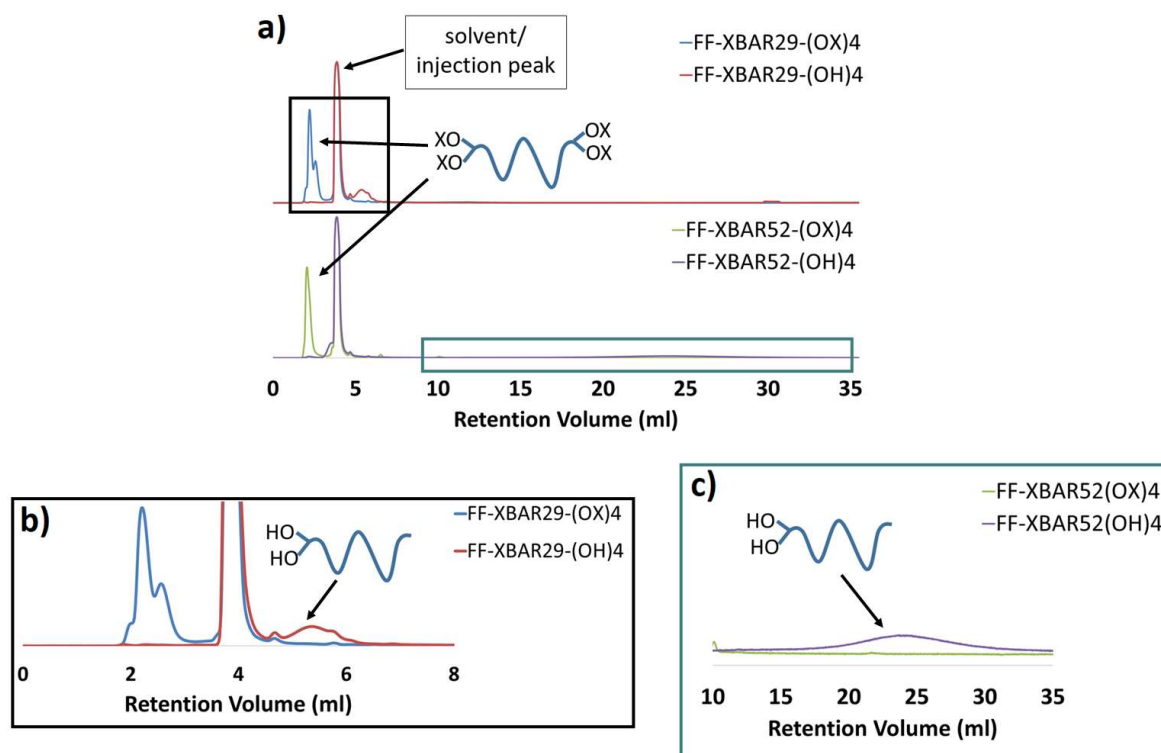


Figure 3.18 - Isothermal (22 °C) NP-IIC chromatogram (UV detector) of FF-XBAR29-(OX)₄ and FF-XBAR52-(OX)₄ at a solvent composition of 87/13 isooctane/THF.

It can be seen in Figure 3.18a, that the chromatogram for FF-XBAR29(OX)₄ obtained at 22 °C with a solvent composition of 87/13 isooctane/THF has resulted in a less resolved chromatogram compared to when the same sample was analysed previously with 88/12 isooctane/THF as the eluent (Figure 3.16). Once again three peaks can be seen although these peaks are less well-resolved, demonstrating the sensitivity of separation to small changes (in this case 1%) in solvent composition. There is a slight shoulder at 2.1 ml, followed by a large peak at 2.2 ml which corresponds to the $\alpha\omega$ -end-capped protected crossbar. A peak can also be seen at 2.8 ml which may represent a partially deprotected or prematurely terminated species. In contrast, the higher molecular weight FF-XBAR52-(OX)₄ shows only one large peak at 2.0 ml (Figure 3.18a), which we believe corresponds to the $\alpha\omega$ -end-capped protected crossbar. The absence of any termination or unexpected peaks when compared to FF-XBAR29-(OX)₄ would also suggest that there are fewer undesired species present in the polymer. The peaks described above for both of these samples elute before the solvent/injection peak (at 4.9 ml), meaning elution under SEC mode is taking place. As such, higher molecular weight polymers should elute before lower molecular weight polymers and this expected behaviour was observed with FF-XBAR52-(OX)₄ eluting slightly before FF-XBAR29-(OX)₄.

The effect of the slight change in solvent composition is seen more clearly in the deprotected samples. For FF-XBAR29-(OH)₄, (Figure 3.18b) there is a broad peak which elutes between c. 5.0 and 6.0 ml, which can be ascribed to the α -end-capped deprotected chains - this peak was observed at 6.6 ml when 88/12 isooctane/THF was used as the eluent. Increasing the polarity of the solvent mixture by increasing the fraction of THF by just 1% weakens the interaction between the -OH end-groups and the polar column, resulting in earlier peak elution. However, the elution of the $\alpha\omega$ -end-capped deprotected crossbars (FF-XBAR29-(OH)₄ and FF-XBAR52-(OH)₄) was not observed at 22 °C, suggesting that the interaction between polymer and column is still too strong at this temperature. The chromatogram for FF-XBAR52-(OH)₄ (Figure 3.18c) first shows a small, broad peak at 24.8 ml, which was attributed to the α -end-capped deprotected chains, which is consistent with previous observations. Attempts to analyse the molecular weight of the broad peak at 24.8 ml, however, gave unreliable and inaccurate data due to the instability of the RI baseline. Moreover, a peak that may represent the $\alpha\omega$ -end-capped deprotected crossbar was, once again, not observed. When considering both FF-XBAR29 and FF-XBAR52, we can see that the peaks corresponding to the α -end-capped deprotected chains (FF-XBAR-(OH)₂) eluted after the solvent/injection peak and separation is taking place in IC mode. As such, and as expected, the higher molecular weight sample (FF-XBAR52-(OH)₂) eluted later (at 24.8 ml) than the lower molecular weight sample (FF-XBAR29-(OH)₂) which eluted earlier at 5.4 ml. Since the change in solvent polarity had a notable impact on elution, it was decided that it would be more efficient to change the solvent composition rather than the elution temperature to promote the complete elution of FF-XBAR52 including the $\alpha\omega$ -end-capped deprotected chains (FF-XBAR-(OH)₄).

Thus, a more polar mobile phase of isooctane/THF at a ratio of 84-16 was used for the complete elution of FF-XBAR52. Three samples - FF-XBAR52-(OX)₄, FF-XBAR52-(OH)₂ and FF-XBAR52-(OH)₄ were analysed at a temperature of 22 °C and their chromatograms are shown in Figure 3.19. The chromatogram for FF-XBAR52-(OX)₄ again differs to that observed when using 87-13 isooctane/THF as the mobile phase with one strong peak at 2.0 ml for the $\alpha\omega$ -end-capped protected crossbar. However, the major differences in elution behaviour are more evident in the chromatograms of the deprotected samples. The analysis of FF-XBAR52-(OH)₂ also shows a peak at 2.0 ml which may correspond to the remnant $\alpha\omega$ -end-capped protected chains. It is also possible that these chains belong to unfunctionalised polymer present in the sample. ¹H-NMR analysis for FF-XBAR52

indicated that an average of 1.80 units of DPE-OSi were present per chain rather than the expected 2 units, which does suggest that there is still a mixture of chains capped at one end and both ends in the final polymer. The peak at 2.0 ml is in the same position as observed in the analysis of FF-XBAR52-(OX)₄ although its much smaller size, confirms that most, or all of these chains have been deprotected. The chromatogram for FF-XBAR52-(OH)₂ also contains a large peak at 2.7 ml which can be attributed to the desired α -end-capped deprotected chains. Molecular weight analysis of the peaks at 2.7 ml and 2.0 ml indicated that each had an identical M_n of 47,900 g mol⁻¹. Although this does not agree perfectly with the molar mass of this sample by SEC (*ca.* 52,000 g mol⁻¹ – see Table 3.3) we think it reasonable to assume that the identical molar masses indicate that separation of the chains arises solely as a functional of end-group functionality.

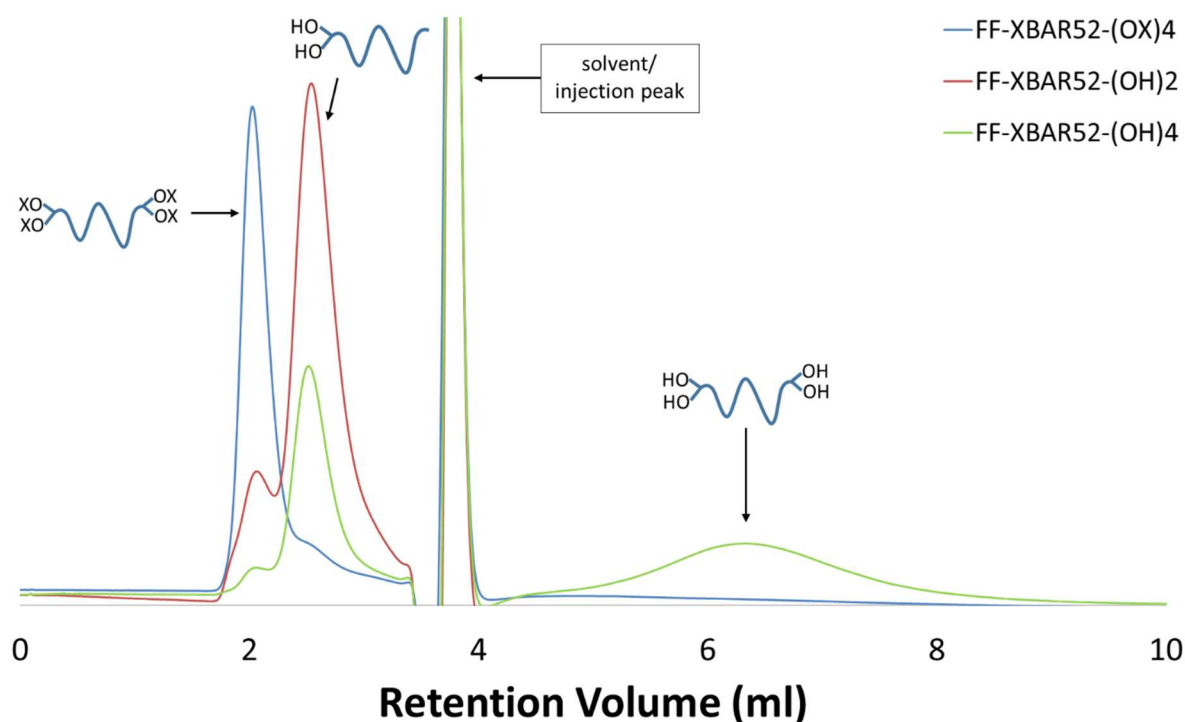


Figure 3.19 - Isothermal (22 °C) NP-IIC chromatograms (UV detector) of samples FF-XBAR52-(OX)₄, FF-XBAR52-(OH)₂ and FF-XBAR52-(OH)₄ at a solvent composition of 84/16 isooctane/THF.

The chromatogram for FF-XBAR52-(OH)₄ also shows a low intensity peak at 2.7 ml and broad peak with a maximum intensity at 6.2 ml – we believe that this latter peak can be ascribed to the $\alpha\omega$ -end-capped deprotected crossbar, as illustrated in Figure 3.19 above. Molar mass analysis of the peak at 6.2 ml revealed an M_n of 53,300 g mol⁻¹ which is in good agreement the expected molar mass (from SEC) and with the molar mass of the peaks at 2.0 and 2.7 ml. This further reinforces the conclusion that all peaks correspond to polymers

of the same molar mass and separation is purely due to the changing nature/number of the end group functionalities. Analysis of the peak areas in the chromatogram of FF-XBAR52-(OH)₄ shows that the peaks at 6.6 ml and 2.7 ml represent 53% and 44% of the sample respectively, again suggesting that FF-XBAR52-(OH)₄ is a more complex and heterogeneous sample than initially indicated by ¹H-NMR spectroscopy.

We believe that this study represents the first time that NP-IC has been used to analyse telechelic, multifunctional polymers. The NP-IC analysis of the crossbar polymers, although challenging, provided significant data and insight into the structure and heterogeneity of the polymers in question, demonstrating the unique ability of NP-IC for the analysis of such complex materials. The initial ¹H-NMR results suggested that high levels of end-capping had been achieved, although NMR only gives an average picture of the molecules under investigation. Moreover, end-group analysis of high molar mass polymers by NMR is inherently challenging given the poor signal to noise ratio of signals associated with the end groups. However, the NP-IC analysis revealed the presence of a number of different species, albeit with the (desired) fully functionalized ω -end-capped deprotected chains being present in the largest concentration in the final samples. Due to the presence of multiple polar -OH end-groups, interactions with the columns can be strong leading to sample retention and non-elution. In order to overcome these issues, the use of higher temperature provides a possible solution although this may lead to other issues such as sample co-elution i.e. different polymer chains eluting at the same time or with the solvent injection peak as was the case for FF-XBAR29-(OX)₄. A temperature gradient may be applied in order to alleviate this issue, but the use of a temperature gradient generates other challenges beyond method development, including very unstable (RI) concentration detector baselines, making any quantitative calculations nearly impossible. Changes to solvent composition were shown to have significant effects on sample elution and a change in just 1% solvent composition from 88/12 isooctane/THF to 87/13 was enough to result in much faster sample elution. The sensitivity of interaction chromatography to many factors, while making it a powerful tool, also hinders its efficacy somewhat due to the need to balance these factors in order to gain good reproducible data.

In order to use NP-IC for the analysis of heterogeneous materials which contain multiple polar chain-end functionalities, very time consuming method development is required to find the optimal elution conditions for each individual crossbar. However, the ¹H-NMR analysis of the fully protected samples, which indicated that end-capping had been

achieved at acceptable levels, combined with the NP-IIC analysis which indicate that the desired crossbars were still present in the highest concentrations in the samples tested, it was decided that the crossbars were viable to be used as macromonomers for the synthesis of H-shaped polymers.

This chapter focused on the synthesis of a range of end-functionalised polymers by living anionic polymerisation for their eventual use as “macromonomers” in the synthesis of H-shaped polymers. The number and range in molecular weight of macromonomers produced as well as their full characterisation allows for the same polymers to be used repeatedly in coupling reactions, allowing, for the first time, for a homologous series of H-shaped polymers to be synthesised by the macromonomer approach.

3.3 Experimental

3.3.1 Materials

Benzene (Sigma–Aldrich, HPLC grade, $\geq 99\%$), and dichloromethane (in-house solvent purification) were dried and degassed over calcium hydride (CaH_2) (Acros Organics, 93%) and stored under high vacuum. Tetrahydrofuran (in-house purification) was dried over sodium wire and benzophenone (Sigma–Aldrich, 99%), and stored under high vacuum. The solvents were degassed by a number of freeze-pump-thaw cycles and freshly distilled prior to use. 1,3-Butadiene (Sigma–Aldrich, $\geq 99\%$) and ethylene oxide (Sigma–Aldrich, $\geq 99.5\%$) were transferred through columns of Carbosorb (Sigma–Aldrich) and molecular sieves (Sigma–Aldrich) to remove any inhibitor and moisture respectively. 4,4'-dihydroxybenzophenone (99%), *tert*-butyldimethylsilyl chloride (TBDMSCl) (97%), imidazole (97%), sodium bicarbonate (99.7%), triphenylphosphine (PPh_3) (99%), methyltriphenylphosphonium iodide (97%), methyllithium solution (1.6 M in diethyl ether), magnesium sulphate, carbon tetrabromide (CBr_4) (99%), and *N,N,N',N'*-tetramethylethylenediamine (TMEDA) (≥ 99.5) (all Sigma–Aldrich) were used as received. *N,N*-dimethylformamide (DMF) (Sigma–Aldrich, anhydrous 99.8%) was stored over 3 Å molecular sieves (Sigma–Aldrich) under inert atmosphere. *sec*-Butyllithium (Sigma–Aldrich, 1.4 M solution in cyclohexane) and *n*-butyllithium (Sigma–Aldrich, 2.5 M in hexanes) were used as received. 2,2,4-Trimethylpentane (isooctane) (HPLC grade, $\geq 99.9\%$), Tetrahydrofuran (HPLC grade, $\geq 99.9\%$) (both Fischer Scientific) were used as received. Tetrahydrofuran, methanol, toluene, acetone, ethanol and petroleum ether (all AR grade) and hydrochloric acid (~ 36 wt. %) (all Fischer Scientific) were used as received.

3.3.2 Characterisation

3.3.2.1 Nuclear Magnetic Resonance (NMR)

^1H -NMR spectra were measured on a Varian VNMRs 700 MHz or a Bruker DRX-400 MHz spectrometer using either CDCl_3 or DMSO-d_6 as solvents.

3.3.2.2 Size Exclusion Chromatography (SEC)

Triple detection size exclusion chromatography (SEC) was carried out for the analysis of molecular weight and dispersity of the synthesised polymers, using a Viscotek TDA 302 with refractive index, right angle light scattering (RALS – 690 nm) and viscosity detectors and two PLgel 5 μm mixed C columns (300 \times 75 mm). Tetrahydrofuran was used as the eluent at a flow rate of 1.0 ml/min and at a temperature of 35 °C. The calibration was carried

out with a single narrow distribution polystyrene standard purchased from Polymer Laboratories. A value of 0.124 mL/g (measured in house) was used as the dn/dc of polybutadiene for the analysis of prepared polymers.

3.3.2.3 Interaction Chromatography (IC)

Isothermal interaction chromatography analysis was carried out under normal-phase conditions. Polymer solution concentrations of approximately 4 mg/ml dissolved in the eluent mixture were used and the injection volume was 100 μ l. Normal-phase isothermal interaction chromatography (NP-IIC) was carried out using a single diol modified silica column (Nucleosil 100-OH Å pore, 250×4.6 mm I.D., 5 μ m) and the eluent was a mixture of isooctane/THF, the composition of which varied as required. The flow rate was set to 1 ml/min. The NP-IIC system used a modified Viscotek TDA 301 with refractive index, viscosity RALS detector and a Viscotek UV 2600 detector set to a wavelength of 215.1 nm for polybutadiene samples. The temperature of the column in the system was controlled by a Thermo Scientific thermostatically controlled circulating bath and a thermostat.

3.3.3 Synthesis

The reaction vessel pictured below, (Figure 3.20), colloquially referred to as a “Christmas tree” is an example of the type of reactor used (in Durham) for all anionic polymerisation experiments. All polymerisations carried out during this work utilised the same general procedure but with varying amounts of monomer, solvents and reagents. The main solvent used in all the following polymerisations was benzene. Any extra steps taken are detailed in that polymer’s synthetic description. Preparation of the Christmas tree for anionic polymerisation is detailed in full in Chapter 2, section 2.3.2.1.

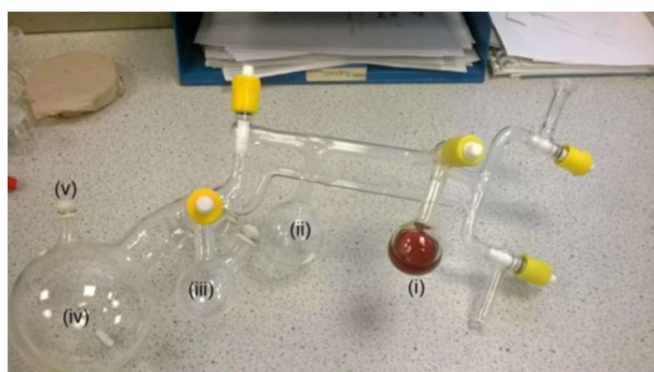


Figure 3.20 - “Christmas tree” reactor used for living anionic polymerisation, (i) Flask A containing living polystyryllithium, (ii) Flask B, (iii) Sidearm Flask, (iv) Reaction Flask, (v) Septum.

3.3.4 Synthesis of Functional Initiator/End-Capping Agent (DPE-OSi)

3.3.4.1 1-Bis(4-*tert*-butyldimethylsiloxyphenyl)benzophenone

In a 2-necked, 250 ml round bottomed flask equipped with a reflux condenser and a nitrogen bubbler, 4,4'-dihydroxybenzophenone (25.33 g, 118.24 mmol) and imidazole (21.64 g, 317.86 mmol) were dissolved in dry DMF under nitrogen. TBDMSCl (35.18 g, 233.41 mmol) was then added to the solution, giving rise to a pale yellow colour, and this mixture was stirred magnetically under nitrogen at 40 °C overnight. The mixture was then washed with NaHCO₃ (100 ml of a 5% solution; 12.5 g in 250 ml high purity water). The protected monomer was then extracted with hexane, dried over MgSO₄, rotary evaporated and dried under vacuum yielding a yellow oil, which was purified with column chromatography (toluene eluent), obtaining white crystals. Yield 93%; ¹H-NMR (400 MHz, CDCl₃): δ (ppm) 7.76 (d, J = 8 Hz, 4H), 6.93 (d, J = 8 Hz, 4H), 1.03 (s, 18H), 0.27 (s, 12H); ¹³C NMR (CDCl₃, 101 MHz): δ (ppm) 194.71, 159.51, 132.14, 131.29, 119.62, 99.98, 77.22, 25.63, 18.27.

3.3.4.2 1,1-Bis(4-*tert*-butyldimethylsiloxyphenyl)ethylene (DPE-OSi)

In a 3-necked, 250 mL round bottomed flask equipped with reflux condenser, nitrogen bubbler and pressure-equalising dropping funnel, methyltriphenylphosphonium iodide (46.56 g, 102.96 mmol) was dissolved in methyllithium (84 ml, 134.04 mmol). 1-bis(4-*tert*-butyldimethylsiloxyphenyl)benzophenone (47.97 g, 108.83 mmol) was dissolved in dry THF (150 ml) and added to the methyllithium solution drop wise at 0 °C, and the reaction mixture stirred overnight at room temperature. The mixture was then terminated with acetone (60 ml), the solid triphenylphosphine oxide was removed by washing the solution with petroleum ether. The ether was then removed via rotary evaporation obtaining a yellow oil, which was purified via recrystallization with ethanol, obtaining off white crystals. Yield (60%); ¹H-NMR (400 MHz, CDCl₃): δ (ppm) 7.24 (d, J = 8 Hz, 4H), 6.82 (d, J = 8 Hz, 4H), 1.02 (s, 18H), 0.24 (s, 12H); ¹³C NMR (CDCl₃, 101 MHz): δ (ppm) 155.39, 149.16, 134.79, 129.36, 119.57, 111.67, 77.22, 25.70, 18.23.

3.3.5 Synthesis of Crossbar Macromonomers (telechelic polybutadiene)

3.3.5.1 Synthesis of Telechelic Polybutadiene - "End-capped" Approach

3.3.5.1.1 EC-XBAR62-αω

DPE-OSi (0.55 g, 1.5 mmol) was added to the reaction vessel which was subsequently sealed and put under vacuum. Benzene (5 ml), was then distilled, under vacuum, into the vessel,

and removed to azeotropically dry the DPE-OSi. This process was repeated three times. Benzene (250 ml) was then distilled, under reduced pressure, into the vessel to dissolve the DPE-OSi and the reaction mixture was freeze-pump-thawed to degas the flask. The vessel was raised to atmospheric pressure with dry nitrogen and TMEDA (0.15 ml, 2.5 mmol) was added. *sec*-Butyllithium was added dropwise (to titrate out any residual impurities) until a red colour persisted and a final addition of 0.50 ml *sec*-butyllithium (1.25 mmol) was added by injection. The solution was stirred at room temperature for 1 hour before butadiene (8.95 g, 165 mmol) was distilled into the reaction vessel. The reaction was allowed to stir at 50 °C for 24 hours, after which a small portion of the reaction mixture was collected into a side flask and terminated with nitrogen-sparged methanol (EC-XBAR62-α). In a separate vessel, DPE-OSi (0.44 g, 1.0 mmol) was titrated with *sec*-butyllithium in benzene (5 ml) until the appearance of a red colour persisted for 1 hour. At this point, this red coloured DPE-OSi solution was injected into the polymerisation mixture and the polymer solution was stirred at 50 °C for a further 5 days before being terminated with nitrogen-sparged methanol, giving EC-XBAR62-αω. The intermediate sample and the final polymer were then precipitated separately into excess methanol in the presence of anti-oxidant butylated hydroxytoluene (BHT), dissolved in THF, precipitated again into BHT/methanol, collected after removing the excess methanol by decanting and the polymer dried to constant mass under vacuum for several days. Yield 78%; ¹H-NMR (400 MHz, CDCl₃): δ (ppm) 0.99 ppm [(CH₃)₃C-Si], 0.19 ppm [(CH₃)₂-Si]; M_n 62,300 g mol⁻¹, M_w 63,700 g mol⁻¹, Đ 1.02.

3.3.5.1.2 EC-XBAR76-αω

Synthesis of EC-XBAR76-αω was prepared according to the procedure described above in 3.3.5.1.1 DPE-OSi (0.55 g, 1.5 mmol), TMEDA (0.15 ml, 2.5 mmol), butadiene (17.11 g, 316 mmol) and 0.50 mL of *sec*-butyllithium (1.0 mmol) were dissolved in benzene (100 ml). DPE-OSi (0.55 g, 1.50 mmol) was dissolved in benzene (5 ml) and injected. Yield 84%; ¹H-NMR (400 MHz, CDCl₃): δ (ppm) 0.99 ppm [(CH₃)₃C-Si], 0.19 ppm [(CH₃)₂-Si]; M_n 76,300 g mol⁻¹, M_w 78,800 g mol⁻¹, Đ 1.03.

3.3.5.2 Synthesis of Telechelic Polybutadiene – Modified “End-capped” Approach

3.3.5.2.1 EC-XBAR32-αω

DPE-OSi (0.69 g, 1.25 mmol) was added to the reaction vessel and dried azeotropically three times with benzene. Benzene (250 ml) was distilled into the vessel to dissolve the DPE-OSi and the reaction mixture was freeze-pump-thawed for further purification. The vessel was

raised to atmospheric pressure with dry nitrogen. *sec*-Butyllithium was added dropwise (to titrate out any residual impurities) until a red colour persisted and a final volume of 0.89 ml *sec*-butyllithium (1.25 mmol) was added by injection. The solution was stirred at room temperature for 24 hours before butadiene (24.03 g, 444 mmol) was distilled into the reaction vessel. The reaction was allowed to stir at 50 °C for 24 hours, after which the reaction mixture was sampled into a side flask (EC-XBAR32- α). In a separate vessel, DPE-OSi (0.83 g, 1.87 mmol) and TMEDA (0.38 ml, 2.5 mmol) were titrated with *sec*-butyllithium in benzene (5 ml) until the appearance of a persistent red colour and allowed to react for 24 hours. At this point, this red mixture was injected into the polymerisation mixture and the polymer solution was stirred at 50 °C for a further 5 days before being terminated with nitrogen-sparged methanol, giving EC-XBAR32- $\alpha\omega$. Both samples were then recovered by precipitation into methanol, dissolved in THF, precipitated again into methanol, collected and dried under vacuum. Yield 96%; $^1\text{H-NMR}$ (700 MHz, CDCl_3): δ (ppm) 0.99 ppm [$(\text{CH}_3)_3\text{C-Si}$], 0.19 ppm [$(\text{CH}_3)_2\text{-Si}$]; M_n 32,900 g mol $^{-1}$, M_w 35,000 g mol $^{-1}$, Đ 1.06.

3.3.5.3 Synthesis of Telechelic Polybutadiene - “Fire and Forget” Approach

3.3.5.3.1 FF-XBAR29- $\alpha\omega$

DPE-OSi (0.66 g, 1.50 mmol) was added to the reaction vessel and dried azeotropically three times with benzene. Benzene (150 ml) was distilled into the vessel to dissolve the DPE-OSi and the reaction mixture was freeze-pump-thawed for further purification. The vessel was raised to atmospheric pressure with dry nitrogen. *sec*-Butyllithium was added dropwise (to titrate out any residual impurities) until a red colour persisted and a final volume of 0.35 ml *sec*-butyllithium (0.50 mmol) was added by injection. The solution was stirred at room temperature for 24 hours before butadiene (10.79 g, 199 mmol) was distilled into the reaction vessel. The reaction was allowed to stir at 50 °C for 24 hours, after which the reaction mixture was sampled into a side flask (FF-XBAR29- α). To the remaining reaction mixture, TMEDA (0.15 ml, 1.0 mmol) was added. The polymer solution was stirred at 50 °C for a further 5 days before being terminated with nitrogen-sparged methanol, giving FF-XBAR29- $\alpha\omega$. Both samples were then precipitated into BHT/methanol, dissolved in THF, precipitated again into BHT/methanol, collected, and dried under vacuum. Yield 90%; $^1\text{H-NMR}$ (700 MHz, CDCl_3): δ (ppm) 0.99 ppm [$(\text{CH}_3)_3\text{C-Si}$], 0.19 ppm [$(\text{CH}_3)_2\text{-Si}$]; M_n 29,000 g mol $^{-1}$, M_w 31,200 g mol $^{-1}$, Đ 1.07.

3.3.5.3.2 FF-XBAR52- $\alpha\omega$

FF-XBAR52 was prepared according to the procedure described above in 3.3.5.3.1 DPE-OSi (1.66 g, 3.75 mmol), butadiene (24.06 g, 445 mmol), 0.89 mL of *sec*-butyllithium (1.25 mmol) and TMEDA (0.37 mL, 2.5 mmol) were dissolved in benzene (250 mL). Yield 82%; $^1\text{H-NMR}$ (400 MHz, CDCl_3): δ (ppm) 0.99 ppm [$(\text{CH}_3)_3\text{C-Si}$], 0.19 ppm [$(\text{CH}_3)_2\text{-Si}$]; M_n 52,100 g mol $^{-1}$, M_w 54,100 g mol $^{-1}$, Đ 1.03.

3.3.5.3.3 FF-XBAR53- $\alpha\omega$

FF-XBAR53 was prepared according to the procedure described above in 3.3.5.3.1. DPE-OSi (1.10 g, 2.50 mmol), butadiene (25.07 g, 463 mmol), 0.59 mL of *sec*-butyllithium (0.83 mmol) and TMEDA (0.25 mL, 1.66 mmol) were dissolved in benzene (250 mL). Yield 98%; $^1\text{H-NMR}$ (400 MHz, CDCl_3): δ (ppm) 0.99 ppm [$(\text{CH}_3)_3\text{C-Si}$], 0.19 ppm [$(\text{CH}_3)_2\text{-Si}$]; M_n 53,000 g mol $^{-1}$, M_w 54,700 g mol $^{-1}$, Đ 1.03.

3.3.5.3.4 FF-XBAR100- $\alpha\omega$

FF-XBAR100 was prepared according to the procedure described above in 3.3.5.3.1. DPE-OSi (0.66 g, 3.75 mmol), butadiene (26.81 g, 496 mmol), 0.35 mL of *sec*-BuLi (1.25 mmol) and TMEDA (0.37 mL, 2.5 mmol) were dissolved in benzene (250 mL). Yield 93%; $^1\text{H NMR}$ (400 MHz, CDCl_3): δ (ppm) 0.99 ppm [$(\text{CH}_3)_3\text{C-Si}$], 0.19 ppm [$(\text{CH}_3)_2\text{-Si}$]; M_n 101,600 g mol $^{-1}$, M_w 115,200 g mol $^{-1}$, Đ 1.13.

3.3.5.4 Deprotection of Crossbar Macromonomers

In a 2-necked 1 L flask equipped with reflux condenser, polymer EC-XBAR32- $\alpha\omega$ (24.00 g, 0.73 mmol) was dissolved in THF (240 mL) to form a 10% w/v solution. To this solution concentrated HCl (2.9 mL, 2.9 mmol) was added in a 10:1 ratio with respect to the four protected phenol groups of the crossbar and reacted overnight at 80 °C. The deprotection was monitored by $^1\text{H-NMR}$ before stopping the reaction. The polymer was precipitated into methanol, redissolved in THF, precipitated again into methanol, collected, and dried to constant mass under vacuum. Yield 98%.

Polymers FF-XBAR29- $\alpha\omega$, FF-XBAR52- $\alpha\omega$, FF-XBAR53- $\alpha\omega$ and FF-XBAR100- $\alpha\omega$ were deprotected using the same procedure above for EC-XBAR32- $\alpha\omega$ and characterised by $^1\text{H-NMR}$ spectroscopy.

3.3.6 Synthesis of Arm Macromonomers

3.3.6.1 Synthesis of Hydroxyl end-functionalised macromonomers

3.3.6.1.1 ARM19-OH

Butadiene (65.41 g, 1209 mmol) and 2.34 mL of *sec*-butyllithium (3.27 mmol) were dissolved in benzene (500 ml) and the polymerisation allowed to proceed under vacuum at 50 °C for 24 hours. Ethylene oxide (0.40 g, 9.1 mmol) was purified with 0.1 ml *n*-butyllithium, then added via vacuum distillation and the reaction continued under vacuum at room temperature for 24 hours, after which it was terminated by injection of nitrogen-sparged methanol/HCl (5:1 v/v ratio). The polymer was precipitated into methanol, redissolved in THF, precipitated again into methanol, collected, and dried under vacuum. Yield 97%; M_n 19,700 g mol⁻¹, M_w 19,900 g mol⁻¹, Đ 1.04. ¹H-NMR (700 MHz, CDCl₃) 3.66 ppm [CH₂-OH].

3.3.6.1.2 ARM23-OH

ARM23-OH was prepared according to the procedure described above in 3.3.6.1.1. Butadiene (22.38 g, 414 mmol) and 0.79 ml of *sec*-butyllithium (1.12 mmol⁻¹) were dissolved in benzene (250 ml) and end-capped with ethylene oxide (0.5 g, 13 mmol). Yield 88%; M_n 23,200 g mol⁻¹, M_w 24,700 g mol⁻¹, Đ 1.06.

3.3.6.1.3 ARM25-OH

ARM25-OH was prepared according to the procedure described above in 3.3.6.1.1. Butadiene (22.38 g, 414 mmol) and 0.79 ml of *sec*-butyllithium (1.12 mmol) were dissolved in benzene (250 ml) and end-capped with ethylene oxide (0.5 g, 13 mmol). Yield 88%; M_n 24,600 g mol⁻¹, M_w 25,600 g mol⁻¹, Đ 1.04.

3.3.6.1.4 ARM31-OH

ARM31-OH was prepared according to the procedure described above in 3.3.6.1.1. Butadiene (26.41 g, 488 mmol) and 0.94 ml of *sec*-butyllithium (1.32 mmol) were dissolved in benzene (250 ml) and end-capped with ethylene oxide (0.88 g, 19 mmol). Yield 94%; ¹H-NMR (700 MHz, CDCl₃) 3.66 ppm [CH₂-OH]; M_n 28,400 g mol⁻¹, M_w 29,700 g mol⁻¹, Đ 1.03.

3.3.6.1.5 ARM40-OH

ARM40-OH was prepared according to the procedure described above in 3.3.6.1.1. Butadiene (64.83 g, 1198 mmol) and 0.93 ml of *sec*-butyllithium (1.12 mmol) were dissolved in benzene (500 ml) and end-capped with ethylene oxide (0.5 g, 13 mmol). Yield 96%; M_n 40,800 g mol⁻¹, M_w 24,700 g mol⁻¹, Đ 1.06.

3.3.6.2 Arm Bromination (conversion of hydroxyl groups)

In a 1 L flask ARM19-OH (63.26 g, 3.21 mmol) and triphenylphosphine (PPh_3) (2.53 g, 9.63 mmol) were azeotropically dried three times with benzene under vacuum. Dry dichloromethane (DCM) (600 ml) was then distilled into the flask to form ca. 10% w/v solution. Carbon tetrabromide (3.99 g, 12.03 mmol) was dissolved in DCM (5 ml) in another flask which was then brought to atmospheric pressure with nitrogen and injected into the polymer solution through a septum at 0 °C. The reaction was then allowed to rise to room temperature and the conversion monitored by ^1H -NMR before stopping of the reaction. The polymer was precipitated into methanol, redissolved in THF, precipitated again into methanol, collected, and dried under vacuum. Yield 98%. ^1H -NMR (700 MHz, CDCl_3) 3.40 ppm [$\text{CH}_2\text{-Br}$].

Hydroxyl end-functionalised macromonomers ARM23-OH, ARM25-OH, ARM31-OH and ARM40-OH were brominated using the same procedure above for ARM19-OH and characterised by ^1H -NMR spectroscopy, SEC and NP-IIC.

3.4 Conclusions

A series of telechelic polybutadiene “crossbars” with molecular weights between 30,000 – 100,000 g mol⁻¹ were synthesised via living anionic polymerisation in reactions using DPE-OSi as both a functionalised initiator and end-capping agent, resulting in polymers with narrow dispersity values. These polymers were produced using two different pathways, an “end-capping” approach in which DPE-OSi is added in two batches, and a “fire and forget” approach in which all DPE-OSi is present from the start. By the exploitation of reactivity ratios and TMEDA it was found that while both pathways have their merits, the “fire and forget” approach proved more beneficial, and facile with the synthesis of telechelic polymers being possible in a one-pot, one shot reaction. A series of linear polybutadiene “arms” with molecular weights between 18-40,000 g mol⁻¹ were also synthesised through the use of living anionic polymerisation and traditional chain end-capping and post-polymerisation end group conversion, also resulting in polymers with narrow dispersity values.

The arms and two of the crossbars were characterised using normal-phase isothermal interaction chromatography (NP-IIC) in order to quantitatively analyse the extent of end-capping for which, in the case of the arms in particular, ¹H-NMR was inadequate. NP-IIC was shown to be very effective at quantifying the success of end-capping with regards to –H, –OH and –Br end-capped arm polymers. In the case for the crossbar polymers, NP-IIC was able to determine that the polymers themselves, rather than consisting of just the final deprotected crossbar with four –OH groups, instead consisted predominantly of a mixture of α-end-capped (2 –OH) and αω-end-capped (4 –OH) chains, revealing a more complex nature of the crossbars which would not have been known without the use of NP-IIC. The analysis of both sets of macromonomers by normal-phase interaction chromatography further states the case for this technique to be used as an additional technique for the analysis of high molecular weight end-functionalised polymers.

3.5 References

1. Trollsås, M.; Atthoff, B.; Claesson, H.; Hedrick, J. L., *Macromolecules* **1998**, *31* (11), 3439-3445.
2. Hutchings, L. R., *Soft Matter* **2008**, *4* (11), 2150-2159.
3. Hutchings, L. R.; Roberts-Bleming, S. J., *Macromolecules* **2006**, *39* (6), 2144-2152.
4. López-Villanueva, F.-J.; Wurm, F.; Kilbinger, A. F. M.; Frey, H., *Macromol. Rapid Commun.* **2007**, *28* (6), 704-709.
5. Hutchings, L. R.; Agostini, S.; Hamley, I. W.; Hermida-Merino, D., *Macromolecules* **2015**, *48* (24), 8806-8822.
6. Hutchings, L. R.; Dodds, J. M.; Roberts-Bleming, S. J., *Macromolecules* **2005**, *38* (14), 5970-5980.
7. Zhao, Y.; Higashihara, T.; Sugiyama, K.; Hirao, A., *Macromolecules* **2007**, *40* (2), 228-238.
8. Quirk, R. P.; Wang, Y., *Polym. Int.* **1993**, *31* (1), 51-59.
9. Hutchings, L. R.; Dodds, J. M.; Rees, D.; Kimani, S. M.; Wu, J. J.; Smith, E., *Macromolecules* **2009**, *42* (22), 8675-8687.
10. Yuki, H.; Okamoto, Y., *Bull. Chem. Soc. Jpn.* **1970**, *43* (1), 148-151.
11. Brooks, P. P.; Natalello, A.; Hall, J. N.; Eccles, E. A. L.; Kimani, S. M.; Bley, K.; Hutchings, L. R., *Macromol. Symp.* **2013**, *323* (1), 42-50.
12. Hutchings, L. R.; Brooks, P. P.; Parker, D.; Mosely, J. A.; Sevinc, S., *Macromolecules* **2015**, *48* (3), 610-628.
13. Agostini, S.; Hutchings, L. R., *Eur. Polym. J.* **2013**, *49* (9), 2769-2784.
14. Clarke, N.; Luca, E. D.; Dodds, J. M.; Kimani, S. M.; Hutchings, L. R., *Eur. Polym. J.* **2008**, *44* (3), 665-676.
15. Quirk, R. P.; Ma, J.-J., *J. Polym. Sci., Part A: Polym. Chem.* **1988**, *26* (8), 2031-2037.
16. Hutchings, L. R.; Agostini, S.; Oti, M. E.; Keth, J., *Eur. Polym. J.* **2015**, *73*, 105-115.
17. Hao, Z.; Xiao, B.; Weng, N., *J. Sep. Sci.* **2008**, *31* (9), 1449-1464.
18. Tanaka, H.; Zhou, X.; Masayoshi, O., *J. Chromatogr. A* **2003**, *987* (1), 119-125.
19. Hawkes, S. J., *J. Chem. Educ.* **1983**, *60* (5), 393.
20. Chang, T.; Lee, H. C.; Lee, W.; Park, S.; Ko, C., *Macromol. Chem. Phys.* **1999**, *200* (10), 2188-2204.

Chapter 4

**Synthesis and characterisation of H-shaped
Polybutadienes**

4.1 Introduction

H-shaped polymers represent a complex class of branched polymers, differing from stars in that there are two branch points i.e. linking agents located at each end of the main chain backbone or “crossbar” instead of just one. The two branch points in essence mean that H-shaped polymers (H-polymers) represent the simplest structure in which long chain hierarchical branching is present in a polymer chain.¹ Long chain branching has been shown to have remarkable effects on polymer properties for both rheological and industrial applications. H-shaped polymers have also been previously studied to show that they may combine the properties of star and linear polymers in novel ways.² The ability to model the rheology of such polymers would allow for the design and synthesis of polymers in which properties such as melt strength and processability could be predicted. These models may also be able to determine what potential branch structures or architectures are present in more complex industrial polymers.³

The synthesis of well-defined, model H-shaped polymers has long been a synthetic challenge for polymer chemists, and as such there are very few reported examples of their synthesis and rheology, especially in comparison to star-branched or hyperbranched polymers. Most synthetic routes to produce H-polymers are based on the use of living anionic polymerisation and multifunctional chlorosilane coupling agents; examples of these methods were discussed previously in Chapter 1 (section 1.5.2.2).⁴⁻⁷ These chlorosilane coupling strategies, however, are not without problems – particularly regarding the production of unwanted, partially-branched by-products which may be difficult to remove by fractionation.

Currently, the development of theories related to the melt rheology of branched polymers relies heavily on the use of model branched polymers most often synthesised by anionic polymerisation. However, previously published work in this field has often neglected the presence of structural heterogeneity in such materials and these imperfections often limit the accuracy of any rheological data obtained.⁸ The synthesis of perfectly homogeneous model branched polymers is not trivial and as such, in lieu of “perfect” branched materials being produced, the next best outcome is to produce fully characterised branched polymers in which the presence of by-products can be detected and quantified. One characterisation technique which has recently emerged to address this characterisation challenge is interaction chromatography. As shown previously in this thesis, interaction

chromatography (IC) has proven to be a vital tool in the analysis of complex polymers. Interaction chromatography has been shown to be able to characterise structural heterogeneity in branched polymers, via reversed-phase IC (RP-IC) for the analysis of star-branched polymers (Chapter 2), whereas normal-phase IC (NP-IC) has been used to characterize the end-functionalized macromonomers (Chapter 3) which serve as precursor building blocks for the synthesis of H-shaped polymers discussed herein.

In this work the “macromonomer” approach has been used for the synthesis of a series of H-shaped polymers. The crossbar and the arm macromonomers were created by living anionic polymerisation in separate reactions, before coupling was achieved via a post polymerisation reaction. This constitutes a distinct advantage of the macromonomer approach, in that it allows for the creation of a homologous series of H-shaped polymers where different samples can be prepared with a crossbar of identical molecular mass, coupled to arms of differing molecular weights. Crucially, complete characterisation data for each linear component of the final H-shaped polymer is known, which would be advantageous in rheological studies. The macromonomer approach has been previously used by this group to produce DendriMacs,⁹ HyperMacs¹⁰⁻¹¹ and more recently, a series of asymmetric three arm stars, in which the molecular weight of two long arms were kept fixed and the remaining short arm molecular weight was systematically varied.¹² The macromonomer approach has not yet, to the best of our knowledge, been adapted for the synthesis of H-shaped polymers.

Ideally, the macromonomer approach should allow for the construction of branched polymers with greater control over properties such as the molecular weight and molecular weight distribution of each segment in a branched polymer. This approach may also reduce the number of potential by-products as well as being able to potentially identify any by-products present in the branched polymers since all the macromonomers have been fully characterised previously. However, the macromonomer approach is not without its difficulties. The use of this approach can be particularly time consuming as it requires the synthesis of various end-functionalised polymers and separate coupling reactions. Although the approach should result in fewer by-products previous reports have shown that side reactions can occur during the coupling step which in turn may limit the overall efficiency of the coupling reactions.¹²

We describe here the use of the macromonomer approach for the synthesis of a series of H-shaped polymers in which control and consistency over the molecular weight of each linear precursor (macromonomer) used in the synthesis of the H-polymer is achieved by using living anionic polymerisation. The telechelic “crossbar” polymers were synthesised using DPE-OSi as both a functionalised initiator and end-capping agent, whereas the end-functionalised “arm” polymers were synthesised through the use of living anionic polymerisation, traditional chain end-capping and post-polymerisation end-group conversion. The macromonomers used in the H-polymer reactions and full details of their synthesis and characterisation are detailed in Chapter 3. The H-shaped polymers themselves were prepared using a Williamson coupling reaction between the alkyl halide chain-end functionality of the arms and the phenol groups at the chain-end of the crossbars. Both this thesis and previously published work has demonstrated that SEC alone is incapable of adequately characterising complex branched polymers. As such, we have combined this synthetic strategy with analysis by both size exclusion chromatography (SEC) and interaction chromatography (IC) for structural characterisation of the resulting H-shaped polymers.

4.2 Results and Discussion

The general schematic of the macromonomer approach for the synthesis of H-polymers is given below (Figure 4.1).

Crossbar:

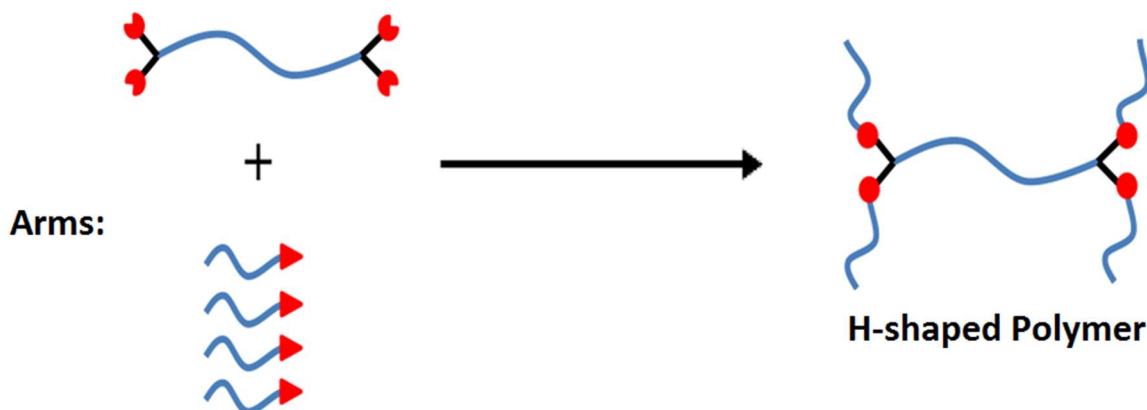


Figure 4.1 - General schematic for the synthesis of H-shaped polymers via the macromonomer approach

In this approach a crossbar polymer is linked to the arm polymers in a post-polymerisation, Williamson coupling reaction. The design and (attempted) optimization of the macromonomer approach for the synthesis of H-shaped polymers is described below. For ease of reference, molar mass data for the crossbars and arms used in the following reactions are provided below in Table 4.1.

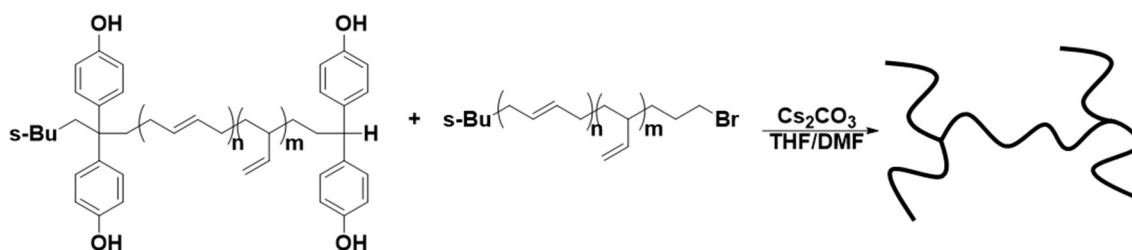
Table 4.1 - Molar mass data of macromonomer polymers (solvent THF; $dn/dc = 0.124 \text{ ml g}^{-1}$)

Molar mass of macromonomers (g mol^{-1})							
<u>Crossbar</u>	<u>M_n</u>	<u>M_w</u>	<u>\bar{D}</u>	<u>Arm</u>	<u>M_n</u>	<u>M_w</u>	<u>\bar{D}</u>
EC-XBAR32	32,900	35,000	1.06	ARM19-Br	19,200	19,900	1.04
FF-XBAR29	29,000	31,200	1.07	ARM23-Br	24,900	26,800	1.08
FF-XBAR52	52,400	54,400	1.04	ARM25-Br	24,300	25,100	1.03
FF-XBAR53	53,000	54,700	1.03	ARM31-Br	31,400	33,800	1.08
FF-XBAR100	101,600	115,200	1.13	ARM40-Br	40,300	41,600	1.03

4.2.1 Synthesis of H-shaped polymers in DMF/THF

The Williamson coupling reaction is a nucleophilic substitution (S_N2) reaction between an alkyl halide and an alcohol group resulting in an ether linkage (Scheme 4.1). The alkyl

halide (in this case an alkyl bromide) of the arms acts as the leaving group whereas the phenol group acts as the nucleophile in this reaction. This reaction and the reaction conditions were chosen as they had previously been reported as suitable for the production of branched polymers.¹²⁻¹³



Scheme 4.1 - Williamson coupling reaction for the synthesis of H-shaped polybutadiene

The Williamson coupling is promoted by the use of polar aprotic solvents with a high dielectric constant such as DMF ($\epsilon = 36.7$ at $30\text{ }^{\circ}\text{C}$)¹⁴; polybutadiene however, is insoluble in DMF. While polybutadiene is highly soluble in THF, the solvent itself has a relatively low dielectric constant ($\epsilon = 7.58$ at $25\text{ }^{\circ}\text{C}$) and the coupling reaction proceeds extremely slowly in THF with low rates of conversion.¹⁵ In order to compensate for both solubility and promote coupling, a 1 : 1 v/v mixed solvent of DMF : THF was initially chosen as the reaction solvent for the Williamson coupling reactions. Highly purified solvents are necessary in Williamson coupling reactions in order to limit side reactions. For this reason, THF was purified over sodium/benzophenone and degassed and DMF was dried over molecular sieves before use. Cesium carbonate (Cs_2CO_3) has been previously reported to promote the Williamson coupling reaction and was employed as a base in these reactions; the base needed in order to deprotonate the phenol groups and form the conjugate base, which acts as the true nucleophile. $60\text{ }^{\circ}\text{C}$ was chosen as the temperature for these reactions based on previous reports, in order to avoid potential side reactions that may occur due to the degradation of DMF at higher temperatures.¹¹

Crossbar macromonomers FF-XBAR29, FF-XBAR52 and FF-XBAR100 were each reacted with linear arm macromonomer ARM31-Br in the presence of cesium carbonate (see Scheme 4.1) to produce H-Pbd_1, H-Pbd_2 and H-Pbd_3 respectively. The reactions were performed at $60\text{ }^{\circ}\text{C}$ using a 1 : 5 : 10 molar ratio of crossbar to arm to cesium carbonate respectively - these ratios were used in an attempt to maximise the extent of coupling and drive the coupling reactions to completion. To begin, the macromonomers were dissolved in dry THF, after which the required quantity of DMF was added to the solution and the temperature raised to $60\text{ }^{\circ}\text{C}$. The final solution concentration of the polymer was 10wt%.

At this point the desired amount of cesium carbonate was added and the reaction was stirred mechanically via the use of an overhead (plastic) paddle stirrer. Mechanical stirring was used in order to ensure good mixing was maintained despite the increasing viscosities of the solutions. A sample was collected at the onset of reaction after the cesium carbonate addition (0 hr), and the coupling reactions were then sampled at various intervals to monitor their progress (by SEC) and the reactions were stopped when no more change in molecular weight was apparent.

Table 4.2 - Molar mass data for H-Pbd_2 (solvent THF; $dn/dc = 0.124 \text{ ml g}^{-1}$)

H-Pbd_2	Peak # (elution time / ml)			
	<u>1</u> (12.1)	<u>2</u> (12.3)	<u>3</u> (12.8)	<u>4</u> (13.3)
$M_n \text{ (g mol}^{-1}\text{)}$	163,000	87,200	56,900	31,200
$M_w \text{ (g mol}^{-1}\text{)}$	181,900	89,200	57,800	32,100
\bar{D}	1.12	1.02	1.01	1.03

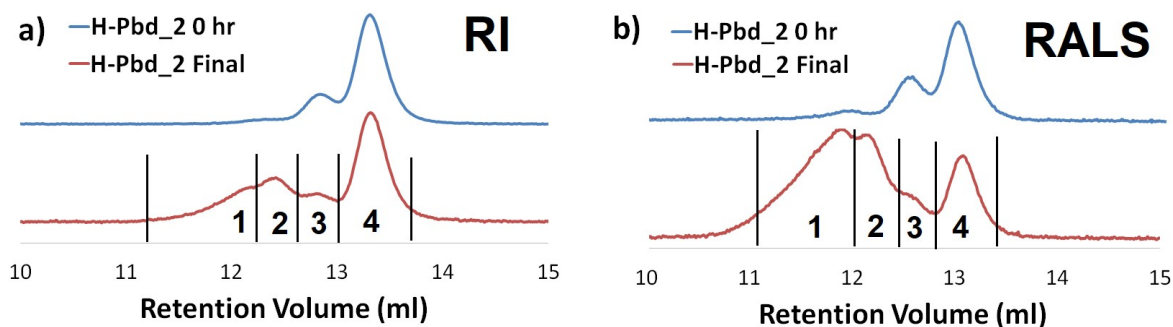


Figure 4.2 - SEC chromatograms ((a) RI and (b) RALS detector) of polymer H-Pbd_2. Comparison of the samples between the start (0 hr) and end of reaction.

In these reactions the coupling is monitored by the appearance and growth of a higher molecular weight peak that should present itself at a lower retention volume than that of the linear macromonomers. SEC analysis of H-Pbd_1 (FF-XBAR29, ARM31-Br) and H-Pbd_3 (FF-XBAR100, ARM31-Br) revealed the absence of a higher molecular weight peak corresponding to the H-shaped polymer, with the chromatograms of the final products being identical to the chromatograms taken at time = 0 hr (discussed later). However, H-Pbd_2 (FF-XBAR52, ARM31-Br) proved somewhat more successful with the appearance of a broad multimodal peak between 11 and 12.5 ml retention volume indicating that chain coupling had taken place – see Figure 4.2 Molar mass analysis was carried out on H-Pbd_2

and the results are presented in Table 4.2; with the integration limits used in the calculation of the peaks also given in Figure 4.2. The target (theoretical) molar mass (M_{nTHEO}) of the H-polymer in this case is 178,000 g mol⁻¹ (Crossbar FF-XBAR52 M_n = 52,400 g mol⁻¹, Arm ARM31-Br M_n = 31,400 g mol⁻¹), however, the highest molar mass fraction (peak 1) with a peak maximum at 12.1 ml had an M_n of 163,000 g mol⁻¹, an M_w of 181,900 and a Đ of 1.12. It should be noted, however, that analysis of the unresolved peaks in this way is susceptible to inaccuracy. Although the M_n of peak 1 is a little lower than the theoretical target molar mass of the H-polymer, this fraction is rather broad and not fully resolved from the rest of the distribution. Moreover, the breadth of this “peak” may indicate that the peak actually arises due to the presence of the desired H-shaped polymer and some lower molar mass, partially coupled product such as the product with only three arms coupled to the backbone (Figure 4.3).

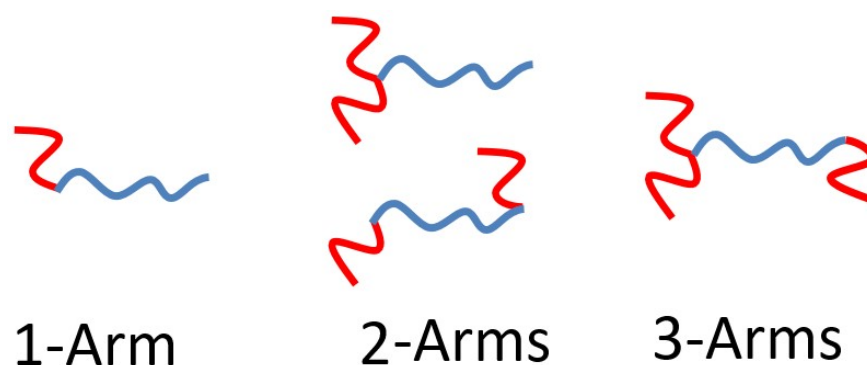


Figure 4.3 - Potential incomplete by-products of H-shaped polymer synthesis by the Williamson coupling reaction.

Although it is clear that high molar mass polymer has been produced via coupling of the macromonomers, and it is likely that at least some of the desired H-shaped polymer has been formed, it is equally clear that the coupling is far from complete and the multimodal SEC trace indicates the presence of lower molar mass, partially coupled polymer. Although the resolution of the peaks is not good, it is still possible to estimate the molar mass of the various fractions. Thus the “peak” at 12.3 ml had an M_n value of 87,900 g mol⁻¹, suggesting it belongs to a product with only one arm attached. The peak at 12.8 ml corresponds to unreacted crossbar still present in the crude polymer and the peak at 13.3 ml corresponds to unreacted arm, confirming that the crossbar had not even been fully consumed, despite the presence of a molar excess of arm polymer.

This initial set of coupling reactions was not terribly successful. Only partial coupling was seen for H-Pbd_2, whilst the other two experiments resulted in no meaningful coupling. Although one might have made an argument for a lack of coupling in H-Pbd_3 due to the high molecular weight crossbar (FF-XBAR100) resulting in a low concentration of functional groups and low rates of reaction, this would not appear to be a viable argument given that the lowest molar mass crossbar (FF-XBAR29) also yielded no coupling. Moreover, NP-IIC analysis of FF-XBAR29 (Chapter 3 section 3.2.4.2), indicated that the functional phenol groups are present on said crossbar macromonomer, and SEC and ^1H -NMR analysis also confirmed the integrity of the crossbar. However, it should also be noted that the NP-IIC analysis did indicate that the degree of functionalisation of FF-XBAR29 was not perfect, consisting of mixtures of one-end capped and both ends-capped functionalised chains. One factor that was suspected to be contributing to the low extent of coupling seen in all of these reactions, was the apparent limited solubility of the polybutadiene in the DMF : THF solvent mixture. The macromonomers dissolved completely in THF, however, the addition of DMF caused the partial precipitation of the macromonomers at room temperature, especially in the case for polymers H-Pbd_2 and H-Pbd_3. Although the solubility of the macromonomers improved as the temperature was raised to 60 °C, in all three cases, after about 36 hours of reaction time, the polybutadiene had become insoluble in the reaction co-solvent, forming a brown, gel-like substance around the paddle of the overhead stirrer and reaction flask. It was therefore decided to explore alternative solvent mixtures.

4.2.2 Synthesis of H-shaped polymers in DMAc/THF

In a subsequent set of coupling reactions, crossbar macromonomers FF-XBAR29, FF-XBAR52 and FF-XBAR100 were again reacted with arm macromonomer ARM31-Br giving polymers H-Pbd_4, H-Pbd_5 and H-Pbd_6 respectively. The solvent was changed from a 1 : 1 v/v DMF : THF mixture to a 1 : 1 v/v DMAc : THF solvent mixture; this solvent combination having been previously used in the synthesis of polybutadiene DendriMacs with reasonable success.¹⁶ DMAc also possesses a slightly higher dielectric constant ($\epsilon = 37.80$), which should favour the Williamson coupling reaction. All other conditions were kept the same as the previous attempts using DMF/THF. The reactions were again followed by SEC analysis and stopped when they showed no further change in molecular weight. Owing to the potential risk of impurities being present in the macromonomers, all

polymers as well as the cesium carbonate were vacuum dried before usage. In all three reactions the polymers remained fully soluble in the DMAc/THF solvent mixture throughout the experiment.

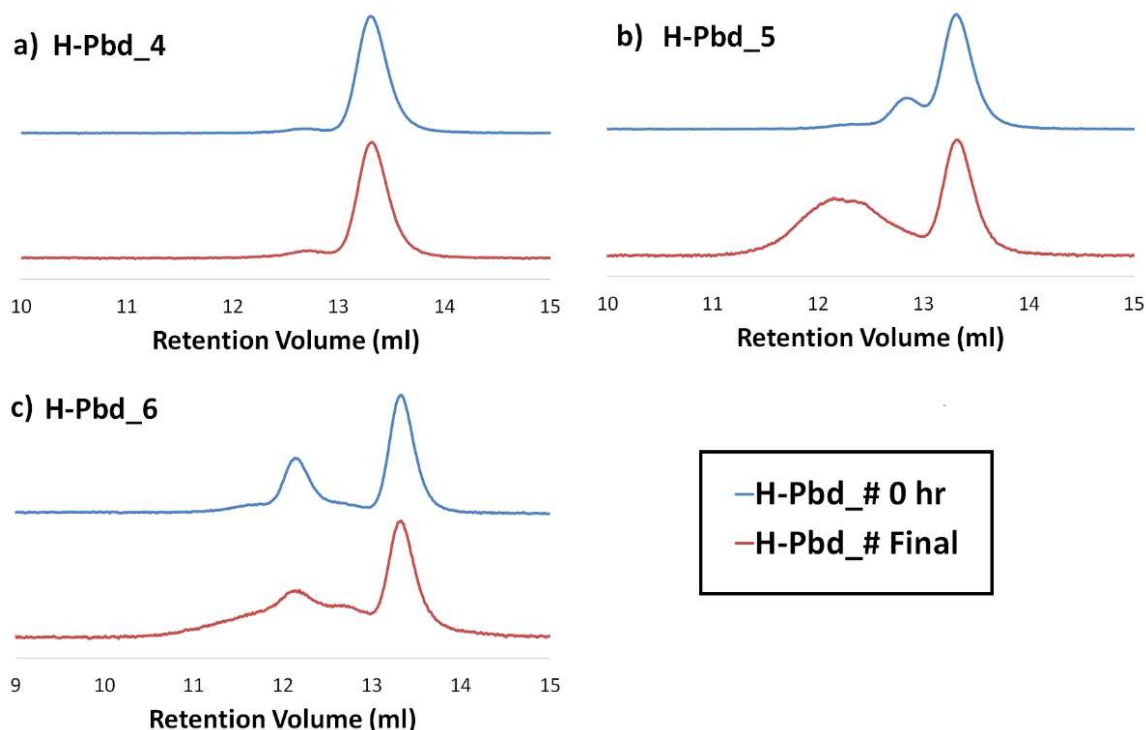


Figure 4.4 - SEC chromatograms (RI detector) of polymers: (a) H-Pbd_4, (FF-XBAR29, ARM31-Br) (b) H-Pbd_5 (FF-XBAR52, ARM31-Br) and (c) H-Pbd_6 (FF-XBAR100, ARM31-Br). Comparison of the samples between the start (0 hr) and end of reaction.

In the case of H-Pbd_4, using FF-XBAR29 and ARM31-Br, it is evident from the SEC data in Figure 4.4a, that there has been almost no coupling at all. This is the same outcome as for the analogous reaction with the same macromonomers using DMF/THF (H-Pbd_1). Given that the arm (ARM31-Br) did undergo successful coupling in other reactions, the consistent absence of coupling points towards some problem with FF-XBAR29, despite ^1H -NMR, SEC and NP-IIC analysis which all indicated that it was viable, with the desired crossbar structures constituting the main component of its product mixture. Conversely, reactions H-Pbd_5 and H-Pbd_6 indicated that coupling had taken place with evidence of crossbar consumption compared to their corresponding starting material chromatograms (Figure 4.4b and c). Reactions 5 and H-Pbd_6 also proved slightly more successful than seen in the analogous reactions carried out in DMF/THF.

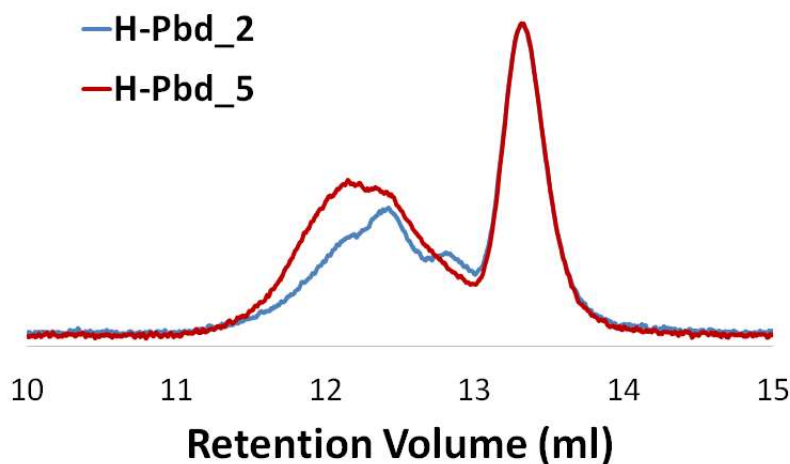


Figure 4.5 - SEC chromatograms (RI detector) of polymers H-Pbd_2 (FF-XBAR52, ARM31-Br; solvent: DMF/THF) (blue line) and H-Pbd_5 (FF-XBAR52, ARM31-Br; solvent: DMAc/THF) (red line)

Firstly considering H-Pbd_5, we can see from Figure 4.5 it has a broad peak in between 11.0 and 13 ml, with a maximum at 11.9 ml, representing a mixture of coupled products. The intensity of the peak between 11.0 and 13 ml is also greater for H-Pbd_5 than observed for H-Pbd_2 indicating a greater extent of coupling. The final chromatogram for H-Pbd_5 also suggests that the crossbar (FF-XBAR52) has been (mostly) consumed in this case, with the peak at 12.8 ml having almost completely disappeared, compared to H-Pbd_2 where there was still an evident peak for the crossbar.

Table 4.3 - Molar mass data for H-Pbd_2 and H-Pbd_5 (solvent THF; $dn/dc = 0.124 \text{ ml g}^{-1}$)

Polymer	<u>Coupled Product Peak</u>		
	<u>M_n</u> (g mol ⁻¹)	<u>M_w</u> (g mol ⁻¹)	<u>Đ</u>
H-Pbd_2	97,600	122,900	1.26
H-Pbd_5	123,600	183,500	1.48

Molar mass analysis (Table 4.3) of the broad peaks showed that H-Pbd_5 has an M_n of 123,600 g mol⁻¹, whereas the broad peak of H-Pbd_2 gave an M_n of 97,600 g mol⁻¹, suggesting that the (mixture of) branched products in H-Pbd_5 have a higher molar mass. Whereas both polymers may contain a mixture of some 1-arm, 2-arm, 3-arm and the desired 4-arm H-polymer, the RI chromatograms combined with molar mass data suggests that H-Pbd_5 consists of products with a greater number of coupled arms than H-Pbd_2, due to the enhanced level of coupling.

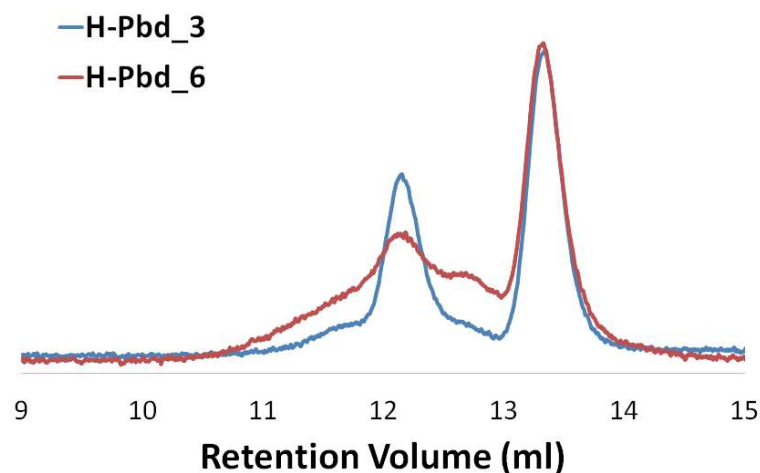


Figure 4.6 - SEC chromatograms (RI detector) of polymers H-Pbd_3 (FF-XBAR100, ARM31-Br; solvent: DME/THF) (blue line) and H-Pbd_6 (FF-XBAR100, ARM31-Br; solvent: DMAc/THF) (red line)

The RI chromatogram for H-Pbd_6, (Figure 4.6) shows that more coupling has taken place compared to H-Pbd_3. For H-Pbd_3, the crossbar (FF-XBAR100) peak at 12.3 ml was identical to the H-Pbd_6 starting material chromatogram. For H-Pbd_6, the crossbar peak has a lower intensity, moreover there is a shoulder between 10.5 and 11.9 ml, at a lower retention volume than the corresponding crossbar peak. Molecular weight analysis reveals that this shoulder has an M_n of 150,200 g mol⁻¹, M_w of 182,000 g mol⁻¹ and a dispersity of 1.21. The data suggests chains represented by this shoulder are comprised of at least two arms coupled to the crossbar (theoretical M_{nTHEO} ca. 164,000 g mol⁻¹), whilst the dispersity is an indication that multiple branched products may be present.

Thus far, all macromonomers, solvents and reactants used were thoroughly dried before usage. However, the cesium carbonate used was a few months old. As cesium carbonate is hygroscopic, it was thought that the participation of the base in the coupling reaction may have been limited due to the presence of water. The Williamson coupling is an S_N2 reaction, any presence of water in these reactions has been known to slow down the rate of reaction, by inhibiting the reactants from forming the S_N2 transition state, with a recent report confirming that as little as three water molecules in reaction is enough to have a marked effect on reaction.¹⁷ As such, a new bottle of cesium carbonate was used in the following set of coupling reactions in order to identify whether the (old sample of) base was the cause for the slow rate of reaction and low coupling. Thus H-Pbd_7, 8 and 9 were otherwise analogous in all respects to H-Pbd_4, 5 and 6 and the coupling reactions were followed by SEC and stopped when no further change was observed.

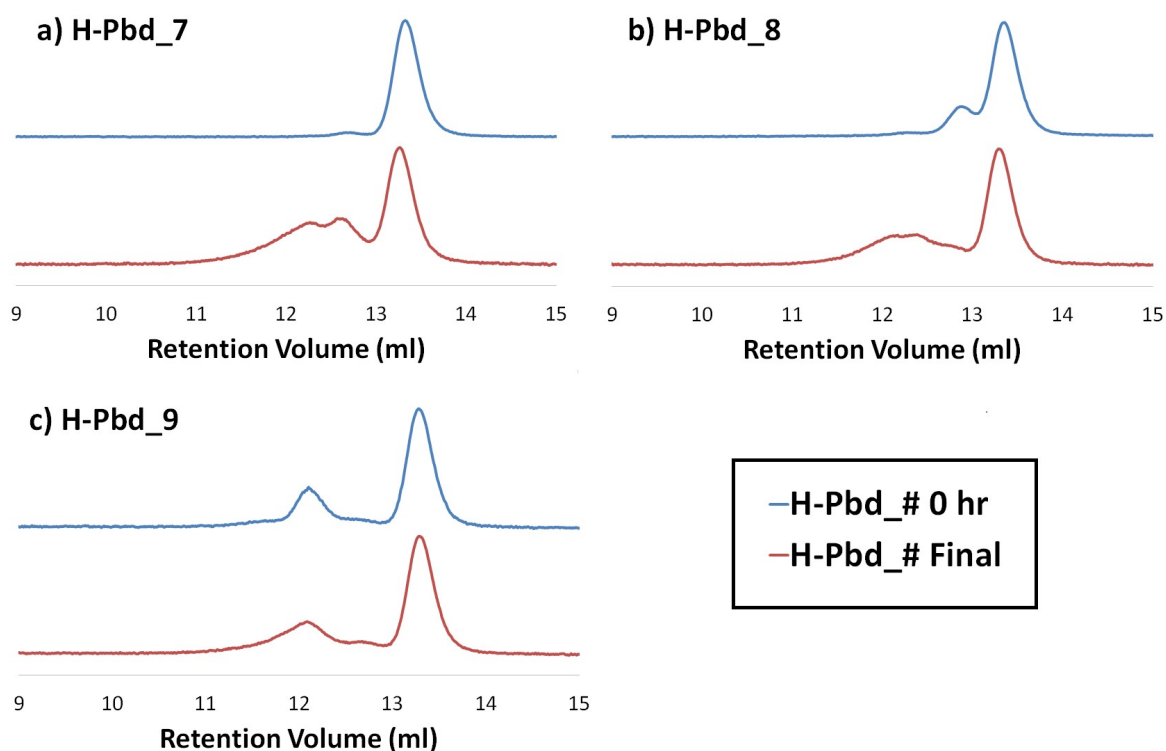


Figure 4.7 - SEC chromatograms (RI detector) of polymers: (a) H-Pbd_7 (FF-XBAR29, ARM31-Br), (b) H-Pbd_8 (FF-XBAR52, ARM31-Br) and (c) H-Pbd_9 (FF-XBAR52, ARM31-Br), from the reactions using a new bottle of cesium carbonate. Comparison of the samples between the start (0 hr) and end of reaction.

The SEC data presented Figure 4.7 illustrates that in each reaction moderate levels of coupling were achieved. Moreover, for the first time, the experiment using the lowest molecular weight crossbar FF-XBAR29 (H-Pbd_7) showed some evidence of undergoing coupling. In the previous two experiments using FF-XBAR29 (H-Pbd_1 and H-Pbd_4) there had been no coupling evident. The use of fresh cesium carbonate in this instance has, to some extent, improved conditions enough for coupling to occur, suggesting that the old cesium carbonate may have been a cause of the failure of the previous two reactions. The SEC chromatogram for H-Pbd_7 (Figure 4.7a) has two distinct high molecular weight peaks with maxima at 12.4 ml and 12.6 ml, and with M_n values of 127,000 g mol⁻¹ and 78,500 g mol⁻¹ respectively. These molar mass values correspond approximately to the theoretical values expected for a crossbar coupled to three-arms (ca. 120,000 g mol⁻¹) and two arms (ca. 90,000 g mol⁻¹) respectively.

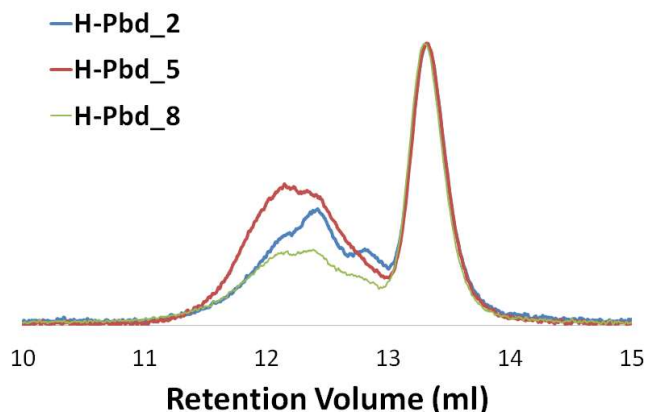


Figure 4.8 - SEC chromatograms (RI detector) of polymers H-Pbd_2 (FF-XBAR52, ARM31-Br; solvent: DMF/THF) (blue line), H-Pbd_5 (FF-XBAR52, ARM31-Br; solvent: DMF/THF) (red line) and H-Pbd_8 (FF-XBAR52, ARM31-Br; solvent: DMF/THF; new bottle cesium carbonate) (green line)

Whilst the use of fresh cesium carbonate resulted in an improvement for the lowest molecular weight crossbar, the SEC chromatograms and molecular weight analysis for the higher molecular weight crossbars FF-XBAR52 (H-Pbd_8), and FF-XBAR100 (H-Pbd_9) were rather similar to the previous, analogous coupling reactions. The RI chromatogram for H-Pbd_8 (Fig 4.8) shows a broad peak between 11 - 13 ml, although it is less intense than seen for H-Pbd_5, indicating that less coupling may have taken place. A greater level of crossbar consumption in comparison to H-Pbd_2 was also observed, with there being no identifiable peak for the crossbar in comparison to the clear peak maxima present at 12.8 ml in H-Pbd_2. Molar mass analysis of the broad peak of H-Pbd-8 gave an M_n of 118,100 g mol⁻¹, M_w of 150,200 g mol⁻¹ and a dispersity of 1.27 all of which were lower than seen for H-Pbd-5 but higher than seen for H-Pbd-2.

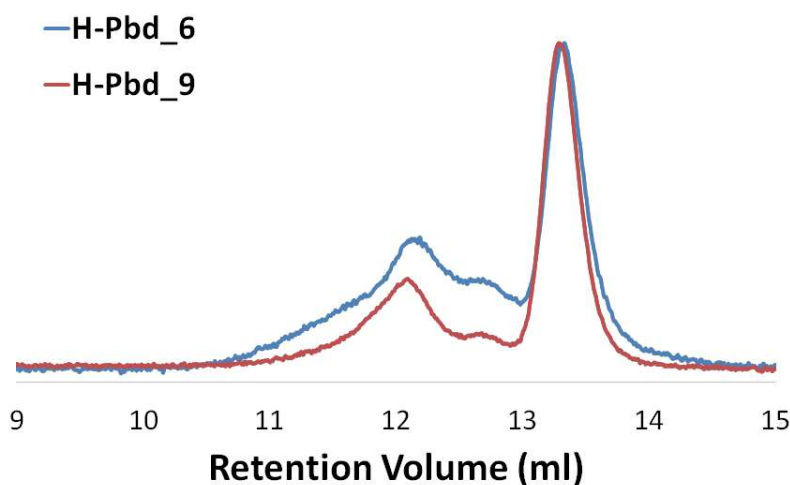


Figure 4.9 - SEC chromatograms (RI detector) of polymers H-Pbd_6 (FF-XBAR100, ARM31-Br; solvent: DMF/THF) (blue line) and H-Pbd_9 (FF-XBAR100, ARM31-Br; solvent: DMF/THF; new bottle cesium carbonate) (red line)

Table 4.4 - Molar mass data for H-Pbd_6 and H-Pbd_9 (solvent THF; $dn/dc = 0.124 \text{ ml g}^{-1}$)

Polymer	<u>Coupled Product Shoulder (10.5-11.9 ml)</u>		
	<u>M_n (g mol⁻¹)</u>	<u>M_w (g mol⁻¹)</u>	<u>\bar{D}</u>
H-Pbd_6	150,200	182,000	1.21
H-Pbd_9	156,200	196,800	1.26

Polymer H-Pbd_9 produced similar results to those seen for H-Pbd_6, with a shoulder between 10.5 ml and 11.9 ml also detected (Fig 4.9) Molecular weight analysis for each of these polymers gave very similar values, signifying a comparable amount of coupling has taken place in both reactions, with the MW data suggesting the shoulder consists of a majority of one-arm coupled or two-arms coupled by-products.

4.2.2.1 RP-TGIC analysis of H-shaped polymers H-Pbd_7, H-Pbd_8 and H-Pbd_9

Although SEC can provide evidence that reaction has occurred, because its mode of separation is based on molecular size, rather than molecular weight, SEC analysis can be somewhat ineffective in complex mixtures of branched and linear polymers, which is certainly the case in these reactions. In contrast, reversed-phase temperature gradient interaction chromatography (RP-TGIC) has been shown to reveal a better understanding of the nature of such complex mixtures.¹⁸⁻²¹ As has been discussed in previous chapters, interaction chromatography (IC) is a separation method in which separation is driven primarily by enthalpic interactions between the solute polymer molecules and the stationary phase and separation/retention is proportional to the molecular weight. The strength of the enthalpic interaction, and therefore retention time, can also be controlled by variation in temperature which allows for superior resolution in TGIC than SEC. The enhanced resolution in TGIC has also been shown to allow the detection of small quantities of residual by-products present in apparently purified samples, that were otherwise undetectable via SEC due to very small differences in their molecular sizes.²¹ With these advantages in mind, TGIC presented itself as a potentially invaluable characterisation tool for the analysis of the crude mixtures of polymers formed during the attempted synthesis of H-shaped polymers. Reversed-phase TGIC analysis was thus carried out on crude polymers H-Pbd_7, H-Pbd_8 and H-Pbd_9, to reveal a more detailed picture of the coupled products being produced. The results of this analysis are presented in Figure 4.10.

The analysis of the polybutadienes was achieved by RP-TGIC using a mobile phase of 1,4-dioxane at a flow rate of 0.4 ml/min. A temperature gradient of 0.13 degrees per minute between a range of 22-30 °C was used. It should also be remembered that due to the separation mechanism of RP-TGIC, the order of elution with respect to molar mass is reversed and lower molecular weight species elute before higher molecular weight species, and this elution occurs after the solvent peak. It can be seen that in all three cases, the superior resolution of TGIC over SEC reveals much more information for each polymer.

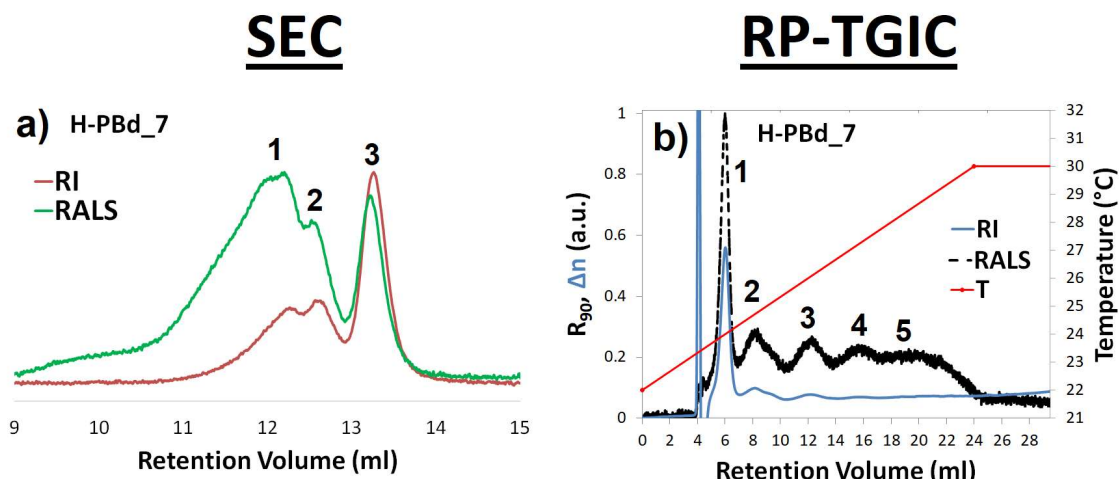


Figure 4.10 - SEC (a) and RP-TGIC (b) chromatograms of polymer H-Pbd_7. TGIC samples were analysed in 1,4-dioxane at a flow rate of 0.4 ml/min. Temperature profiles are shown on the plot.

The TGIC chromatogram for polymer H-Pbd_7 (FF-XBAR29, ARM31-Br) (Figure 4.10a) shows a well-defined peak at about 13.3 ml, corresponding to unreacted arm (ARM31-Br) and two overlapping peaks between 11 – 13 ml. In contrast the TGIC data (Figure 4.10b) shows five overlapping, polymer peaks – more clearly visible in the RALS signal as light scattering is more sensitive to the presence of larger polymer chains. The first extremely sharp peak at 4.0 ml (RI detector) is the solvent injection peak, which is then followed by an intense, narrow peak at 6.1 ml which corresponds to the excess unreacted arm still present in the sample. The macromonomer approach used in these reactions allows us to speculate with confidence about the underlying polymer structure corresponding to each peak, by considering that each corresponds to a crossbar with an increasing number of coupled arms. As both the crossbar (FF-XBAR29) and arm (ARM31-Br) had almost equivalent molar masses it may be assumed that any residual crossbar was co-eluted with peak 1. As such, the four peaks detected at 8.2 ml, 12.1 ml, 15.9 ml and 20.1 ml, may

reasonably be assumed to represent the crossbar with one, two, three and four coupled arms respectively.

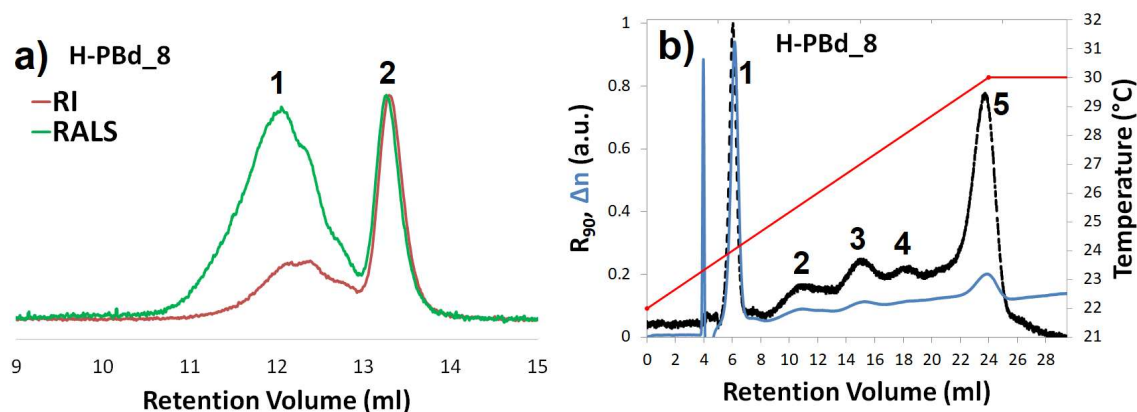


Figure 4.11 - SEC (a) and RP-TGIC (b) chromatograms of polymer H-Pbd_8. TGIC samples were analysed in 1,4-dioxane at a flow rate of 0.4 ml/min. Temperature profiles are shown on the plot.

The TGIC analysis for H-Pbd_8 (FF-XBAR52, ARM31-Br) (Figure 4.11b) particularly exemplifies the superior resolution of TGIC and evidences the best chain coupling result thus far. The SEC chromatogram for this sample (Figure 4.11a) shows a well-defined peak at about 13.3 ml corresponding to unreacted arm, and a broad peak to lower retention volumes, which has some evidence of structure – a shoulder can be seen in the RALS trace at about 12.5 ml. Conversely, the TGIC data shows five clear, albeit overlapping, peaks. For this sample there is the characteristic solvent injection peak (RI detector) at 4.0 ml, as well as the intense peak representing the excess unreacted arm at 6.1 ml. There are then three further peaks (peaks 2 – 4) at 10.6 ml, 14.8 ml and 17.9 ml which, although not fully resolved, are clearly evident especially in the light scattering trace. It would seem reasonable therefore to suggest that peaks 2 - 4 correspond to a crossbar coupled to one, two and three arms respectively and the large peak at 23.9 ml consists of the fully coupled H-shaped polymer. The RI (concentration) detector also indicates that the peak at 23.9 ml may be the product present in the mixture in the highest concentration, ignoring the unreacted excess arm (peak 1).

In order to confirm the assignment of the peak at 23.9 ml as the H-shaped polymer, a linear polybutadiene standard with a molecular weight of $170,000 \text{ g mol}^{-1}$, which is very similar to the theoretical M_n of the H-polymer ($177,600 \text{ g mol}^{-1}$) was analysed under the same conditions, and was shown to elute at an almost identical retention volume. It is worth recalling the RP-TGIC separates polymers on the basis of the molecular weight, not hydrodynamic volume and thus, the co-elution of these two samples of nearly identical

molar mass supports the assignment of the peak at 23.9 ml as the H-shaped polymer (Figure 4.12). However, it is also worth noting that the multimodal nature of H-Pbd_8 shows that the efficiency and extent of the coupling reaction is far from ideal.

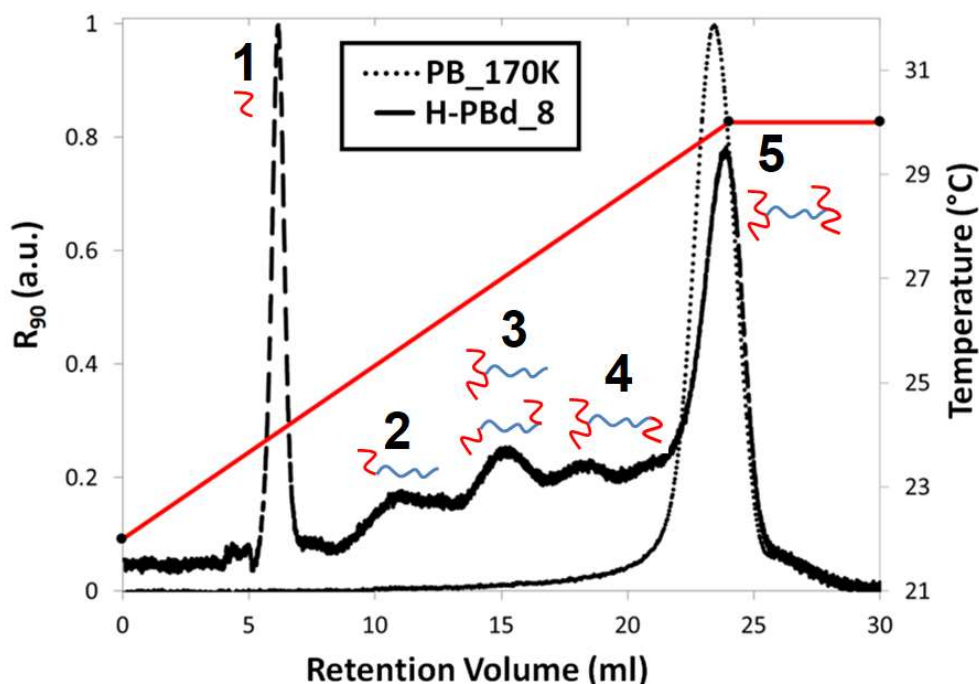


Figure 4.12 - TGIC chromatograms (RALS detector) of polymers H-PBD_8 and linear polybutadiene standard PB170K. TGIC samples were analysed in 1,4-dioxane at a flow rate of 0.4 ml/min. Temperature profile is shown on the plot.

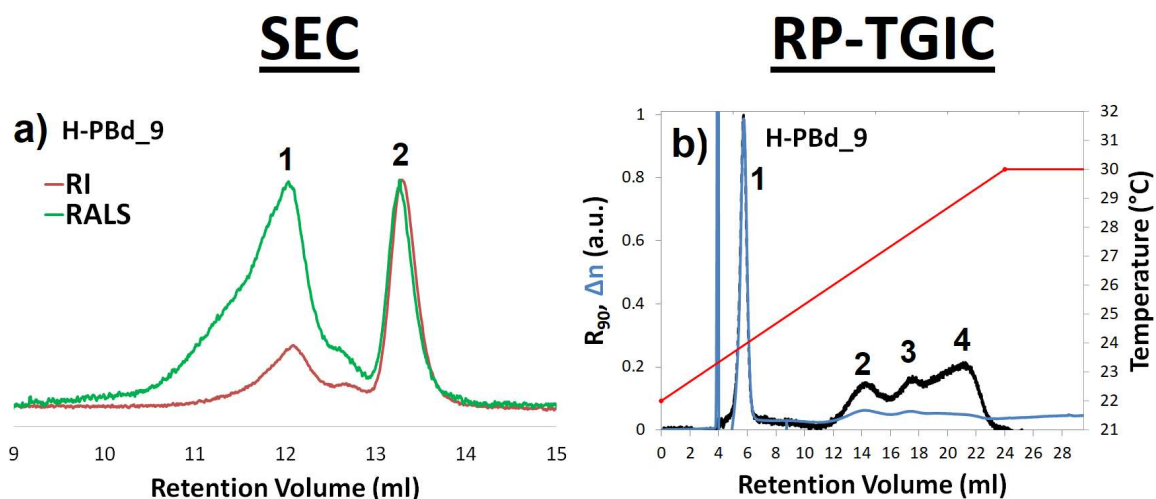


Figure 4.13 - SEC (a) and RP-TGIC (b) chromatograms of polymer H-Pbd_9. TGIC samples were analysed in 1,4-dioxane at a flow rate of 0.4 ml/min. Temperature profiles are shown on the plot.

The SEC analysis (Figure 4.13a) of H-Pbd_9 (FF-XBAR100, ARM31-Br) showed that there was still a significant amount of unreacted crossbar and arm (peaks 1 and 2). There also seems to be a shoulder between the crossbar and arm peaks at 12.7 ml, which may be a

result of the high MW FF-XBAR100 crossbar degrading during reaction. The RALS signal indicated more clearly the presence of coupled material with a high MW shoulder detected between 10.5 – 11.9 ml. The TGIC analysis (Figure 4.13b) showed that after the unreacted arm (peak 1) there are only three peaks detected at 14.3 ml, 17.8 ml and 21.3 ml which may represent the excess crossbar (peak 2), with peaks 3 and 4 corresponding to the crossbar with one and two arms attached respectively and the final peak which may belong to a crossbar with three arms attached. The lower number of peaks, overlapping of the peaks and low peak intensity would also confirm that the coupling reaction using the highest molecular weight crossbar has been the least successful.

The RI (concentration detector) trace from the TGIC analysis of polymers H-Pbd_7 (FF-XBAR29, ARM31-Br), H-Pbd_8 (FF-XBAR52, ARM31-Br) and H-Pbd_9 (FF-XBAR100, ARM31-Br), indicates in each case the extent of coupling and fraction of branched products was not high; this is in agreement with their respective SEC chromatograms. The instability of the RI baseline, due to temperature sensitivity, in all the TGIC chromatograms prevented any accurate molecular weight data being obtained from these chromatograms. However, RP-TGIC has clearly shown that it is capable of revealing far more information about these complex mixtures than SEC is able to and, moreover, that the coupling reactions worked to some extent, with small quantities of the desired H-shaped polymer made in at least two cases.

Thus, although the use of DMAc in place of DMF as a co-solvent with THF resulted in somewhat higher levels of macromonomer chain coupling (excluding H-Pbd_4); it can also be concluded that the rate and, therefore, extent of coupling seen in all the coupling reactions discussed thus far, has been modest at best. This is evidenced by the fact that in all cases there are still relatively large amounts of the unreacted arm polymer, even when taking into account it is present in a slight molar excess. Henceforth, it was decided that further optimization would be required in order to adapt the macromonomer approach for successful H-shaped polymer synthesis. Two possible ways in which the extent of coupling could be improved were considered – increasing the molar ratio of arm macromonomer to crossbar and/or increasing the molar ratio of base to crossbar. Increasing the amount of arm macromonomer present is likely to increase coupling simply based on there being more material available for reaction. A previous report on the synthesis of polystyrene stars using the macromonomer approach and Williamson coupling reactions¹² showed that the use of very high temperatures (150 °C) was beneficial for the efficiency of the coupling

reaction, however, prolonged exposure of polybutadiene to such high temperatures would undoubtedly lead to thermal/oxidative degradation. Moreover, the addition of common anti-oxidants such as butylated hydroxytoluene is not possible since this phenolic species may take part in the reaction itself. Previous work done by the Hutchings' group on the synthesis of polystyrene and polybutadiene HyperMacs, focused on the effect of the base on the rate and extent of chain coupling, concluding that cesium carbonate resulted in the greatest amount of coupling among the commonly used metal carbonates.¹³ Although cesium carbonate was already used in the reactions described above, the amounts of base used although present in a 10 molar excess with respect to the crossbar, were vanishingly small (20 – 60 mg). Due to the high viscosity of the reaction mixtures it was surmised that inefficient mixing of the base with the starting materials may be occurring and so we also decided to explore the outcome of increasing the molar ratio of cesium carbonate to crossbar.

4.2.2.2 Synthesis of H-shaped polymers in DMAc/THF – Varying the Molar Ratio of Arms to Crossbar

The rate (and potentially the extent) of the coupling reaction is in part dependent on the number of chain-end functional groups available for reaction on both the crossbar and arm macromonomers. In the previous reactions, the molar ratio of crossbar to arm (1 : 5) delivers only one molar excess of arm with respect to functional groups on the crossbar, and (surprisingly) has still resulted in a relatively large amount of uncoupled arm macromonomer present in the final polymers. It was considered possible that the chain-end functionalities were being affected by side reactions, lowering their availability for coupling to the crossbar. As such, it was decided to explore whether increasing the molar ratio of arm macromonomer relative to that of the crossbar at the start of reaction (0 hr) would have a beneficial effect on the coupling reactions. Two reactions were carried out, both using crossbar FF-XBAR52 and ARM23-Br in a 10 wt% solution in DMAc/THF (50/50 v/v), with 10 mol equivalents of Cs_2CO_3 (relative to crossbar), at 60 °C. In the first reaction (H-Pbd_10) 7 equivalents of arm were used relative to the crossbar and in the second reaction (H-Pbd_11) 10 equivalents of arm were used. In each case the reaction was followed by SEC until no further coupling was detected.

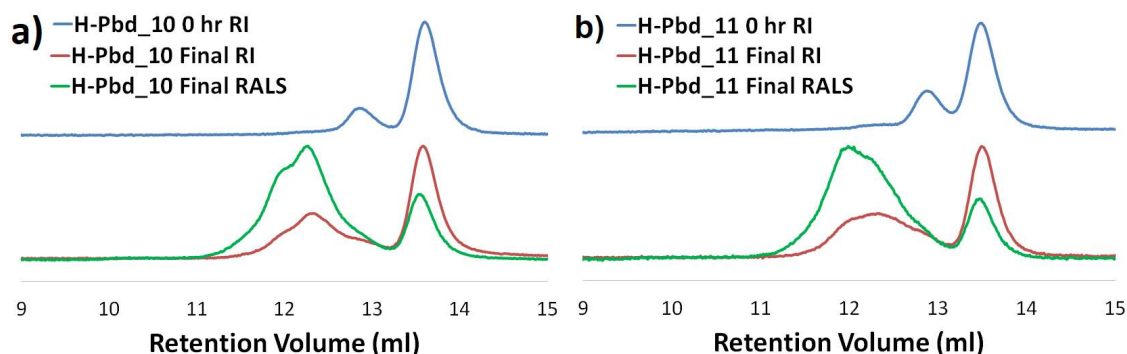


Figure 4.14 - SEC chromatograms (RI and RALS detectors) of polymers: (a) H-Pbd_10 (FF-XBAR52, ARM23-Br (7 equivalents arm : crossbar)), and (b) H-Pbd_11 (FF-XBAR52, ARM31-Br (10 equivalents arm : crossbar)). Comparison of the samples between the start (0 hr) and end of reaction.

Table 4.5 - Molar mass data for H-Pbd_10 and H-Pbd_11 (solvent THF; $dn/dc = 0.124 \text{ ml g}^{-1}$)

Polymer	H-polymer theoretical M_{nTHEO} (g mol^{-1})	Coupled Product Peak (11-13 ml)		
		M_n (g mol^{-1})	M_w (g mol^{-1})	\bar{D}
H-Pbd_10	152,000	98,400	117,000	1.19
H-Pbd_11	152,000	108,100	130,400	1.20

The SEC chromatograms of samples of H-Pbd_10 and H-Pbd_11 (Figure 4.14) clearly show that increasing the molar ratio of arms to crossbar has produced a higher degree of coupling. Molar mass analysis for both polymers is given in Table 4.5. In H-Pbd_10, using 7 equivalents of arm has resulted in a multimodal higher molecular weight peak between 11 and 13 ml with an M_n value of approximately $98,400 \text{ g mol}^{-1}$. The theoretical values expected for crossbar FF-XBAR52 coupled to two ARM23-Br arms ($102,200 \text{ g mol}^{-1}$) is in good agreement with the obtained M_n value. Molar mass analysis of H-Pbd_11, using ten equivalents gave slightly higher results ($M_n = 108,100 \text{ g mol}^{-1}$, suggesting that higher MW material may be present.

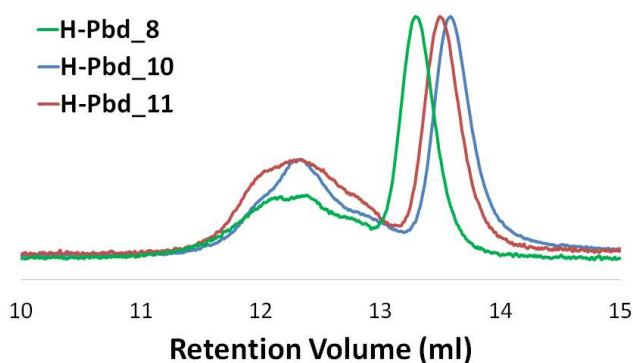


Figure 4.15 - SEC chromatograms (RI detector) of polymers H-Pbd_8 (5 equivalents arm : crossbar), H-Pbd_10 (7 equivalents arm : crossbar) and H-Pbd_11 (10 equivalents arm : crossbar).

Moreover, it is clear that increasing the molar ratio of arms has resulted in a slight increase in the extent of coupling when compared to using just 5 equivalents of arm. Figure 4.15 shows the RI (concentration) signal for H-Pbd_8 (FF-XBAR52, ARM31-Br; 1 : 5; crossbar : arm) compared to H-Pbd_10 ((FF-XBAR52, ARM31-Br; 1 : 7; crossbar : arm) and H-Pbd_11 ((FF-XBAR52, ARM31-Br; 1 : 10; crossbar : arm). Measuring the area under the curve for the peaks representing the branched products reveals that 41% of H-Pbd_8 is coupled, 47% of H-PB_10 is coupled and 50% of H-Pbd_11 is coupled, demonstrating the benefit of increasing the molar ratio of the arms. However, it is also worth noting that even with a large excess of arms, and an improved extent of coupling, the SEC traces of the resulting polymers are still broad, suggesting a significant degree of (unwanted) heterogeneity.

To investigate the nature of the heterogeneity, RP-TGIC analysis was carried out on H-Pbd_10 and H-Pbd_11 using the previously established conditions, and the results for H-Pbd_10 are presented below in Figure 4.16. The TGIC chromatogram for H-Pbd_10 (Figure 4.16b) in particular is far more detailed than its corresponding SEC chromatogram (Figure 4.16a), and seven distinct peaks can be detected.

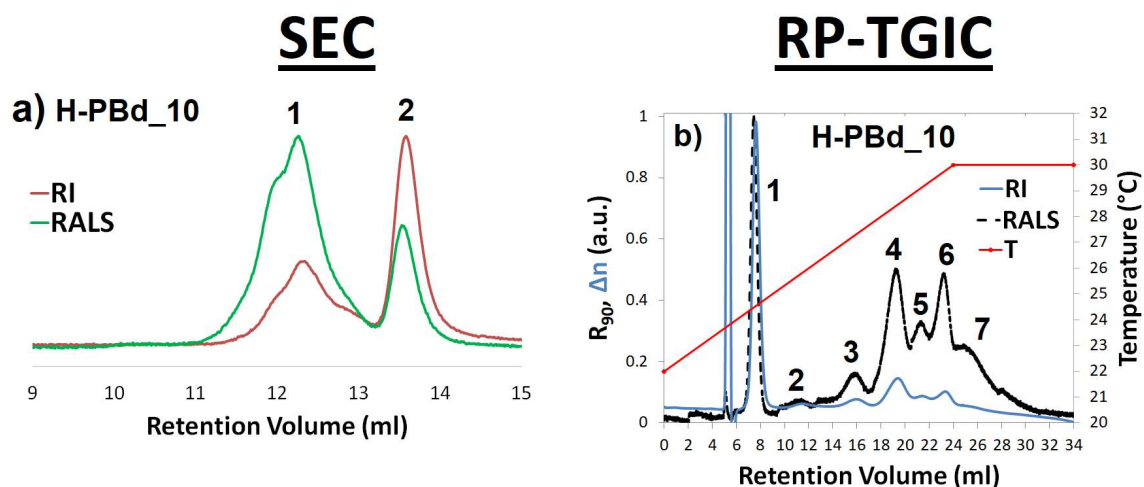


Figure 4.16 - SEC (a) and RP-TGIC (b) chromatograms of polymer H-Pbd_10 (FF-XBAR52, ARM23-Br (7 equivalents arm : crossbar)). TGIC samples were analysed in 1,4-dioxane at a flow rate of 0.4 ml/min. Temperature profiles are shown on the plot.

Although this extent of complexity is far from ideal as a synthetic outcome, the level of detail revealed by the TGIC data is remarkable. The peak at 5.3 ml is the solvent peak, followed by an intense peak at 7.3 ml (peak 1) corresponding to the unreacted arm. A small peak at 11.5 ml (peak 2) may correspond to a trace of unreacted crossbar. Peaks 3, 4, 5 and 6 can reasonably be assigned to the product of cross bar plus one arm, two arms, three arms and four arms respectively. There was also clear evidence of further species eluting beyond

24 ml (peak 7) which is only really evident in the RALS signal. Given the high sensitivity of light scattering to high molar mass species, we can assume that peak 7 corresponds to a very low concentration of a very high molecular weight by-product. Table 4.6 lists the theoretical molar masses of the starting materials and the expected products of the reactions. Due to the reasonable stability of the RI detector baseline in the TGIC chromatogram for H-Pbd_10, molecular weight data was obtainable for each peak and the results are given in Table 4.7. A triple detection calibration using a linear polybutadiene standard ($M_n = 86,000 \text{ g mol}^{-1}$, $\bar{D} 1.01$) was used for the RP-TGIC molar mass analysis, with a dn/dc of 0.095 ml g^{-1} used for polybutadiene in 1,4-dioxane, obtained from previously published work.²² However, it should be noted that dn/dc is a temperature dependent parameter and the use of a temperature gradient may result in errors arising in MW calculations. The RI peaks present in the TGIC chromatogram are also not fully resolved, which may also result in inaccuracies.

Table 4.6 - Theoretical molar masses for the expected polymeric species in H-Pbd_10 (7 equivalents arm : crossbar)) and H-Pbd_11 (10 equivalents arm : crossbar)).

Expected Species Theoretical Molar Mass ($M_{n\text{THEO.}}$) (g mol^{-1})					
<u>ARM23-Br</u>	<u>FF-XBAR52</u>	<u>XBAR</u>	<u>XBAR</u>	<u>XBAR</u>	<u>XBAR</u>
<u>(ARM)</u>	<u>(XBAR)</u>	<u>+1 ARM</u>	<u>+2 ARMS</u>	<u>+3 ARMS</u>	<u>+4 ARMS</u>
24,900	52,400	77,300	102,200	127,100	152,000

Table 4.7 - Molar mass data for H-Pbd_10 obtained by triple detection RP-TGIC analysis (solvent 1,4-dioxane; $dn/dc = 0.095 \text{ ml g}^{-1}$)

H-Pbd_10	Peak # (ml)						
	<u>1</u>	<u>2</u>	<u>3</u>	<u>4</u>	<u>5</u>	<u>6</u>	<u>7</u>
	(7.3)	(11.5)	(16.0)	(19.4)	(21.5)	(23.4)	(24.8)
$M_n \text{ (g mol}^{-1}\text{)}$	20,300	54,200	80,000	103,800	129,700	151,100	181,900
$M_w \text{ (g mol}^{-1}\text{)}$	21,900	54,800	80,300	104,800	129,900	152,200	182,900
\bar{D}	1.081	1.010	1.004	1.010	1.001	1.007	1.005
Total RI Area (%)	49	5	8	18	6	9	5

The calculated M_n values for peaks 1 to 6 (Table 4.7) are in good agreement with the predicted values given in Table 4.6. The calculated M_n in for Peak 2 ($54,200 \text{ g mol}^{-1}$) confirms that this peak does correspond to a remnant of unreacted crossbar. There is then an increase in molar mass of approximately $24,000 \text{ g mol}^{-1}$ between peaks from Peak 2 to Peak 6 which

is concurrent with the incremental addition of one extra arm to the crossbar, and these M_n values are again in good agreement with the expected values. The molar mass data suggest that peak 6 (M_n 151,100 g mol⁻¹) is the desired H-shaped polymer (theoretical M_n 152,000 g mol⁻¹) even if the TGIC (RI) data indicates it is present in rather modest amounts in the final product. The calculated molecular weight for Peak 7 (M_n 181,900 g mol⁻¹) would imply that a species with 5 arms may be present. This high molecular weight by-product may be a result of a small subset of chains present in FF-XBAR52 that have an additional unit of DPE-OSi in chain, creating some chains with 3 (or more) DPE-OSi units. This in turn opens up the possibility of forming a polymer with 5 or 6 arms. NP-IIC analysis of FF-XBAR52 indicated that the crossbars are more complex than initially assumed and as such the potential for a small subset of chains containing extra DPE-OSi units capable of coupling, although undesired, is still possible. The RI baseline stability of H-Pbd_10 cases also allowed for an estimate of the concentration of each component present in the crude polymer, by measuring the area under the RI curve (Table 4.7). The main component of interest in this case is Peak 6, representing the desired H-shaped polymer, which was calculated to represent 9% of the total polymer's mass including the unreacted starting material. While this is a relatively poor yield of the desired product, it confirms that the generation of H-shaped polymers is possible by this route.

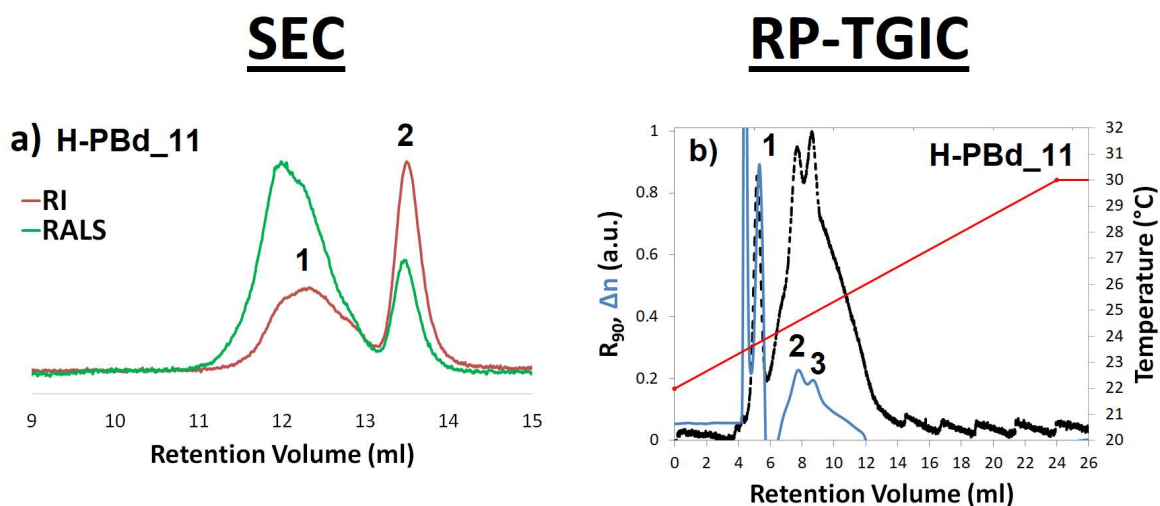


Figure 4.17 - SEC (a) and RP-TGIC (b) chromatograms of polymer H-Pbd_11 (FF-XBAR52, ARM31-Br (10 equivalents)). TGIC samples were analysed in 1,4-dioxane at a flow rate of 0.4 ml/min. Temperature profiles are shown on the plot.

The TGIC chromatogram for H-Pbd_11 (Figure 4.17b) showed multiple peaks but was far less well-resolved than in the case for H-Pbd_10, yet still provided more information than its comparative SEC (Figure 4.17a). Three defined peaks were identified with the intense

peak at 5.8 ml corresponding to the unreacted arm. Two less well-resolved peaks can be seen at 7.9 and 8.5 ml; however, the RI baseline was too unstable for any accurate molecular weight data to be obtained. It was surmised that eluent purity may have been the reason for this polymer's less resolved chromatogram, as evidenced by the erratic behaviour of the RALS detector. The 1,4-dioxane used is hygroscopic, and any impurities in the solvent may also negatively affect any chromatograms produced. However, it still remains the case that for both H-Pbd_10 and 11, increasing the molar ratio of arms to crossbar (using either seven or ten mol equivalents) has resulted in increased coupling and evidence of the desired H-polymer was strong for the crossbar synthesised using 7 mol equivalents.

4.2.2.3 Synthesis of H-shaped polymers in DMAc/THF - Varying the Molar Ratio of Cesium Carbonate

With the small benefit demonstrated of increasing the molar ratio of arms relative to crossbar established, the impact of varying the molar ratio of cesium carbonate was then explored. Cesium carbonate is used as the base in these reactions, in preference to potassium carbonate, due to the previously reported significantly higher degrees of coupling in the synthesis of HyperMacs.¹³ However, although the base was added in a 10 molar excess with respect to the crossbar, this resulted in only small amounts of base (ca. 20 - 60 mg) being added to the relatively viscous reaction mixtures, which may have limited its participation in reaction. It was theorised that increasing the molar ratio of carbonate present would allow for a more thorough dispersion of carbonate throughout the solvent mixture, thereby increasing the homogeneity of the mixture and hence participation of the base in reaction. Two reactions were carried out, the first using crossbar FF-XBAR29 (H-Pbd_12) and the second using crossbar FF-XBAR52 (H-Pbd_13). Both reactions used 10-mol equivalents of ARM23-Br as the arm macromonomer, analogous to reactions H-Pbd_7 and H-Pbd_11 respectively. A 10wt% solution in DMAc/THF (50/50 v/v), with 50 mol eq of Cs₂CO₃ (a fivefold increase from all previous reactions using 10 mol eq) relative to crossbar at 60 °C were used in H-Pbd_12 and H-Pbd_13 reactions and reaction stopped when no further coupling was detected.

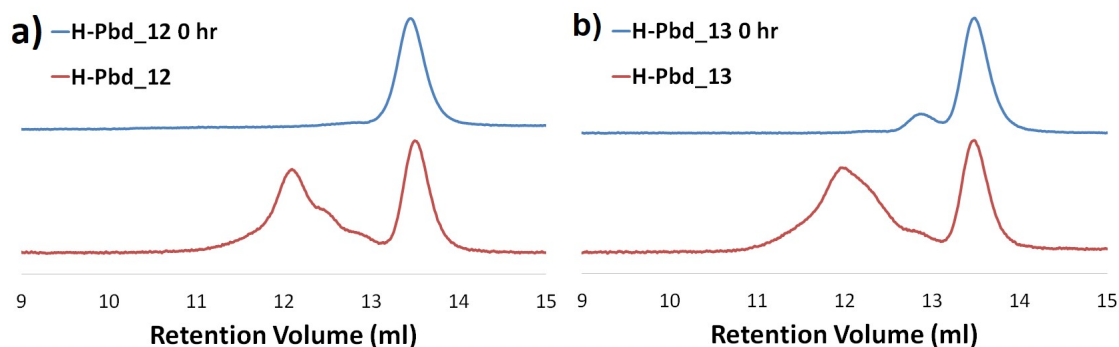


Figure 4.18 - SEC chromatograms (RI detector) of polymers: (a) H-Pbd_12 (FF-XBAR29, ARM23-Br), and (b) H-Pbd_13 (FF-XBAR52, ARM23-Br). Comparison of the samples between the start (0 hr) and end of reaction. Reaction conditions: 10 equivalents arm : crossbar; 50 equivalents cesium carbonate : crossbar.

The increased amount of cesium carbonate has had a dramatic effect on the extent on coupling, as seen in Figure 4.18. There is a broad high molecular weight peak evident in H-Pbd_12 at 12.4 ml, with two shoulders with maxima at 12.6 and 12.8 ml respectively. Molecular weight analysis of broad region between 11 – 13 ml gave an M_n of 120,000 g mol⁻¹ and an M_w of 147,400 g mol⁻¹, suggesting in this instance coupling has been quite successful and there is a significant portion of high molecular weight material. H-Pbd_13 has a high molecular weight peak between 10.5 and 12.7 ml gives an M_n of 102,000 g mol⁻¹, also confirming the existence of high molecular weight products in this sample.

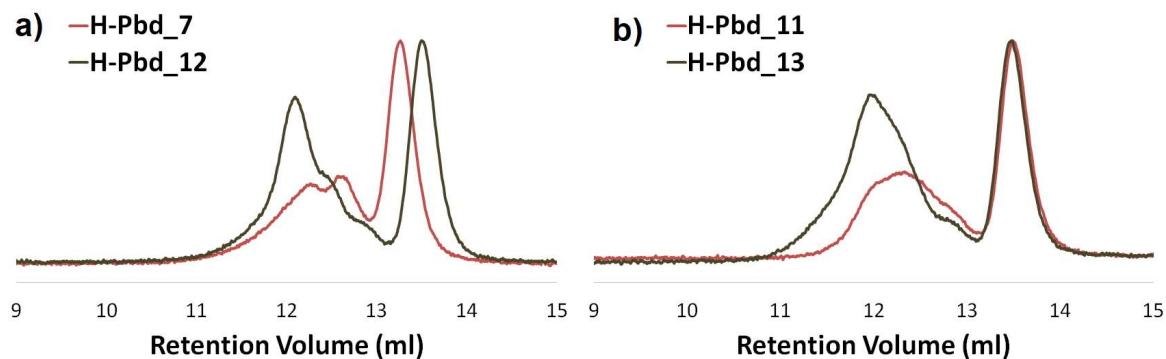


Figure 4.19 - SEC chromatograms (RI detector) of polymers: (a) H-Pbd_7 and H-Pbd_12, and (b) H-Pbd_11 and H-Pbd_13.

Figure 4.19 compares the RI (concentration) chromatograms of H-Pbd_12 (FF-XBAR29, ARM23-Br) and H-Pbd_13 (FF-XBAR52, ARM23-Br), which both used 50 equivalents of carbonate, to analogous reactions H-Pbd_7 and H-Pbd_11 respectively, which were identical in every way except for using 10 equivalents of carbonate. There is a slight offset between the chromatograms of H-Pbd_7 and H-Pbd_12 due to the samples being run on different SEC calibration profiles. For both H-Pbd_12 and H-Pbd_13 the area of the high molecular weight coupling peak has increased when compared to all previous reactions,

signifying that a greater level of coupling has been achieved in both reactions. For H-Pbd_12 the peak area for the high molecular weight peak (retention volume 11-13 ml) showed that 59% of the total mass of polymer was coupled, compared to 40% for H-Pbd_7. Similarly, for H-Pbd_13, 60% of the polymer was coupled, compared to 50% for H-Pbd_11.

RP-TGIC analysis was carried out on H-Pbd_12 and 13 using the previously established conditions, and the results are presented below in Figure 4.20 and 4.21 respectively and compared to SEC data for the same polymers.

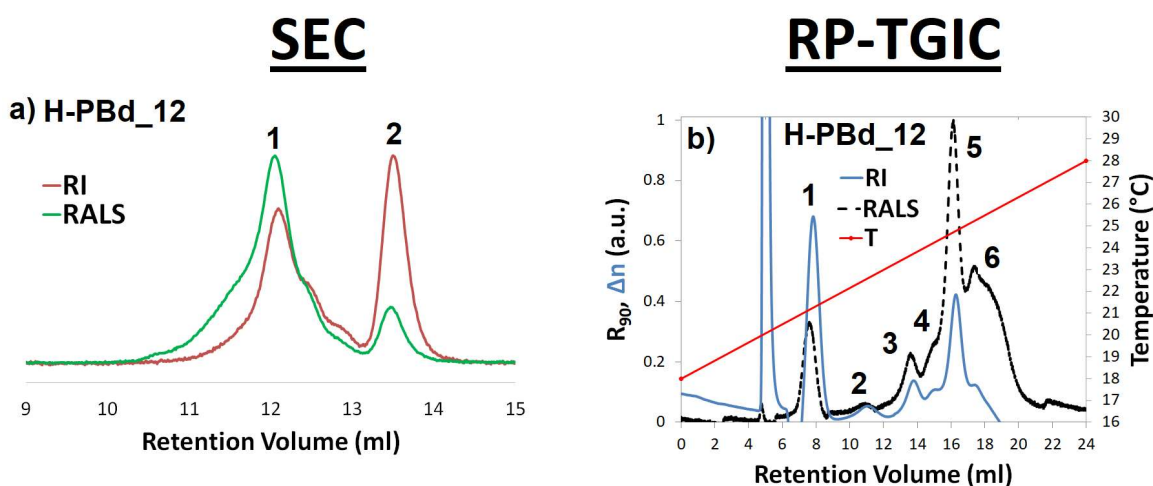


Figure 4.20 - SEC (a) and RP-TGIC (b) chromatograms of polymer H-Pbd_12 (FF-XBAR29, ARM23-Br). TGIC samples were analysed in 1,4-dioxane at a flow rate of 0.4 ml/min. Temperature profiles are shown on the plot.

As can be seen in the RP-TGIC chromatogram above, TGIC again reveals far more information about the polymers than SEC. The TGIC analysis (Figure 4.20b) shows that H-Pbd_12 is comprised of at least six species. Considering H-Pbd_12, it should be noted that the temperature range of the gradient was lowered from 22 - 30 °C to 18 - 28 °C due to the use of a lower molecular weight crossbar and therefore expected lower molecular weight products. The peak at 5.1 ml is the solvent peak, followed by a sharp peak at 7.9 ml (peak 1) corresponding to the unreacted arm. Both the crossbar (FF-XBAR29) and arm (ARM31-Br) have very similar molar masses any residual crossbar is co-eluted with peak 1. As such, peaks 2 - 5 from 11.1 ml to 16.4 ml can be assigned to the product of the crossbar plus one arm to four arms respectively, and the intensity of peak 5 at 16.4 ml is an encouraging indication that the desired H-polymer is present in the sample in a much larger quantity than the other by-products. There was also evidence of a further peak at a higher retention volume (17.7 ml), especially evident in the RALS signal, which may be assigned to high

molecular weight by-products, which again may be a result of arms coupling to crossbar chains with more than two DPE-OSi units incorporated.

Table 4.8 - Theoretical molar masses for the expected polymeric species in H-Pbd_12. Reaction conditions: 10 equivalents arm : crossbar; 50 equivalents cesium carbonate : crossbar.

Expected Species Molar Mass (M_n) (g mol ⁻¹)					
<u>ARM23-Br</u>	<u>FF-XBAR29</u>	<u>XBAR</u>	<u>XBAR</u>	<u>XBAR</u>	<u>XBAR</u>
(<u>ARM</u>)	(<u>XBAR</u>)	<u>+1 ARM</u>	<u>+2 ARMS</u>	<u>+3 ARMS</u>	<u>+4 ARMS</u>
24,900	29,000	53,900	78,800	103,700	128,600

Table 4.9 - Molar mass data for H-Pbd_12 obtained by triple detection RP-TGIC analysis (solvent 1,4-dioxane; dn/dc = 0.095 ml g⁻¹)

H-Pbd_12	Peak # (ml)					
	<u>1</u>	<u>2</u>	<u>3</u>	<u>4</u>	<u>5</u>	<u>6</u>
	(7.9)	(11.1)	(13.9)	(15.1)	(16.4)	(17.7)
M_n (g mol⁻¹)	22,200	45,700	79,200	108,900	125,000	213,700
M_w (g mol⁻¹)	23,000	45,800	79,300	109,000	125,200	236,500
\bar{D}	1.033	1.002	1.001	1.001	1.002	1.107
Total RI area (%)	44	5	9	6	23	13

The predicted M_n values for the expected products from peaks 1 to 5 are given in Table 4.8 and are in good agreement with the obtained values presented in Table 4.9. Moreover, the peak with the highest intensity, corresponding to the coupled component present in the highest concentration, is peak 5. It was speculated above that this peak could be assigned to the desired fully coupled H-shaped polymer. For H-Pbd_12, the desired H-polymer has a theoretical M_n value of *ca.* 128,000 g mol⁻¹, which is in good agreement with the M_n value obtained for peak 5 of 125,000 g mol⁻¹. An estimate of the concentration of each species present was taken by measuring the area under the RI curve and is also given in Table 4.9. It shows that the area of peak 5 was calculated to represent 23% of the total polymer, which is a marked improvement compared to H-Pbd_10, in which the H-polymer constituted 9% of the total polymer.

For sample H-PBd-13, RPIC analysis (Figure 4.21) revealed the familiar solvent and unreacted arm peaks at 5.1 ml and 7.8 ml respectively. There was a small peak at 9.8 ml (peak 2) which is believed to correspond to unreacted crossbar, followed by four peaks

(peaks 3 - 6) which we believe represent the crossbar attached with one arm up to four arms respectively. There were also two peaks detected at 20.6 ml and 22.2 ml that again must be a result of higher MW by-products.

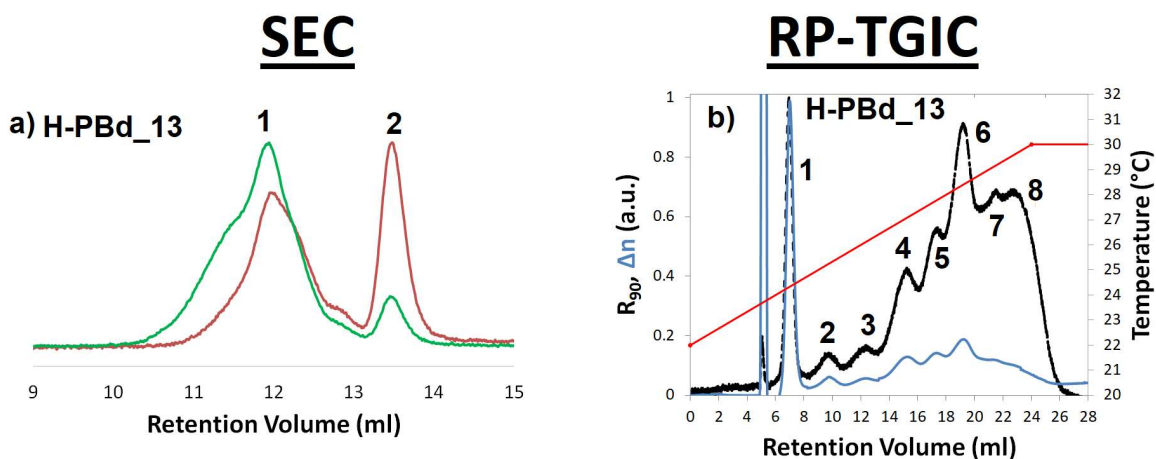


Figure 4.21 - SEC (a) and RP-TGIC (b) chromatograms of polymer H-Pbd_13. TGIC samples were analysed in 1,4-dioxane at a flow rate of 0.4 ml/min. Temperature profiles are shown on the plot.

Table 4.10 - Theoretical molar masses for the expected polymeric species in H-Pbd_13. Reaction conditions: 10 equivalents arm : crossbar; 50 equivalents cesium carbonate : crossbar.

Expected Species Theoretical Molar Mass (M_{nTHEO}) (g mol ⁻¹)					
<u>ARM23-Br</u>	<u>FF-XBAR52</u>	<u>XBAR</u>	<u>XBAR</u>	<u>XBAR</u>	<u>XBAR</u>
(ARM)	(XBAR)	+1 ARM	+2 ARMS	+3 ARMS	+4 ARMS
24,900	52,400	77,300	102,200	127,100	152,000

Table 4.11 - Molar mass data for H-Pbd_13 obtained by triple detection RP-TGIC analysis (solvent 1,4-dioxane; $dn/dc = 0.095$ ml g⁻¹)

H-Pbd_13	Peak # (ml)							
	<u>1</u>	<u>2</u>	<u>3</u>	<u>4</u>	<u>5</u>	<u>6</u>	<u>7</u>	<u>8</u>
	(7.0)	(9.8)	(12.3)	(15.6)	(17.3)	(19.2)	(20.6)	(22.2)
M_n (g mol ⁻¹)	23,000	55,800	80,600	97,200	120,400	146,200	212,400	342,300
M_w (g mol ⁻¹)	24,000	56,000	80,900	97,500	120,500	146,600	214,100	397,700
\bar{D}	1.052	1.005	1.003	1.002	1.002	1.011	1.005	1.066
Total RI area (%)	36	6	5	13	10	20	5	5

The theoretical molecular weight data for the expected species is given in Table 4.10, and the experimental molar mass data for each peak is given in Table 4.11 respectively. Peak 2 has an M_n of 55,800 g mol⁻¹, confirming it represents the fraction of unreacted crossbar FF-

XBAR52 (M_n 52,400 g mol⁻¹). The M_n value obtained for peak 6 (146,200 g mol⁻¹) is in excellent agreement with the M_n expected for the desired H-polymer (152,000 g mol⁻¹), confirming that peak 6 corresponds to the H-polymer. The total RI peak area for peak 6 was calculated to represent 20% of the total polymer.

One of the key objectives of this study was to provide quantities of pure H-polymer for rheological studies and to achieve this the crude samples require purifying by fractionation. In order to obtain an adequate quantity of sample (1 – 2 grams of pure material), the desired H-shaped polymer will need to be present in the crude mixture at a reasonable level. Given the rather limited efficiency of the coupling reactions it was considered that a coupled product containing 20 - 25% H-shaped polymer would be sufficient to provide adequate pure H-shaped polymer following purification of the crude samples by fractionation – see later – provided the reactions were scaled-up from the current scale (1 – 4 g) to around 20 – 40 grams. The increase in the amount of cesium carbonate present in the reaction mixture has resulted in a significant increase in the extent of coupling and resulted in the production of a satisfactory fraction of the desired H-shaped polymers.

4.2.2.4 Synthesis of H-shaped polymers in DMAc/THF - Improved Conditions

The previous series of experiments enabled the development of a methodology that, whilst far from perfect, should result in both adequate coupling and higher conversion rates for the generation of H-shaped polybutadienes via the macromonomer approach.

A molar ratio of 7 equivalents of arm to crossbar was chosen over 10 equivalents, as previous results indicated that 10 equivalents only generated a 3% increase in coupling over 7 equivalents and requires the use of much more starting material, which is a concern for the eventual scale up reactions. When the molar ratio of cesium carbonate to crossbar was increased from 10 to 50 equivalents results showed a beneficial impact on the extent of coupling. However, the use of this amount of carbonate also seemed to increase the production of high molecular weight by-products which may be difficult to remove during purification, and it was thought that even higher molar ratios would exacerbate this problem. As such, the amount of carbonate used was kept as 50 mol equivalents. The solvent mixture (DMAc/THF 50/50 v/v; 10 wt% concentration) should ensure that all macromonomers remain in solution for the duration of reaction. The temperature (60 °C)

should ensure that the rate of reaction is increased to a suitable enough level without the oxidative degradation of polybutadiene as detailed in previous work.

With these conditions identified, a further small scale, test reaction was carried out in order to confirm the effectiveness of the chosen conditions. Polymer H-Pbd_14 was synthesised using crossbar, FF-XBAR52 and ARM25-Br and the SEC chromatograms of the starting materials and crude product are presented in Figure 4.22.

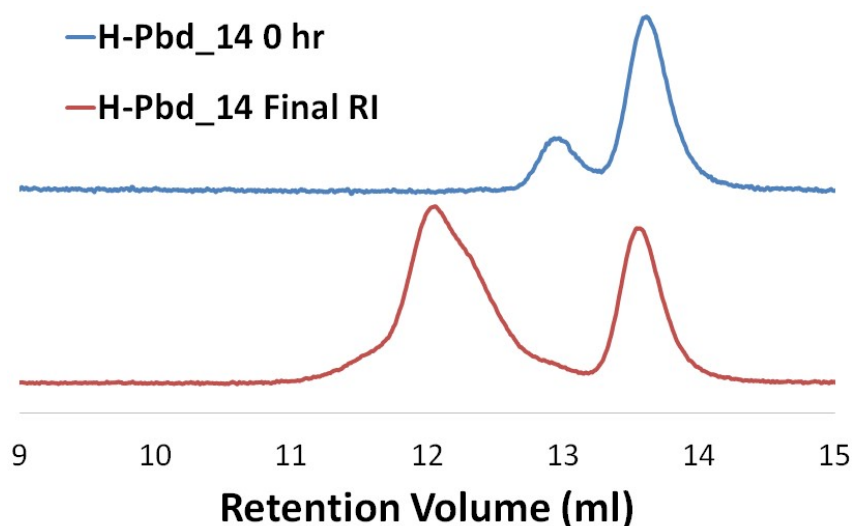


Figure 4.22 - SEC chromatograms (RI and RALS detectors) of polymer H-Pbd_14 (FF-XBAR52 and ARM25-Br). Reaction conditions: 7 equivalents arm : crossbar; 50 equivalents cesium carbonate : crossbar. Comparison of the samples between the start (0 hr) and end of reaction.

The data in Figure 4.22 suggests that these conditions have been successful with the broad peak between 11 and 13 ml indicating that the majority of product present in the final crude polymer is that of the mixture of coupled products. Measuring the area under the RI (concentration) curve reveals that 67% of the polymer is coupled, the highest percentage obtained of any reaction so far. The use of a different macromonomer, ARM25-Br may have also contributed to the increased amount of coupling, as NP-IIC analysis confirmed that 92% of the chains in this sample were end-capped compared to ARM23-Br (85% end-capped). RP-TGIC analysis was carried out on H-Pbd_14 to determine the extent of by-product formation and the chromatogram is given in Figure 4.23.

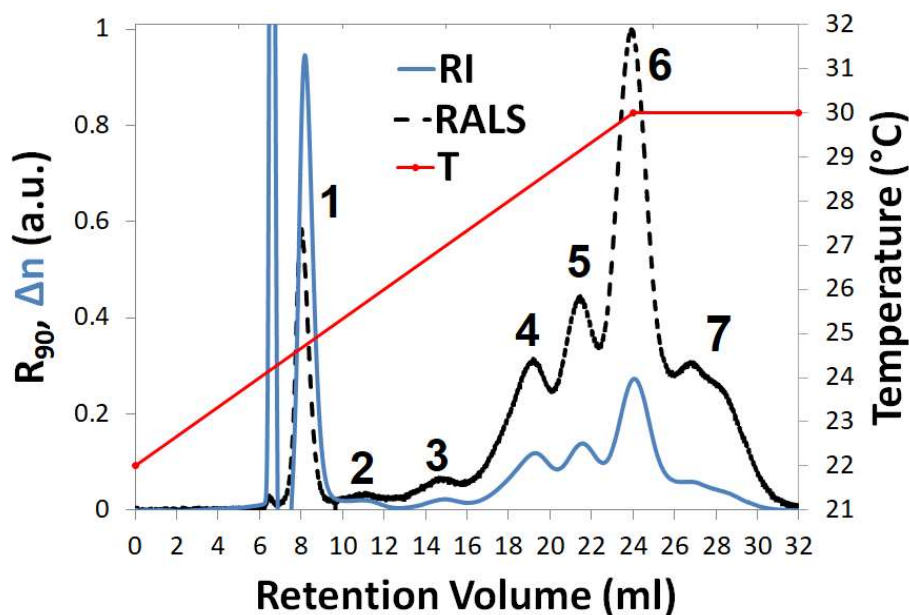


Figure 4.23 - TGIC chromatograms of polymer H-Pbd_14 recorded with RI and RALS detectors. TGIC samples were analysed in 1,4-dioxane at a flow rate of 0.4 ml/min. Temperature profile is shown on the plot.

Once again, when compared to SEC, TGIC (Figure 4.23) reveals much more quantifiable information about the complex mixture of products. The solvent peak is detected at 6.7 ml, with the unreacted arm peak (peak 1) at 8.2 ml and the unconsumed crossbar peak (peak 2) at 11.0 ml. Peaks 3 – 6 at 14.9 ml, 19.3 ml, 21.6 ml and 24.1 ml can be ascribed to the crossbar coupled to 1 arm, 2 arms, 3 arms, and the H-polymer respectively. There is again evidence of higher molecular weight by-product, with a peak (peak 7) at higher retention volume.

Table 4.12 - Molar mass data for H-Pbd_14 obtained by triple detection RP-TGIC analysis (solvent 1,4-dioxane; $dn/dc = 0.095 \text{ ml g}^{-1}$)

H-Pbd_14	Peak # (ml)						
	<u>1</u> (8.2)	<u>2</u> (11.0)	<u>3</u> (14.9)	<u>4</u> (19.3)	<u>5</u> (21.6)	<u>6</u> (24.1)	<u>7</u> (26.0)
$M_n \text{ (g mol}^{-1}\text{)}$	14,600	34,400	118,200	100,100	126,000	142,900	241,900
$M_w \text{ (g mol}^{-1}\text{)}$	20,000	39,100	118,300	100,200	126,600	146,800	244,900
\bar{D}	1.373	1.137	1.001	1.001	1.005	1.027	1.012
Total RI Area (%)	37	2	2	14	12	27	7

Molecular weight analysis was conducted based on the TGIC data and the results are presented in Table 4.12. Peak 6 (H-shaped polymer) should have a theoretical M_n value of *ca.* 144,000 g mol^{-1} and the value obtained of 142,900 g mol^{-1} confirms that this peak

represents the desired product. The experimental M_n for peak 4 (100,100 g mol⁻¹) and peak 5 (126,000 g mol⁻¹) also closely match their expected M_n values (*ca.* 100,000 g mol⁻¹ and *ca.* 127,000 g mol⁻¹ respectively), whereas the M_n values of peaks 1 and 2 are slightly lower than their corresponding macromonomers. However, for peak 3 the M_n obtained (118,200 g mol⁻¹) is much higher than what was expected for its by-product of one arm coupled to crossbar (M_n *ca.* 77,300 g mol⁻¹). As stated earlier, molecular weight calculations are more susceptible to error in TGIC compared to SEC due to the use of a temperature gradient, which causes baseline instability in the RI (concentration) signal and can also affect the dn/dc value for polymers. The mass fraction (as a %) of the various components of H-Pbd_14 was also calculated. As expected the amount of unreacted arm still represents a major fraction of the polymer at 37%, but for peak 6, a fraction of 27% was obtained, indicating that the final H-polymer is present in a good amount.

Hitherto, all reactions have been carried out on a relatively small scale (1 - 4 g). The main aim of the previous reactions was to improve the operating reaction conditions and IC methodology for the synthesis and analysis of H-shaped polybutadienes by the macromonomer approach. It has been shown that the synthesis of H-polymers is feasible by this route, but the degree of coupling was not altogether successful, resulting in the generation of a mixture of partially coupled products, alongside the desired H-polymer. Although the macromonomer approach allows for the synthesis of a homologous series of H-shaped polymers, with identical molar mass linear segments, a distinct advantage over more traditional routes, the incomplete coupling means that the synthesis needs to be scaled up to allow enough H-shaped polymer to be recovered by fractionation. This first required the re-synthesis of the macromonomers on a larger scale (*ca.* 30 - 50 g), followed by larger scale coupling reactions which proved to be more challenging than anticipated.

4.2.3 Synthesis of H-shaped polymers - Large Scale Synthesis

4.2.3.1 Initial attempts

Based on the previous results it was decided to scale up by using the exact same reaction conditions as used in the synthesis of H-Pbd_14, including the use of the same crossbar (FF-XBAR52) and arm (ARM25-Br) macromonomers. This reaction was carried out with the aim of generating enough of the crude H-polymer to allow for the production of a few grams of purified H-polymer after fractionation. Polymer H-Pbd_15 was synthesised (on a

30 g gram scale) and SEC and RP-TGIC analysis were conducted on the resulting polymer mixture – see below in Figure 4.24.

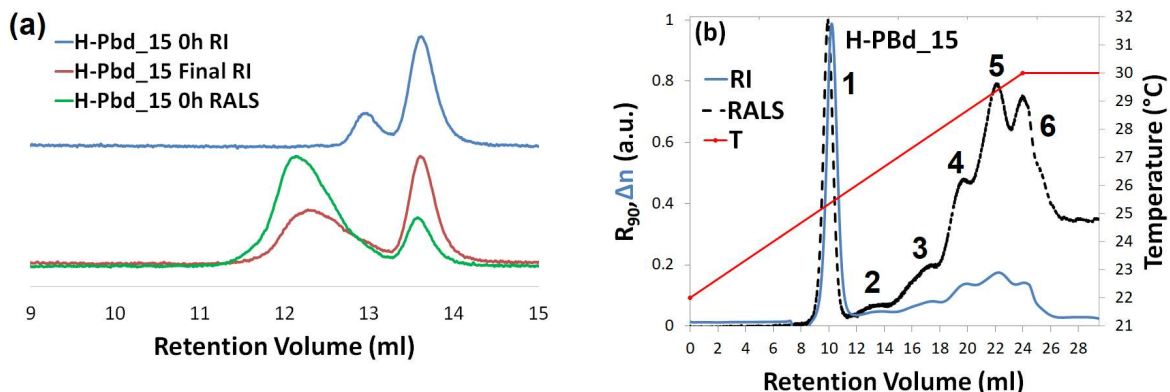


Figure 4.24 - SEC (a) and RP-TGIC (b) chromatograms of H-Pbd_15 (FF-XBAR52, ARM25-Br) recorded with RI and RALS detectors. Reaction conditions: 7 equivalents arm : crossbar; 50 equivalents cesium carbonate : crossbar. TGIC analysis was carried out in 1,4-dioxane at a flow rate of 0.4 ml/min. Temperature profile is shown on the plot.

Table 4.13 - Molar mass data for H-Pbd_15 obtained by triple detection RP-TGIC analysis (solvent 1,4-dioxane; $dn/dc = 0.095 \text{ ml g}^{-1}$)

H-Pbd_15	Peak # (ml)					
	<u>1</u>	<u>2</u>	<u>3</u>	<u>4</u>	<u>5</u>	<u>6</u>
	(10.2)	(13.3)	(17.4)	(19.9)	(22.2)	(24.1)
$M_n \text{ (g mol}^{-1}\text{)}$	15,100	51,000	72,500	95,900	116,100	145,400
$M_w \text{ (g mol}^{-1}\text{)}$	22,400	51,100	72,700	96,000	116,200	145,600
\bar{D}	1.482	1.002	1.003	1.001	1.001	1.001
Total RI Area (%)	49	4	9	11	17	10

The SEC analysis (Figure 4.24a) indicates that although coupling has been achieved, it was not achieved to the same extent as for H-Pbd_14 (Figure 4.23). RP-TGIC analysis resulted in a relatively familiar chromatogram, although there is much peak overlap in this instance. As it can be seen in (Figure 4.24b), six peaks were detected. Peaks 1 and 2 at 10.2 ml and 13.3 ml are of the unreacted arm and crossbar respectively. Peaks 3 - 6 at 17.4 ml, 19.9 ml, 22.2 ml and 24.1 ml represent the expected series of partially and fully coupled products. Molar mass data for the sample were calculated and are presented in Table 4.13, although the light scattering baseline drift undoubtedly introduced some error into the data. The molar mass of peaks 3 - 6 are broadly in line with the predicted values for the expected products and peak 6 has an M_n of 145,400 g mol^{-1} , which is only slightly lower than the theoretical value for the H-polymer (ca. 152,000 g mol^{-1}). Peak area analysis (RI

chromatogram) indicated that peak 6 represents about 10% of the final polymer which, although not as high as seen previously, was deemed sufficient to warrant purifying to obtain a sample for rheological analysis.

Unfortunately, subsequent large scale reactions using the previously established, and reasonably successful conditions resulted in polymers with very low degrees of coupling, as evidenced by both SEC and TGIC. The larger scale experiments, conducted on 20 to 30 gram scales consistently failed to achieve the levels of macromonomer coupling seen on a smaller scale regardless of which macromonomers were used, the purity of the cesium carbonate used or the age of the DMAc/THF solution used. The macromonomers were re-characterised to ensure that there had been no loss of functionality, and indeed, when the smaller scale reactions were repeated, the previously observed higher extents of coupling were once again obtained. Two factors were considered as potential reasons for lower coupling on a larger scale. The first was the mixing efficiency of the overhead mechanical stirrer. As stated previously, if the cesium carbonate is not homogeneously dispersed throughout the reaction mixture, coupling efficiency is lowered. In these larger scale reactions, it was noted that the mechanical stirrer was unable to provide adequate mixing of cesium carbonate in the larger reaction flasks. The paddles used in the mechanical stirring may have not been sufficient to provide mixing in the larger flasks. In an attempt to overcome this issue, the reaction procedure was modified in two ways – firstly the solution concentration was lowered from 10 wt% to 5 wt% to reduce solution viscosity and aid mixing, and the stirring was switched from using mechanical stirring to magnetic stirring. There was a concern that lowering the concentration would reduce the rate of the coupling reaction, but nonetheless, it was decided that it was worth pursuing in order to ensure coupling. Another concern was that the use of magnetic stirring rather than mechanical stirring would result in the case of local stirring in the reaction flask rather than involving the entire mixture. However, mechanical stirring with each of the previous scale up attempts was inefficient hence the switch was seen as worthwhile.

Four further large scale reactions were carried out (15 – 30 g) using a 5 wt% solution in DMAc/THF (50/50 v/v), with 50 mol equivalents of Cs_2CO_3 (relative to crossbar) at 60 °C. H-Pbd_16 and H-Pbd_17 both used crossbar EC-XBAR32; H-Pbd_18 and H-Pbd_19 both used crossbar FF-XBAR53. Each crossbar was reacted with both ARM19-Br (H-Pbd_16 and H-Pbd_18) and ARM40-Br (H-Pbd_17 and H-Pbd_19) and reactions were deemed complete when no further coupling was detected by SEC. The SEC chromatograms of the four

polymers and molecular weight data are presented in Figure 4.25 and Table 4.14 respectively.

Table 4.14 - Molar mass data for the large scale synthesis of polymers H-Pbd_16, H-Pbd_17, H-Pbd_18 and H-Pbd_19 via a Williamson coupling reaction

Code	Crossbar	Arm	H-polymer theoretical M_{nTHEO} (g mol ⁻¹)	Coupled peak M_n (g mol ⁻¹)	Coupled peak M_w (g mol ⁻¹)	\bar{D}	Coupled peak RI area (%)
H-Pbd_16	EC-XBAR32	ARM19-Br	109,700	119,200	197,700	1.66	64
H-Pbd_17	EC-XBAR32	ARM40-Br	194,100	140,400	182,700	1.30	35
H-Pbd_18	FF-XBAR53	ARM19-Br	129,200	122,000	226,000	1.85	57
H-Pbd_19	FF-XBAR53	ARM40-Br	213,600	179,200	238,100	1.32	52

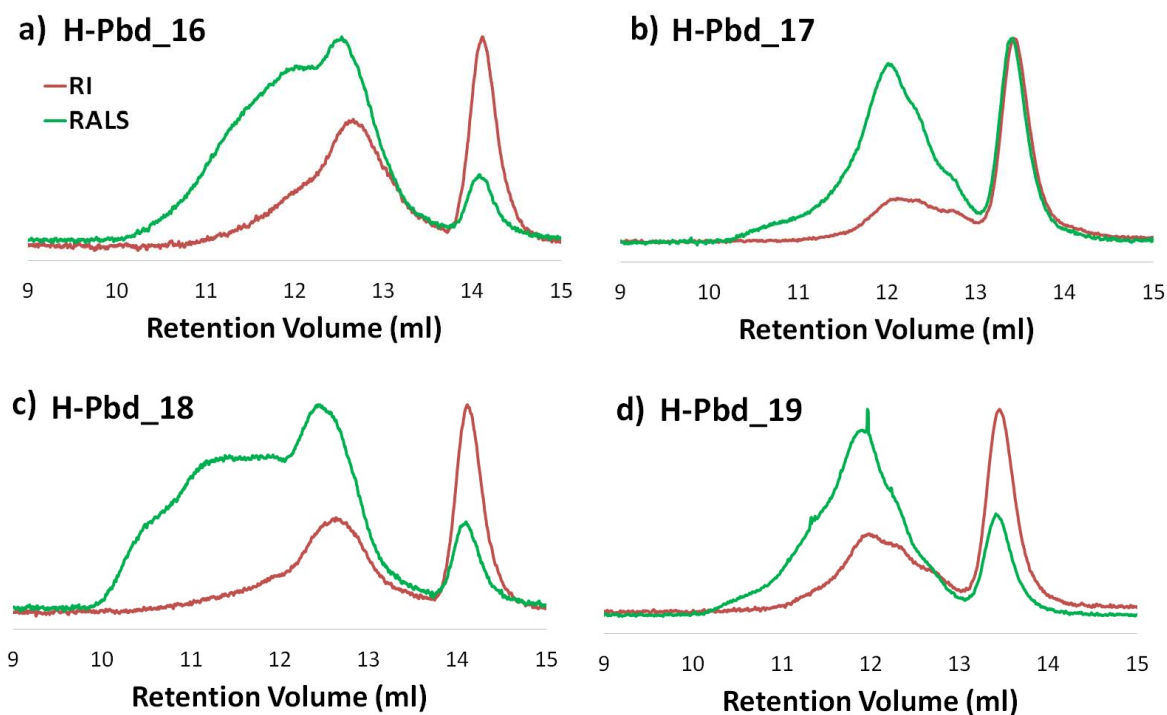


Figure 4.25 - SEC chromatograms (RI and RALS detectors) of polymers: (a) H-Pbd_16, (b) H-Pbd_17, (c) H-Pbd_18 and (d) H-Pbd_19 via a Williamson coupling reaction. Reaction conditions: 7 equivalents arm : crossbar; 50 equivalents cesium carbonate : crossbar.

From the SEC chromatograms presented in Figure 4.25 it can be seen that in each case chain coupling has occurred to a greater or lesser extent, although for H-Pbd_17, the degree of coupling is rather more modest than for H-Pbd_16, H-Pbd_18 and H-Pbd_19. Measurements of the RI area for the three more successful reactions indicate that at least 50% of the product mixture consisted of coupled polymer, whereas for H-Pbd_17 only 35%

of the polymer was coupled. Molecular weights of the high molar mass, coupled product only, for each sample are reported in Table 4.14, as is the theoretical M_n of the desired H-polymer. The molar mass values obtained for H-Pbd_16 and H-Pbd_18 are in fair agreement with their predicted H-polymer M_n values, however, for H-Pbd_17, both the obtained M_n (140,400 g mol⁻¹) and M_w (182,700 g mol⁻¹) are lower than the predicted H-polymer molecular weight (M_n 194,100 g mol⁻¹). The dispersity values in all cases also indicate that a mix of products is contained within each sample. For both H-Pbd_16 and H-Pbd_18, the light scattering signal between 10 and 12 ml also suggests the formation of high MW by-products, arising from coupling between polymer chains containing more than two DPE units. RP-TGIC analysis was also carried out on the four polymers and the chromatograms are presented overleaf in Figure 4.26.

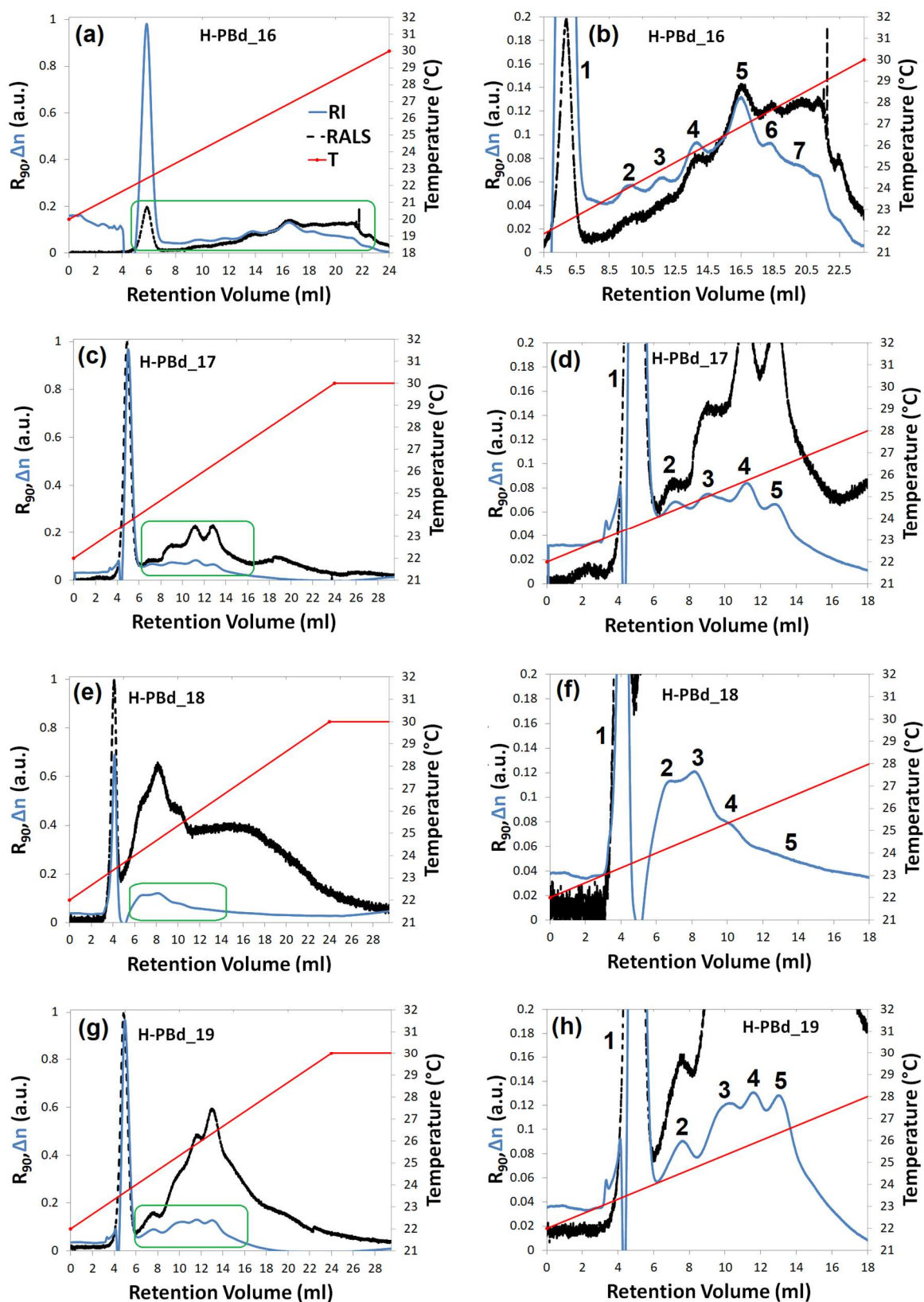


Figure 4.26 - TGIC chromatograms of polymers: (a,b) H-Pbd_16, (c,d) H-Pbd_17, (e,f) H-Pbd_18 and (g,h) H-Pbd_19 recorded with RI and RALS detectors. Expansions of the chromatograms on the left are presented on the right, to better observe the presence of peaks due to coupled products. TGIC samples were analysed in 1,4-dioxane at a flow rate of 0.4 ml/min. Temperature profiles are shown on the plot.

The TGIC chromatograms once again provide more detailed information on the mix of coupled products present in each polymer. Upon expansion of the polymers TGIC chromatograms (Figure 4.26 b d, f, h), the peaks and shoulders present can be more clearly distinguished, and in the case of H-Pbd_18 it is evident that there is much peak overlap.

In the case of H-Pbd_16 (EC-XBAR32, ARM19-Br) and H-PBD_18 (EC-XBAR53, ARM19-Br), the light scattering signal again confirms the existence of high molecular weight by-products as seen in their SEC chromatograms. These higher molecular weight by-product peaks have been seen in previous examples and may be due to coupling reactions involving the linear arms and a presence of crossbar polymer chains with more than two DPE units per chain. However, it can be seen from the RI signals, which are proportional to concentration, that these elements may not be present at high levels. In order to identify and quantify which peaks corresponded to the desired H-polymers, molecular weight analysis and peak area estimations were carried out using the RI signal for H-Pbd_16 to H-PBD_19 and the results are summarised in Table 4.15 to Table 4.18 respectively.

The instability of the RI baseline introduced some error into the molecular weight calculations, however, the obtained MW data supported the existence of the H-shaped polymer in each sample; the theoretical M_n for each sample is included in the tables below and the peak identified as the H-shaped polymer is highlighted in red text. In the TGIC chromatogram for H-Pbd_16 peak 5 (M_n 106,200 g mol⁻¹) was identified as the H-polymer due to its agreement with the theoretical H-polymer molecular weight. Peak 5 was also classified as the H-polymer for both H-Pbd_17 (EC-XBAR32, ARM40-Br) (Peak 5 M_n = 198,100 g mol⁻¹) and H-Pbd_19 (EC-XBAR53, ARM40-Br) (Peak 5 M_n = 215,200 g mol⁻¹). Due to the level of peak overlap in H-Pbd_18, peak 4 was identified as the H-polymer (Peak 4 M_n = 138,100 g mol⁻¹). There was no peak observed for the product of one arm attached to the crossbar, which would have had a theoretical M_n of 72,100 g mol⁻¹, however, this species may have been obscured due to overlap with the solvent peak at 5.0 ml. Peak area estimations suggest that the H-polymers constituted 17%, 4%, 10% and 13% of polymers H-Pbd_16, 17, 18 and 19 respectively.

RP-TGIC analysis indicated that the proportion of the product mixture which was the desired H-polymer was somewhat more modest than hoped. However, polymers H-Pbd_16, H-Pbd_18 and H-Pbd_19 were taken forward along with H-Pbd_15 (FF-XBAR52, ARM25-Br) for purification by fractionation. Due to the low degree of both coupling and

H-polymer present in H-Pbd_17, and concerns that not much material would be left after purification, it was not taken forward from this point.

Table 4.15 - Molar mass data for H-Pbd_16 (EC-XBAR32, ARM19-Br) obtained by triple detection RP-TGIC analysis (solvent 1,4-dioxane; dn/dc = 0.095 ml g⁻¹)

H-Pbd_16	H-polymer M_{nTHEO} (g mol ⁻¹)	Peak # (ml)						
		<u>1</u> (5.8)	<u>2</u> (9.9)	<u>3</u> (11.8)	<u>4</u> (13.8)	<u>5</u> (16.5)	<u>6</u> (18.2)	<u>7</u> (20.1)
M_n (g mol ⁻¹)	109,700	17,200	-	72,900	90,200	106,200	145,700	215,700
M_w (g mol ⁻¹)	-	18,500	-	73,100	90,400	106,300	145,500	237,500
\bar{D}	-	1.076	-	1.002	1.002	1.001	1.003	1.101
Total RI Area (%)	-	52	5	5	8	17	5	9

Table 4.16 - Molar mass data for H-Pbd_17 (EC-XBAR32, ARM40-Br) obtained by triple detection RP-TGIC analysis (solvent 1,4-dioxane; dn/dc = 0.095 ml g⁻¹)

H-Pbd_17	H-polymer M_{nTHEO} (g mol ⁻¹)	Peak # (ml)				
		<u>1</u> (5.0)	<u>2</u> (7.2)	<u>3</u> (9.3)	<u>4</u> (11.3)	<u>5</u> (12.9)
M_n (g mol ⁻¹)	194,100	39,100	77,000	113,900	147,200	198,100
M_w (g mol ⁻¹)	-	41,700	77,100	114,200	147,500	198,600
\bar{D}	-	1.066	1.002	1.002	1.002	1.003
Total RI Area (%)	-	71	7	10	8	4

Table 4.17 - Molar mass data for H-Pbd_18 (EC-XBAR53, ARM19-Br) obtained by triple detection RP-TGIC analysis (solvent 1,4-dioxane; dn/dc = 0.095 ml g⁻¹)

H-Pbd_18	H-polymer M_{nTHEO} (g mol ⁻¹)	Peak # (ml)				
		<u>1</u> (4.1)	<u>2</u> (7.3)	<u>3</u> (8.2)	<u>4</u> (10.1)	<u>5</u> (14.0)
M_n (g mol ⁻¹)	129,200	23,300	86,600	99,500	138,100	258,300
M_w (g mol ⁻¹)	-	23,900	87,200	100,100	139,400	284,100
\bar{D}	-	1.025	1.007	1.006	1.009	1.100
Total RI Area (%)	-	43	15	21	10	10

Table 4.18 - Molar mass data for H-Pbd_19 (EC-XBAR53, ARM40-Br) obtained by triple detection RP-TGIC analysis (solvent 1,4-dioxane; dn/dc = 0.095 ml g⁻¹)

H-Pbd_19	H-polymer M_{nTHEO} (g mol ⁻¹)	Peak # (ml)					
		<u>1</u> (5.0)	<u>2</u> (7.7)	<u>3</u> (10.2)	<u>4</u> (11.7)	<u>5</u> (13.2)	<u>6</u> (15.5)
M_n (g mol ⁻¹)	213,600	40,200	87,500	122,500	166,600	215,200	380,500
M_w (g mol ⁻¹)	-	43,300	87,600	123,100	166,900	216,500	437,000
\bar{D}	-	1.077	1.001	1.005	1.001	1.006	1.149
Total RI Area (%)	-	50	8	14	9	13	6

4.2.3.2 Purification of Large Scale H-shaped polymers

Polymers H-Pbd_15 (FF-XBAR52, ARM25-Br), H-Pbd_16 (EC-XBAR32, ARM19-Br), H-Pbd_18 (EC-XBAR53, ARM19-Br), and H-Pbd_19 (EC-XBAR53, ARM40-Br) were selected for purification by fractionation. Due to the complex nature of the polymers, the objective was to remove the excess low molecular weight arm and any potential high molecular weight by-products still present in the samples that may have adverse effects on their rheology. However, it was expected that the partially coupled products (i.e. the one-arm, two arm and three-arm coupled polymers) would most likely still make up significant portions of the “purified” materials as they are harder to separate due to the very similar molar masses. TGIC was intended to be used to characterise the purified products. Purification was achieved by using toluene/methanol solvent/non-solvent solution fractionation, using SEC to monitor the progress. A full description of the fractionation process is given in section 4.3.4, but to summarize here, the process works by initially dissolving the entire polymer in a dilute solution of toluene, in a separating funnel which is placed in a water bath. Methanol (a non-solvent) is then added slowly, with stirring until the mixture becomes cloudy, at which point the polymer is redissolved by gentle warming of the mixture. The process of adding non-solvent to reach the cloud point, followed by warming to clarify, is repeated over a pre-defined temperature range. The stirrer is then removed and the mixture is allowed to cool down slowly to room temperature resulting in phase-separation leaving a lower fraction which is rich in high molecular weight material which is collected. This process is repeated resulting in multiple fractions for a given cycle (e.g. Series A, fraction A1, A2....). Each subsequent fraction collected has a lower molecular weight than the previous one i.e. fraction A5 will have less high molecular weight material and more low molecular weight material than fraction A1. After a cycle is completed, the

isolated fractions are analysed and then can then be combined with similar molar mass fractions, and the fractionation process repeated to purify the material further. The SEC results are presented for each polymer in the figures below (Figure 4.27 – Figure 4.30). It can be seen from the SEC results that many of the fractions obtained from each polymer still retain a portion of the high molecular weight material, however, the majority of the lower molecular weight unreacted macromonomers have been removed.

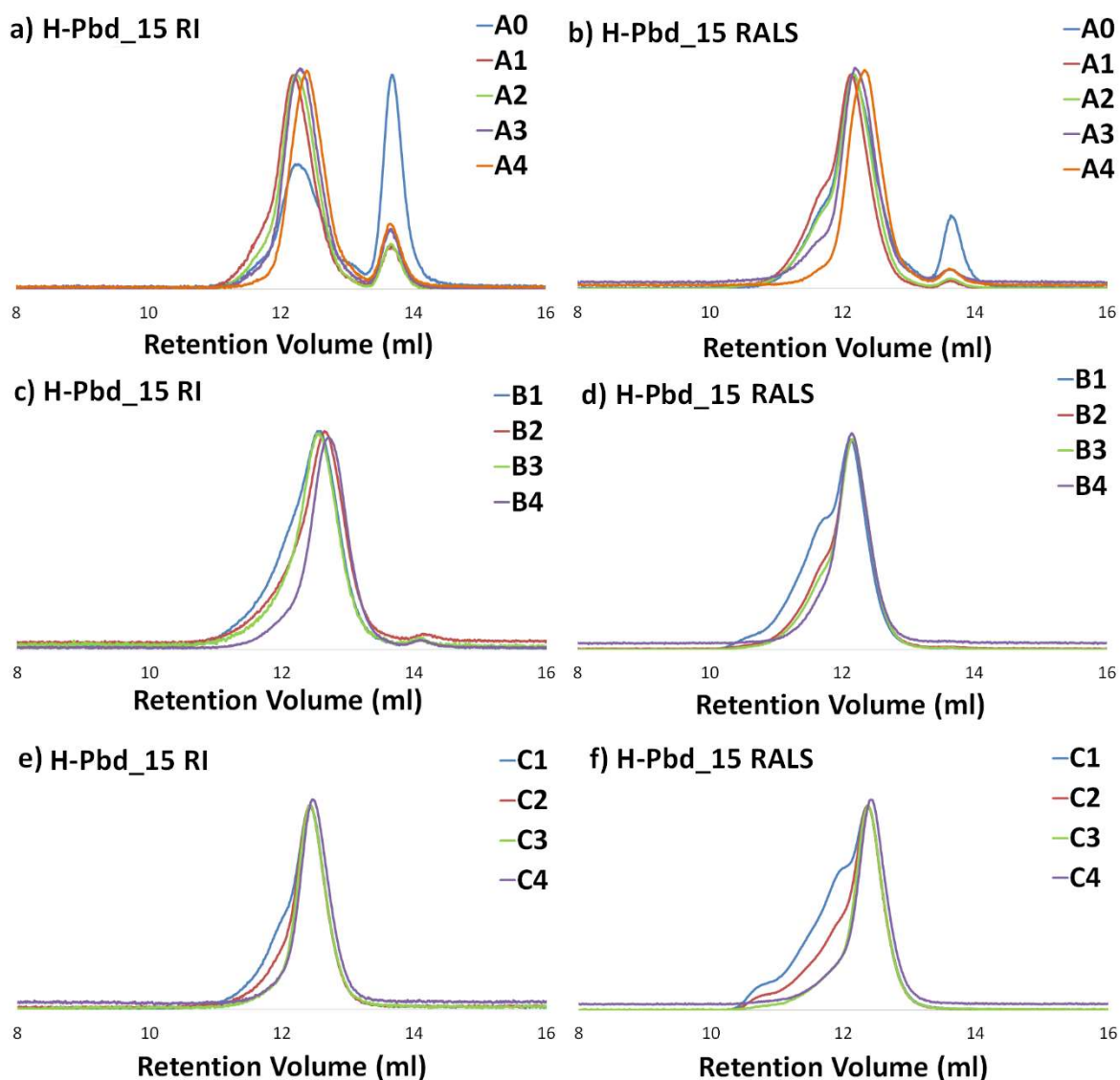


Figure 4.27 - SEC chromatograms (RI and RALS detectors) of H-Pbd_15 through three cycles of fractionation

Polymer H-Pbd_15 (FF-XBAR52, ARM25-Br) underwent three cycles of fractionation, the SEC results of which are given in Figure 4.27. It can be seen that the first fractionation cycle was relatively successful in the removal of a majority of the lower molecular weight excess arm which had been indicated by the sharp peak between 13 – 14 ml. All fractions from the

A-Series (besides A0 which represented the starting crude material) were combined and taken through to the next cycle, where the existence of high molecular weight by-products becomes more apparent in the B-fractions. This is more clearly evidenced in the light scattering SEC chromatograms for the fractions, with fraction B1 in particular containing a high level of impurities. As such B1 was discarded and fractions B2, B3 and B4 were combined and taken through to the final series of fractionation (C-series). The RALS and RI detectors again indicated the existence of higher molecular weight by-products, however, in fractions H-Pbd_15_C3 and H-Pbd_15_C4 (Figure 4.27f), most of the high molar mass impurity had been removed, and the low molecular weight arm had been completely removed. During this process we have found that high molecular weight products are much more difficult to separate out from the desired H-polymer and this proved to be a bigger challenge in the purification of the other large scale polymers.

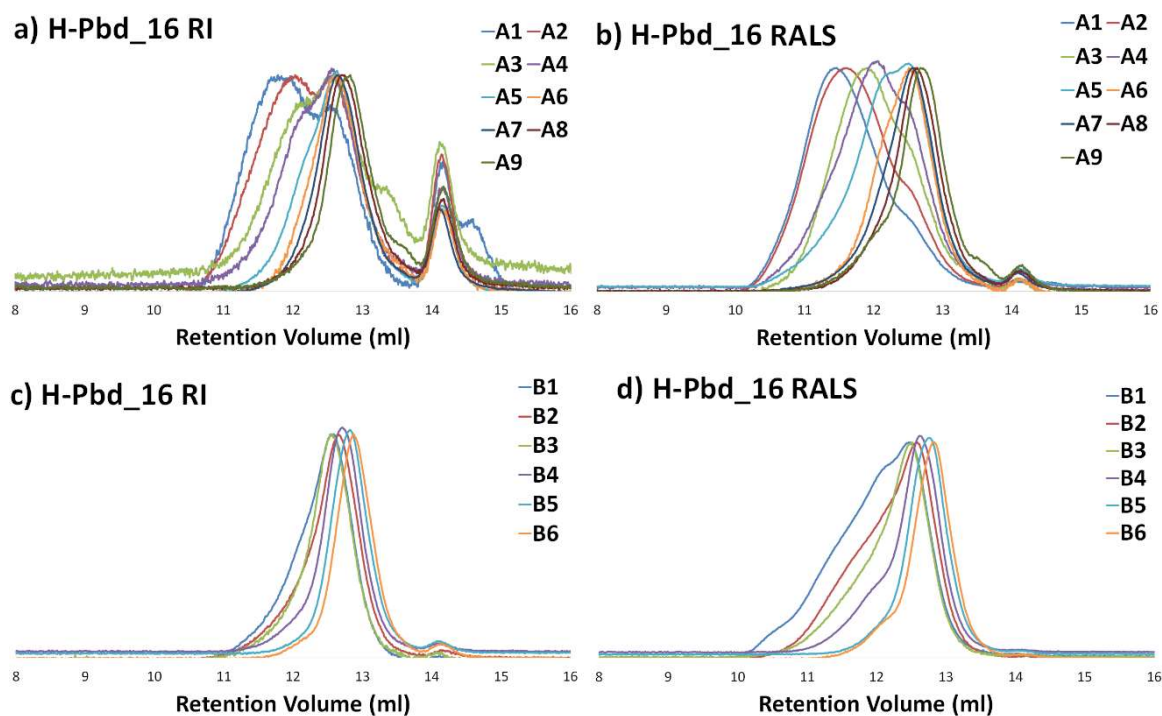


Figure 4.28 - SEC chromatograms (RI and RALS detectors) of H-Pbd₁₆ through two cycles of fractionation
Polymer H-Pbd₁₆ (EC-XBAR32, ARM19-Br) underwent two cycles of fractionation and the SEC chromatograms are shown in Figure 4.28 above. In the first fractionation cycle, there is a large amount of high molecular weight material, and as such the first four fractions (H-Pbd₁₆_A1 to H-Pbd₁₆_A4) were discarded to remove these high molecular weight by-products whilst the remaining fractions were taken forward to the next series of fractionations. This second series removed the majority of lower molecular weight material

(although some was still evident). Fractions H-Pbd_16_B5 and H-Pbd_16_B6 produced the purest samples and were deemed to be the most suitable for rheological testing.

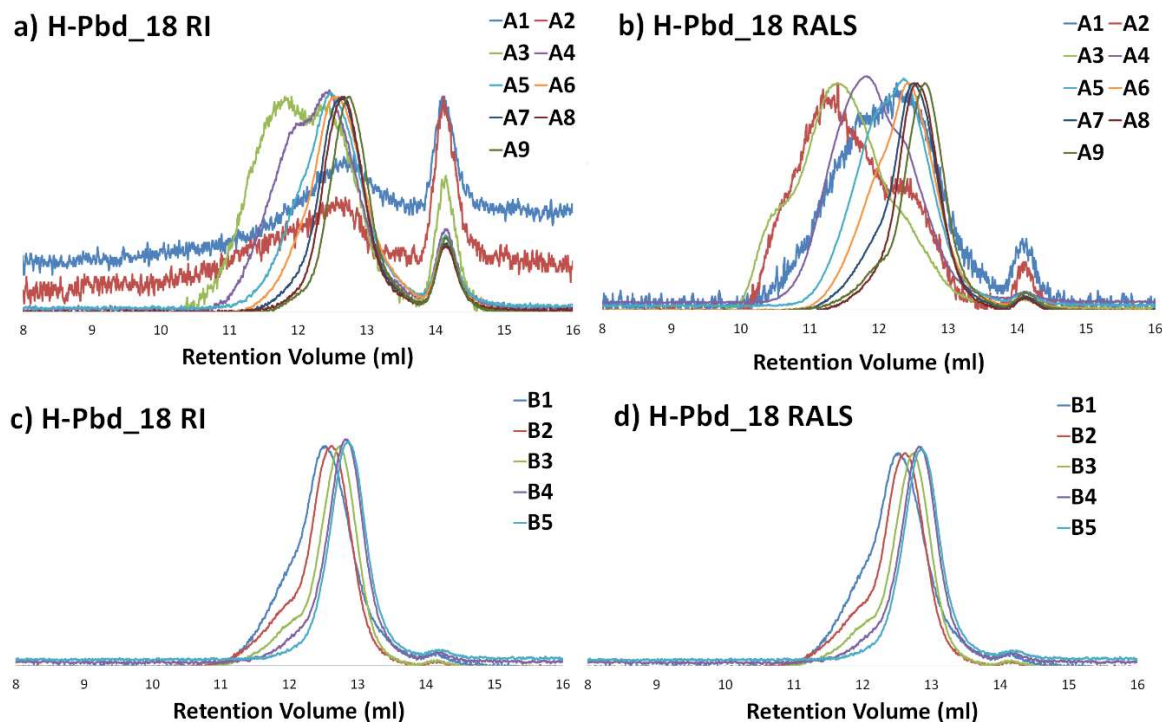


Figure 4.29 - SEC chromatograms (RI and RALS detectors) of H-Pbd_18 through two cycles of fractionation

Polymer H-Pbd_18 (EC-XBAR53, ARM19-Br) underwent two fractionation cycles (Figure 4.29). The presence of high molecular weight material was again noted, and again as for H-Pbd_16, the first four fractions (H-Pbd_18_A1 to H-Pbd_18_A4) were discarded and the remaining fractions taken forward to the next series of fractionations. The RALS chromatograms more clearly illustrated the presence of the high MW impurities, although, the RI chromatograms indicated that they were present in a relatively minor concentrations compared to the overall polymer. The entire series was retained for testing, with H-Pbd_18_B4 and H-Pbd_18_B5 appearing to be the lowest disperse samples obtained. In all fractions there still remained a slight trace of lower molecular weight arm.

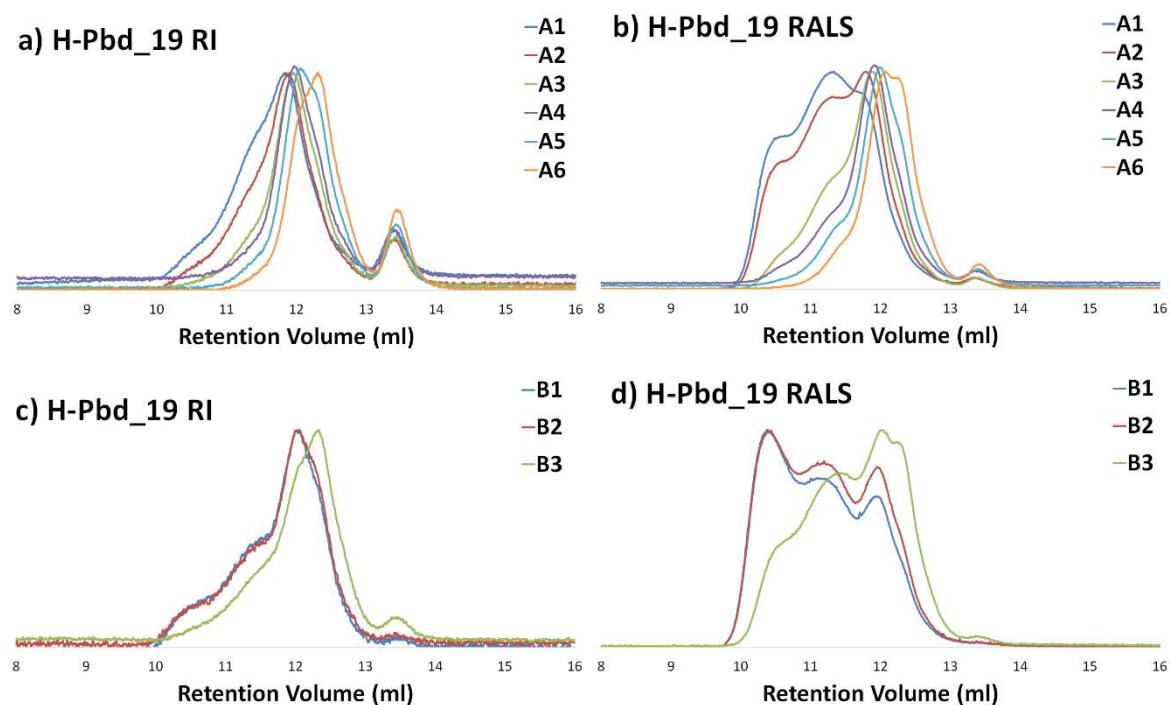


Figure 4.30 - SEC chromatograms (RI and RALS detectors) of H-Pbd_19 through two cycles of fractionation

Polymer H-Pbd_19 (EC-XBAR53, ARM40-Br) underwent two cycles of fractionation (Figure 4.30). This polymer, which has the lowest degree of coupling of all the large scale polymerisations, proved the most difficult to purify, with all fractions obtained in both series containing large amounts of impurities. This series of fractions was retained but the mixtures remain highly complex. Molar mass data on the complete series of final fractions following purification are given overleaf in Table 4.19. The theoretical H-polymer M_n for each sample is included in the tables below and the fractions identified as pure enough for rheological testing are highlighted in red text. The molar mass data of the crude large scale H-shaped polymers is also presented here for comparison. Table 4.19 shows that the dispersity values of the fractions obtained for all samples have been reduced from their crude starting materials, with the exception of H-Pbd_19, which still recorded high MW and dispersity values. What is also interesting to note is that the purest samples (based on the dispersity value) also have M_n values lower than the target M_n of what would be expected of the fully coupled H-shaped polymer (M_{nTHEO}). It is very likely that the “pure” fractions still retain some amount of partially coupled “impurities” i.e. 2-arms and 3-arm coupled by-products, which may be lowering the overall MW of the samples.

Table 4.19 - Molar mass data for the initial crude polymer and the final series of fractionations for large scale polymers H-Pbd_15, H-Pbd_16 H-Pbd_18 and H-Pbd_19 (solvent THF; $dn/dc = 0.124 \text{ ml g}^{-1}$)

H-Pbd_15				
Fraction	$M_n (\text{g mol}^{-1})$	$M_w (\text{g mol}^{-1})$	\bar{D}	$M_{n\text{THEO}} (\text{g mol}^{-1})$
H-Pbd_15_Crude	30,400	82,900	2.73	152,000
H-Pbd_15_C1	165,300	206,100	1.25	152,000
H-Pbd_15_C2	149,000	175,500	1.17	152,000
H-Pbd_15_C3	132,600	148,200	1.12	152,000
H-Pbd_15_C4	136,400	150,100	1.10	152,000
H-Pbd_16				
Fraction	$M_n (\text{g mol}^{-1})$	$M_w (\text{g mol}^{-1})$	\bar{D}	$M_{n\text{THEO}} (\text{g mol}^{-1})$
H-Pbd_16_Crude	76,700	133,600	1.74	109,700
H-Pbd_16_B1	139,700	192,700	1.38	109,700
H-Pbd_16_B2	129,400	168,700	1.30	109,700
H-Pbd_16_B3	129,600	121,700	1.25	109,700
H-Pbd_16_B4	114,000	127,500	1.12	109,700
H-Pbd_16_B5	87,400	97,500	1.12	109,700
H-Pbd_16_B6	87,800	97,700	1.11	109,700
H-Pbd_18				
Fraction	$M_n (\text{g mol}^{-1})$	$M_w (\text{g mol}^{-1})$	\bar{D}	$M_{n\text{THEO}} (\text{g mol}^{-1})$
H-Pbd_18_Crude	73,900	143,300	1.94	129,200
H-Pbd_18_B1	127,000	164,800	1.29	129,200
H-Pbd_18_B2	125,200	159,000	1.27	129,200
H-Pbd_18_B3	71,500	90,200	1.26	129,200
H-Pbd_18_B4	93,500	104,800	1.12	129,200
H-Pbd_18_B5	88,000	96,900	1.10	129,200
H-Pbd_19				
Fraction	$M_n (\text{g mol}^{-1})$	$M_w (\text{g mol}^{-1})$	\bar{D}	$M_{n\text{THEO}} (\text{g mol}^{-1})$
H-Pbd_19_Crude	69,400	141,800	2.04	213,600
H-Pbd_19_B1	283,000	623,000	2.20	213,600
H-Pbd_19_B2	263,800	595,700	2.25	213,600
H-Pbd_19_B3	193,900	258,100	1.33	213,600

Fractionation is unable to remove these by-products due to their similarity in molecular weight to both themselves and the desired H-polymer. Unfortunately attempts to carry out RP-TGIC analysis on the “purified” samples proved unsatisfactory and resulted in chromatograms that did not reveal additional level of detail beyond that revealed by SEC. Given more time, it is hoped that these samples can be satisfactorily submitted for further RP-TGIC analysis to provide detail on the nature and quantity of any remaining structural heterogeneity.

4.3 Experimental

4.3.1 Materials

Tetrahydrofuran (in house purification) was dried over sodium wire and benzophenone (Sigma-Aldrich, 99%), degassed over calcium hydride and stored under high vacuum. The solvent was degassed by a number of freeze-pump-thaw and freshly distilled prior to use. Cesium carbonate (99.995%) and *N,N,N',N'*-tetramethylethylenediamine (TMEDA) (both Sigma-Aldrich) were used as received. *N,N*-dimethylformamide (anhydrous, 99.8%) and *N,N*-dimethylacetamide (DMAC) (Acros Organics, 99.5%, Extra Dry) were used as received. Tetrahydrofuran and methanol (both AR grade) (both Fischer Scientific) were used as received. 1,4-dioxane (HPLC grade, Fischer Scientific) was used as received.

4.3.2 Characterisation

4.3.2.1 Nuclear Magnetic Resonance (NMR)

¹H-NMR spectra were measured on a Varian VNMRs 700 MHz or Bruker DRX-400 MHz spectrometer using CDCl₃ as the solvent.

4.3.2.2 Size Exclusion Chromatography (SEC)

Triple detection size exclusion chromatography (SEC) was carried out for the analysis of molecular weight and dispersity of the synthesised polymers, using a Viscotek TDA 302 with refractive index, right angle light scattering (RALS – 690 nm) and viscosity detectors and two PLgel 5 µm mixed C columns (300×75 mm). Tetrahydrofuran was used as the eluent at a flow rate of 1.0 ml/min and at a temperature of 35 °C. The calibration was carried out with a single narrow distribution polystyrene standard purchased from Polymer Laboratories. A value of 0.124 mL/g (measured in house) was used as the dn/dc of polybutadiene for the analysis of prepared polymers.

4.3.2.3 Temperature Gradient Interaction Chromatography (TGIC)

Temperature gradient interaction chromatography analysis was carried out in reversed-phase conditions. Polymer solution concentrations of approximately 4 mg/ml dissolved in the eluent mixture were used and the injection volume was 100 µl. Reversed-phase temperature gradient interaction chromatography (RP-TGIC) analysis was carried out using a single C18 bonded silica column (Nucleosil C18, 100 Å pore 250×4.6 mm I.D., 5 µm or Nucleosil C18, 300 Å pore 250×4.6 mm I.D., 5 µm). 1,4-dioxane was used as the eluent at a flow rate of 0.40 ml/min. The RP-TGIC system used a modified Viscotek TDA 302 with

refractive index, viscosity, RALS detectors (Viscotek) and an external UV detector (Knauer). The temperature of the column in both systems was controlled by a Thermo Scientific thermostatically controlled circulating bath. A value of 0.095 mL/g was used as the dn/dc of polybutadiene which was obtained from a previous report.²²

4.3.3 Synthesis

All Williamson coupling reactions carried out during this work utilised the same general procedure, but with varying amounts of macromonomer, solvents and reagents. Any extra steps taken are detailed in that polymer's synthetic description.

4.3.3.1 Synthesis of H-Pbd_1

To a three-necked 250 ml flask, equipped with a reflux condenser and overhead mechanical stirrer, "crossbar" FF-XBAR29 (1.03 g, 0.020 mmol), brominated "arm" ARM31-Br (3.16 g, 0.105 mmol), and cesium carbonate (Cs_2CO_3) (0.066 g, 0.20 mmol) were dissolved in vacuum distilled dry THF (20 ml). Dry dimethylformamide (DMF) (20 ml) was then added to this solution and the reaction was heated with an oil bath to 60°C, with the progress followed by SEC and stopped when no further change in molecular weight was recorded. The polymer was precipitated into methanol, dissolved in THF, precipitated again into methanol, collected by filtration and dried under vacuum. Yield 57%.

H-Pbd_1: Yield 57%; M_n 32,600 g mol⁻¹, M_w 41,400 g mol⁻¹, Đ 1.27.

4.3.3.2 Synthesis of H-Pbd_2

H-Pbd_2 was prepared according to the procedure described in 4.3.3.1. Crossbar FF-XBAR52 (0.52 g, 0.015 mmol), brominated "arm" ARM31-Br (1.68 g, 0.053 mmol), and cesium carbonate (Cs_2CO_3) (0.036 g, 0.11 mmol) were dissolved in dry THF (12 ml) and 12 ml dry DMF (12 ml). Yield 71%.

H-Pbd_2: M_n 47,500 g mol⁻¹, M_w 75,500 g mol⁻¹, Đ 1.57.

4.3.3.3 Synthesis of H-Pbd_3

H-Pbd_3 was prepared according to the procedure described in 4.3.3.1. Crossbar FF-XBAR100 (0.5 g, 0.0049 mmol), brominated "arm" ARM31-Br (0.77 g, 0.024 mmol), and cesium carbonate (Cs_2CO_3) (0.017 g, 0.049 mmol) were dissolved in dry THF (7 ml) and dry DMF (7 ml). Yield 72%.

H-Pbd_3: M_n 41,500 g mol⁻¹, M_w 70,000 g mol⁻¹, Đ 1.69.

4.3.3.4 Synthesis of H-Pbd_4

H-Pbd_4 was prepared according to the procedure described in 4.3.3.1. Crossbar FF-XBAR29 (1.03 g, 0.020 mmol), brominated “arm” ARM31-Br (3.15 g, 0.105 mmol), and cesium carbonate (Cs_2CO_3) (0.067 g, 0.20 mmol) were dissolved in dry THF (7 ml) and dry DMAc (7 ml). Yield 78%.

H-Pbd_4: M_n 34,000 g mol⁻¹, M_w 37,000 g mol⁻¹, Đ 1.10.

4.3.3.5 Synthesis of H-Pbd_5

H-Pbd_5 was prepared according to the procedure described in 4.3.3.1. H-Polymer 5 was prepared according to the procedure described above in 4.14.1. Crossbar FF-XBAR52 (0.50 g, 0.010 mmol), brominated “arm” ARM31-Br (1.71 g, 0.054 mmol), and cesium carbonate (Cs_2CO_3) (0.034 g, 0.10 mmol) were dissolved in dry THF (12 ml) and dry DMAc (12 ml). Yield 72%.

H-Pbd_5: M_n 53,200 g mol⁻¹, M_w 87,800 g mol⁻¹, Đ 1.65.

4.3.3.6 Synthesis of H-Pbd_6

H-Pbd_6 was prepared according to the procedure described in 4.3.3.1. Crossbar FF-XBAR100 (0.50 g, 0.0050 mmol), brominated “arm” ARM31-Br (0.84 g, 0.027 mmol), and cesium carbonate (Cs_2CO_3) (0.020 g, 0.050 mmol) were dissolved in dry THF (7 ml) and dry DMAc (7 ml). Yield 42%.

H-Pbd_6: M_n 52,200 g mol⁻¹, M_w 113,700 g mol⁻¹, Đ 2.18.

4.3.3.7 Synthesis of H-Pbd_7

H-Pbd_7 was prepared according to the procedure described in 4.3.3.1. Crossbar FF-XBAR29 (0.18 g, 0.0058 mmol), brominated “arm” ARM31-Br (0.91 g, 0.029 mmol), and cesium carbonate (Cs_2CO_3) (0.020 g, 0.058 mmol) were dissolved in dry THF (20 ml) and dry DMAc (20 ml). Yield 79%.

H-Pbd_7: M_n 53,500 g mol⁻¹, M_w 98,400 g mol⁻¹, Đ 1.84.

4.3.3.8 Synthesis of H-Pbd_8

H-Pbd_8 was prepared according to the procedure described in 4.3.3.1. Crossbar FF-XBAR52 (0.52 g, 0.010 mmol), brominated “arm” ARM31-Br (1.68 g, 0.053 mmol), and

cesium carbonate (Cs_2CO_3) (0.036 g, 0.11 mmol) were dissolved in dry THF (12 ml) and dry DMAc (12 ml). Yield 70%.

H-Pbd_8: M_n 44,300 g mol⁻¹, M_w 81,100 g mol⁻¹, \bar{D} 1.83.

4.3.3.9 Synthesis of H-Pbd_9

H-Pbd_9 was prepared according to the procedure described in 4.3.3.1. Crossbar FF-XBAR100 (0.45 g, 0.0045 mmol), brominated “arm” ARM31-Br (0.98 g, 0.031 mmol), and cesium carbonate (Cs_2CO_3) (0.020 g, 0.062 mmol) were dissolved in dry THF (8 ml) and dry DMAc (8 ml). Yield 72%.

H-Pbd_9: M_n 44,300 g mol⁻¹, M_w 81,100 g mol⁻¹, \bar{D} 1.83.

4.3.3.10 Synthesis of H-Pbd_10

H-Pbd_10 was prepared according to the procedure described in 4.3.3.1. Crossbar FF-XBAR52 (0.50 g, 0.0095 mmol), brominated “arm” ARM23-Br (2.38 g, 0.095 mmol), and cesium carbonate (Cs_2CO_3) (0.031 g, 0.095 mmol) were dissolved in dry THF (15 ml) and dry DMAc (15 ml). Yield 73%.

H-Pbd_10: M_n 36,500 g mol⁻¹, M_w 80,700 g mol⁻¹, \bar{D} 2.21.

4.3.3.11 Synthesis of H-Pbd_11

H-Pbd_11 was prepared according to the procedure described in 4.3.3.1. Crossbar FF-XBAR52 (0.50 g, 0.0095 mmol), brominated “arm” ARM23-Br (1.66 g, 0.066 mmol), and cesium carbonate (Cs_2CO_3) (0.031 g, 0.095 mmol) were dissolved in dry THF (10 ml) and dry DMAc (10 ml). Yield 77%.

H-Pbd_11: M_n 36,400 g mol⁻¹, M_w 65,500 g mol⁻¹, \bar{D} 1.80.

4.3.3.12 Synthesis of H-Pbd_12

H-Pbd_12 was prepared according to the procedure described in 4.3.3.1. Crossbar FF-XBAR29 (0.50 g, 0.0017 mmol), brominated “arm” ARM23-Br (4.28 g, 0.017 mmol), and cesium carbonate (Cs_2CO_3) (0.28 g, 0.86 mmol) were dissolved in dry THF (24 ml) and dry DMAc (24 ml). Yield 74%.

H-Pbd_12: M_n 49,600 g mol⁻¹, M_w 100,500 g mol⁻¹, \bar{D} 2.02.

4.3.3.13 Synthesis of H-Pbd_13

H-Pbd_13 was prepared according to the procedure described in 4.3.3.1. Crossbar FF-XBAR52 (0.57 g, 0.0011 mmol), brominated “arm” ARM23-Br (2.71 g, 0.11 mmol), and cesium carbonate (Cs_2CO_3) (0.18 g, 0.54 mmol) were dissolved in dry THF (16 ml) and dry DMAc (16 ml). Yield 72%

H-Pbd_13: M_n 79,200 g mol⁻¹, M_w 131,400 g mol⁻¹, \bar{D} 1.66.

4.3.3.14 Synthesis of H-Pbd_14

H-Pbd_14 was prepared according to the procedure described in 4.3.3.1. Crossbar FF-XBAR52 (0.45 g, 0.0076 mmol), brominated “arm” ARM25-Br (1.33 g, 0.053 mmol), and cesium carbonate (Cs_2CO_3) (0.12 g, 0.38 mmol) were dissolved in dry THF (8 ml) and dry DMAc (8 ml). Yield 77%

H-Pbd_14: M_n 57,500 g mol⁻¹, M_w 112,300 g mol⁻¹, \bar{D} 1.95.

4.3.3.15 Synthesis of H-Pbd_15

H-Pbd_15 was prepared according to the procedure described in 4.3.3.1, substituting the 250 ml reaction flask for a 500 ml three-necked flask. Crossbar FF-XBAR52 (4.0 g, 0.079 mmol), brominated “arm” ARM23-Br (13.5 g, 0.055 mmol), and cesium carbonate (Cs_2CO_3) (1.30 g, 3.97 mmol) were dissolved in dry THF (90 ml) and dry DMAc (90 ml). Yield 76%

H-Pbd_15: M_n 30,400 g mol⁻¹, M_w 82,900 g mol⁻¹, \bar{D} 1.83.

4.3.3.16 Synthesis of H-Pbd_16

To a two-necked 1 L flask, equipped with a reflux condenser and magnetic, “crossbar” EC-XBAR32 (5.50 g, 0.16 mmol), brominated “arm” ARM19-Br (22.13 g, 1.15 mmol), and cesium carbonate (Cs_2CO_3) (2.68 g, 8.23 mmol) were dissolved in vacuum distilled dry THF (270 ml). Dry dimethylacetamide (DMAc) (270 ml) was then added to this solution and the reaction was heated with an oil bath to 60 °C, with the progress followed by SEC and stopped when no further change in molecular weight was recorded. The polymer was precipitated into methanol, dissolved in THF, precipitated again into methanol, collected by filtration and dried under vacuum. Yield 78%.

H-Pbd_16: M_n 76,700 g mol⁻¹, M_w 133,600, g mol⁻¹, \bar{D} 1.74.

4.3.3.17 Synthesis of H-Pbd_17

H-Pbd_17 was prepared according to the procedure described in 4.3.3.16. Crossbar EC-XBAR32 (1.50 g, 0.045 mmol), brominated “arm” ARM40-Br (12.67 g, 0.31 mmol), and cesium carbonate (Cs_2CO_3) (0.020 g, 2.26 mmol) were dissolved in dry THF (130 ml) and dry DMAc (130 ml). Yield 74%.

H-Pbd_17: M_n 44,300 g mol⁻¹, M_w 81,100 g mol⁻¹, \bar{D} 1.83.

4.3.3.18 Synthesis of H-Pbd_18

H-Pbd_18 was prepared according to the procedure described in 4.3.3.16. Crossbar FF-XBAR52 (7.00 g, 0.14 mmol), brominated “arm” ARM19-Br (19.08, 0.99 mmol), and cesium carbonate (Cs_2CO_3) (2.31 g, 7.10 mmol) were dissolved in dry THF (270 ml) and dry DMAc (270 ml). Yield 76%.

H-Pbd_18: M_n 73,900 g mol⁻¹, M_w 143,300 g mol⁻¹, \bar{D} 1.94.

4.3.3.19 Synthesis of H-Pbd_19

H-Pbd_19 was prepared according to the procedure described in 4.3.3.16. Crossbar FF-XBAR52 (2.00 g, 0.041 mmol), brominated “arm” ARM40-Br (11.44 g, 0.28 mmol), and cesium carbonate (Cs_2CO_3) (0.66 g, 2.02 mmol) were dissolved in dry THF (130 ml) and dry DMAc (130 ml). Yield 78%.

H-Pbd_19: M_n 69,400 g mol⁻¹, M_w 141,800 g mol⁻¹, \bar{D} 2.04.

4.3.4 Fractionation of H-shaped polymers

To a three-necked, 3 litre separating funnel the recovered polymer (ca. 30 g) was dissolved in 2 litres of toluene. The separating funnel was then transferred to a temperature controlled water bath and equipped with an overhead stirrer. The temperature of the water bath was set to 25 °C. While stirring, methanol was added dropwise to the funnel until the polymer solution becomes cloudy, after which point the temperature was raised slowly until the solution becomes clear. Methanol was added again until the solution turns cloudy again, and this process was repeated until a suitable temperature was reached (5-10 °C above original temperature). The overhead stirrer was then removed from the separating funnel and the clear solution was allowed to cool overnight to 25 °C. The lower phase fraction, containing the higher molecular weight material was then precipitated into methanol and the fractionation process was repeated for the upper phase of the solution.

4.4 Conclusions

This chapter presented, for the first time, an adaptation of the “macromonomer” approach to synthesise H-shaped polymers using a variety of different chain end functionalised linear polybutadienes with different molecular weights. Telechelic “crossbar” polybutadienes with molecular weights between 30,000 - 100,000 g mol⁻¹ were synthesised via living anionic polymerisation in a one-pot, one-shot reaction using DPE-OSi as both a functionalised initiator and end-capping agent, resulting in polymers with narrow dispersity values. Various “arms” with molecular weights between 20,000 - 40,000 g mol⁻¹ were synthesised using living anionic polymerisation combined with traditional chain end-capping and post-polymerisation end-group conversion, also resulting in polymers with narrow dispersity values. We have synthesised a number of branched polymers using the aforementioned macromonomers via a Williamson coupling reaction and analysed the resulting polymers using both SEC and reversed-phase temperature gradient interaction chromatography (RP-TGIC). The use of this synthetic strategy generated polymers with complex mixtures, containing a number of by-products as well as the desired H-polymer architectures.

We found that while SEC was able to confirm that reaction had taken place, it was unable to accurately define or quantify the mixture of structures present in the polymers generated. However, interaction chromatography, specifically reversed-phase temperature gradient interaction chromatography (RP-TGIC) was able to provide a much more complete picture of the complex polymer mixtures generated. In contrast to SEC, which could mostly only confirm the existence of coupling, in many cases TGIC was able to give a complete, quantitative analysis of the constituents of the entire polymer mixture in question, specifically identifying all species present within a given sample.

Not only did TGIC provide information about the presence of low molecular weight by-products, there was also the case of high molecular weight by-products detected by TGIC, which allowed for their full characterisation. On a small scale, the Williamson coupling reaction itself resulted in instances of low coupling at first, but further reactions were carried out to improve the extent of coupling. This was achieved in two ways, firstly by increasing the molar ratio of arm to crossbar with attempts using both 7 and 10 equivalents of arm, which increased the extent of coupling compared to using 5 equivalents. The second strategy to improve the extent of coupling involved increasing the molar ratio of cesium

carbonate to crossbar, with the use of 50 equivalents proving far more successful than 10 equivalents resulting in a dramatic increase in the extent of coupling. Combining these changes with the previously established reaction conditions resulted in the generation of polymers with reasonable levels of coupling, and in which the desired H-shaped polymer was generated as the major product. However, the scaling-up of this method to larger quantities (20 - 40 g) provided only one suitable polymer mixture for purification (H-Pbd_15). As such, the procedure was modified further to improve stirring/ mixing, first by changing the stirring method from mechanical to magnetic, and then by lowering the solution concentration from 10% to 5%. These modifications allowed for the generation of four branched polymers, three of which were purified by fractionation in order to remove low and high molecular weight by-products and isolate the final H-polymers.

Interaction Chromatography has shown itself to be an invaluable analytical method, which is complementary to SEC, especially for the analysis of very complex polymer mixtures. Full characterisation data which is not obtainable by the use of SEC alone has been possible, and the ability to both identify and quantify the composition of the various constituents of such a polymer mixture is a vital tool that will aid complex polymer characterisation and rheological studies.

4.5 References

1. McLeish, T. C. B., *Macromolecules* **1988**, *21* (4), 1062-1070.
2. Daniels, D. R.; McLeish, T. C. B.; Kant, R.; Crosby, B. J.; Young, R. N.; Pryke, A.; Allgaier, J.; Groves, D. J.; Hawkins, R. J., *Rheol. Acta* **2001**, *40* (5), 403-415.
3. Chen, X.; Lee, H.; Rahman, M. S.; Chang, T.; Mays, J.; Larson, R., *Macromolecules* **2012**, *45* (14), 5744-5756.
4. Roovers, J.; Toporowski, P. M., *Macromolecules* **1981**, *14* (5), 1174-1178.
5. Hakiki, A.; Young, R. N.; McLeish, T. C. B., *Macromolecules* **1996**, *29* (10), 3639-3641.
6. Iatrou, H.; Avgeropoulos, A.; Hadjichristidis, N., *Macromolecules* **1994**, *27* (21), 6232-6233.
7. Rahman, M. S.; Aggarwal, R.; Larson, R. G.; Dealy, J. M.; Mays, J., *Macromolecules* **2008**, *41* (21), 8225-8230.
8. Perny, S.; Allgaier, J.; Cho, D.; Lee, W.; Chang, T., *Macromolecules* **2001**, *34* (16), 5408-5415.
9. Hutchings, L. R.; Roberts-Bleming, S. J., *Macromolecules* **2006**, *39* (6), 2144-2152.
10. Clarke, N.; Luca, E. D.; Dodds, J. M.; Kimani, S. M.; Hutchings, L. R., *Eur. Polym. J.* **2008**, *44* (3), 665-676.
11. Hutchings, L. R.; Dodds, J. M.; Roberts-Bleming, S. J., *Macromolecules* **2005**, *38* (14), 5970-5980.
12. Agostini, S.; Hutchings, L. R., *Eur. Polym. J.* **2013**, *49* (9), 2769-2784.
13. Hutchings, L. R.; Dodds, J. M.; Roberts-Bleming, S. J., *Macromol. Symp.* **2006**, *240* (1), 56-67.
14. Corradini, F.; Marcheselli, L.; Tassi, L.; Tosi, G., *Can. J. Chem.* **1992**, *70* (12), 2895-2899.
15. Hutchings, L. R.; Dodds, J. M.; Rees, D.; Kimani, S. M.; Wu, J. J.; Smith, E., *Macromolecules* **2009**, *42* (22), 8675-8687.
16. Kimani, S. M.; Hutchings, L. R., *Macromol. Rapid Commun.* **2008**, *29* (8), 633-637.
17. Doi, K.; Togano, E.; Xantheas, S. S.; Nakanishi, R.; Nagata, T.; Ebata, T.; Inokuchi, Y., *Angew. Chem. Int. Ed.* **2013**, *52* (16), 4380-4383.
18. Hutchings, L. R., *Macromolecules* **2012**, *45* (14), 5621-5639.
19. Chang, T., *J. Polym. Sci., Part B: Polym. Phys.* **2005**, *43* (13), 1591-1607.
20. Lee, W.; Cho, D.; Chun, B. O.; Chang, T.; Ree, M., *J. Chromatogr. A* **2001**, *910* (1), 51-60.
21. Snijkers, F.; van Ruymbeke, E.; Kim, P.; Lee, H.; Nikopoulou, A.; Chang, T.; Hadjichristidis, N.; Pathak, J.; Vlassopoulos, D., *Macromolecules* **2011**, *44* (21), 8631-8643.
22. Li, S. W.; Park, H. E.; Dealy, J. M.; Maric, M.; Lee, H.; Im, K.; Choi, H.; Chang, T.; Rahman, M. S.; Mays, J., *Macromolecules* **2011**, *44* (2), 208-214.

Chapter 5

**Synthesis and characterisation of Randomly Branched
Polybutadienes**

5.1 Introduction

Branched polymers are of significant industrial interest due to the favourable rheological properties they possess in comparison to their linear analogues, including low solution and melt viscosities, and improved solubility.¹⁻² As such, there is much industrial interest in a facile, cheap, one-step synthetic methodology for producing large quantities of branched materials using commercially available starting materials. There are few industrial methods for the generation of long-chain, randomly-branched materials, with the synthesis of low density polyethylene being the most commercially recognisable. For the synthesis of long-chain, randomly-branched vinyl polymers other methods also exist, such as the previously mentioned self-condensing vinyl polymerisation (SCVP) (Chapter 1), however, SCVP requires the use of functionalised or specialised monomers. The standard synthetic strategies for the production of many branched architectures on an industrial scale are limited. Academically, many more examples exist, but often involve the use of either complex multistep synthetic strategies, or as in the case of hyperbranched polymers, the synthesis of preformed small molecules or macromolecules that can then undergo polymerisation. The generation of the branched materials described above, require synthetic methods which, although effective, are often time-consuming, labour-intensive, costly, and often result in modest amounts of material.

5.1.1 The Strathclyde Route

In 2000, Sherrington and co-workers reported a novel yet facile synthetic technique for the synthesis of highly branched polymers. The Sherrington approach, also known as the Strathclyde route, describes the use of free radical polymerisation to copolymerise a vinyl monomer with a difunctional monomer and a radical chain transfer agent.³ The use of small amounts of difunctional monomer in most chain-growth polymerisation mechanisms can result in gelation and the formation of insoluble networks, either through macrogelation in concentrated solutions or microgelation in highly dilute solutions. However, Sherrington *et al.* were able to demonstrate that the use of a transfer agent promotes the termination of enough chains to counterbalance the effect of crosslinking, thus avoiding network formation and obtaining soluble branched polymer; this is illustrated in Figure 5.1.³

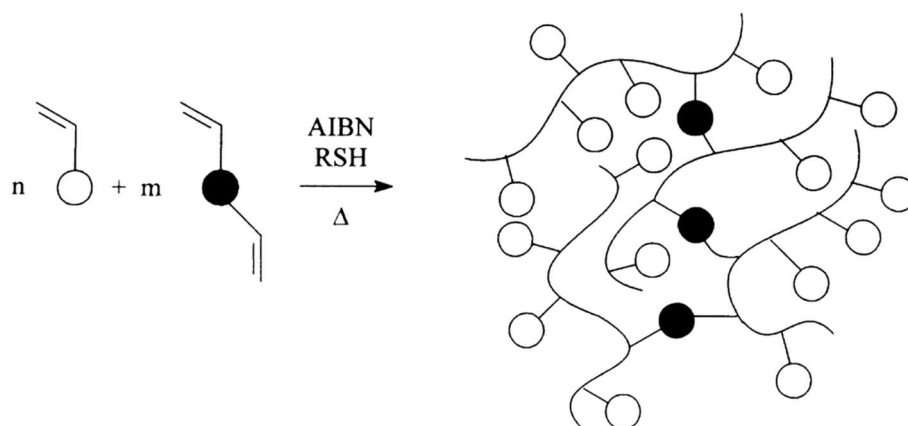


Figure 5.1 - Synthesis of branched vinyl polymer using a balance of divinyl monomer and radical transfer agent³ Reprinted with permission from [O'Brien, N.; McKee, A.; Sherrington, D. C.; Slark, A. T.; Titterton, A., *Polymer* 2000, 41 (15), 6027-6031]. Copyright [2000] Elsevier

This approach has since been adopted and modified in some cases for use with other polymerisation mechanisms, with Sherrington *et al.* themselves modifying the approach to synthesise branched polystyrene via cationic polymerisation, using divinylbenzene as a chain-coupling agent.⁴ Interestingly, chain transfer to monomer occurred by this route and no additional chain transfer agent was needed. Normally unwanted proton-transfer side reactions, which are a frequent occurrence in vinyl cationic polymerisations, can instead be used to inhibit the degree of crosslinking. Cationic polymerisation is not widely used industrially, but this again demonstrated the versatility of the Strathclyde route.

Controlled radical polymerisation techniques have also been used successfully to exploit this approach. Perrier and co-workers first demonstrated its use to form randomly branched PMMA via RAFT polymerisation using ethylene glycol dimethacrylate (EGDMA) as a chain-coupling agent and 2-2'-cyanopropyl dithiobenzoate (CPDB) as a chain transfer agent.⁵

5.1.2 Adapting the Strathclyde Route for Anionic Polymerisation

In living anionic polymerisation, chain transfer and termination reactions are, by definition, completely absent. However, dependent on certain reaction conditions, chain transfer reactions can be introduced to anionic polymerisation. It is generally perceived that these reactions are unwanted and it is true that chain transfer leads to increased dispersity of the resulting polymers synthesised which will also possess lower molecular weights than their initial targets. However, chain transfer can be very useful and is commercially exploited

for the synthesis of low molecular weight liquid polybutadiene by anionic polymerisation, where the cost of initiator would be prohibitively high in the absence of chain transfer.

A classic example of chain transfer in anionic polymerisation is chain transfer to solvent, especially in the case of diene (butadiene/isoprene) polymerisation in toluene, the mechanism of which is given below in Figure 5.2. When diene polymerisation is initiated by an alkyl lithium initiator, the corresponding propagating polymer chain can be terminated by the abstraction of a hydrogen atom from the solvent (toluene) itself – this chain-transfer process is usually promoted by the addition of an additive such as potassium *tert*-butoxide. This hydrogen abstraction in turn generates a new initiating species which can re-initiate chain growth. In turn, the newly initiated chain can be terminated by another solvent molecule with the process repeated until the reaction is either completely terminated or all monomer has been consumed. This (usually) unwanted side reaction may also be desirable when it is used to control the polymerisation of a diene monomer in the presence of a chain-coupling agent which will be explained further.

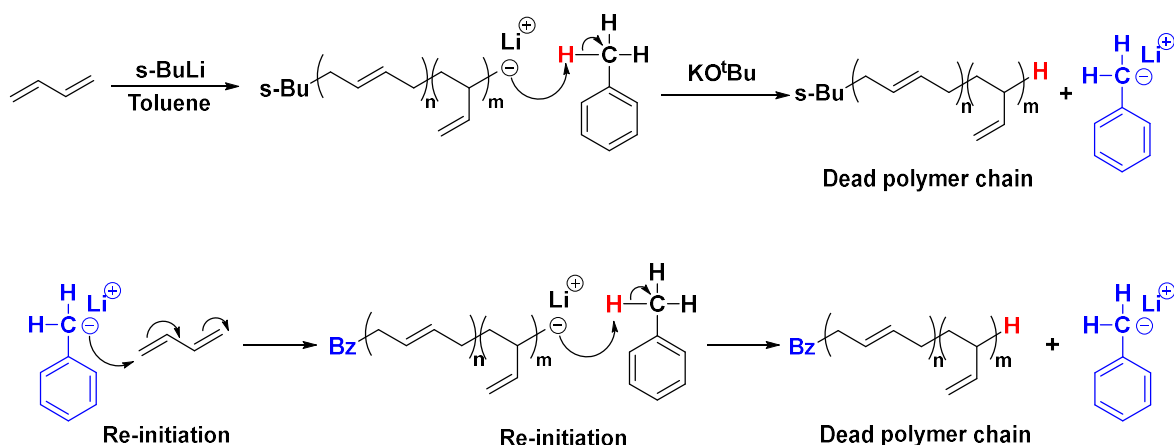


Figure 5.2 - Mechanism of chain transfer to solvent in the presence of potassium *tert*-butoxide in the anionic polymerisation of butadiene.

Divinylbenzene (DVB) is a chain-coupling agent which is often used in the synthesis of randomly branched or crosslinked polymers. In anionic polymerisation, it has most commonly been employed as a coupling agent for the synthesis of star-branched polymers.⁶

DVB has seen use in anionic polymerisation for the synthesis of highly/hierarchically long-chain branched polymers.⁷ However, its usage has been quite limited due to the rapid onset of crosslinking, often resulting in gelation, even at very low mole fractions of DVB. When both vinyl groups of the DVB have reacted with propagation chains, and the propagation continues after incorporation of the DVB, the DVB will link two chains together via a

tetrafunctional branch point. As the polymerisation proceeds, it can eventually lead to the formation of highly-branched chains and if not impeded, highly crosslinked networks – gelation; this is illustrated below in Figure 5.3.

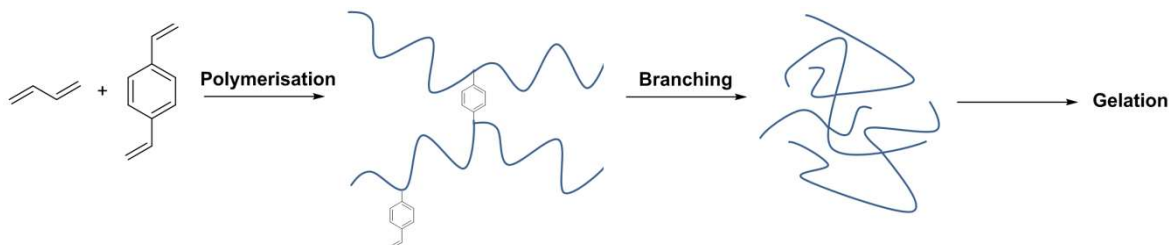


Figure 5.3 - Reaction of butadiene and divinylbenzene in the absence of chain transfer

The main reason for the rapid gelation is due to there being no inherent termination reactions in anionic polymerisation, unlike in free radical polymerisation. Sherrington, previously posited (and demonstrated) that for a “living” polymerisation with no chain transfer or termination, the ratio of difunctional monomer (DVB) : initiator is key. Thus, if the ratio of difunctional monomer : initiator is ≤ 1 , soluble lightly branched polymer should be obtained, however, if this ratio is > 1 , gelation is inevitable and insoluble crosslinked polymer will be obtained. This hypothesis was validated using ATRP.⁸ However, the introduction of chain transfer into such a reaction inhibits gelation by terminating chains and creating new chains in competition with chain-coupling, allowing for the generation of branched polymers that remain soluble.³ As mentioned previously, in the anionic polymerisation of polybutadiene, toluene can be used as both the chain transfer agent and solvent. This is favourable from an industrial standpoint as toluene is a cheap solvent and also removes the need to use another material as the chain transfer agent. Anionic polymerisation is used extensively industrially, which again made the adaptation of this route to anionic polymerisation desirable.

To date, the only previous attempt to adapt the Strathclyde route to produce branched polybutadiene via anionic polymerisation was carried out by a Masters’ student in the Hutchings’ group in 2013.⁹ The target of this preliminary (unpublished) work was the synthesis of highly branched, soluble, LOW molecular weight ($<20,000 \text{ g mol}^{-1}$) polybutadiene. Randomly branched polymers were prepared from butadiene via anionic chain-transfer polymerisation using DVB as the difunctional monomer and toluene as both the solvent and chain transfer agent.

The aforementioned preliminary work resulted in some key findings, specifically related to suitable reactions conditions. The first finding was that a promoter such as potassium *tert*-butoxide (KO^tBu) was necessary in order to increase the rate of chain transfer from monomer to solvent. The increase in the rate of chain transfer arises due to the combination of potassium *tert*-butoxide with the propagating alkylolithium species – polybutadienyl lithium. The mixing of these two reagents forms an *in-situ* extremely reactive system, which is much higher in basicity than its constituent parts, known as a superbases.¹⁰ Superbases, also known as Schlosser bases, LICKOR bases,¹¹ or Lochmann bases are most often used as powerful metallation and transmetallation agents in organic synthesis.¹² The use of a potassium *tert*-butoxide/alkylolithium system, often referred to specifically as Schlosser's base,¹³ in this instance promotes proton extraction from the methyl group situated on toluene, in turn transferring the negative charge from the propagating species to the solvent, which then goes on to participate and continue throughout the polymerisation. While superbases can be formed with the use of many heavier (than Li) metal alkoxides and alkylolithium reagents, the use of *n*-butyllithium or *sec*-butyllithium in the presence of potassium *tert*-butoxide only promotes a hydrogen/metal exchange with a benzylic methyl group such as the one present on toluene.¹⁰ When no potassium *tert*-butoxide was present in the polymerisation, there was little to no evidence of chain transfer, in agreement with expectations,¹⁴⁻¹⁵ and gelation occurred if the DVB : Initiator (in this case the initiator was *sec*-BuLi, which will be referred to as Li from this point) ratio was > 1. However, the addition of potassium *tert*-butoxide (KO^tBu : Li = 0.2) was sufficient to promote chain transfer and inhibit gelation when the DVB : Li ratio was > 1, and soluble branched polybutadiene resulted.

It was also found that increasing the ratio of DVB : Li increased the degree of branching, evidenced by the increasing molar mass in the resultant polymers; with gelation inhibited even when using DVB : Li ratios up to 1.5. The presence of potassium *tert*-butoxide also dramatically increased the rate of propagation and whilst one might have expected that increasing the ratio of KO^tBu : Li, would increase the contribution of chain transfer, in some cases the enhanced rate of propagation resulted in very rapid crosslinking. The potassium *tert*-butoxide also had an (expected) impact on the resultant polymers' microstructures – increasing the vinyl content to between 30 and 40% - which can be undesirable for some applications.

The principal aim of the current work was to develop the previous preliminary work on the adaptation of the Strathclyde route to anionic polymerisation, with key attention being focused on the generation of high molecular weight, highly (randomly) branched polymers, as most polybutadiene rubbers used in the tyre industry are high MW and branched. High molecular weight polymers with tetrafunctional branch points in particular are of significant rheological interest to the tyre industry; it has been documented that at molecular weights exceeding $60,000 \text{ g mol}^{-1}$ (trichain) and $100,000 \text{ g mol}^{-1}$ (tetrachain) rubbers possess lower viscosities than equivalent linear ones, reducing their cold flow and improving their processability.¹⁶ There was also some attention paid to the microstructure of these materials as it is known that microstructure also has a significant impact on other key properties, such as the glass transition temperature. A secondary aim involved a study into the use of alternative chain transfer promoters such as tetramethylethylenediamine (TMEDA) on this process and in particular the impact on the contribution of chain transfer and on the resultant microstructure.

5.2 Results and Discussion

Randomly branched polymers were prepared by anionic polymerisation via the adaptation of the “Strathclyde” route first reported by the Sherrington group.³ This was accomplished by using toluene as solvent and chain transfer agent, and divinylbenzene (DVB) as a chain-coupling agent. Chain transfer reactions limit the number of polymer chains available for chain branching, inhibiting the formation of a network polymer or gelation. To generate high molecular weight, highly branched polymers, the chain transfer process had to be robust enough to inhibit gelation. In order to investigate the efficacy of chain transfer, two common modifiers – potassium *tert*-butoxide and TMEDA were investigated for their effectiveness in controlling the degree of crosslinking in the polymerisations via the promotion of chain transfer. Moreover, some interesting and useful observations were made about the relationship between the amount of modifier used and the resulting polymer microstructure. The successful adaptation of this approach should allow for the synthesis of soluble, high molecular weight, highly branched, polybutadienes.

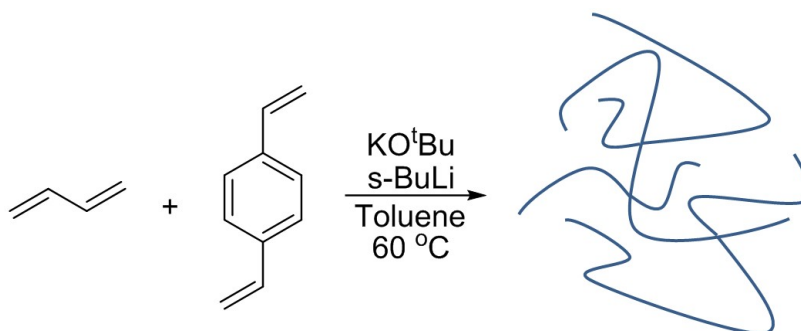
5.2.1 Synthesis of Randomly Branched Polybutadiene with Divinylbenzene

For diene polymerisation in toluene, the extent of chain transfer (CT) in the absence of a CT promoter is negligible. However, the addition of a CT promoter such as potassium *tert*-butoxide enhances the rate and therefore the amount of chain transfer in the resultant polymerisation. The most common additives used to enhance chain transfer are potassium *tert*-butoxide (KO^tBu) and N,N,N',N'-tetramethylethylenediamine (TMEDA). The current investigation focussed on these two promoters and their influence on the extent on gelation, chain transfer, molecular weight and microstructure of the obtained polymers.

5.2.1.1 Synthesis of Randomly Branched Polybutadiene with Divinylbenzene using Potassium *tert*-butoxide

Preliminary (unpublished) work first carried out by the Hutchings group had established the basic reaction conditions to allow the synthesis of soluble branched polymers from DVB and butadiene via anionic chain-transfer polymerisation, however, they were repeated in this instance to confirm the previous conditions to provide baseline data before moving to higher molar mass polymers.⁹ DVB was assumed to have similar reactivity (in regards to the first reacting double bond) to styrene when in a copolymerisation with butadiene. The

reaction scheme is given in Scheme 5.1. In these reactions, the potassium *tert*-butoxide is added to the reactor first, followed by the solvent and then monomer.



Scheme 5.1 - Synthesis of randomly branched polybutadiene in toluene

A series of polymers was produced and the reaction conditions, resulting microstructure and molar mass data are given in Table 5.1. A reaction temperature of 60 °C was used in all polymerisations. The “target” M_n for all polymerisations was 20,000 g mol⁻¹. This number represents the M_n value that one would expect, assuming that there had been zero chain transfer or chain branching reactions in these polymerisations – hence the target M_n is based on the ratio of monomer to initiator. The polymers in all cases were recovered by precipitation, rather than solvent evaporation and *ca.* 5 grams of polybutadiene in 50 ml of toluene was used in order to make results as comparable and reproducible as possible.

Table 5.1 - Reaction conditions, molar mass data and microstructure values for randomly branched polybutadienes using solid potassium *tert*-butoxide

Sample	DVB : Li	KO ^t Bu : Li	Time (min)	M_n (g mol ⁻¹)	M_w (g mol ⁻¹)	\bar{D}	Yield (%)	1,4-content (%)
R-Pbd_1	1.2	0.2	720	2800	41,700	16	72	66
R-Pbd_2	1.2	0.2	720	16,200	59,700	3.69	86	83
R-Pbd_3	1.2	0.2	60	1600	72,500	44	91	67
R-Pbd_4	1.2	0.2	60	33,500	83,000	2.48	93	86
R-Pbd_5	1.5	0.2	120	11,800	392,000	33	98	67
R-Pbd_6	1.5	0.2	120	54,900	427,400	7.78	85	84

DVB was added in a molar ratio relative the amount of *sec*-BuLi, i.e. initiator in the reactions. The DVB : Li ratios were set to above 1.0 as the preliminary work indicated that ratios above 1.0 could result in polymers with enhanced branching whilst still avoiding gelation. Potassium *tert*-butoxide (KO^tBu) was added in a 0.2 mole ratio relative to the

amount of initiator present. It should be noted that despite the reaction times used varying from one hour (for polymers R-Pbd_3 and R-Pbd_4) two hours (R-Pbd_5 and R-Pbd_6) and 12 hours (R-Pbd_1 and R-Pbd_2) there was no gelation seen in any of these polymerisations with the entire recovered polymer remaining soluble. These results are very encouraging in that they indicate that chain transfer is not only occurring, but doing so at a level which is inhibiting gelation, which is also reflected in the SEC results obtained.

In all cases the polymerisations resulted in good yields, however, as can be seen in Table 5.1, poor reproducibility of the results was an issue. Each pair of polymers R-Pbd_1 & R-Pbd_2; R-Pbd_3 & R-Pbd_4; and R-Pbd_5 & R-Pbd_6 were produced under identical reaction conditions that were intended to explore the reproducibility of this system. However, the microstructures and molecular weight data obtained show that there are large discrepancies between the sets of polymers. Initially there was no obvious explanation for the variation in results however a closer look at the data, and in particular the microstructure data, may help explain why the experiments were less reproducible than initially expected.

Polymers R-Pbd_1, R-Pbd_3 and R-Pbd_5 all possess between 66 – 67% 1,4-microstructure (calculated from $^1\text{H-NMR}$) whereas polymers R-Pbd_2, R-Pbd_4 and R-Pbd_6 (highlighted in red in Table 5.1) possess between 83-86% 1,4-microstructure.

The above microstructure analysis, in addition the SEC data, allows the polymers to be split into two groups, which for simplicity's sake, will be classified as the High Vinyl Content polymers (HVC) and the Low Vinyl Content (LVC) polymers. The HVC polymers are samples R-Pbd_1, R-Pbd_3 and R-Pbd_5 and the LVC polymers are R-Pbd_2, R-Pbd_4 and R-Pbd_6 which are highlighted in red in Table 5.1.

The molecular weight data in Table 5.1 reveals much valuable information about the nature of both the HVC and LVC polymers. It is evident that the HVC polymers have M_n values which are much lower than the target M_n of 20,000 g mol $^{-1}$ with R-Pbd_1, R-Pbd_3 and R-Pbd_5 having M_n values of 2800 g mol $^{-1}$, 1600 g mol $^{-1}$ and 11,800 g mol $^{-1}$ respectively. This in contrast to the LVC polymers, which in general have M_n values which are approximately equal to, or much higher than the target M_n , with R-Pbd_2, R-Pbd_4 and R-Pbd_6 having M_n values of 16,200 g mol $^{-1}$, 33,500 g mol $^{-1}$ and 54,900 g mol $^{-1}$ respectively. This can be better illustrated by the SEC chromatograms for the polymers in both groups, which are presented in Figure 5.4.

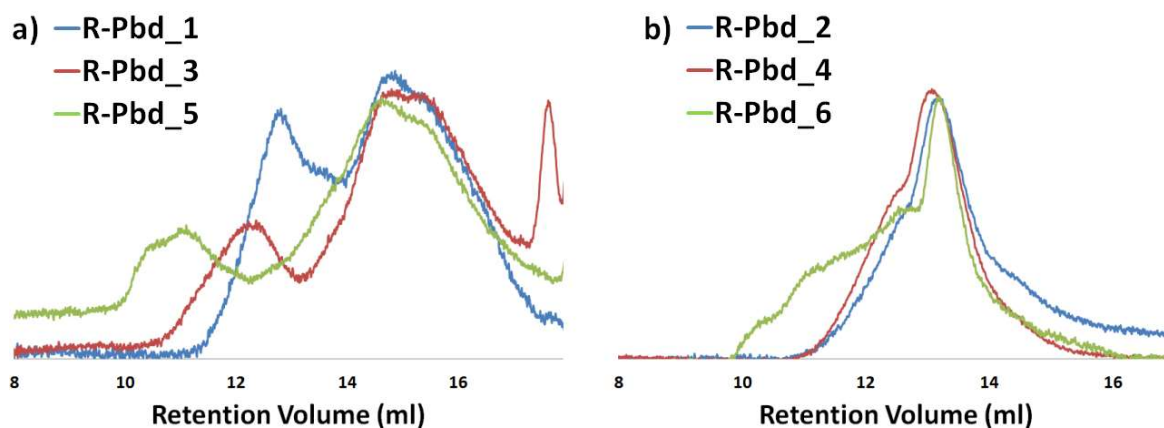


Figure 5.4 - SEC chromatograms (RI Detector) of random polybutadienes. Group (a) represents high vinyl content (HVC) polymers R-Pbd_1, R-Pbd_3 and R-Pbd_5. Group (b) represents low vinyl content (LVC) polymers R-Pbd_2, R-Pbd_4 and R-Pbd_6.

In each case it is clear from the SEC chromatograms that the polymers are highly disperse, although the odd-numbered samples, where chain transfer appears to have played a more significant role are unsurprisingly much more highly disperse than the even-numbered samples in Figure 5.4b.

For the HVC polymers (Figure 5.4a) complex, multimodal chromatograms were obtained, with the major peaks detected at higher retention volumes (13-17 ml). However, in each case a higher molecular weight peak was observed at retention volumes in the region of 10-13 ml. SEC analysis of the high molecular weight peaks of the HVC polymers was carried out, however, as these peaks were not fully resolved, the analysis cannot be completely accurate. Nevertheless, the analysis suggests the existence of very high molecular weight (several hundred thousand g mol^{-1}) products within each sample. The bimodality present in the HVC samples suggests the presence of two overlapping distributions with probable variation in molecular architecture – one distribution is probably comprised of predominantly high molecular weight, branched polymer whilst the other comprises of predominantly low molecular weight, lightly branched or linear polymer chains.

The LVC polymers have very different looking chromatograms, but still clearly show evidence of some chain transfer, this is clear from the tailing to low molecular weight from approximately 14 ml retention time, present in the chromatograms for all samples. There is also however, significant evidence of high molecular weight polymer due to chain branching/chain coupling, between 10 - 13 ml for all LVC samples. Examination of the SEC chromatogram of polymers R-Pbd_2, R-Pbd_4 and R-Pbd_6 (Figure 5.4b) shows they are in marked contrast to those chromatograms in Figure 5.4a. The SEC chromatograms for the

even-numbered samples are much less complex and less disperse, but still broad and not mono-modal. However, the shape of the peak and the absence of a second distinct peak to lower retention volume suggests that these samples are comprised (predominantly) of a single distribution of branched, high molecular weight product. Although the generation of these high molecular weight, high 1,4-microstructure, soluble branched polymers may have arisen not by design, a route to produce such materials could have significant advantages in certain industrial and rheological applications. Low vinyl polybutadienes (<20% 1,2-microstructure) have low glass transition temperatures (between -85 °C and -100 °C) which improves the processability of the materials, along with other tire specific factors such as abrasion resistance.¹² Branched polybutadiene also features improved rheological properties over its linear analogues such as lower melt viscosities at identical molecular weights.¹⁶

It is well-known that in anionic polymerisation, potassium *tert*-butoxide has a major impact on the microstructure of a diene polymer^{12, 15, 17} and this in turn allows us to begin to understand what may be the cause of the large (but oddly repeatable) discrepancies between both sets of polymers. Potassium *tert*-butoxide's primary function in these reactions was to increase the rate of chain transfer to the solvent, thereby controlling the extent of chain-coupling to inhibit gelation. The use metal alkoxides, however, also leads to other changes in behaviour. Firstly, the rate of propagation is increased dramatically (8 – 100 fold)¹⁵ by the addition of alkali metal butoxides with alkyllithium initiators in diene polymerisations, thus limiting the amount of potassium *tert*-butoxide that could be used in these reactions. Secondly, the presence of potassium *tert*-butoxide has an impact on the microstructure of diene polymerisations. Hsieh and Wofford found that higher ratios of KO^tBu : Li resulted in higher levels of vinyl content (1,2-microstructure) in polybutadiene. Thus when no potassium *tert*-butoxide is present, the 1,2-microstructure content of the resulting polymers was less than 10%. A KO^tBu : Li ratio of 0.1 resulted in 15% 1,2-microstructure, a KO^tBu : Li ratio of 0.2 resulted in 35% 1,2-microstructure, and a KO^tBu : Li ratio of ≥0.5 resulted in a maximum 48% 1,2-microstructure, at 30 °C.¹⁵

Due to the relatively small scale of these reactions (5 g), the very small amounts of potassium *tert*-butoxide required in each case was often on the milligram scale (*ca.* 5-6 mg). Potassium *tert*-butoxide is a moisture sensitive, white crystalline solid and the procedure used for both measuring out and addition to the reactors, namely under a nitrogen

atmosphere with the use of a glove bag, may have led to inaccuracies in the actual amount of potassium *tert*-butoxide added.

As the ratio of potassium *tert*-butoxide to initiator has a significant impact on the polymerisation, the following can be surmised from the microstructure data, SEC analysis and previous reports – the HVC polymers R-Pbd_1, R-Pbd_3 and R-Pbd_5 probably have (approximately) the desired amount of potassium *tert*-butoxide present in the polymerisation mixtures ($\text{KO}^t\text{Bu} : \text{Li} = 0.2$). This is primarily evident from the level of 1,2-vinyl content (ca. 33 – 34%) present in the resultant polymers, which is consistent with the desired ratio of potassium *tert*-butoxide : Li as reported previously.¹⁵ It is also clear from the SEC data that R-Pbd_1, R-Pbd_3 and R-Pbd_5 have rather low values of molar mass and high dispersity – both observations are consistent with a high degree of chain transfer. This is in contrast to the LVC polymers R-Pbd_2, R-Pbd_4 and R-Pbd_6 which all appear to have LOWER than the expected amount of potassium *tert*-butoxide present in their polymerisations, resulting in a lower contribution of chain transfer, lower levels of vinyl content (ca. 14 – 17%) and higher molecular weights. These results suggest that the even numbered polymers most likely contain $\text{KO}^t\text{Bu} : \text{Li}$ ratios closer to 0.1 based on previous reports.

The LVC polymers suggest that the use of a lower ratio of potassium *tert*-butoxide : Li can result in high molecular weight branched polymers, with a higher 1,4 microstructure whereby enough potassium *tert*-butoxide is present to promote sufficient chain transfer to inhibit gelation.

Although the SEC data strongly suggests chain coupling and chain branching, the molar masses, dispersities and shapes of the chromatograms do not provide direct evidence of chain branching. However a plot of $\log(\text{intrinsic viscosity})$ against $\log(\text{molecular weight})$, also known as a Mark-Houwink (MH) plot is able to give direct qualitative information about the branched nature of a polymer. Branched polymers are more compact and as a result have lower intrinsic viscosities compared to a linear polymer with the same molecular weight, and the polymer architecture can be induced from the gradient of the MH plot. MH plots are given for both the HVC and LVC polymers in Figure 5.5. It can be seen that in some cases, there is a change in gradient with increasing molar mass, where a decrease in gradient indicates chain branching. The reason for the change in gradient is almost certainly a result of the different molecular architectures present within a sample.

The lower molecular weight chains produced from chain transfer and re-initiation are probably linear and correspond to the initial steeper gradient, whereas the high molecular weight chains arise from chain coupling/chain branching which accounts to a change in gradient to a lower value. For polymers R-Pbd_1, R-Pbd_2, and R-Pbd_3 (Figure 5.5a, b, c), there is very strong correlation between the log(intrinsic viscosity) and log(molecular weight) over the entire molecular weight distribution suggesting that these polymers most likely consist predominantly of chains with a linear architecture. This is in line with the SEC chromatograms for HVC polymers R-Pbd_1 and R-Pbd_3 where it is evident that there is a lot of low molecular weight material as a result of chain transfer. The SEC chromatogram for R-Pbd-2 shows that it is the LVC polymer with the lowest fraction of high molecular weight chains, that is, it has the lowest amount of chain branching present and must consist of mostly linear chains. These are in marked contrast to the MH plots for polymers R-Pbd_4, R-Pbd_5 and R-Pbd_6, (Figure 5.5d, e, f) where a very clear change in gradient can be seen for each polymer, suggesting the samples have a more significant fraction of branched polymer present.

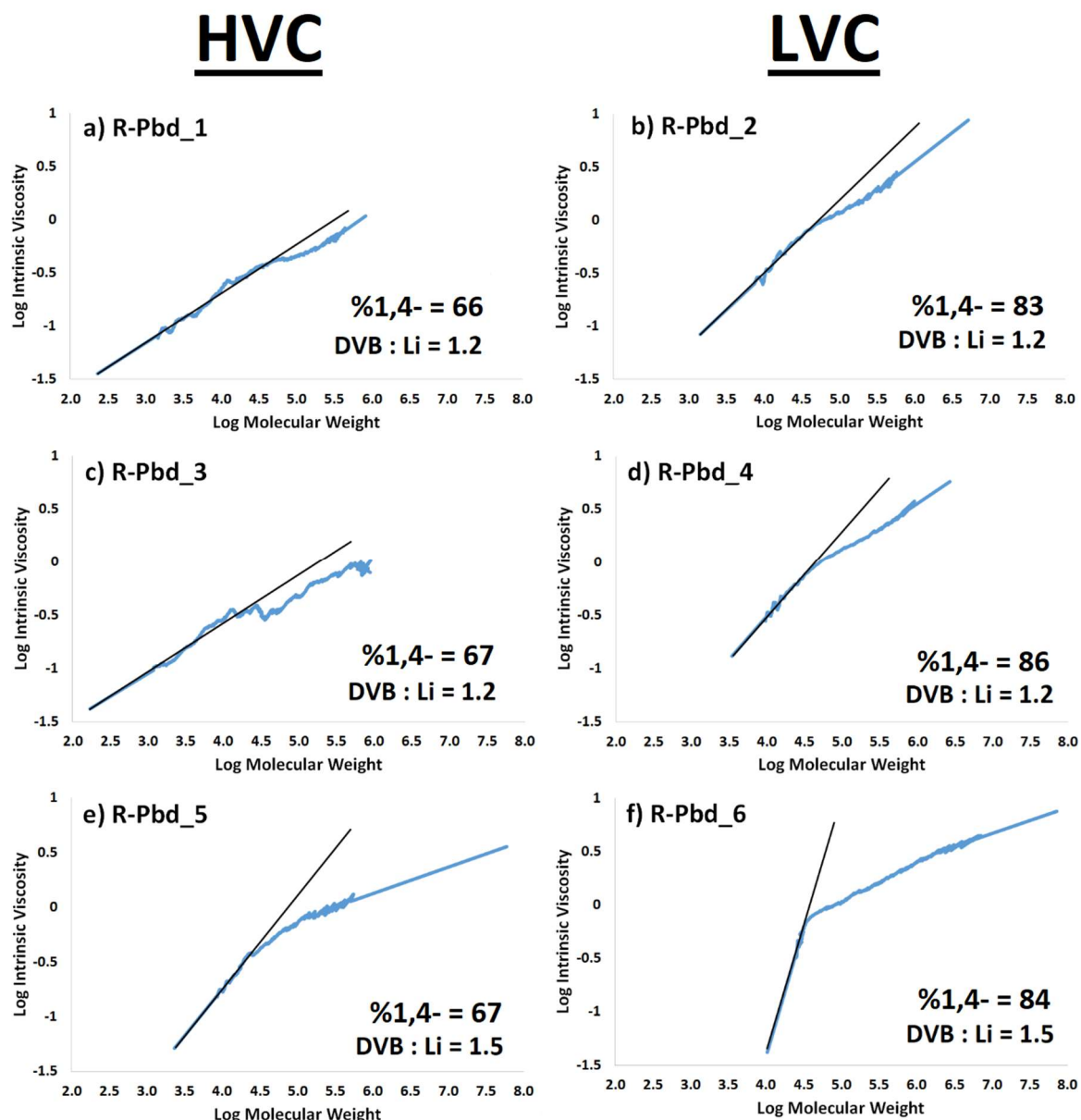


Figure 5.5 - Mark-Houwink plots for HVC polymers: R-Pbd_1, R-Pbd_3 and R-Pbd_5; and LVC polymers: R-Pbd_2, R-Pbd_4 and R-Pbd_6

What also should be noted is that a small increase in the DVB : Li ratio greatly enhanced the degree of branching. Thus, a DVB : Li ratio of 1.2 (R-Pbd_1 to R-Pbd_4) resulted in M_w values between 40,000 g mol⁻¹ and 85,000 g mol⁻¹. However, increasing the DVB : Li ratio to 1.5 resulted in the M_w values of R-Pbd_5 and R-Pbd_6 being 392,000 g mol⁻¹ and 427,000 g mol⁻¹ respectively. These small changes in the amount of DVB used, very much highlight the sensitivity of anionic polymerisation to the presence of any difunctional monomer. It is also worth reinforcing the fact that in all cases the ratio of DVB : Li is greater than 1.0 and according to Sherrington, under these conditions gelation is expected in the absence of chain transfer. This would suggest that in all cases, even those with apparently much lower

levels of the chain transfer promoter potassium *tert*-butoxide, sufficient chain transfer occurs to inhibit gelation! The results clearly demonstrate that the Strathclyde route can be applied using anionic polymerisation, but at the scale of reaction used, reproducibility was poor. This was almost certainly due to the difficulty in accurately measuring the exact amount of potassium *tert*-butoxide that is present at the onset of polymerisation. However, this challenge, whilst resulting in poor reproducibility, (serendipitously) revealed that it is possible to prepare high molecular weight, soluble branched polymers by the described methodology whilst maintaining a high degree of 1,4-microstructure.

Attempts were made to overcome this irreproducibility by producing a stock solution of potassium *tert*-butoxide in toluene; however, the potassium *tert*-butoxide proved insoluble at any meaningful concentration in toluene. The low solubility of the potassium *tert*-butoxide in the toluene of the stock solutions meant this was not a viable approach, although several unsuccessful polymerisations were carried out. It was then decided to use a commercially available solution of potassium *tert*-butoxide in THF (1.0 M), which should have allowed a high degree of control over the amount of potassium *tert*-butoxide used and more control and reproducibility over the molecular weight and microstructures of the final polymers. However, there were some concerns about the potential impact of the THF on the reaction since THF itself results in a higher 1,2 microstructure and moreover, the propagating alkylolithium chain-ends may react with THF, leading to further inaccuracies.¹⁸⁻
¹⁹ Three attempts to produce branched polybutadiene using the THF solution of potassium *tert*-butoxide were carried out and the results are given in Table 5.2, with the SEC chromatograms shown in Figure 5.6. The reaction conditions used were identical to the analogous polymerisation reaction described above, with the exception of the use of the THF solution of potassium *tert*-butoxide which was injected into the reactor as a first step, to allow the (attempted) removal of THF by vacuum distillation. This was carried out in an attempt to obviate the potential issues alluded to above. The target M_n for all polymerisations was 20,000 g mol⁻¹.

Table 5.2 - Reaction conditions, molar mass data and microstructure values for randomly branched polybutadienes using potassium *tert*-butoxide in THF (1.0 M)

Code	M_n (g mol ⁻¹)	M_w (g mol ⁻¹)	\bar{D}	Yield (%)	1,4- (%)
R-Pbd_7	164,500	1,922,000	11.69	7	63
R-Pbd_8	73,400	257,100	3.69	42	64
R-Pbd_9	6,830	67,400	9.87	47	64

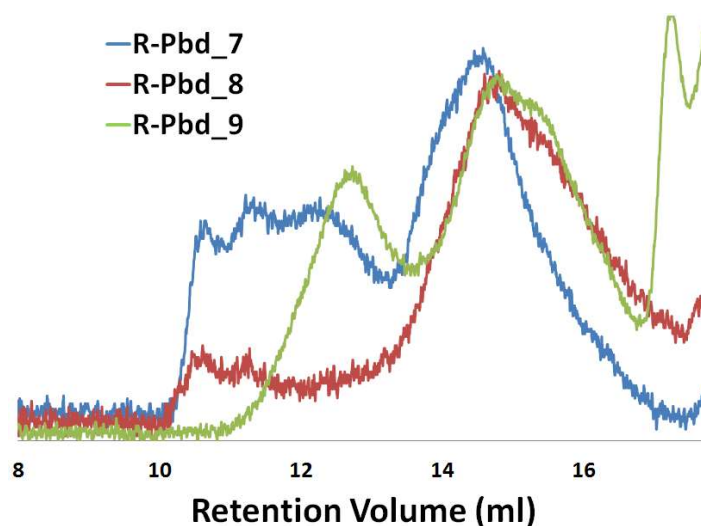


Figure 5.6 - SEC chromatograms (RI Detector) of random polybutadienes using potassium *tert*-butoxide in THF (1.0 M)

It is immediately evident for the polymers obtained using potassium *tert*-butoxide in THF, that the reactions are less controlled than seen previously. For polymers R-Pbd_7, R-Pbd_8 and R-Pbd_9, the yields were much lower than expected, the target M_n values were also very far from target values and the microstructures again indicating high levels of vinyl content (36-37% 1,2-microstructure). The SEC chromatograms (Figure 5.6) also indicate that similar levels of chain transfer are occurring to those seen for the previous HVC polymers. The multimodality evident in the chromatograms for R-Pbd_7, R-Pbd_8 and R-Pbd_9 suggests the possible formation of high molecular weight, branched polymers along with a lower molecular weight, lightly branched or linear polymers. The very low yield and high molecular weight of sample R-Pbd_7 was probably due to impurities deactivating either the initiator or propagating chains. For R-Pbd_8 and R-Pbd_9, impurities may have also affected the final yield of polymer. In these reactions the required amount of potassium *tert*-butoxide was directly injected into the flask, as the THF solution, and the 1,4-microstructure values obtained are in agreement with the previous HVC polymers, which suggests that the correct $\text{KO}^t\text{Bu} : \text{Li}$ ratio of 0.2 must have been present in the reaction. However, the lower yields of these reactions, may have been due in some part to residual THF still being present in the reaction flasks during polymerisation, which can lead to chain termination. To ensure no impact from residual THF in these polymerisations, the reaction was repeated but in this case the potassium *tert*-butoxide was azeotropically dried to remove any residual traces of THF, however, none of these attempts were successful (no polymer obtained).

In summary, potassium *tert*-butoxide has been shown to be an effective chain transfer promoter for the anionic polymerisation of butadiene in toluene and enables the synthesis of branched polymers when the polymerisation is carried out in the presence of divinylbenzene. However, there have been significant reproducibility problems associated with the process of using both solid and solutions of potassium *tert*-butoxide. Although this irreproducibility was frustrating, the series of reactions using solid potassium *tert*-butoxide did reveal some unexpectedly positive results. In some experiments the data obtained strongly suggested that the amount of potassium *tert*-butoxide used was less than intended, which in turn led to a lower contribution of chain transfer. Despite this, the outcome of these particular reactions was still branched soluble polymers with significantly higher molar masses and a much higher than anticipated 1,4-microstructures – both key aims for this short study. It would appear that far lower levels of potassium *tert*-butoxide are required to suppress gelation than previously thought. However, the challenge in delivering accurate quantities of potassium *tert*-butoxide led to the investigation of another chain transfer promoter – TMEDA.

5.2.1.2 Synthesis of Randomly Branched Polybutadiene with Divinylbenzene using TMEDA

Owing to the reproducibility difficulties in the synthesis of highly branched polymers using the potassium *tert*-butoxide as a chain transfer promoter, a new strategy was adopted – namely substituting TMEDA for the potassium *tert*-butoxide. Lewis bases such as TMEDA are also known to promote chain transfer reactions; TMEDA for example, has been used to prepare very low molecular weight ($<8,000 \text{ g mol}^{-1}$) polybutadiene in toluene by anionic chain-transfer polymerisation.^{12, 14} TMEDA is also a liquid, which allows for much better control over the addition of small quantities when compared to the solid potassium *tert*-butoxide used previously. Moreover, TMEDA is a very common, cheap material, already in wide use industrially. A series of reactions was carried out using TMEDA, with the aim of understanding the impact that TMEDA has on the control of branching, dispersity, molecular weight and chain transfer. As stated previously, Sherrington proposed for a “living” polymerisation that at DVB : Li ratios above 1.0, gelation is inevitable unless chain transfer is able to inhibit this. We have previously shown that polymerisations carried out using DVB : Li ratios of 1.2 and 1.5, in the presence of potassium *tert*-butoxide, produced soluble polymers, suggesting that gelation was sufficiently inhibited in these cases by chain

transfer. Reactivity ratios of $r_1 = 1.266$ and $r_2 = 1.310$ were reported for styrene and butadiene respectively, in a styrene/butadiene rubber (SBR) (20/80) statistical copolymerisation initiated by BuLi with a TMEDA : Li ratio of 0.97 at 50 °C. Moreover, the resultant polymers comprised of 48% 1,4-microstructure.²⁰ In a styrene/butadiene copolymerisation, TMEDA acts as a randomiser, resulting in random placement of styrene units in polybutadiene chains. By using TMEDA instead of potassium *tert*-butoxide, similar results to previously published work should be observed. Namely, that TMEDA should ensure that DVB incorporation is randomly incorporated into the polybutadiene chains, although there should also be high levels of 1,2-microstructure (*ca.* 50%) present in the final polymers.

With this in mind it was decided that the “TMEDA-controlled” polymerisations would be carried out initially with a DVB : Li ratio of 1.2, to explore whether TMEDA is similarly able to suppress gelation and produce soluble, high molecular weight, branched polymer. Four polymers were produced using varying fractions of TMEDA and the reaction conditions and results are summarised in Table 5.3. A reaction temperature of 60 °C was used in all polymerisations. The target M_n for R_PBd_10, R_PBd_11, R_PBd_12 was 20,000 g mol⁻¹ whereas the target M_n for R_PBd_13 was 40,000 g mol⁻¹.

Table 5.3 - Reaction conditions, molar mass data and microstructure values for randomly branched polybutadienes prepared using TMEDA as chain transfer agent

Sample	TMEDA : Li	Target M_n (g mol ⁻¹)	M_n (g mol ⁻¹)	M_w (g mol ⁻¹)	\bar{D}	Yield (%)	1,4- (%)
R_PBd_10	1	20,000	10,100	13,700	1.36	2	38
R_PBd_11	0.75	20,000	28,900	65,700	2.28	91	37
R_PBd_12	0.5	20,000	41,900	122,200	2.92	96	51
R_PBd_13	0.5	40,000	115,500	586,500	5.07	89	48

A series of three reactions was carried out (R_PBd_10, R_PBd_11, and R_PBd_12) on the same scale and under the same reaction conditions (60°C, toluene solvent, overnight), with the only variable being the amount of TMEDA added (with respect to *sec*-BuLi). The TMEDA can be seen to have a pronounced effect on many factors in these polymerisations and some trends are clear. As expected, the presence of TMEDA has a dramatic effect on the microstructure of the polymers. The 1,4-microstructure obtained for these polymers ranged from 37 to 51%, increasing slightly with decreasing TMEDA as shown in Table 5.3,

in line with previously reported values.^{15, 21} In all cases this is significantly lower than what would be expected in a reaction with no TMEDA present where greater than 90% 1,4-enchainment is expected. It would also appear that lowering the TMEDA : Li ratio results in an increase in the total molecular weight of the polymer. This suggests that increasing TMEDA : Li ratio results in a greater contribution of chain transfer during polymerisation.

R_PBd_10, was carried out with a 1 : 1 ratio of TMEDA : Li. This produced a soluble polymer, but in very low yield (2%). Recovery of this polymer was very difficult due to the polymer's poor separation from the methanol it was recovered from. The experimental M_n of the fraction of R_PBd_10 which was recovered (M_n 10,100 g mol⁻¹), was much lower than the target of 20,000 g mol⁻¹ and the polymer itself was disperse (\bar{D} 1.36). The SEC chromatogram of this sample (Figure 5.7a) shows a peak with a long tail suggesting chain transfer had occurred in the polymerisation. It was presumed that a 1 : 1 ratio of TMEDA : Li resulted in too much chain transfer and in a polymer with a very low molecular weight and little branching, if any. It was surmised that much of the lower molecular weight material was lost, with only a fraction of the higher molecular weight material being recovered.

As a result, in subsequent polymerisations the ratio of TMEDA : Li was lowered. However, the SEC analysis of the polymers produced with TMEDA : Li < 1.0 resulted in very different chromatograms to R-Pbd_10. The SEC chromatograms of R_PBd_11, R_PBd_12 and R_PBd_13 in Figure 5.7 show the presence of a major, low dispersity peak at between 13.5 and 14 ml retention volume. This was a consistent feature for samples R-Pbd_11, 12 and 13. SEC analysis of just the sharp peak at 13.6 ml (for R-Bbd_12) reveals a molar mass which is very close to the target molecular weight and with a narrow dispersity which suggests little or no chain transfer (M_n 23,800 g mol⁻¹, M_w 24,700 g mol⁻¹, \bar{D} 1.04). However, it is clear from the SEC chromatogram that chain coupling reactions have taken place in each polymer, as evidenced by the broad, multimodal peak to lower retention volumes.

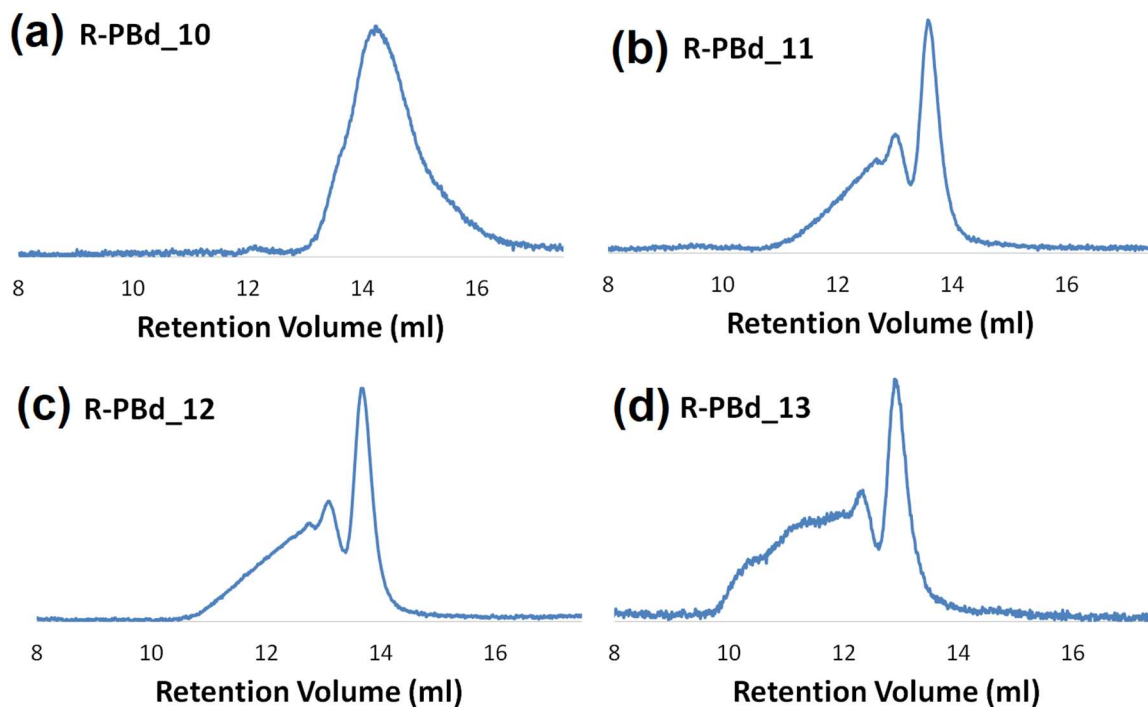


Figure 5.7 - SEC chromatograms (RI detector) of randomly branched polybutadienes prepared using TMEDA as chain transfer agent

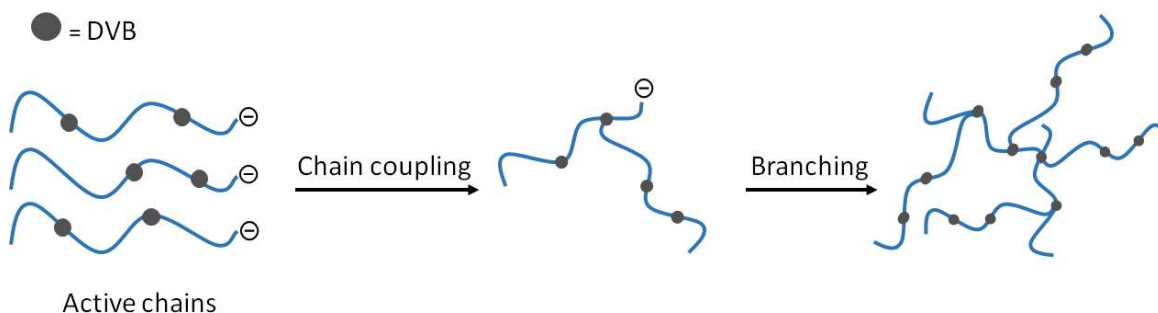


Figure 5.8 - Proposed route of branching of randomly branched polybutadienes prepared using TMEDA as chain transfer agent

The SEC chromatograms of samples R-Pbd_11, 12 and 13 also display little or no evidence of chain transfer occurring, with no characteristic tailing of the peaks between 13.5 and 14 ml being observed. Instead, these chromatograms appear to indicate that post-polymerisation, chain-on-chain coupling may be occurring, leading to high molecular weight branched architectures (Figure 5.8). A large, sharp peak can be seen in the chromatograms of these three polymers (at 13.5 – 14.0 ml), which is then followed by a smaller, also sharp peak at a slightly higher retention volume, which is further followed by a large, broad shoulder peak that continues until *ca.* 10 ml. As reported above, the initial large sharp peak at the lowest retention volume has a molar mass which is approximately equal to the target molecular weight; the next peak, to shorter retention volume, whilst not

fully resolved from a broader, higher molar mass peak, is probably the consequence of two chains coupled together. The broad dispersity shoulders to lower retention volume arise from multiple chains being coupled together in a randomly branched architecture. The nature of these distributions is in contrast to the polymers produced with potassium *tert*-butoxide polymers which were less well-defined and more disperse due to the contribution of chain transfer.

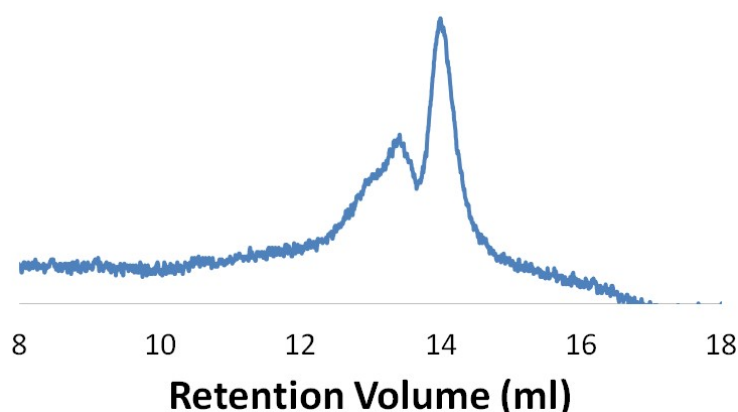
An additional important aspect of the previously mentioned polymers produced with TMEDA (R_PBd_10, R_PBd_11 and R_PBd_12) is that they all showed some evidence of microgelation. During reaction these gel particles were not visible but upon termination and precipitation of the polymer they became evident. Separation of these particles from the soluble polymer was particularly simple, as the small gel fractions tended stick to the bottom of the reactor and not precipitate out with the rest of the polymer. These gel fragments themselves proved insoluble in THF or toluene once they had been separated from the reaction. This coupled with the SEC data which showed no evidence of chain transfer suggested that the ratios of TMEDA : Li were insufficient to inhibit all crosslinking from taking place.

In order to see the impact of the target molecular weight on the polymerisation, R_PBd_13 was produced with a target M_n of 40,000 g mol⁻¹. A TMEDA ratio of 0.5 : 1 was selected as this produced the polymer with the highest reported dispersity thus far (R_PBd_12). The reaction time was also increased to three days for this polymerisation in order to see what effect time may have on the reaction, specifically whether a prolonged period of time would lead to complete gelation of the product, however, soluble polymer was obtained and total gelation did not occur. The polymer obtained (R_PBd_13) was very disperse ($\bar{D} = 5.07$) and with a high molecular weight ($M_n = 115,500$ g mol⁻¹, $M_w = 586,500$ g mol⁻¹); shown by its SEC chromatogram (Figure 5.7d). However, its SEC chromatogram possessed an intense high molecular weight shoulder, still suggested that random coupling/branching had occurred. Two further experiments were carried out in order to see how far the DVB and TMEDA levels could be increased before the onset of total gelation. The DVB level was increased in part, to see if it would be possible to produce more high molecular weight branched material. The experimental details as well as the molar mass data for these two experiments are given in Table 5.4.

Table 5.4 - Reaction conditions, molar mass data and microstructure values for randomly branched polybutadienes R_PBd_14 and R_PBd_15 prepared using TMEDA as chain transfer agent

Code	TMEDA : Li	Time (min)	DVB : Li	M _n (g mol ⁻¹)	M _w (g mol ⁻¹)	Đ	Yield (%)	1,4- (%)
R_PBd_14	2	15	1.5	gelation	gelation	-	-	-
R_PBd_15	2	5	1.2	75,600	322,300	4.26	25	51

The target M_n of these two polymerisations was 20,000 g mol⁻¹ with 60 °C again used as the reaction temperature. The first attempt at synthesis of a polymer using a TMEDA : Li ratio of 2 : 1 and a DVB : Li ratio of 1.5 : 1 resulted in total gelation within 15 minutes (R_PBd_14). In this case no soluble fraction was recovered. A 2 : 1 TMEDA : Li ratio seemingly increased the rate of propagation to such a high rate that its ability to promote chain transfer was ineffective in stopping gelation. This was not seen for ratios of TMEDA : Li of 1 : 1 or lower, as in those reactions the polymerisation had continued with only low levels of microgelation. It may also be that this ratio of TMEDA combined with the aforementioned ratio of DVB : Li was too high to prevent gelation. In a subsequent polymerisation reaction a TMEDA : Li ratio of 2 : 1 and a lower DVB : Li ratio of 1.2 : 1 was used. After 5 minutes, a portion of the reaction mixture was collected and terminated, whilst the remainder was allowed to continue polymerizing, resulting in total gelation within 30 minutes. A soluble polymer was recovered from the sample collected after 5 minutes (R_PBd_15), in a low yield (25% of the total polymer) which may also be due to the fact that polymerisation had not gone to completion due to the short reaction time. The SEC results for R_PBd_15 are given in Table 5.4 and Figure 5.9.

**Figure 5.9 - SEC chromatogram (RI detector) of randomly branched polybutadiene R-Pbd_15 using TMEDA as chain transfer agent.**

The SEC chromatogram for R_PBd_15 showed some evidence of chain transfer, with peak tailing being evident at retention volumes greater than for the peak at 14.5 ml. The product also shows what looks like evidence of branching, due to its bimodality and similarity to other TMEDA “controlled” polymerisations. It would appear that, if a TMEDA : Li ratio of 2 or higher is to be used for such reactions, it may be necessary to terminate the reactions before the onset of gelation or use lower levels of DVB.

In contrast with potassium *tert*-butoxide, the polymerisations carried out in the presence of TMEDA as chain transfer promoter produced very different results. The resultant polymers although randomly branched, contained very little evidence of chain transfer being promoted by TMEDA in most cases. There were also instances of microgelation detected with total gelation when the levels of TMEDA and DVB were both increased. TMEDA may prove itself to be a less effective additive for the synthesis of randomly branched polymers than potassium *tert*-butoxide, but the use of potassium *tert*-butoxide did lead to difficulties in the reproducibility of reactions carried out. However, these issues did lead to a serendipitous and highly significant result – the discovery of a route to highly branched, high molecular weight, soluble polymers with high 1,4-microstructure.

5.3 Experimental

5.3.1 Materials

Toluene (Aldrich, HPLC grade, $\geq 99.9\%$) and divinylbenzene (technical grade, 80%) were dried and degassed over calcium hydride (CaH_2) (Acros Organics, 93%) and stored under high vacuum. 1,3-Butadiene (Aldrich, +99%) was passed through columns of Carbosorb (Aldrich) and molecular sieves (Aldrich) to remove any inhibitor and moisture respectively. Potassium *tert*-butoxide (sublimed grade, 99.99% trace metals basis), Potassium *tert*-butoxide solution (1.0 M in THF) and N,N,N',N' -tetramethylethylenediamine (TMEDA) (≥ 99.5) (all Sigma-Aldrich) were used as received. The solvents were degassed by a number of freeze-pump-thaw cycles and freshly distilled prior to use. *sec*-Butyllithium (Aldrich, 1.4 M solution in cyclohexane) and *n*-butyllithium (Sigma-Aldrich, 2.5 M in hexanes) were used as received. Tetrahydrofuran and methanol (both AR grade) (both Fischer Scientific) were used as received.

5.3.2 Characterisation

5.3.2.1 Nuclear Magnetic Resonance (NMR)

^1H -NMR spectra were measured on Varian VNMRs 700 MHz or Bruker DRX-400 MHz spectrometer using CDCl_3 as the solvent.

5.3.2.2 Size Exclusion Chromatography (SEC)

Triple detection size exclusion chromatography (SEC) was carried out for the analysis of molecular weight and dispersity of the synthesised polymers, using a Viscotek TDA 302 with refractive index, right angle light scattering (RALS – 690 nm) and viscosity detectors and two PLgel 5 μm mixed C columns (300 x 75 mm). Tetrahydrofuran was used as the eluent at a flow rate of 1.0 ml/min and at a temperature of 35 $^\circ\text{C}$. The calibration was carried out with a single narrow distribution polystyrene standard purchased from Polymer Laboratories. A value of 0.124 mL/g (measured in house) was used as the dn/dc of polybutadiene for the analysis of prepared polymers.

5.3.3 Synthesis

The reaction vessel pictured below, (Figure 5.10), colloquially referred to as a “Christmas Tree” is an example of the type of reactor used in all anionic polymerisation experiments. All polymerisations carried out during this work utilise the same general procedure but with varying amounts of monomer, solvents and reagents used. The main solvent used in

all the following polymerisations was toluene. Any extra steps taken are detailed in that polymer's synthetic description. Preparation of the Christmas tree for anionic polymerisation is detailed in full in Chapter 2, section 2.3.2.1.

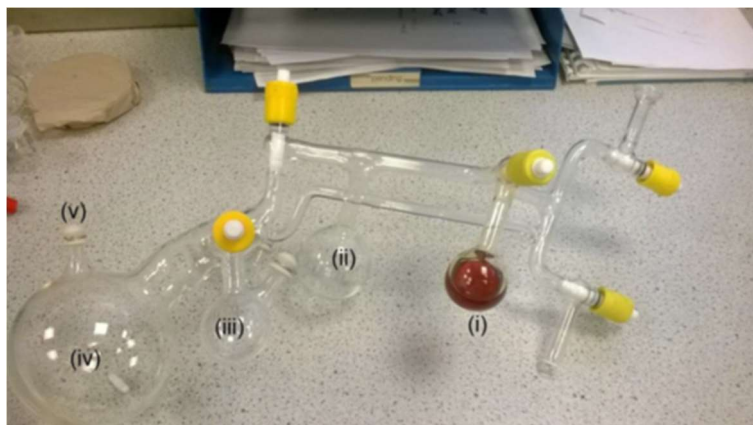


Figure 5.10 - "Christmas tree" reactor used for living anionic polymerisation, (i) Flask A containing living polystyryllithium, (ii) Flask B, (iii) Sidearm Flask, (iv) Reaction Flask, (v) Septum.

5.3.3.1 Synthesis of Randomly Branched Polybutadiene with Potassium *tert*-Butoxide

5.3.3.1.1 R-Pbd_1

Under a nitrogen atmosphere, potassium *tert*-butoxide (0.0056 g, 0.050 mmol) was added to the reaction flask of the Christmas tree. Toluene (50 ml) was also added via distillation under vacuum into the reaction flask and the potassium *tert*-butoxide allowed to dissolve. Divinylbenzene (0.041 ml, 0.29 mmol) was injected directly into the reaction flask via the septum, after which the solution was frozen for one hour and evacuated to remove any air which may be present. Butadiene (5.00 g, 92 mmol) was then added via distillation under vacuum into the reaction flask of the Christmas tree. In order to obtain the target arm M_n of 20,000 g mol⁻¹, 0.18 ml of *sec*-BuLi in cyclohexane (0.25 mmol) was injected directly into the reaction flask via the septum and reacted under vacuum at 60 °C for 12 hours, after which the polymerisation mixture was terminated via injection of nitrogen-sparged methanol. The polymer was precipitated in methanol in the presence of anti-oxidant, butylated hydroxytoluene (BHT). The supernatant liquor was then removed, the polymer dissolved in THF and the polymer then precipitated again in BHT/methanol, recovered and dried to constant mass under vacuum for several days. Yield 72%.

R-Pbd_1: M_n 2800 g mol⁻¹, M_w 41,700 g mol⁻¹, Đ 16

5.3.3.1.2 R-Pbd_2

R-Pbd_2 was prepared according to the procedure described above in 5.3.3.1.1. To a solution of potassium *tert*-butoxide (0.0088 g, 0.078 mmol), divinylbenzene (0.064 ml, 0.45 mmol) and butadiene (7.83 g, 145 mmol) in toluene (80 ml) was added. *sec*-BuLi (0.28 ml, 0.39 mmol) was injected and the polymerisation allowed to react under vacuum at 60 °C for 12 hours. Yield 86%.

R-Pbd_2: M_n 16,200 g mol⁻¹, M_w 59,700 g mol⁻¹, Đ 3.69

5.3.3.1.3 R-Pbd_3

R-Pbd_3 was prepared according to the procedure described above in 5.3.3.1.1. To a solution of potassium *tert*-butoxide (0.0062 g, 0.055 mmol), divinylbenzene (0.045 ml, 0.32 mmol) and butadiene (5.53 g, 102 mmol) in toluene (50 ml), *sec*-BuLi (0.20 ml, 0.28 mmol) was injected and the polymerisation allowed to react under vacuum at 60 °C for 1 hour. Yield 91%.

R-Pbd_3: M_n 1600 g mol⁻¹, M_w 72,500 g mol⁻¹, Đ 44

5.3.3.1.4 R-Pbd_4

R-Pbd_4 was prepared according to the procedure described above in 5.3.3.1.1. To a solution of potassium *tert*-butoxide (0.0065 g, 0.058 mmol), divinylbenzene (0.047 ml, 0.33 mmol) and butadiene (5.75 g, 106 mmol) in toluene (50 ml), *sec*-BuLi (0.21 ml, 0.29 mmol) was injected and the polymerisation allowed to react under vacuum at 60 °C for 1 hour. Yield 93%.

R-Pbd_4: M_n 33,500 g mol⁻¹, M_w 83,000 g mol⁻¹, Đ 2.48

5.3.3.1.5 R-Pbd_5

R-Pbd_5 was prepared according to the procedure described above in 5.3.3.1.1. To a solution of potassium *tert*-butoxide (0.0087 g, 0.077 mmol), divinylbenzene (0.063 ml, 0.44 mmol) and butadiene (7.72 g, 143 mmol) in toluene (50 ml), *sec*-BuLi (0.28 ml, 0.39 mmol) was injected and the polymerisation allowed to react under vacuum at 60 °C for 2 hours. Yield 98%.

R-Pbd_5: M_n 11,800 g mol⁻¹, M_w 392,000 g mol⁻¹, Đ 33

5.3.3.1.6 R-Pbd_6

R-Pbd_6 was prepared according to the procedure described above in 5.3.3.1.1. To a solution of potassium *tert*-butoxide (0.0069 g, 0.062 mmol), divinylbenzene (0.050 ml, 0.35 mmol) and butadiene (6.17 g, 114 mmol) in toluene (50 ml), *sec*-BuLi (0.22 ml, 0.31 mmol) was injected and the polymerisation allowed to react under vacuum at 60 °C for 2 hours. Yield 85%.

R-Pbd_6: M_n 54,900 g mol⁻¹, M_w 427,400 g mol⁻¹, Đ 7.78

5.3.3.2 Synthesis of Randomly Branched Polybutadiene with Potassium *tert*-Butoxide solution (1.0 M in THF)

5.3.3.2.1 R-Pbd_7

Potassium *tert*-butoxide solution (1.0 M in THF) (0.050 ml, 0.50 mmol) was injected directly to the reaction flask of the Christmas tree and the vessel evacuated for one hour to remove any residual THF. Toluene (50 ml) was also added via distillation under vacuum into the reaction flask and the potassium *tert*-butoxide allowed to dissolve. Divinylbenzene (0.068 ml, 0.48 mmol) was injected directly into the reaction flask via the septum, after which the solution was frozen for one hour and evacuated to remove any air which may be present. Butadiene (8.29 g, 153 mmol) was then added via distillation under vacuum into the reaction flask of the Christmas tree. In order to obtain a target M_n of 20,000 g mol⁻¹, 0.30 ml of *sec*-BuLi in cyclohexane (0.41 mmol) was injected directly into the reaction flask via the septum and allowed to react under vacuum at 60 °C for 12 hours, after which the polymerisation mixture was terminated via injection of nitrogen-sparged methanol. The polymer was precipitated in methanol in the presence BHT. The excess solution was then removed, the polymer fully dissolved in THF and the polymer then precipitated again in BHT/methanol and dried to constant mass under vacuum for several days. Yield 7%.

R-Pbd_7: M_n 164,500 g mol⁻¹, M_w 1,922,000 g mol⁻¹, Đ 11.69

5.3.3.2.2 R-Pbd_8

R-Pbd_8 was prepared according to the procedure described above in 5.3.3.2.1. To a solution of potassium *tert*-butoxide (0.049 ml, 0.049 mmol), divinylbenzene (0.040 ml, 0.28 mmol) and butadiene (4.92 g, 91 mmol) in toluene (50 ml), *sec*-BuLi (0.18 ml, 0.25 mmol) was injected and the polymerisation allowed to react under vacuum at 60 °C for 12 hours. Yield 42%.

R-Pbd_8: M_n 73,400 g mol⁻¹, M_w 257,100 g mol⁻¹, Đ 16

5.3.3.2.3 R-Pbd_9

R-Pbd_9 was prepared according to the procedure described above in 5.3.3.2.1. To a solution of potassium *tert*-butoxide (0.051 g, 0.051 mmol), divinylbenzene (0.042 ml, 0.29 mmol) and butadiene (5.10 g, 94 mmol) in toluene (50 ml), *sec*-BuLi (0.18 ml, 0.26 mmol) was injected and the polymerisation allowed to react under vacuum at 60 °C for 12 hours. Yield 47%.

R-Pbd_9: M_n 6830 g mol⁻¹, M_w 67,400 g mol⁻¹, Đ 16

5.3.3.3 Synthesis of Randomly Branched Polybutadiene with TMEDA

5.3.3.3.1 R-Pbd_10

Toluene (50 ml), Divinylbenzene (0.046 ml, 0.32 mmol) and TMEDA (0.042 ml, 0.28 mmol) were both injected directly into the reaction flask via the septum, after which the solution was frozen for one hour and evacuated to remove any air which may be present. Butadiene (5.61 g, 104 mmol) was then added via distillation under vacuum into the reaction flask of the Christmas tree. In order to obtain the target arm M_n of 20,000 g mol⁻¹, 0.20 ml of *sec*-BuLi in cyclohexane (0.28 mmol) was injected directly into the reaction flask via the septum and reacted under vacuum at 60 °C for 12 hours, after which the polymerisation mixture was terminated via injection of nitrogen-sparged methanol. The polymer was precipitated in methanol in the presence of BHT. The excess solution was then removed, the polymer fully dissolved in THF and the polymer then precipitated again in BHT/methanol and dried to constant mass under vacuum for several days. Yield 2%.

R-Pbd_10: M_n 10,100 g mol⁻¹, M_w 13,700 g mol⁻¹, Đ 1.36

5.3.3.3.2 R-Pbd_11

R-Pbd_11 was prepared according to the procedure described above in 5.3.3.3.1. To a solution of TMEDA (0.040 ml, 0.27 mmol), divinylbenzene (0.058 ml, 0.41 mmol) and butadiene (7.11 g, 131 mmol) in toluene (50 ml), *sec*-BuLi (0.25 ml, 0.36 mmol) was injected and the polymerisation allowed to react under vacuum at 60 °C for 12 hours. Yield 91%.

R-Pbd_11: M_n 28,900 g mol⁻¹, M_w 65,700 g mol⁻¹, Đ 2.28

5.3.3.3.3 R-Pbd_12

R-Pbd_12 was prepared according to the procedure described above in 5.3.3.3.1. To a solution of TMEDA (0.026 ml, 0.17 mmol), divinylbenzene (0.057 ml, 0.40 mmol) and butadiene (6.93 g, 128 mmol) in toluene (50 ml), *sec*-BuLi (0.25 ml, 0.35 mmol) was injected and the polymerisation allowed to react under vacuum at 60 °C for 12 hours. Yield 96%.

R-Pbd_12: M_n 41,900 g mol⁻¹, M_w 122,200 g mol⁻¹, Đ 2.92

5.3.3.3.4 R-Pbd_13

R-Pbd_13 was prepared according to the procedure described above in 5.3.3.3.1. To a solution of TMEDA (0.011 ml, 0.08 mmol), divinylbenzene (0.025 ml, 0.18 mmol) and butadiene (6.09 g, 113 mmol) in toluene (50 ml), *sec*-BuLi (0.11 ml, 0.15 mmol) was injected and the polymerisation allowed to react under vacuum at 60 °C for 12 hours. Yield 89%.

R-Pbd_13: M_n 115,500 g mol⁻¹, M_w 586,500 g mol⁻¹, Đ 5.07

5.3.3.3.5 R-Pbd_14

R-Pbd_14 was prepared according to the procedure described above in 5.3.3.3.1. To a solution of TMEDA (0.086 g, 0.58 mmol), divinylbenzene (0.062 ml, 0.43 mmol) and butadiene (5.76 g, 106 mmol) in toluene (50 ml), *sec*-BuLi (0.21 ml, 0.29 mmol) was injected and the polymerisation allowed to react under vacuum at 60 °C for 15 minutes. Yield n/a - gel.

5.3.3.3.6 R-Pbd_15

R-Pbd_15 was prepared according to the procedure described above in 5.3.3.3.1. To a solution of TMEDA (0.0091 g, 0.61 mmol), divinylbenzene (0.065 ml, 0.46 mmol) and butadiene (6.10 g, 113 mmol) in toluene (50 ml), *sec*-BuLi (0.22 ml, 0.31 mmol) was injected and the polymerisation allowed to react under vacuum at 60 °C for 30 minutes. Yield 25%.

R-Pbd_15: M_n 75,600 g mol⁻¹, M_w 322,300 g mol⁻¹, Đ 4.26

5.4 Conclusions

In contrast to linear polymers, highly branched polymers possess a variety of advantageous properties such as enhanced melt strength effecting their processability.²² The adaptation of anionic polymerisation for the synthesis of highly branched, high molecular weight vinyl polymers therefore represents both academic and industrial interest. Anionic polymerisation remains one of the most widely utilised industrial techniques for the synthesis of polymers. The creation of highly branched polymers using inexpensive starting materials could potentially allow for the simple generation of a wealth of materials with desirable properties without major modification to existing facilities or processes. However, a significant problem facing the production of highly (randomly) branched polymers by anionic polymerisation is that the degree of chain coupling often leads to gelation. The Strathclyde route has previously shown great potential for the facile synthesis of soluble branched vinyl polymers using free radical polymerisation in which chain transfer reactions are introduced to inhibit crosslinking, and its adaptation to anionic polymerisation is reported in this chapter. Building upon previous work carried out by the Hutchings' group⁹ which was mostly concerned with the synthesis of low molecular weight highly branched polymer, the main aim in this work was to synthesise higher molecular weight, highly branched soluble product by inhibiting gelation by chain transfer. This was achieved by the synthesis of polybutadiene using divinylbenzene as the chain-coupling agent. The reactions were carried out using toluene which acts as both solvent and chain transfer agent. Chain transfer is promoted by the use of additives such as metal alkoxides or Lewis bases. The effect of two additives – potassium *tert*-butoxide and TMEDA on the chain transfer process and resultant polymers were also investigated.

Polymers were produced using both potassium *tert*-butoxide in its solid powder form and also as a solution in THF as chain transfer promoting modifiers. The polymers obtained from polymerisation using potassium *tert*-butoxide (powder) were indeed branched materials, but with inconsistencies arising from the difficulty of accurately dosing very small quantities of the powder form of potassium *tert*-butoxide. The resulting polymers could be split into two groups, polymers containing a high level (>30%) of 1,2 microstructure (vinyl) content (HVC) and polymers containing a low level of 1,2 content (<15%) (LVC). It was concluded that due to the difficulties in obtaining consistent levels of potassium *tert*-butoxide in the reactor, varying amounts of potassium *tert*-butoxide present in the polymerisations resulted in a varying contributions of chain transfer. However, the

use of potassium *tert*-butoxide also inevitably had an effect on the microstructure of all the aforementioned polymers, increasing the level of 1,2-content present to levels of 13 - 33%. It was determined that the polymers with lower potassium *tert*-butoxide to initiator ratios, purported to be around *ca.* KOtBu : Li = 0.1, resulted in the generation of highly branched, yet still soluble material with low levels of vinyl content (<15%), which is quite a significant find for the synthesis of highly branched 1,4-polybutadiene. Sherrington had predicted that the ratio of DVB to initiator is the key variable and using DVB : Li ratios ≥ 1.0 in “living” polymerisations inevitably results in gelation unless chain transfer is prevalent. For every polymerisation in this chapter a DVB : Li ratio above 1.0 was used. The amount of DVB used in the reactions proved to have a drastic impact on the degree of chain coupling. Increasing the DVB to initiator ratio from 1 : 1.15 Li : DVB to 1 : 1.48 Li : DVB resulted in polymers with M_w values in the hundreds of thousands g mol^{-1} as opposed to tens of thousands of g mol^{-1} . In order to gain more consistency in the results, the use of a potassium *tert*-butoxide solution (in THF) was also investigated. The resultant polymerisations however, resulted in further inconsistencies and low yielding reactions, which was put down to the effect of more impurities being present in the polymerisations. Gelation was avoided in all instances of polymerisation using either the potassium *tert*-butoxide powder or solution with soluble polymers obtained.

The polymers produced using TMEDA as the chain transfer promoter resulted in randomly branched polymers as the result of post-polymerisation, linear chain coupling. The polymers prepared using TMEDA were also more susceptible to gelation, with microgelation observed for the polymers where the initiator to TMEDA : Li ratio was less than one, and total gelation observed at a TMEDA : Li ratio of 2 : 1, if the reaction was not terminated prematurely.

Adapting the Strathclyde route to anionic polymerisation has not been without challenges, however the ability to synthesise highly randomly branched, high molecular weight soluble vinyl materials has been demonstrated. Moreover, it was also possible to attain high (85%) 1,4-content branched polybutadiene, by the (serendipitous) inaccurate addition of potassium *tert*-butoxide at an assumed potassium *tert*-butoxide : Li ratio of 0.1. Such an observation was unplanned and unexpected and suggests that the production of high 1,4 branched polybutadiene is viable by the Strathclyde approach. These materials could be of particular interest in a variety of applications where the desirable rheological properties of branched polybutadiene can be matched with the low glass transition temperature of high

1,4 polybutadiene. As a result, the aims of this chapter were met, albeit with some unintended good fortune. Further investigations are surely needed for optimization and the creation of a truly, reproducible procedure. The materials synthesised in this chapter are of rheological interest and samples are being investigated in Durham by a PhD student in a related project.

5.5 References

1. England, R. M.; Rimmer, S., *Polym. Chem.* **2010**, *1* (10), 1533-1544.
2. Hutchings, L. R.; Kimani, S. M.; Hoyle, D. M.; Read, D. J.; Das, C.; McLeish, T. C. B.; Chang, T.; Lee, H.; Auhl, D., *ACS Macro Letters* **2012**, *1* (3), 404-408.
3. O'Brien, N.; McKee, A.; Sherrington, D. C.; Slark, A. T.; Titterton, A., *Polymer* **2000**, *41* (15), 6027-6031.
4. Camerlynck, S.; Cormack, P. A. G.; Sherrington, D. C., *Eur. Polym. J.* **2006**, *42* (12), 3286-3293.
5. Liu, B.; Kazlauciunas, A.; Guthrie, J. T.; Perrier, S., *Macromolecules* **2005**, *38* (6), 2131-2136.
6. Young, R. N.; Fetters, L. J., *Macromolecules* **1978**, *11* (5), 899-904.
7. Halasa, A. F.; Robertson-Wilcox, S. E.; Zanzig, D. J.; Arconti, R. J.; Hsu, W. L. Anionic diene polymerization process with branching. US4845165A, 1987.
8. Isaure, F.; Cormack, P. A. G.; Graham, S.; Sherrington, D. C.; Armes, S. P.; Butun, V., *Chem. Commun.* **2004**, (9), 1138-1139.
9. Kempe, F. Synthesis of Branched Polybutadienes by Anionic Polymerisation with a Divinyl Crosslinker. Masters, Durham University, Durham, 2013.
10. Schlosser, M., Superbases for organic synthesis. In *Pure Appl. Chem.*, 1988; Vol. 60, pp 1627-1634.
11. Schlosser, M.; Strunk, S., *Tetrahedron Lett.* **1984**, *25* (7), 741-744.
12. Hsieh, H. L.; Quirk, R. P., *Anionic Polymerization: Principles and Practical Applications*. Marcel Dekker: New York, 1996.
13. Schlosser, M., *Angew. Chem. Int. Ed.* **2005**, *44* (3), 376-393.
14. Luxton, A. R., *Rubber Chem. Technol.* **1981**, *54* (3), 596-626.
15. Hsieh, H. L.; Wofford, C. F., *J. Polym. Sci., Part A-1: Polym. Chem.* **1969**, *7* (2), 449-460.
16. Kraus, G.; Gruver, J. T., *J. Polym. Sci., Part A: Gen. Pap.* **1965**, *3* (1), 105-122.
17. Cheng, T. C.; Halasa, A. F., *J. Polym. Sci., Part A: Polym. Chem.* **1976**, *14* (3), 573-581.
18. Bywater, S.; Firat, Y.; Black, P. E., *J. Polym. Sci., Part A: Polym. Chem.* **1984**, *22* (3), 669-672.
19. Mykhaylyk, O. O.; Fernyhough, C. M.; Okura, M.; Fairclough, J. P. A.; Ryan, A. J.; Graham, R., *Eur. Polym. J.* **2011**, *47* (4), 447-464.
20. Chang, C. C.; Halasa, A. F.; Miller, J. W.; Hsu, W. L., *Polym. Int.* **1994**, *33* (2), 151-159.
21. Antkowiak, T. A.; Oberster, A. E.; Halasa, A. F.; Tate, D. P., *J. Polym. Sci., Part A-1: Polym. Chem.* **1972**, *10* (5), 1319-1334.
22. Dodds, J. M.; De Luca, E.; Hutchings, L. R.; Clarke, N., *J. Polym. Sci., Part B: Polym. Phys.* **2007**, *45* (19), 2762-2769.

Chapter 6

Concluding Remarks

6.1 Conclusions

In this project, the syntheses and characterisations of a range of branched polymer architectures were realised. They were achieved via a number of synthetic methods, predominantly involving the use of living anionic polymerisation and in some cases involving post-polymerisation coupling reactions. The polymers were characterised using a range of methods. Three different branched polymer architectures were targeted for synthesis: star-branched polymers, H-shaped polymers and randomly long-chain branched polymers. The project was funded by Michelin and the materials were of interest principally as model polymers for various rheological tests and structure-property correlation studies of direct relevance to the tyre industry. As such 1,3-butadiene was used as the base monomer for all polymers synthesised in this work.

The synthesis of well-defined three-arm and four-arm star-branched polybutadiene was achieved using a combination of living anionic polymerisation and chlorosilane coupling agents. An arm-first methodology was used to firstly generate the living polymer chains (arms) of the desired molecular weight which were subsequently coupled via termination with methyltrichlorosilane for the three-arm star and silicon tetrachloride for the four-arm star. Before purification, both the linear arm segments and the final star polymers were characterised by both ^1H -NMR spectroscopy and size exclusion chromatography (SEC), with both techniques confirming the composition and molar mass data of the polymers respectively. Purification of the stars was carried out using solvent/non-solvent fractionation in order to remove the excess unreacted linear arm and SEC analysis suggested that the polymers had been purified completely. However, this was proven not to be the case by the use of a powerful chromatographic technique known as interaction chromatography (IC) and in particular temperature gradient interaction chromatography (TGIC). Reversed-phase TGIC (RP-TGIC) was used to analyse the star-branched polymers before and after purification and provided a wealth of information which was not accessible by SEC. In the crude polymer samples, RP-TGIC was able to identify the existence of partially coupled by-products in both the three-arm and four-arm star polymers. While SEC analysis for an attempted synthesis of a four-arm star indicated that only a three-arm star had been achieved, RP-TGIC revealed the existence of multiple products within the polymer mixture including the desired four-arm star, although in a lower concentration compared to the three-arm by-product.

RP-TGIC analysis of the purified polymers was able to reveal traces of unwanted impurities arising from incomplete coupling present in the polymers. Although the generation of “perfect” homogenous materials is the ideal goal for the synthesis of model polymers, this is often rather challenging. However, the ability to completely characterise such polymers with TGIC; to identify and quantify the presence of heterogeneities, not possible by SEC alone, is crucial in allowing such materials to be used for accurate structure-property correlation studies.

For the synthesis of H-shaped polymers the macromonomer approach was adopted. In this approach, the macromonomers are well-defined, chain-end functionalised polymers synthesised by living anionic polymerisation, which are then coupled together in a post polymerisation reaction. This approach was chosen to allow the synthesis of a “mix-and-match” series of H-shaped polymers where every linear unit of the constituent H-polymer is completely characterised. The macromonomers are divided into two classes – telechelic polymers with four functionalities (two at each chain-end) to serve as the “crossbar” for the H-polymers and single chain-end functionalised polymers to serve as the “arms” of the H-polymers. The crossbar polymers were synthesised using two strategies, both of which used the same protected moiety, DPE-OSi – that served as both a functionalised initiator and as an end-capping agent. The first strategy was an “end-capping” approach in which DPE-OSi was added in two batches: firstly, at the beginning of the reaction to initiate polymerisation, and then at the end of polymerisation as a terminating agent to end-cap the polymer chains. The second strategy used a “fire and forget” approach in which all DPE-OSi was present from the start of polymerisation, exploiting the inability of DPE-OSi to either homopolymerise or copolymerise with butadiene, in order to generate the telechelic polymers. TMEDA was added in both pathways in order to promote the end-capping reactions although it was concluded that if TMEDA was present from the beginning of reaction, DPE-OSi incorporation was uncontrolled. Both pathways resulted in a number of well-defined, telechelic polybutadiene crossbars with molar masses in the ranges of 30,000 g mol⁻¹ to 100,000 g mol⁻¹, although the polymers produced by the “fire and forget” pathway proved to be more satisfactory with a higher degree of end-capping, which was confirmed by ¹H-NMR. The most suitable crossbars generated by both routes were then deprotected for use in the subsequent coupling reactions. The crossbars were also analysed using interaction chromatography, in this case normal-phase isothermal interaction chromatography (NP-IIC). NP-IC separates polymers based on both their

molecular weight and chain end functionality, in contrast to RP-IC which is only able to separate polymers based on molecular weight. In the case of the crossbars, ^1H -NMR analysis was able to indicate the average number of DPE-OSi units per chain, but could say nothing about the distribution of DPE-OSi units per chain. NP-IIC was able to provide a much more complete picture of the extent of end-capping, which was more complex than anticipated, revealing that the crossbars consisted of mixtures of chains capped at one end and at both ends (as desired). Although from a synthetic standpoint this was clearly not desirable, this is another case of IC analysis revealing the true nature of the materials in question, which would not have been possible with only a combination of SEC and NMR. The linear “arm” polybutadiene macromonomers were synthesised using living anionic polymerisation and subsequently end-functionalised by terminating the polymers with ethylene oxide. The resulting hydroxyl chain-end functionality was converted to a bromine functionality. A series of linear polybutadiene “arms” with molecular weights between 18,000 and 40,000 g mol⁻¹ was produced and normal-phase isothermal interaction chromatography (NP-IIC) was used to determine the extent of end-capping, as ^1H -NMR was not able to accurately quantify the degree of end-capping in these high molecular weight samples. Non-functionalised, hydroxyl-functionalised and bromine-functionalised samples of each arm macromonomer were analysed and it was possible to quantitatively determine the percentage of chain ends that has been successfully end-capped for each polymer. NP-IIC has showed itself to be an invaluable tool for the analysis of high molecular weight chain-end functionalised polymers. We have shown for the first time that NP-IIC can be used to characterise end-functionalised polymers and allow quantitative analysis of the degree of end-capping at molar masses where other techniques such as NMR and MALDI-MS are completely ineffective.¹

H-shaped polymers synthesised by both ionic and radical polymerisation methods have been previously reported although relatively few examples exist in the literature, especially in comparison to reports of the synthesis and characterisation of stars and other highly/hyperbranched polymers. It was expected that the macromonomer approach would allow for a facile approach to produce H-shaped polymers and moreover, to allow the synthesis of a series of H-polymers in which the polymers could all be completely characterised. Previously this (macromonomer) approach had been used by the Hutchings’ group for the synthesis of asymmetric three-arm polystyrene stars,² but we believe that this is the first reported attempt to prepare H-shaped polymers by the macromonomer

approach. A number of H-shaped polymers were synthesised using the various crossbar and arm macromonomers with the main aim being the adaptation of the macromonomer approach to the synthesis of these materials. The Williamson coupling reaction was chosen for these syntheses as it had been successfully used previously for the synthesis of a variety of branched polymers from macromonomers. Small scale reactions were initially carried out in order to develop a methodology that would maximize coupling and the generation of the desired H-shaped polymer. The Williamson coupling requires a solvent with a high dielectric constant such as DMF, however, due to polybutadiene's insolubility in DMF a 1 : 1 co-solvent combination of THF : DMF was used for the initial reactions, which resulted in little coupling, largely due to polybutadiene's poor solubility in the solvent mixture. The solvent mixture was then changed to 1 : 1 THF : DMAc which resulted in greater solubility as well as an improved coupling efficiency. A number of factors were then investigated to understand their effect on the extent of coupling, including the molar ratio of arms to crossbar as well as the molar ratio of the base. It was concluded that increasing the molar ratio of arms to crossbar had a positive effect on coupling efficiency, as did using cesium carbonate in a very large molar excess to the crossbar. A combination of both effects greatly enhanced macromonomer conversion. The coupling efficiency was monitored by both SEC and RP-TGIC analysis, although TGIC analysis proved difficult, in particular for disperse samples with low rates of conversion and coupling. In many cases, however, RP-TGIC revealed significantly greater levels of detail about the nature of the heterogeneity of the samples including by-products arising from incomplete coupling and high molecular weight by-products that were present, with the high molar mass impurities suggesting that in some cases the crossbars did in fact include a small fraction of chains with three or more DPE-OSI units. This analysis clearly illustrates the advantages of TGIC and the limitations of SEC. Improved reaction conditions were eventually established for the generation of H-shaped polymers using the macromonomer approach although coupling reactions were incomplete, leading to complex mixtures which, as revealed by TGIC, comprised of up to 25 - 30% of desired H-shaped polymer. Attempts to scale up these coupling reactions initially ran into numerous difficulties. We believe the ability to provide adequate mixing of the components of the reaction mixture was an issue and the degree of coupling was lower than seen in the smaller scale reactions. However, a number of modifications, including the lowering of the solution concentration from 10 wt% polymer to 5 wt% polymer and the use of magnetic stirring rather than mechanical stirring resulted in polymers synthesised on a large scale with an adequate degree of coupling to allow for the

production of (nearly) homogeneous samples (by fractionation) for rheological characterisation. The final samples were not as well-defined as had been hoped, but still proved to be of rheological interest.

In conclusion, the adaptation of the macromonomer approach for the synthesis of H-shaped polymers resulted in something of a mixed story. It is clear that this approach allows (in theory) for the synthesis of a homologous series of H-shaped polymers and allows for the complete characterisation of the individual building blocks. However, the efficiency of the coupling reaction was disappointing and remains a crucial factor in the success of the approach. The Williamson coupling reaction is an extremely useful reaction, however, it performs best at very high temperatures in polar aprotic solvents. The coupling of polybutadiene macromonomers was in part limited by poor solubility in the optimal solvents, and the use of modest reaction temperatures was necessary due to the thermal/oxidative degradation butadiene undergoes at higher temperatures. On a much more positive note, interaction chromatography showed itself to be an invaluable complementary analytical method, especially in regards to the analysis of complex polymer mixtures. NP-IIC has shown itself to be a valuable tool for the analysis of high molecular weight chain-end functionalised polymers, able to provide quantitative information where other techniques fail. RP-TGIC was able to provide extremely detailed compositional analysis of complex polymer mixtures, in much greater detail than SEC analysis is capable of. The characterisation data to the level of detail described for the functionalised macromonomers, as well as the star and H-shaped polymers would not have been possible without the use of interaction chromatography, showcasing the necessity of this technique for the analysis of highly complex polymers.

Finally, a study into the synthesis of randomly branched polybutadiene concluded that the "Strathclyde" route can be successfully adapted to allow the formation of high molecular weight, randomly-branched polybutadiene, with a high 1,4-microstructure, by anionic polymerisation. The Strathclyde route involves the copolymerisation of a vinyl monomer with a difunctional (crosslinking) monomer and a chain transfer agent to inhibit gelation. This was adapted to living anionic polymerisation by using butadiene as the vinyl monomer, divinylbenzene (DVB) as the crosslinking agent and toluene as both the chain transfer agent and the polymerisation solvent. Two modifiers that enhance chain transfer and their effects on the resultant polymers were investigated, potassium *tert*-butoxide and TMEDA.

Previous (unpublished) work in the Hutchings' group had established the base reaction conditions for the synthesis of low molecular weight branched polymers, and established that potassium *tert*-butoxide at a molar ratio of 0.2 with respect to the initiator (Li) was sufficient to enhance chain transfer in toluene.³ Building on this work it was discovered that it was possible to use DVB : Li ratios greater than 1.0, which would ordinarily result in gelation, provided that there is sufficient chain transfer to inhibit gelation. Potassium *tert*-butoxide was found to be by far the most effective chain transfer promoter, although TMEDA was also found to be capable of inhibiting gelation, but to a much lesser extent than potassium *tert*-butoxide. The small scale of the reactions resulted in significant challenges in accurately adding the (very small) required amounts of potassium *tert*-butoxide and this resulted in some irreproducibility between what should have been identical reactions. However, serendipitously this allowed us to conclude that lower mole fractions of potassium *tert*-butoxide (approximately 0.1 mole equivalents with respect to Li) could be used to promote sufficient chain transfer to inhibit gelation whereas the previous study had used double this amount. This in turn led to the realization that although lower levels of potassium *tert*-butoxide being present would lower the contribution of chain transfer, a much lower amount of potassium *tert*-butoxide could be used to produce polymers with the desired much higher molar masses whilst still inhibiting gelation. However, the most important aspect regarding this discovery was that lower levels of potassium *tert*-butoxide also resulted in microstructures with much higher levels of 1,4-content (85% c.f. 65%) which in combination with the properties of branched architectures could prove highly beneficial for some applications. In conclusion, soluble, randomly branched high molecular weight polybutadienes were synthesised in a one-pot reaction by successfully adapting the Strathclyde route to anionic polymerisation. In addition, a route was found to the synthesis of low vinyl branched polybutadiene which could be of significant benefit especially regarding the tyre and rubber industries.

6.2 Future Work

The research described in this thesis could be explored in the following ways to further exploit the combined use of anionic polymerisation, the macromonomer approach and interaction chromatography for the synthesis of branched polymers.

H-shaped polymers

Improving the coupling reaction in the macromonomer approach. There was a number of issues regarding the Williamson coupling reaction's efficacy, specifically due to the use of butadiene which suffered from poor solubility in ideal solvents requiring the use of a co-solvent, the concern of thermal/oxidative degradation limiting the temperature range and poor mixing being observed when these reactions were scaled up. Butadiene is a highly important industrial monomer and in order to improve the macromonomer approach for this monomer, other coupling reactions could be investigated. Reactive functionality to enable the coupling reactions is provided in most cases post-polymerisation; different chain-end functional groups and their effectiveness at coupling could be explored. Above all, the coupling reaction should be possible in a good solvent for high molecular weight polybutadiene. One such possible reaction is the Steglich esterification, which involves the coupling of an acid group to an alcohol group using *N,N'*-dicyclohexylcarbodiimide (DCC) as the coupling reagent and 4-dimethylaminopyridine (DMAP) as the catalyst. An advantage of this reaction is that it can be performed in dichloromethane (DCM), which is known to be a good solvent for polybutadiene. The use of this reaction would require the synthesis of either the arm or crossbar polymers end functionalized with carboxylic acid groups and this could be achieved quantitatively for the arm macromonomers by using carbon dioxide as the end-capping agent. Another possibility is the azide-alkyne "click" reaction which couples together an azide group to an alkyne group through a cycloaddition. This reaction was used previously by Hutchings' group to synthesise star polystyrenes using a copper (I) catalyst in DMF, however, for butadiene a ruthenium (I) based catalyst in dioxane may be more suitable, due to solubility. If the coupling reaction efficiency can be increased by using these more monomer-friendly conditions, this would hopefully provide more well-defined materials for study.

The synthesis of H-shaped polymers using different monomers may also be of interest. In this work, polybutadiene was the monomer of choice primarily because the resulting materials were required for rheological study and to underpin understanding of industrial

polymers produced by the tyre industry. However, for more academic purposes the synthesis of H-shaped polymers of other monomers such as styrene or isoprene may provide another novel synthetic application of the macromonomer approach which still remains the only method of synthesis that allows for full characterisation of the “building blocks” of any branched polymers that may be synthesised, also allowing for the use of the same polymer for multiple reactions.

Another way in which the work could be extended would be the synthesis of miktoarm H-shaped polymers. This would involve the reaction of macromonomers of different compositions for the creation of novel materials. For example, the synthesis of an H-shaped polymer with a polybutadiene backbone and polystyrene arms. The macromonomer approach could again be used for the synthesis of the materials separately. There are very few reports on the synthesis of H-shaped block copolymers, with the ones reported focused on the use of ATRP to synthesise low molecular weight ($< 10,000 \text{ g mol}^{-1}$) polymers,⁴ and none on copolymerising styrene and butadiene. An investigation into the potential impact of the branched architecture on micro-phase separated morphologies could also be of interest.

Randomly branched polymers

Optimization of the use of potassium *tert*-butoxide in the synthesis of randomly branched polymers would be one of the most immediate ways to develop the work presented in this thesis. It was effectively shown that gelation could be avoided with the use of this chain transfer promoter but there still remains the challenge of optimizing the reaction to provide consistent results. There can also be exploration in the best method of delivering the potassium *tert*-butoxide to the reaction in order to generate the desired polymers reproducibly, with an option being to scale up the reactions (in either laboratory or perhaps on industrial scale), in order to gain a better control over the amount of potassium *tert*-butoxide addition.

The exploration of different metal alkoxides and their effect on inhibiting gelation, chain transfer and the resultant branched products could also be tested. In this study, potassium *tert*-butoxide was used, building upon the previous study, as well as for its well-known usage in industry. However, while it has been reported that polar promoters including metal alkoxides increase chain transfer to solvent,⁵ there has not been any investigation regarding their usage in inhibiting gelation in the synthesis of branched polymers.

Further investigation could also be conducted with the use of TMEDA as the chain transfer modifier. A more detailed investigation into the effects of TMEDA and the polymers obtained would confirm more about the structure of the materials obtained.

Exploration of other chain transfer modifying agents besides metal alkoxides also remains feasible. A number of modifiers exist for anionic polymerisation, such as 2,2'-ditetrahydrofurylpropane (DTHFP), as well as other Lewis bases such as N,N-dimethylaminoethoxyethane which may also have an impact on microstructure as well as chain transfer.

The impact of DVB on the final molecular weight and architecture of polymers could also be investigated. Molar ratios of up to 1.5 : 1 of DVB to initiator resulted in branched polymers without gelation, it would be of interest to determine the maximum level of DVB which can be added before gelation occurs. If combined with more potassium *tert*-butoxide investigation, both the minimum and maximum levels of DVB : Li as well as KO^tBu : Li before gelation could be established, which could then further be used to accurately tune the resultant branched polymer architecture, microstructures and molar masses.

The synthesis of randomly branched styrene-butadiene rubber by anionic polymerisations. Solution styrene-butadiene rubber (sSBR) is widely used in the tyre industry. The adaptation of the Strathclyde route to this polymer may allow for a facile and direct one-pot route to branched sSBR architectures which may be of significant interest to many industries.

6.3 References

1. Hutchings, L. R.; Agostini, S.; Oti, M. E.; Keth, J., *Eur. Polym. J.* **2015**, *73*, 105-115.
2. Agostini, S.; Hutchings, L. R., *Eur. Polym. J.* **2013**, *49* (9), 2769-2784.
3. Kempe, F. Synthesis of Branched Polybutadienes by Anionic Polymerisation with a Divinyl Crosslinker. Masters, Durham University, Durham, 2013.
4. Han, D.-H.; Pan, C.-Y., *J. Polym. Sci., Part A: Polym. Chem.* **2006**, *44* (9), 2794-2801.
5. Luxton, A. R., *Rubber Chem. Technol.* **1981**, *54* (3), 596-626.